Phase behaviour of supported lipid bilayers studied by neutron reflectivity

Stidder, Barry David

Award date:
2004

Awarding institution:
University of Bath

Phase Behaviour of Supported Lipid Bilayers studied by Neutron Reflectivity

Barry David Stidder

A thesis submitted for the degree of Doctor of Philosophy

University of Bath

Department of Chemistry

October 2004

ProQuest LLC
789 East Eisenhower Parkway
P.O. Box 1346
Ann Arbor, MI 48106-1346

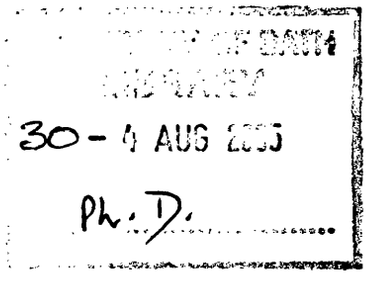
30 - 4 AUG 2005
Ph. D.

Dedicated to my Mum, Dad, brother Tom, sister Amy and my late incredible Nan,
for all things and everything!

Abstract

The aim of this thesis was to incorporate new components into a supported lipid double bilayer system and study their effect on the phase behaviour and stability. This would increase the understanding of mixed lipid planar systems and increase the applicability of the system as a biomembrane mimic.

The fabrication and phase behaviour of DPPC double bilayers containing 0 – 10 mol% cholesterol was investigated. During the transition phase the DPPC sample exhibited large increases in the upper bilayer roughness and thickness of water layer separating the bilayers. This was interpreted as the presence of a ripple phase. Very low concentrations of cholesterol progressively reduced the level of increase in the two parameters; whilst with higher amounts of cholesterol, only a small swelling of the water layer was observed. It is likely therefore that low amounts of cholesterol progressively reduce the size of the ripple structure. These studies add to the understanding of the effect cholesterol near the main transition, which is currently a source of debate.

The phase behaviour of DPPE double and single bilayers with and without cholesterol was investigated. The double bilayer was unstable, forming an irreversible repeat unit in the fluid phase. The single bilayer exhibited stable gel and fluid structures. The addition of 10 mol% cholesterol destabilised the upper bilayer, which detached below the gel – fluid transition temperature.

The effect on the phase behaviour of three different asymmetric lipid distributions was investigated. In one study the asymmetric nature increased the temperature of the gel – fluid transition of lipids with different transition temperatures. In another study the presence of a deuterated lipid leaflet reduced the transition phase behaviour of hydrogenated lipids. In the final study the presence of a lower bilayer with a higher concentration of cholesterol reduced the transition phase behaviour of the upper bilayer.

Contents

Abstract v
Acknowledgements xi
Glossary of Abbreviations xiii

Chapter 1 Introduction 1

1.1 Cell membranes and their components 1
1.2 Phase behaviour of lipids 4
1.3 Modelling cell membranes 8
1.4 Double bilayer system 14
1.5 Forces acting on bilayers 16
1.6 References 18

Chapter 2 Fabrication, Techniques and characterisation 23

2.1 Langmuir monolayers and Langmuir Blodgett films 23
2.2 Fabrication of Double bilayers 28
2.3 Materials and Equipment 29
2.4 Deposition procedure 31
2.5 Principles of neutron reflectivity 35
2.6 Analysis of reflectivity data 43
2.7 Application of reflectivity to double bilayers 49
2.8 Double Bilayer Parameters 51
2.9 D17 Reflectometer at Institut Laue-Langevin 52
2.10 References 55

Chapter 3 DPPC bilayers with low amounts of cholesterol.. 59

3.1 Abstract 59
3.2 Introduction 57
3.3 Fabrication results 62
3.4 Modelling of DPPC-cholesterol neutron reflectivity 64
3.5 Phase behaviour of DPPC double bilayers 65

3.6 Phase behaviour of 1 mol% Cholesterol 99 mol% DPPC 81
3.7 Phase behaviour of 2 mol% Cholesterol 98 mol% DPPC 95
3.8 Phase behaviour of 4 mol% Cholesterol 96 mol% DPPC 108
3.9 Phase behaviour of 6 mol% Cholesterol 94 mol% DPPC 118
3.10 Phase behaviour of 10 mol% Cholesterol 90 mol% DPPC 126
3.11 Deuterated DPPC double bilayers 136
3.12 Single bilayers of d-DPPC and h-DPPC and cholesterol 139
3.13 Comparison of double bilayer parameters 142
3.14 Overall conclusion 150
3.15 References 153

Chapter 4 DPPE bilayers with and without Cholesterol 156

4.1 Introduction 156
4.2 Fabrication of DPPE bilayers 160
4.3 Modelling of DPPE neutron reflectivity 164
4.4 DPPE double bilayers 165
4.5 DPPE single bilayer 183
4.6 DPPE and 10 mol% cholesterol double bilayer 188
4.7 Overall conclusion of DPPE samples 198
4.8 References 200

Chapter 5 Phase behaviour of asymmetric samples 203

5.1 Introduction 203
5.2 Asymmetric bilayers of DPPC, DPPE and cholesterol 205
5.3 Asymmetric hydrogenated and deuterated bilayers 212
5.4 Asymmetric distributions of cholesterol 218
5.5 Asymmetric samples conclusion 231
5.6 References 233

Chapter 6 Thesis Conclusion 235

6.1 DPPC cholesterol phase behaviour 232
6.2 DPPE with and without cholesterol phase behaviour 237
6.3 Phase behaviour of asymmetric samples 238

Chapter 7 Future Perspectives..... 240

7.1 Future samples 240

7.2 Application of different analytical methods..... 241

7.3 References 241

Acknowledgements

My Mum, Dad, brother Tom, sister Amy and my late incredible Nan

Many thanks to Giovanna Fragneto and Steve Roser for their help and patience. Also thanks to Bob Cubitt of the D17 reflectometer.

Acknowledgements to my Grenoble friends for many novel and deep times

Alex 'English Alex', Anne 'Bella Doward', Elisa 'mi sorella', Matt 'remember Bonn and l'Entre-pot?' German Alex of crazy days, Gary 'guys, it's only a Porsche!' Louise 'it was wicked!' Intellectual Bob, Gianluca 'guitar legend', Fred 'the craziest Frenchman ever!' Manuel 'Astorius cider', Carlos 'the smiling footballer', Fabrizio 'the grinning Napoletano', Marcelo 'Jamie Oliver II', Fabrizio 'buon cibo italiano', David 'Capitán español, hey we've still another 15mins to play?' Maria 'loca mademoisella', Stephan 'Stephhannn', Paola 'I'm Italian honest', Tiziana 'no, really', Nico, Tatiana, Angela, Rosella, Simon 'VTT', Pedro 'more relaxed than a Madrid siesta', Rebeca of beautiful Cantabria, Mun 'muy loca!' Arach the second craziest Frenchman ever, Arwel, Adam of white feet, Sarah of English cuisine, Ingrid et le belle chien, crazy Valeria, Susanna, JB, Phil, The Levett, and all the other locos Italians, Spanish, Argentines, Francais and Grenoblois.

Glossary of Abbreviations

Chemicals

DMPC	1,2-Dimyristoyl-sn-Glycero-3-Phosphocholine
DOPC	1,2-Dioleoyl-sn-Glycero-3-Phosphocholine
DOPE	L-α-dioleoyl-phosphatidylethanolamine
DPPC	1,2-Dipalmitoyl-sn-Glycero-3-phosphocholine
DPPE	1,2-Dipalmitoyl-sn-Glycero-3-phosphoethanolamine
DPPG	1,2-Dipalmitoyl-sn-Glycero-3-[Phospho-rac-(1-glycerol)](Na Salt)
DPPS	1,2- Dipalmitoyl -sn-Glycero-3-[Phospho-L-Serine](Na Salt)
DSPC	1,2-Distearoyl-sn-Glycero-3-phosphocholine
DSPE	1,2-Distearoyl-sn-Glycero-3-Phosphoethanolamine
DSPG	1,2-Distearoyl-sn-Glycero-3-[Phospho-rac-(1-glycerol)](Na Salt)
OTS	Octadecanetrichlorosilane
PC	Phosphatidylcholines
PE	Phosphatidylethanolamines
PS	Phosphatidylserines
SAM	Self-assembled monolayer
SMW	Silicon matched water
4MW	4-matched water

Prefixes

h-	Hydrogenated versions of lipid
d-	Deuterated versions of lipid
l-	Lower bilayer
u-	Upper bilayer

Parameters

APM	Area per molecule
Cov	Coverage
Dc	Upper bilayer chain thickness
Dc	Lower bilayer chain thickness
Dw	Thickness of water layer separating bilayers

Dw	Thickness of water layer separating lower bilayer and substrate
Rou	Roughness
T_m	Transition temperature of gel – fluid transition
T_H	Transition temperature of lamellar to hexagonal phase

1. Introduction

1.1 Cell Membranes and their Components

Cell membranes compartmentalise the cell and provide a whole range of vital tasks. They act as a selective barrier to substances entering and leaving the cell, they control cell to cell recognition, transduce extra-cellular signals to regulate internal cellular activity, and control many other cellular activities. Membranes are omnipresent in biological materials; the human brain for example consists of complex network of membranes with a total surface area of 10^3 - 10^4 m^2.

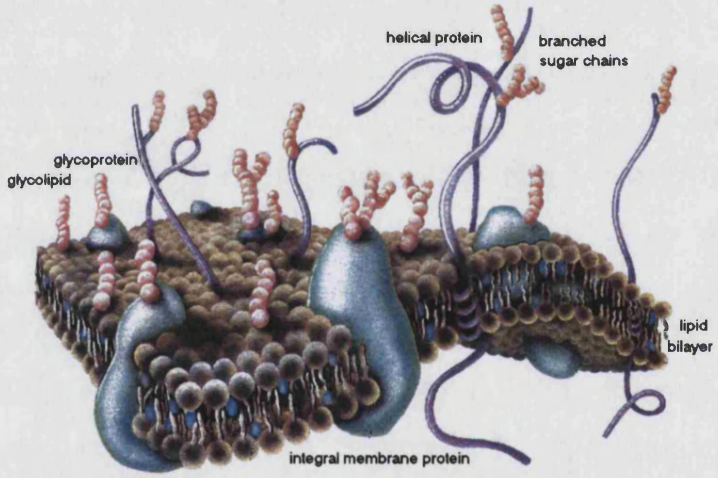

Figure 1.1 Schematic of portion of cell membrane, consisting of a basic lipid bilayer structure with imbedded proteins

Membranes vary widely in their composition and function, but they all have the same fundamental architecture of a lipid bilayer (Figure 1.1). This is due to the molecular structure of the lipids, with their amphiphilic nature that creates the hydrophilic exterior and hydrophobic interior of the bilayer. Each membrane contains a specific set of proteins that enables it to carry out its own highly specialised functions. The traditional view was of the lipids acting purely as a solvent for the proteins, but recent research has shown certain lipids form dynamic clusters to aid the movement of proteins along the axis and may even activate certain proteins (Simons 1997; Barenholz 2002).

Lipids

Nearly all lipids have a polar amphiphilic structure, consisting of a hydrophilic head-group (often charged) and hydrophobic hydrocarbon chain region (Figure 1.2). This amphiphilic structure causes the lipids to spontaneously form monolayers at the air – water and form bilayers in bulk water conditions.

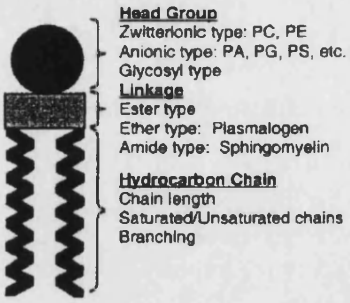

Figure 1.2 Lipids generally consist of three segments of varying types.

The head-groups, chain length and chain saturation vary greatly in nature (Lipidat database). Head-groups vary from amides to saccharides. They can be charged or exist as a zwitterion. Nearly all hydrocarbon chains found in eukaryotic cells have an even number of carbon atoms, normally 16, 18 or 20 carbons, with up to four double bonds present. There are two common types of lipids; phospholipids and glycolipids (Harrison 1975). Common phospholipids are phosphatidylcholines (PC), phosphoethanolamines (PE) and phosphoserines (PS) (Darnel 1995). Glycolipids contain saccharides in their head-groups. The main lipids and sterol used in this study are 1,2-dipalmitoyl-sn-glycero-3-phosphocholine (DPPC), 1,2-dipalmitoyl-sn-glycero-3-phosphoethanolamine (DPPE) and cholesterol (Figure 1.3). DPPC and DPPE are identical apart from the amide part of the head-group. Both consist of alkyl chains, glycero-carbonyl and functionalised phosphate head-groups.

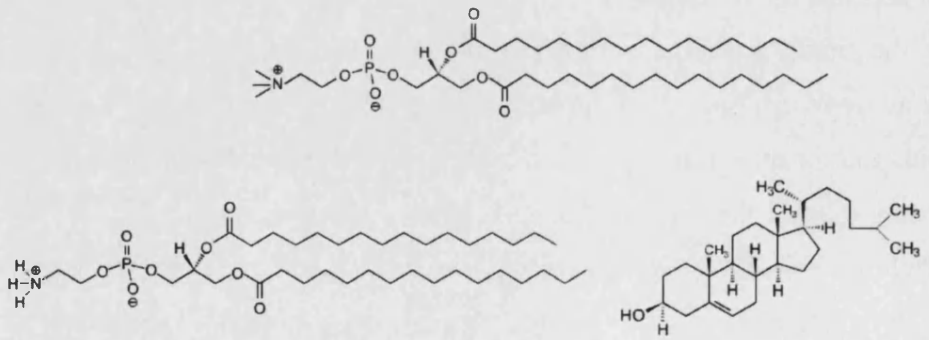

Figure 1.3 The main lipids used in this study. DPPC top, DPPE bottom left and cholesterol bottom right.

Many types of membranes have an asymmetric lipid distribution between the two leaflets. Figure 1.4 shows the asymmetric nature of three types of membranes. It can be seen that phosphatidylcholines are predominantly found in the exterior facing leaflet, whilst phosphoethanolamines are found predominantly in the interior facing leaflet. The asymmetric nature is crucial to the membrane's function.

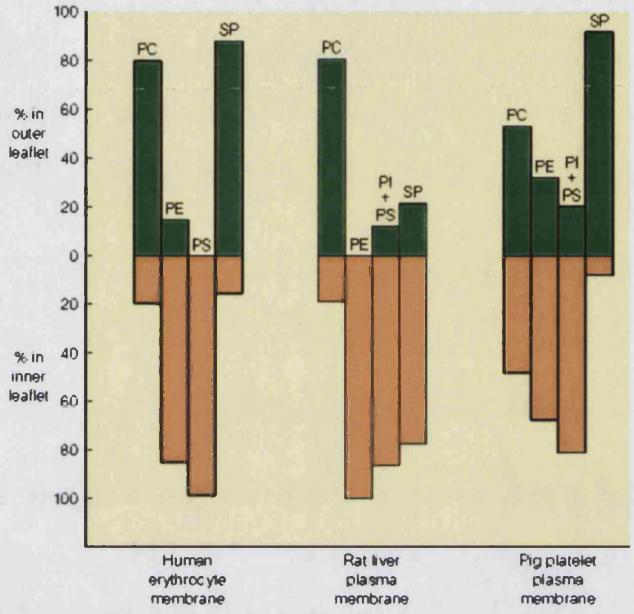

Figure 1.4 Examples of the asymmetric lipid nature of membranes. (PC phosphatidylcholines; PE phosphoethanolamines; PS phosphoserines; PI phosphoinositol; SP sphingomyelin)

1.2 Phase behaviour of lipids

1.2.1 Introduction

The phase behaviour of phospholipids has been extensively studied in vesicles (Koynova 2002, Lipidat database). Lipids generally exhibit three types of different phases. Like liquid crystals they can exhibit gel phases, transition phases and the disordered fluid phases, each with different levels of short range and long range ordering. The type of phase exhibited depends on the lipid composition and physical conditions. Lipids can form lamellar, hexagonal, cubic, and various other partially ordered phases (Koynova 2002). What follows is an overview of the lamellar gel phase, liquid crystalline phase and transition phases.

1.2.2 Gel Phases

In the gel phase (L_β) the molecules are ordered in quasi-hexagonal arrays in the plane of the bilayer, with the chains fully extended in an all-trans configuration. The gel phases of phosphatidylcholines (designated $L_{\beta'}$) are special in that the molecules are tilted with respect to the normal of the bilayer plane, due to their head-groups having an area that is greater than twice the natural packing area of the parallel chains (two per lipid). This frustration is relieved by the chain tilt (Nagle 2000).

1.2.3 Fluid Phase

The fluid phase (L_α) is the biologically relevant phase. In this phase the chains are conformationally disordered and thinner compared to the gel phase. The lipids are free to rotate around their long axis and can diffuse laterally within the membrane leaflet. Exchange of lipids between the bilayer leaflets can occur (flip – flop) but is much less frequent and is often catalysed by specific proteins.

1.2.4 Transitional Phases

Bilayers exhibit a range of transitional phases, from a simple melting of the chains (as in the case of phosphoethanolamines) to a rippling structural transition (as in the case of phosphatidylcholines).

Gel – liquid transition

The main transition that occurs for most lipid types is the first order gel – fluid transition consisting of the melting of the chains. The temperature at which this occurs depends on the type of lipid, the chain length and the composition of the bilayer. The pathway from gel to fluid does not exactly retrace the pathway from fluid to gel. This is because of a difference in the free energies of the solid and fluid domains from those formed in one direction from those formed in the other. This hysteresis is more pronounced in bilayers of charged lipids and lipid mixtures than in bilayers of neutral lipids (Datta 1987).

Ripple phase

Phosphatidylcholines with saturated chains (e.g. DPPC, DSPC) exhibit a distinct rippling phase ($P_{\beta'}$) at temperatures just below the main transition T_m (Nagle 2000). The temperature at which the rippling structure occurs is known as the pre-transition temperature. The predominant profile found in pure PC systems has an asymmetric saw-tooth cross section and a wavelength of about 12–16 nm. Small areas of macro-ripple and other types of ripple of different symmetry and wavelength also occur in pure PC dispersions (Cunningham 1998). Literature values vary though, with the wavelength varying between 100 – 160Å and the amplitude between 5 – 50Å (Zasadzinski 1988). The amplitude of the main ripple has been observed to increase with temperature until the transition to the fluid phase in some studies (Woodward 1996). The essential requirements for a ripple phase are a large head-group, high hydration and molecular tilt. The ripple phase can occur in mixed PC systems and also with low cholesterol ratios (Mortensen 1988). The formation of the ripple phase is an endothermic event and leads to a slight reduction in chain tilt (Banerjee 2002).

Many models have been proposed to explain the formation of ripples (Cunningham 1998 *and references therein*). They can be broadly grouped into two categories,

those that explain it by minimisation of Landau – Ginzburg free energy using mean field approximation (Ishibashi 1995) and others concerning molecular theories based on packing frustration between the head-group and chain regions that change in this temperature range. In the latter, interfacial energy is thought to play a crucial role in the formation, as it is governed by a delicate balance between the attractive hydrophobic interactions in the chain region and the repulsion interactions between the head-group at the interface. Increases in area per molecule by an increase in temperature and increased hydration disturb the latter. Ripples appear to compensate this packing frustration of the head-group and chains (Banerjee 2002). The formation of the ripple was previously thought to be not coupled to the main transition event, but recent studies are starting to propose a linkage (Heimburg 2000).

Anomalous Swelling

While the ripple phase has been well studied and characterised, less attention has been paid to the phenomenon observed when cooling the bilayer in the fluid phase towards the main fluid – gel transition temperature (T_m). As the temperature is decreased close to the T_m, the lamellar repeat spacing increases slightly in some types of phosphatidylcholines (such as DPPC and DMPC) and phosphatidylethanolamine bilayers (DMPE). This behaviour is known as anomalous swelling (AS), but has also been referred to as pseudo-critical or pre-critical behaviour, as it is thought to be linked to the presence of a critical point obscured by the events of the main transition (Mason 2000).

Anomalous swelling has only been observed upon cooling in the fluid phase, it has not been observed when heating in the gel phase. The swelling is non-linear with temperature (Pabst 2003). Evidence suggests that anomalous swelling is not coupled to the formation of a ripple phase (Mason 2001), whilst other studies seem to suggest it is (Richter 1999).

Anomalous swelling has been interpreted as an indication of the bilayer softening near the transition and as a thermal reduction in the bending rigidity, which allows increased fluctuations and an increase in the water layer thickness separating the bilayers (Lemmich 1997). It is still not fully understood why anomalous swelling occurs. Different groups have shown that the hydrophobic part of the bilayer partially

swells, along with the dominant swelling of the water layer (Mason 2001, Pabst 2003).

The magnitude of the swelling varies in literature; examples include a maximum increase of 1.7Å for DMPC (Pabst 2003), 2 – 3Å for DMPC (Richter 1999), 6Å for DMPC and 4Å for DPPC (Hønger 1994). The swelling of only the bilayer has been measured at 2.3Å for DMPC (Mason 2001). All of the studies cited above have been conducted on multilayer systems either in solution or stacked.

1.3 Modelling cell membranes

1.3.1 Introduction

Crystallographically it is not possible to obtain the atomic-level structure of fluid phase bilayers, due to the inherent disorder in the bilayer. A range of other systems has been developed, that are able to give information on the angstrom scale of the fluid phase structure, along with the gel and transition phase structures. Structures are usually obtained through a combination of experimental data and model interpretation.

Whilst the fluid phase is the most biologically relevant phase, the study of the overall phase behaviour is necessary to enable a greater understanding of the function of lipid bilayers and also because it is believed that certain physiologically processes may be dependent on membrane gelation (Hazel 1995). Also it has recently been suggested that the close proximity of certain membranes to the gel state structure is of principal importance for certain processes occurring in the brain, as in the physiology of thermo-regulation, and in the mechanisms of general anaesthesia (Kharakoz 2000).

1.3.2 Requirements for Membrane Mimics

The main requirement for any membrane mimic is to have a similar fluidity level to that of cell membranes. The lipids must not be impeded by external forces that restrict the freedom of movement or behaviour within the leaflet of the bilayer. It is also useful for the bilayers to be fully hydrated. Another requirement is that the composition of the system is controllable, and that components such as proteins can be easily incorporated. Another preferable ability is being able to fabricate the bilayer asymmetrically, that is having the ability to have different components in each of the leaflets of the bilayer.

For certain analytical techniques, such as in many scattering techniques, it is necessary that the bilayer is planar and supported upon a substrate. The presence of the substrate must not hinder the fluidity and freedom of the bilayer. This is essential when studying the properties and behaviour of proteins, where the fluidity of the

bilayer can affect the nature behaviour of the protein. The lack of influence of the substrate is also of a premium when studying the phase behaviour of the bilayer. What follows is a brief overview of some of the commonly used membrane mimic and a discussion of whether the systems meet the requirements.

1.3.3 Monolayers

Although it is preferable to use bilayers in membrane studies, monolayers at the air-liquid interface have proved to be a very useful mimic system (Figure 1.5a). They are perhaps the simplest form of systems used and have a high level of lipid fluidity and hydration of the head-groups. The composition of the monolayer and sub-phase is highly controllable, as is the temperature. Proteins can easily be added to the sub-phase, allowing studies of their interactions with different lipid compositions. Monolayers of biological components are easily formed by spreading the components onto an aqueous sub-phase (Chapter 2.1). Monolayers have been utilised in a vast number of studies with the use of many different analytical techniques. Recent examples include the study interaction of lipid monolayer – DNA complexes by x-ray reflectometry (Kago 1999); the study of the crystallisation of Streptavidin monolayers by Brewster Angle Microscopy (Frey 1996) and the study of the penetration of proteins into lipid monolayers (Vollhardt 2000). The disadvantage of the use of monolayers is that they do not exhibit the same phase behaviour as bilayers, also the fact that they only represent one leaflet of the bilayer.

(a) (b) (c) (d)

Figure 1.5 Common systems used to model membranes. (a) Monolayers, (b) multilamellar vesicles, (c) unilamellar vesicles, (d) stacked multilayers. *(Courtesy G. Fragneto)*

1.3.4 Vesicles

Vesicles are the most common way to study lipid behaviour and allow a diverse range of analytical techniques to be employed. There are two main types of vesicles, the spherical vesicles in solution (Figure 1.5b, 1.5c) and those that have been deposited upon substrates to form planar multilamellar vesicles (Figure 1.5d). Two types of vesicles in solution are possible; unilamellar vesicles consist only of one bilayer (Pabst 2003), whilst multilamellar vesicles consist of bilayers that are arranged like skins of an onion (Kinoshita 1996). Vesicles in solution exhibit a full range of phase behaviour and are fully hydrated and of a controllable composition (Nagle 2000). Vesicles have been used to obtain various bilayer structural attributes such as thickness, area per molecule and the number of water molecules per lipid for different lipids. This enables the study of the bilayer phase behaviour as a function of temperature (Rock 1989, Hønger 1994, Sun 1994, Petrache 1998, Richter 1999, Nagle 2000, Mason 2000, Balgavy 2001, Lee 2001, Pabst 2003). Vesicles have been greatly utilised in studies of interactions of peptides with the bilayer, as detailed in the review by White (1998). Vesicles can also be used to form bilayers on solid substrates by adsorption techniques (Puu 1997, Leonenko 2000, Johnson 2002). Although vesicles in solution are the most common method of studying bilayers, another common method is the use of stacked multilayers on solid substrates (Figure 1.5d). These oriented multilayers allow the utilisation of a range of diffraction methods and can provide information such as the chain tilt, in-plane order (Karmakar 2003) and other structural parameters similar to those obtained from vesicles in solution (Lemmich 1996, Nielsen 2000, Petrache 2000, Salditt 2002, Tristram-Nagle 2002). The number of bilayers can vary from ten bilayers (Mennicke 2002), to hundreds (Darkes 2000), to several thousand (Goormaghtigh 1999). Recent uses are the investigation of lipid diffusion by fluorescence recovery after photo-bleaching (Adalsteinsson 2000), investigation of the structure and fluctuations of bilayers with and without peptides (Salditt 2000) and the orientation of molecules within bilayers using attenuated total reflection infrared spectroscopy (Goormaghtigh 1999).

1.3.5 Supported Biomembrane mimics

Single bilayers (Tamm 1985) on solid supports provide a useful way of utilising many surface and interfacial techniques, that are not possible with vesicles, such as

AFM (Nielsen 1999), impedance analysis (Plant 1999, Terrettaz 2003), surface plasmon resonance (Cooper 1998), reflectivity (Fragneto 2000) and ellipsometry (Benes 2002). They can be used to model cell – cell interactions (Grakoui 1999, Sackmann 1996, Brian 1984) and for various biotechnological applications (Groves 1997, Boxer 2000). Single bilayers can be fabricated on a range of different substrates, varying from gold surfaces (Lahiri 2000) to printed patterned silicon (Orth 2003). The bilayers are usually fully hydrated and are of controlled composition. The main advantage that single bilayers have over multilamellar samples is that the information is bilayer specific; it is not averaged over hundreds or thousands of bilayers. Another advantage is that very small amounts of components are needed to make them, which is very useful when using expensive compounds. One of the main disadvantages though, is that forces from the substrate can often restrict the freedom of the components in the bilayer, for example it has been found to restrict the bilayer phase behaviour (Fragneto 2000). Another disadvantage is that only a very thin film of water separates the bilayer from the substrate. This can restrict the incorporation of transmembrane proteins (Wagner 2000).

There are two main ways of forming single bilayers on substrates. The most common method is by vesicle adsorption (Puu 1997, Leonenko 2000). With this method it is thought that the vesicles first adsorb to the surface, then fuse together, after which they rupture to form a uniform single bilayer (Seifert 1990, Reviakine 2000, Johnson 2002). The adsorption mechanism has been investigated by AFM (Fang 1997). The other common method used in the fabrication is that of the Langmuir – Blodgett technique (Chapter 2). With this method the substrate is drawn though the monolayer two times to deposit two monolayers onto the substrate (Tamm 1985).

The type of substrate supported single bilayers varies greatly. Examples range from a single bilayer adsorbed onto silicon (Puu 1997, Yang 2000), to elaborate polymer supported bilayers (Majewski 1998, Wagner 2000, Saccani 2003) to hybrid bilayers, where one leaflet does not consist of lipids (Krueger 2001). One type of hydrid bilayer consists of a non-lipid self-assembled monolayer as the lower leaflet and a lipid layer as the upper leaflet. This has the advantage of being very robust, but the lipids have very restricted fluidity (Hollinshead 2001). Recent single bilayer studies include investigation of the interactions of living cells with functionalised planar

bilayers (Grakoui 1999), interactions of simple peptides with bilayers (Michielin 1998, Fragneto 2000, Krueger 2001, Zhao 2003) and structural studies (Koenig 1996, Dufrene 1997, Dufrêne 2000, Perez 2003). The dynamics and heterogeneity of supported bilayers have also been probed by fluorescence spectroscopy (Krishnamoorthy 1998). Single bilayers have also been used to study the influence of an electric field on voltage-gated membrane proteins, lipid-lipid interactions, and lipid-protein interactions (Jones 1998) and in the development of novel electrochemical sensors (Knoll 2000).

1.3.5 Supported Bilayers in Biosensors

One of the great hopes with many supported bilayers is that they can be successfully utilised in biosensors. Often membrane proteins are the active component of the biosensor. For the protein to properly function their environment needs to mimic that of the living cell. The use of bilayers allows the proteins to function is a pseudo-natural environment. The ability to deposited bilayers and proteins on a variety of different substrates allows a range of analytical techniques to be utilised. One of the main difficulties with lipid biosensors is to make them robust enough to function outside the laboratory environment. One method is the use of hybrid bilayers on electrodes. In this system the layer next to the metal electrode is not lipids but an organic silane attached to the electrodes that then supports the upper lipid monolayer (Scandia group 2003). Proteins containing ion channels are then incorporated into the bilayer, which open and close repeatedly in response to specific biological agents. In the presence of agents, the ion channels change the bilayer's electrical impedance by permitting the conduction of ions through it. The type and concentration of an agent can thus be identified by measuring the electrical resistance of the bilayer.

Another approach is the use of an ion-channel switch comprising of a gold electrode to which is tethered a lipid membrane that contains gramicidin ion channels linked to antibodies (Rickert 1996, Cornell 1997 *and references therein*). The molecular composition of the tethered membrane results in an ionic reservoir being formed between the gold electrode and the membrane. The binding of agents to the antibodies alters the conductance of the ion channels, altering the composition of the

ionic reservoir. The ionic reservoir can be accessed electrically via the gold electrode, and the presence of a specific agent is detected.

A different approach to biosensors consists of the formation of self-assembled membranes supported on silver wire, which can be used to detect triazine herbicides. The interaction of the triazine and the bilayer producing an electrochemical ion current that is then easily detectable (Siontorou 1997)

Another type of bilayer biosensor is being developed to estimate the fraction of a drug absorbed in the human intestine (Danelian 2000 *and references therein*). Vesicles are attached to a sensor surface and the interactions between drugs and vesicles are monitored directly using surface plasmon resonance technology (SPR). The phenomenon of SPR is sensitive to changes in refractive index at the sensor surface caused by changes in mass. In the SPR method laser light is shone onto a glass prism in contact with a gold surface. Light is reflected at all angles except for the critical angle, at which the light excites the metal surface electrons (plasmons) generating the evanescent field and causing a dip in intensity of the reflected light. The critical angle is sensitive to refractive index changes occurring close to the sensor surface and thus, by monitoring the change in critical angle with time, details of the events at the surface can be probed. The SPR signal shows the binding of the compound to the vesicles and the release of the compound from the vesicle surfaces. The next step in this method is the use of surface modified vesicles to increase the interaction between the vesicles and the drugs, thus increasing the sensitivity of the method.

Surface plasmon resonance can also be used to monitor the adsorption of vesicles onto micro-patterned self-assembled monolayer, to create bio-mimetic membrane on a surface to study the functioning of incorporated proteins and peptides (Jenkins 2001). This method may form the basis of the next generation of biosensors.

There are many other types of optical biosensors as detailed in the review by Leatherbarrow et al. (1999).

1.4 Double Bilayer System

The double bilayer system (DBS) (Figure 1.6) consists of two bilayers deposited on silicon substrates by Langmuir-Blodgett and Langmuir-Schaefer techniques (Charitat 1999, Fragneto 2001). The lower bilayer acts purely as a support for the upper bilayer, which is used as the membrane mimic. It was originally developed to minimise the interactions between single bilayers and the substrate, which can restrict the phase behaviour and thus the biological realism of the mimic. It was also desirable to increase the water layer, allowing the study of transmembrane proteins.

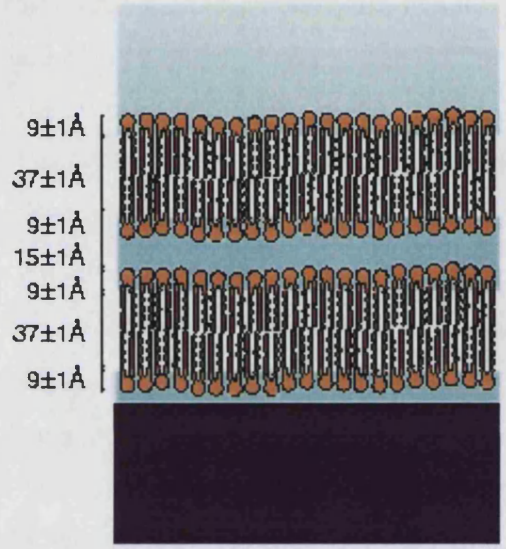

Figure 1.6 Schematic of DSPC double bilayer systems *(Courtesy G. Fragneto)*

When fabricated with the lipid DPPC, it was found that the bilayers were separated by a water layer of approximately 30Å, enabling the upper bilayer to exhibit full phase behaviour and fluctuations. Both bilayers are fully hydrated, with one side open to a semi-infinite reservoir of water and have been found to be stable for days. The composition of the bilayer is fully controllable, as is the water reservoir (Fragneto 2003). The composition of each bilayer leaflet is also fully controllable (Chapter 5). Very small amounts of lipids and proteins are needed in fabrication. Proteins can be incorporated either by co-spreading in the monolayer that is deposited or by adding to the final water reservoir and adsorbing. The information obtained from studies is bilayer specific, as it is not an average of the structure of hundreds of bilayers. A range of different surface and interfacial techniques have

been used to study the double bilayer, from reflectivity, to AFM to surface plasma resonance.

A variation on the system has also recently been developed. In this version the first leaflet of the monolayer has been replaced by a self-assembled monolayer of octadecyltrichlorosilane (Hughes 2002a). The advantage of this system is that it enables the fabrication of double bilayers of lipids with shorter chains, which have a fluid phase at biologically relevant temperatures, such as the lipid DMPC. With this lipid it is not possible to deposit four monolayers as the third layer peels off during deposition. Like the fully lipid double bilayer, this system was found to have similar phase behaviour to multilamellar vesicles (Hughes 2002b). It has recently been used to study the flipping of a simple antimicrobial peptide towards a transmembrane configuration on application of a potential (Hughes, *in preparation*).

Studies involving the double bilayer have revolved around two areas of interest; the phase behaviour of different lipid compositions and the study of in-plane features and fluctuations of the floating bilayer. Specular neutron reflectivity is used to study the phase behaviour, whilst off-specular synchrotron radiation is used to study the in-plane features (Daillant et al., *in preparation*). An overview of the neutron reflectivity work is given below.

When the phase behaviour of the initial double bilayer was investigated it was found that the water layer separating the two bilayers swelled near the main transition and was accompanied by a high increase in the roughness of the upper bilayer (Fragneto 2001). A maximum was reached before the literature value of T_m. The swelling was observed for a range of different chain lengths of phosphatidylcholines and also in selected deuterated versions (Fragneto 2003). The cause of this swelling is not fully understood, but has been interpreted in terms of competition between the inter-bilayer potential and membrane fluctuations. This allows an estimation of the bending rigidity of the bilayer (Mecke 2003). Off-specular synchrotron studies have been undertaken to aid the understanding as, unlike specular neutron reflectivity which gives information perpendicular to the bilayer plane, the technique gives detailed information on the in-plane structure.

1.5 Forces acting on the bilayers

1.5.1 Forces present in multilamellar vesicles

It is well known that adjacent bilayers in multilamellar vesicles associate with each other through attractive Van der Waals forces and repulsive undulations, with the addition of hydration forces at smaller separations (Helfrich 1977, McIntosh 1993). These forces are collectively known as Helfrich forces and they control the mean separation of the membranes. Below is given an overview of the Helfrich forces.

Van der Waals forces are the main attraction force for membrane separations greater than 15Å, if the bilayers carry no electric charge and the solvent contains no macromolecules (Lipowsky 1995). They are also thought to remain as the main attractive force even with bilayer spacings as large as 150Å (Walz 1999).

Undulations are the main source of repulsive forces present in stacked bilayers (Lipowsky 1995, Rand 1989). There are several different types of fluctuations present in bilayers with the most important being the bending mode fluctuations. With bending modes the surface area does not change, the bilayer just undulates. The level of fluctuations is connected to the temperature and the bending rigidity of the bilayer. The length scales are usually large compared to thickness of the bilayer. When a bilayer is confined between bilayers the level of fluctuations are restricted to a maximum wavelength by the external potential of these. Helfrich (1977) demonstrated that undulation repulsion can act over relatively large bilayer spacings and could account for the large swelling seen in planar bilayers.

At smaller bilayer separations hydration forces also contribute to the repulsion. Water molecules near the surface of the bilayers have molecular translational and rotational properties that are markedly different from those in dilute aqueous solution. This arises from structuring of water molecules around the bilayer surface and from the polarising of the water molecules by the hydrophilic bilayer surface (McIntosh 1993). This creates repulsive forces between the hydrated bilayers. The hydration force is found to decay approximately exponentially with increasing separation of the bilayers, giving a typical influential range of force on a few

Angstrom scale. They are only usually dominant on the short-range scale of the order of 5Å (Lipowsky 1986, 1993; McIntosh 1993).

1.5.2 Forces present in double bilayer system

The phase behaviour and structural parameters of the DBS and stacked MLV have been found to be very similar. One may therefore assume that the same forces present in the stacked MLV which maintain the bilayer separation are also the main forces present in the DBS (Hughes 2002b). In the case of the DBS though, forces from the substrate need to be considered more. The substrate forces are thought to be electrostatic from the negatively charged silicon surface. The system also differs in that the bilayers are not confined between two bilayers, and that the two bilayers are in different local environments to each other.

The influence of the substrate forces on the DBS bilayers is currently being investigated by off-specular synchrotron studies. It has been found in neutron reflectivity studies that the lower bilayer does not respond as fully to temperature as the upper bilayer (Fragneto 2001). A significantly higher temperature was needed to transform it to a fluid phase. The fact that the upper bilayer behaves similar to stacked MLV infers that it is not strongly inhibited by substrate forces, but its close proximity suggests that substrate forces are likely to have some form of bearing on the upper bilayer, but to what extent is currently unclear. In stacked MLV it has been proposed that adsorption of bilayers to a solid surface creates attractive stabilising forces throughout the multilamellar arrays (Podgornik 1997). One effect of the surface is to suppress mechanical undulations of the layers, either because of surface tension or because of the forces attaching the bilayers to the substrate, and to increase the effect of the Van der Waals forces.

1.6 References

- Adalsteinsson T, Yu H. (2000) *Lipid lateral diffusion in multi-bilayers, and in monolayers at the air/water and heptane/water interfaces* Langmuir 16, 9410 – 9413
- Balgavý P, Dubniková M, Kuerka N, Kiselev MA, Yaradaikin SP, Uhríková D. (2001) *Bilayer thickness and lipid interface area in unilamellar extruded 1,2-diacylphosphatidylcholine liposomes: a small-angle neutron scattering study* Biochim. Biophys. Acta 1512, 40 – 52
- Banerjee S. (2002) *Exploring the ripple phase of biomembranes* Physica A 308, 89 – 100
- Barenholz Y. (2002) *Cholesterol and other membrane active sterols in rafts* Prog, Lipid. Research 41, 1 – 5
- Benes M, Billy D, Hermens W T, Hof M. (2002) *Muscovite allows for the characterisation of supported bilayers by confocal fluorescence sorrelation spectroscopy* Biological Chemistry 383, 337 - 341
- Boxer S G. (2000) *Molecular transport and organization in supported lipid membranes* Curr. Opin. Chem. Biol. 4, 704 – 709.
- Brian A A, McConnel H M. (1984) *Allogenic stimulation of cytotoxic T cells by supported planar membranes* Proc. Natl. Acad. Sci. 81, 6159 – 6163.
- Charitat T, Bellet-Amalric E, Fragneto G. et al. (1999) *Adsorbed and free lipid bilayers at the solid-liquid interface* Eur. Phys. J. B. 8, 583 – 593
- Cooper M A, Try A C, Carroll J, Ellar D J, Williams D H. (1998) *Surface plasmon resonance analysis at a supported lipid monolayer* Biochem. Biophys. Acta 1373, 101 – 111
- Cornel B A, Braach-Maksvytis V L B, King L G, Osman P D J, Raguse B, Wieczorek L, Pace R J. (1997) *A biosensor that uses ion-channel switches* Nature 387, 580 – 583
- Cunningham B, Brown A D, Wolfe D H, Williams WP, Brain A. (1998) *Ripple phase PC Effect chain length, position, and unsaturation* Phys. Rev. E. 58, 3662 –3672
- Danelian T, Karlen A, Karlsson R, et al. (2000) *SPR biosensor studies of the direct interaction between 27 drugs and a liposome surface: correlation with fraction absorbed in humans* J. Medicinal Chem. 43, 2083 – 2086
- Darkes MJM, Bradshaw J. (2000) *Real-time swelling-series method improves the accuracy of lamellar neutron-diffraction data* Acta. Cryst. D, 56, 48 – 54
- Darnel (3ed 1995) *Molecular cell biology* Scientific American books, New York
- Datta (1987) *A comprehensive introduction to membrane biochemistry,* Flora Publishing, Madison.
- Dufrene Y F, Barger W R, Green J B D. et al (1997) *Nanometer-scale surface properties of mixed phospholipid monolayers and bilayers* Langmuir 13, 4779 – 4784
- Dufrêne YF, Lee G U. (2000) *Advances in the characterisation of supported lipid films with the atomic force microscope* Biochem. Biophys. Acta 1509, 14 – 41
- Fang Y, Yang J. (1997) *The growth of bilayer defects and the induction of interdigitated domains in the lipid-loss process of supported phospholipid bilayers* Biochem. Biophys. Acta 1324, 309 – 319
- Fragneto G, Graner F, Charitat T. et al. (2000) *Interaction of the third helix of antennapedia homeodomain with a deposited phospholipid bilayer: a neutron reflectivity structural study* Langmuir 16, 4581-4588
- Fragneto G, Charitat T, Graner F. et al. (2001) *A fluid floating bilayer* Europhys. Lett. 53, 100 – 106
- Fragneto G, Charitat T, Bellet-Amalric E. et al. (2003) *Swelling of phospholipid floating bilayers: the effect of chain length* Langmuir 19, 7695 – 7702
- Frey W, Schief Jr. W R, Vogel V. (1999) *Two-dimensional crystallisation of Streptavidin studied by quantitative Brewster Angle Microscopy* Langmuir 12, 1312 – 1320
- Grakoui A, Bromley S K, Sumen C. et al. (1999) *Immunological Synapse: molecular machine controlling T cell activation* Science 285, 221 – 227

- Groves J T, Boxer S G. (1995) *Electric-field-induced concentration gradients in planar supported bilayers* Biophys. J. 69, 1972 – 1975
- Harrison (1975) *Biological Membranes.* John Wiley and Sons Inc, New York.
- Hazel J R. (1995) *Thermal adaptation in biological membranes – is homoviscous adaptation the explanation* Annu. Rev. Physiol. 57, 19 – 42
- Helfrich W. (1977) *Steric interaction of fluid membranes in multilayer systems* Z. Naturforsch 33a, 305 – 315
- Heimburg T. (2000) *A model for the lipid pretransition: coupling of ripple formation with the chain-melting transition* Biophys. J. 78, 1154 – 1165
- Hollinshead C M, Hanna M, Barlow D J. et al. (2001) *Neutron reflection from a DMPC monolayer adsorbed on a hydrophobised silicon support* Biochem. Biophys. Acta 1511, 49 – 59
- Hønger T, Mortensen K, Ipsen J H. et al. (1994) *AS of multilamellar lipid bilayers in the transition region by renormalisation of curvature elasticity* Phys. Rev. Lett. 72, 3911 – 3914
- Hughes A V, Goldar A, Gerstenberg M C. et al. (2002a) *Hybrid SAM phospholipid approach to fabricating free supported lipid bilayer* PCCP 4, 2371 –2378
- Hughes A V, Roser S J, Gerstenberg M C. et al. (2002b) *Phase behaviour of DMPC free supported bilayers studied by neutron reflectivity* Langmuir 18, 8161 – 8171
- Hughes AV et al., (2004) *in preparation*
- Ishibashi Y, Iwata M. (1995) *A phase diagram inc. ripple phase of Phos. bi.* J. Phys. Soc. Japan 64, 155 - 158
- Jenkins A T A, Neumann T, Offenhäusser A. (2001) *Surface plasmon microscopy measurements of lipid vesicle adsorption on a micropatterned self-assembled monolayer* Langmuir 17, 265 – 267
- Johnson J M, Ha T, Chu S. et al. (2002) *Early steps of supported bilayer formation probed by single vesicle fluorescence assays* Biophys. J. 83, 3371 – 3379
- Jones S W. (1998) *Overview of Voltage-Dependent Calcium Channels* J. Bioenergetics and Biomembranes 30, 299 – 312
- Kago K, Matsuoka H, Yoshitome R. et al. (1999) *Direct in-situ observation of a lipid monolayer – DNA complex at the air-water interface by x-ray reflectometry* Langmuir 15, 5193 – 5196
- Karmakar S, Raghunathan V A. (2003) *Chol. Induced Modulated Phase in Phospholipid Membranes* Phys. R. Lett. 91, 9, 098102-1
- Kharakoz D P. (2000) *Phase transition in lipids and the problem of homoiothermaia* Biofizika 45, 569 – 572
- Kinoshita K, Yamazaki M. (1996) *Organic solvents induce interdigitated gel structures in multilamellar vesicles of DPPC* Biochem. Biophys. Acta 1284, 233 - 239
- Knol W. (2000) *Functional tethered lipid bilayers* Rev. Molecular Biotech. 74, 137
- Koenig B W, Krueger S, Orts W J. et al. (1996) *Neutron reflectivity and atomic force microscopy studies of a lipid bilayer in water adsorbed to the surface of a silicon single crystal* Langmuir 12, 1343 – 1350
- Krishnamoorthy IG. (1998) *Probing the dynamics of planar supported membranes by nile red fluorescence lifetime distribution* Biochim. Biophys. Acta 1414, 255 – 259
- Krueger S, Meuse C W, Majkrzak C F. et al.(2001) *Investigation of hybrid bilayer membranes with neutron reflectometry: Probing the interactions of Melittin* Langmuir 17, 511 – 521
- Koynova R, Caffrey M. (2002) *An index of lipid phase diagrams.* Chem. and Physics of Lipids 115 (2002) 107–219
- Lahiri J, Kalal P, Frutos A G. et al. (2000) *Method for Fabricating Supported Bilayer Lipid Membranes on Gold.* Langmuir 16, 7805 - 7810

- Leatherbarrow R J, Edwards P R. (1999) *Analysis of molecular recognition using optical biosensors* Curr. Opn. Chem.Biology, 3 544 – 547
- Lee C H, Lin W C, Wang J. (2001) *All-optical measurements of the bending rigidity of lipid-vesicle membranes across structural phase transitions* Phys. Rev. E. 64, 020901
- Leonenko Z V, Carnini A, Cramb D T. (2000) *Supported bi formation by vesicle fusion.* Biochem. Biophys. Acta 1509, 131 - 147
- Lemmich J, Mortensen K, Ipsen J H. et al. (1996) *Small-angle neutron scattering from multilamellar lipid bilayers: Theory, model, and experiment* Phys. Rev. E. 53, 5169 –5180
- Lemmich J, Mortensen K, Ipsen J H. et al. (1997) *The effect of cholesterol in small amounts on lipid-bilayer softness in the region of the main phase transition* Eur. Biophys. 25, 293 – 304
- Lipidat database – www.lipidat.chemistry.ohio-state.edu/
- Lipowsky R, Leibler S. (1986) *Unbinding transitions of interacting membranes.* Phys. Rev. Lett. 56, 2541
- Lipowsky (1995) Handbook of Biological Physics: Structure and Dynamics of Membranes Vol. 1B. Elsevier.
- McIntosh T, Simon S A. (1993) *Contrib. Hydr. Steric Press. to interactions between PC bilayers* Biochemistry 32, 8374 - 8384
- Majewski J, Wong J Y, Park C K. et al. (1998) *Structural studies of polymer cushioned lipid bilayers* Biophys. J. 75, 2363 – 2367
- Mason P C, Gaulin B D, Epand R M. et al. (2000) *Critical swelling in single phospholipid bilayers* Phys. Rev. E. 61, 5634 – 5639
- Mason P C, Nagle J F, Epand R M. et al. (2001) *Anomalous swelling in phospholipid bilayers is not coupled to the formation of a ripple phase* Phys. Rev. E. 63, 030902
- Mecke K R, Charitat T, Graner F. (2003) *Fluctuating lipid bilayer in an arbitrary potential: theory and experimental determination of bending rigidity* Langmuir 19, 2080 – 2087
- Mennicke U, Salditt T. (2002) *Preparation of solid supported lipid bilayers by spin coating* Langmuir 18, 8172 – 8177
- Michielin O, Ramsden J J, Vergeres G. (1998) *Unmyristoylated MARCKS-related protein (MRP) binds to supported planar phosphatidylcholine membranes* Biochem. Biophys. Acta 1375, 110 – 116
- Mortensen K, Pfeiffer W, Sackmann E. et al. (1988 *Structural properties of a phosphatidylcholine-cholesterol system as studied by small-angle neutron scattering: ripple structure and phase diagram* Biochem. Biophys. Acta 945, 221 – 245
- Nagle J F, Tristram-Nagle S. (2000) *Structure of lipid bilayers* Biochim. Biophys. Acta 1469 159 – 195
- Nielsen L K, Risbo J, Callisen T H. et al. (1999) *Lag-burst kinetics in phospholipase A2 hydrolysis of DPPC bilayers visualised by atomic force microscopy* Biochem. Biophys. Acta 1420, 266 – 271
- Nielsen L K, Bjornholm T, Mouritsen O G. (2000) *Fluctuations caught in the act* Nature 404, 352
- Orth R N, Kameoka J, Zipfel W R. et al. (2003) *Creating biological membranes on the micron scale: forming patterned lipid bilayers using a polymer lift-off technique* Biophys. J. 85, 3066 – 3073
- Pabst G, Katsaras J, Raghunathan V A. et al. (2003) *Structure and interactions in the AS regime of phospholipid bilayers* Langmuir 19, 1716 – 1722
- Perez U A, Faucher K M, Majkrzah C F. et al. (2003) *Characterisation of a biomimetic polymeric lipid bilayer by phase sensitive neutron reflectometry* Langmuir 19, 7688 – 7694
- Petrache H I, Gouliaev N, Tristam-Nagle S. et al. (1998) *Interbilayer interactions from high-resolution x-ray scattering* Phys. Rev. E. 57, 7014 – 7024
- Petrache H I, Dodd SW, Brown M F. (2000) *Area per lipid and acyl length distributions in fluid phosphatidylcholines determined by ^2H NMR spectroscopy* Biophys. J. 79, 3172 – 3192

- Podgornik R, Parsegian V A. (1997) *On a possible microscopic mechanism underlying the vapour pressure paradox* Biophys. J. 72, 942 – 952
- Puu G. Gustafson I. (1997) *Planar lipid bilayers on solid supports from liposomes – factors of importance for kinetics and stability* Biochem. Biophys. Acta 1327, 149 – 161
- Rand R P, Parsegian V A. (1989) *Hydration forces between phospholipid bilayers* Biochem. Biophys. Acta 988, 351 – 376
- Reviakine I, Brisson A. (2000) *Formation of supported phospholipid bilayers from unilamellar vesicles investigated by atomic force microscopy* Langmuir 16, 1806 – 1815
- Richter F, Finegold L, Rapp G. (1999) *Sterols sense swelling in lipid bilayers* Phys. Rev. E. 59, 3483 – 3491
- Rickert J, Weiss T, Kraas W. et al. (1996) *A new affinity biosensor: self-assembled thiols as selective monolayer coatings of quartz crystal microbalances* Biosens. Bioelectron. 11, 591 – 598
- Rock P, Thompson T E, Tillack T W. (1989) *Persistence at low temperature of the P' ripple in dipalmitoyl-phosphatidylcholine multilamellar vesicles containing either glycosphingolipids or cholesterol* Biochem. Biophys. Acta 979, 347 – 351
- Saccani J, Castano S, Desbat B. et al. (2003) *A phospholipid bilayer supported under a polymerised Langmuir film* Biophys. J. 85, 3781 – 3787
- Sackmann E. (1996) *Supported membranes: scientific and practical applications* Science 271, 43 – 48.
- Salditt T. (2000) *Strut. Fluc. of highly oriented phospholipid membranes.* Curr. Opin. Coll. Intf. Sci. 5 19-26
- Salditt T, Li C, Spaar A. et al. (2002) *X-ray reflectivity of solid-supported, multilamellar membranes* Eur. Phys. J. E. 7, 105 – 116
- Scandia group (2003) SENSORS Magazine - Advanstar Communications Inc. Peterborough, USA May 2003
- Seifert U, Lipowsky R. (1990) *Adhesion of Vesicles* Phys. Rev. A. 42, 4768 – 4771.
- Simons K, Ikonen E (1997) *Functional rafts in cell membranes* Nature 387, 569-572
- Siontorou S G, Nikolelis D P, Krull U J. et al. (1997) *A triazine herbicide minisensor based on surface-stabilized bilayer lipid membranes* Anal. Chem. 69, 3109 – 3114
- Sun W J, Suter M A, Worthington C R. et al. (1994) *Order and disorder in fully hydrated unorientated bilayers of gel phase DPPC* Phys. Rev. E. 49, 4665 – 4676
- Tamm L K, McConnell H M. (1985) *Supported phospholipid bilayers* Biophys. J. 47, 105 – 113
- Terrettaz S, Mayer M, Vogel H. (2003) *Highly electrically insulating tethered lipid bilayers for probing the function of ion channel proteins* Langmuir 19, 5567 – 5569
- Tristram-Nagle S, Liu Y, Legleiter. et al. (2002) *Structure of gel phase DMPC determined by x-ray diffraction* Biophys. J. 83, 3324 – 3335
- Vollhardt D, Fainerman V B. (2000) *Penetration of dissolved amphiphiles into two-dimensional aggregating lipid monolayers* Adv. Coll. Inf. Sci., 86, 103 – 151
- Wagner M L, Tamm L K. (2000) *Tethered polymer-supported planar lipid bilayers for reconstitution of integral membrane proteins: silane-polyethyleneglycol-lipid as a cushion and covalent linker* Biophys. J. 79, 1400 – 1414
- Walz J Y, Ruckenstein E. (1999) *Comparison of Van der Waals and Undulation interactions between uncharged lipid bilayers* J. Phys. Chem. B. 130, 7461 – 7468
- White S H, Wimley W C. (1998) *Hydrophobic interactions of peptides with membrane interfaces* Biochem. Biophys. Acta 1376, 339 – 352
- Woodward J T, Zasadzinski J A. (1996) *Amplitude, wave form, and temperature dependence of bilayer ripples in the Pbeta' phase* Phys. Rev. E. 53, R3044

- Yang J, Appleyard J. (2000) *The main phase transition of mica-supported phosphatidylcholine membranes* J. Phys. Chem. B. 104, 8097 – 8100
- Zasadzinski J, Schneir J, Gurley J. et al. (1988) *Scanning tunnelling microscopy of freeze-fracture replicas of biomembranes* Science 239, 1013 – 1015
- Zhao J, Tamm L K. (2003) *FTIR and fluorescence studies of interactions of synaptic fusion proteins in polymer-supported bilayers* Langmuir 19, 1838 – 1846

2. Fabrication, Techniques and Characterisation Methods

2.1 Langmuir Monolayers and Langmuir-Blodgett Films

2.1.1 Introduction

Monolayers enable the study and exploitation of the physical behaviour and interactions of nanometer thick films by a range of different surface and interfacial techniques. A Langmuir monolayer (Roberts 1990, Petty 1996) consists of a single layer of insoluble amphiphilic molecules spread on an aqueous sub-phase. They are formed by spreading the amphiphilic molecules in a volatile solvent (typically chloroform) on an aqueous sub-phase. The solvent evaporates, leaving the hydrophilic head-groups immersed in the water and the hydrophobic tail orientated away.

Phase behaviour of the monolayers can be determined by the change in surface pressure versus area per molecule at constant temperature to form an isotherm (Figure 2.1). Surface pressure (Π) is defined as the difference between the surface tension in the absence of a monolayer (γ_o) and the value with a monolayer present (γ)

$$\Pi = \gamma_o - \gamma \tag{2.1}$$

Surface tension (γ) is defined by the partial differential of the excess free energy (G) and the surface area (s), at constant temperature (T), pressure (P) and composition (n_i)

$$\gamma = \left(\frac{\partial G}{\partial s}\right)_{T,P,n_i} \tag{2.2}$$

The surface tension of water (73 mN/m at 20°C and atmospheric pressure) has an exceptionally high value compared to other liquids. When compressed, monolayers usually lower the surface tension by modifying the hydrogen bonds of the water at the surface and increasing the repulsive effect between the hydrocarbon chains. This leads to an increase in the surface pressure. Monolayers exhibit a range of different two-dimensional phase behaviour when the area per molecule is reduced. The rich phase diagram consists of two-dimensional analogs to gas, liquid (L1) and crystalline (CS) phases as well as a variety of tilted mesophases (hexatic) similar to smetic crystals

(Schwartz 1993, Rivière-Cantin 1996). The appearance of these phases is dependent on the compound or compounds, the temperature and pH. In the crystalline phase the molecules are closely packed (Petty 1996). Domain formation can also occur in the gaseous phase. Some molecules such as phosphatidylcholine lipids can exhibit co-existence of liquid and crystalline phases. Figure 2.1 shows the isotherm of DPPC measured at room temperature at neutral pH. Brewster angle microscopy images at three different surface pressures are shown. At low and high pressure the monolayer is homogeneous, whilst at the constant pressure plateau between an area per molecule range of 65 – 47Å^{-2} a coexistence region of crystalline and liquid phases occurs. This is observed in the Brewster angle microscopy as a series of dotted domains.

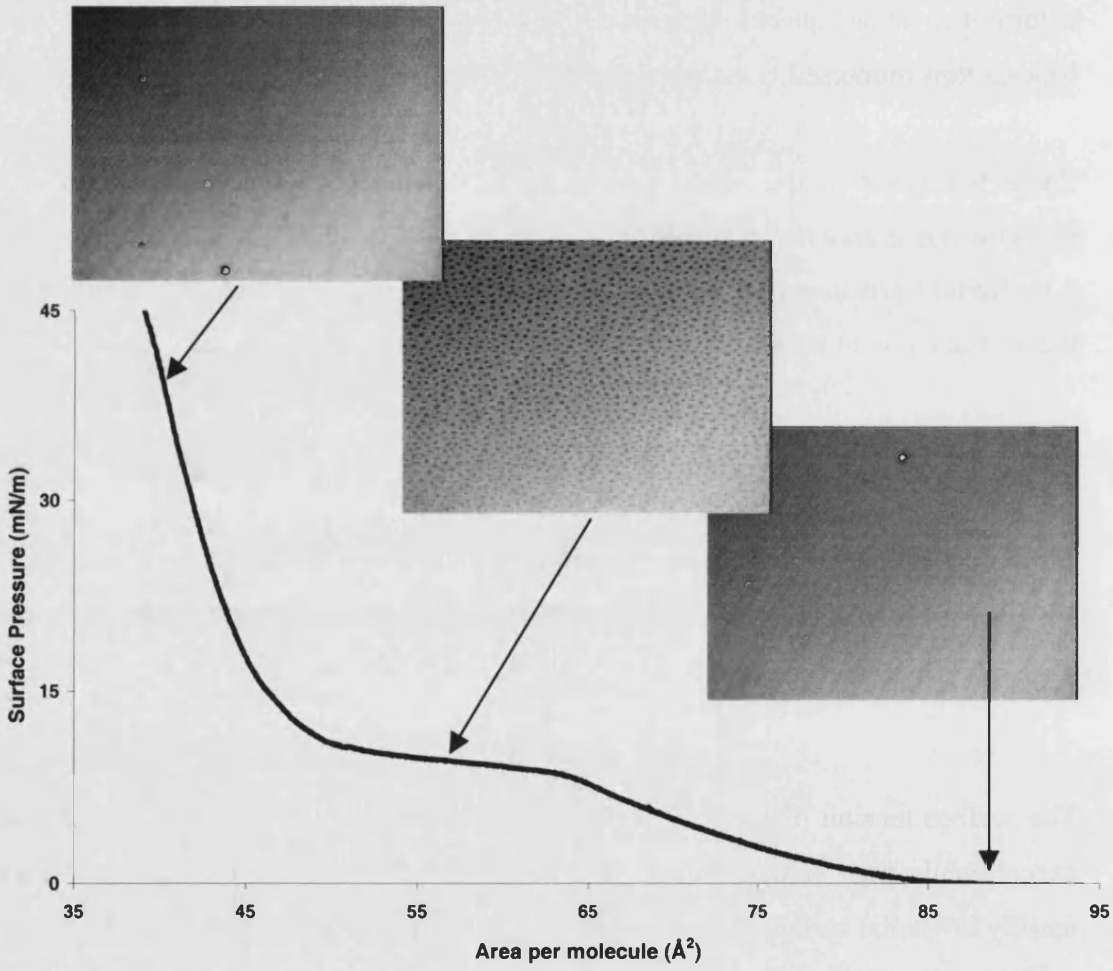

Figure 2.1 Isotherm of DPPC lipid measured at measured at room temperature at neutral pH. BAM images show the different phases present. The middle image is of coexistence of liquid and crystalline phases.

Isotherms of a particular compound can have many different shapes dependent on factors such as the sub-phase used, ion content of sub-phase and temperature variations. Contamination of the monolayer is usually visible in its isotherm, usually taking on the form of additional bumps.

2.1.2 History

Langmuir monolayers have a varied and colourful history. Early research ranges from Benjamin Franklin's observations of the spreading of oil on a pond in Clapham Common in London, to the pioneering research by Agnes Pockles in the late 19th century. Agnes Pockles's method, conducted in her kitchen with cooking trays later became the basis of the Langmuir trough. The 20th century saw huge increase in monolayer work mainly due to the immense work of the Noble Prize winner Irvine Langmuir and by Katherine Blodgett. Langmuir, amongst many other things, developed the surface film balance, while Blodgett conducted pioneering work on the deposition of monolayers onto solid substrates.

2.1.3 Langmuir – Blodgett films

The Langmuir – Blodgett technique enables the deposition of organic films of nanometer thickness on to a range of different substrates. The monolayers are deposited by drawing the substrate slowly through the monolayer at a constant surface pressure. The technique enables the molecular engineering of samples, making it possible to position certain molecular groups at precise distances to others. Thin films can be built up at the molecular level and the interaction between this artificial structure and real cells can be studied (Petty 1996). Depositions can be performed vertically (Langmuir-Blodgett technique) and horizontally (Langmuir-Schaefer technique). Horizontal depositions are the most common due to their simplicity, whilst vertical depositions are usually used when horizontal depositions are not viable. The success of a deposition and the number of layers that can be deposited are heavily dependent on the attributes of the compound, the properties of the sub-phase and the type of substrate used (Roberts 1990). Cleanliness of apparatus and all the components are also a major factor on the success of a deposition. The quality of the deposition can be followed by calculating the transfer ratio, which is simply the area of monolayer deposited, divided by the surface area of block dipped.

2.1.4 Monolayer and Langmuir-Blodgett film studies

Many varied techniques have been used to study the properties and behaviour of monolayers. Grazing incident scattering is able to give information on the conformation of the molecules and the dynamics of monolayer formation (Carino 2001), whilst techniques such as Brewster angle microscopy allow the morphological changes of monolayers caused by area compression to be easily visualised. Domain formation can easily be observed without the addition of fluorescent components as needed in fluorescence microscopy (Ramos 1999, Lawie 2000). X-ray and neutron reflectivity enables full characterisation of the structure both in-plane and out of plane (Daillant 1990). AFM has been used to study the topology when the monolayers are deposited on substrates (Ekelund 1999).

Monolayers and Langmuir-Blodgett films have been used in many studies involving lipid and proteins (Gershfeld 1979, McConlogue 1997, Krueger 2001, Schalke 2000, Brezesinski 2003, Bolze 2002). The interaction of proteins and ions injected into the sub-phase and the monolayer can be easily followed using isotherms and Brewster angle microscopy (Flach 2000, Wu 2001). The Langmuir-Blodgett technique can be used to fabricate model bilayers, which allows a greater range of surface and interfacial techniques to be utilised, which are not possible when bilayers are in solution. Langmuir-Blodgett films of polymerised components can be formed either by directly depositing polymerised films (Mumby 1986, Brinkhuis 1991, Teerenstra 1992) or by depositing monomers, which are then polymerised by an appropriate method (Hatada 1977, Fukuda 1981, Miyashita 1991). The use of polymerisation films increases the thermal, mechanical and chemical stability of organic films thus increasing their suitability for use in practical devices (Tieke 1979, Swalen 1987, Miyashita 1993).

The properties of alkylsilanes have been studied by use of monolayers and Langmuir-Blodgett films. Alkylsilanes are used as components in hybrid materials (Wen 1996, Judeinstein 1996) and to modify surface properties (Finnie 2000, Zheng 2000). Langmuir monolayers have been used in this field to study the dynamics of the formation and possible cross-linking (Sagiv 1980) of polymerisation of alkylsilanes

monolayers at the air/water interface by grazing incident x-ray diffraction (Carino 2001). Miscibility and non-ideality of mixed films can be readily studied by use of Langmuir techniques (Motomura 1986, Matsuki 1990, Ikeda 1994, Iyota 1998).

2.2 Fabrication of Double Bilayers

2.2.1 Introduction

Once fabricated, double bilayers have been found to be stable and robust with respect to the temperature and type of lipids. The difficult part however is the fabrication. The depositions are very sensitive to any contamination and irregularities in the method. During this thesis the method was optimised to a stage where three out of four attempts would succeed. What follows here is a detailed explanation of the method, with all its intricacies. The materials used will also be given.

2.2.2 Overview

As mentioned in Chapter 1, fabrication of the double bilayer consists of three vertical monolayer depositions (Langmuir – Blodgett) followed by a horizontal deposition (Langmuir – Schaefer). The samples can be made from a range of different monolayer types including asymmetric leaflet bilayers (Chapter 6).

First the silicon substrate and the Langmuir trough are thoroughly cleaned and then the monolayer is spread. The first deposition involves drawing the substrate up through the monolayer; the second deposition involves lowering it through and the third drawing it up once again. This ensures that all the monolayers are orientated in the correct way. Single bilayer samples were fabricated by one vertical and one horizontal deposition (Charitat 1999). Peptides and proteins can be incorporated either by co-spreading in the monolayer or by adding to the reservoir and adsorbing.

2.2.3 Factors necessary for successful fabrication

One of the main factors needed for a successful fabrication is the cleanliness and purity of all components, from the trough, to the lipids, water and silicon substrates. The other main factors are patience, good laboratory skills and time.

2.3 Materials and Equipment

2.3.1 Materials

All the lipids used in this experiment were purchased either from Sigma – Aldrich chemicals, (St. Quentin Fallavier, France) or Avanti Polar Lipids (Alabama, USA). Cholesterol was purchased from Sigma Chemicals. All were used without further purification.

The solvents used in cleaning and in solutions were of analytical grade (99.8+ % purity). Deuterium oxide (99%) was supplied by the Institut Laue-Langevin. All were used without further purification. Ultra-pure water used was of Millipore grade (resistivity 18MΩ cm).

Silicon substrates (8cm x 5cm x 2cm) were highly polished on one side to an average root-mean-squared of 3±3Å by the ESRF optics laboratory (Grenoble, France). Angstrom roughness is highly important for deposition reasons and to enable reflectivity measurements. The other sides of the substrates are not polished for economic reasons. All substrates are thoroughly cleaned before use.

2.3.2 Equipment

The samples were prepared using a custom built Langmuir trough (Nima, Coventry, England) with a large dipping well and monolayer surface area of 20x30cm (Figure 2.2 *left*). Vertical depositions were performed using the computer controlled Nima dipper. A novel manual dipper was developed for the horizontal Schaefer deposition to improve its quality and reproducibility (Figure 2.2. *Right*). It consists of micro-controlled adjuster mounted on a sturdy support. The silicon substrate mounts on to the arm via the level adjuster. The level adjuster allows the horizontal level of the substrate to be adjusted.

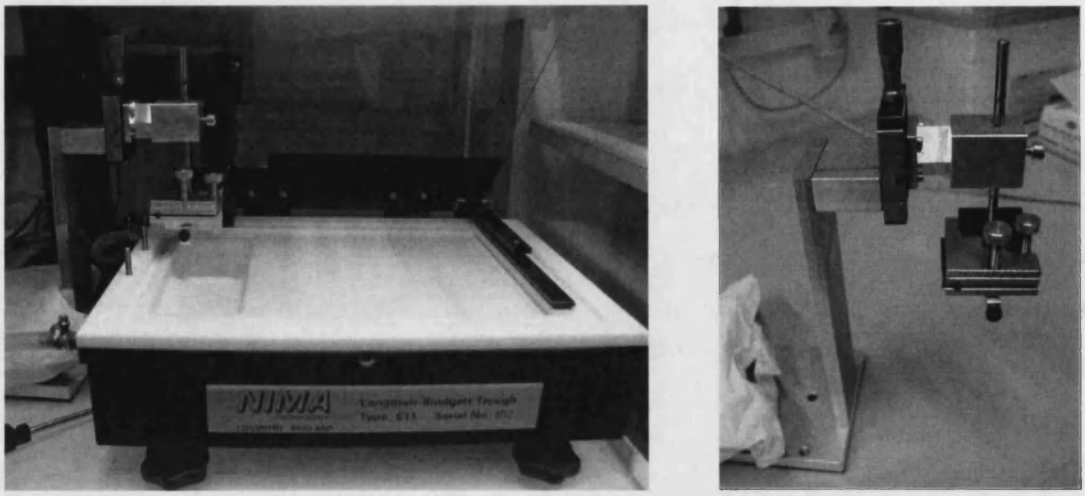

Figure 2.2 *Left.* Langmuir trough with dipper positioned. *Right.* Custom built Schaefer dipper.

2.3.3 Solutions

All solutions were made by dissolving the lipids in chloroform to a 1mg/1mL concentration (which approximates to 10^{-3}M). Phosphatidylcholines, both hydrogenated and deuterated dissolved readily in chloroform, whilst hydrogenated phosphatidylethanolamine needed mild heating. It was not found possible to dissolve deuterated phosphatidylethanolamine, despite heating and adding small amounts of methanol to the chloroform. Phosphatidylserines were found to dissolve when very small amounts of methanol were added. Solutions of DPPC and cholesterol were made to molar ratios.

2.3.4 Trough housing

As with all monolayer work, the trough should be protected from dust by housing in either a lamellar flow cabinet or enclosed in a Perspex box. In general it was found that the lipids deposited better if the temperature around the trough was below 20°C. This may be linked to the low transition temperatures of lipids like DPPC (37.7°C).

2.4 Deposition Procedure

2.4.1 Silicon Substrates

Thorough cleaning of the silicon substrates is essential before deposition. Due to the high degree of polishing it is necessary to use passive techniques for cleaning the silicon surface. The method used here was solvent cleaning in an ultrasound bath. The silicon was cleaned in the ultrasound in chloroform, ethanol, and ultra pure water for 25 minutes per solvent. It is essential that gloves be used when handling the silicon, with care taken to never touch the polished side. Hand grease is very difficult to remove by solvent cleaning. Prior to deposition the surface silicon was treated with the UV/ozone method (Vig 1985). This involves exposing the substrate to UV under a constant flow of oxygen for 30 minutes to form hydrogen oxide groups at the surface to ensure a highly hydrophilic surface. The silicon was then lowered into the water sub-phase so that the required dipper area was submerged. It is not necessary to dip the whole substrate as footprint of beam is smaller than size of substrate.

2.4.2 Monolayers

Solutions of the lipids were spread on the water usually to a surface pressure of approximately 10mN/m. This ensures that there is enough monolayer area for three depositions. The monolayer was left for 20 minutes to allow the solvent to evaporate. After which it was then compressed slowly at 30cm²/minute until a surface pressure of 40mN/m was obtained. The surface pressure was then held at this value using the automated pressure control.

2.4.3 Depositions

Depositions were performed at a constant surface pressure of 40mN/m using a dipper speed of 5mm/min. Decreasing the deposition speed below 5mm/min was not found to increase the transfer ratio, whilst increasing above this speed reduced the transfer ratio. Depositions consisted of three vertical depositions followed by the horizontal Schaefer deposition (Figure 2.3). Single bilayers are fabricated by one vertical and one horizontal deposition. The same procedure as for the double bilayer is used. The depositions were monitored by calculation of transfer ratios, which is the ratio of the area of monolayer deposited to the surface area of substrate dipped.

2.4.4 First deposition

The substrate is drawn up through the monolayer until it is fully out of the water. The first deposition is usually the most robust. Occasionally optical fringes are observed due to the draining of the thin layer of water between the silicon and the first deposited layer. The transfer ratio is normally unity regardless of the type of lipid used.

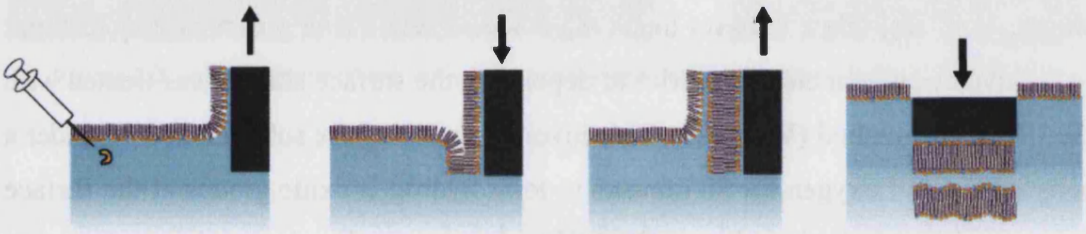

Figure 2.3 Schematic of first, second and third vertical depositions and final Schaefer deposition.

2.4.5 Second deposition

Best results are obtained with a wait of 20 minutes between the first and second deposition. This allows the monolayer to equilibrate after the first deposition. When the substrate is lowered back towards the monolayer it is preferable to touch the monolayer at the slowest possible speed (1mm/min), then stop and wait 2 minutes before starting the deposition at speed of 5mm/min. This allows the monolayer to settle after the impact. The second deposition is usually the most temperamental. Unlike the passive like coating style of the first and third depositions with their raised meniscuses, this deposition has a downward meniscus leading to the monolayer being compressed onto the first monolayer. It is therefore more sensitive.

Irrespective of the type of lipid used the transfer ratios of the second deposition were always found to be around 0.3 – 0.4. However, when fitting the lower bilayer generally needed a coverage of between 0.9 - 1. The low transfer ratio can be explained when considering the ratio of polished surface to unpolished of the substrate as only one face of the silicon is polished. This gives a ratio of 30% polished area to unpolished area. It is likely that deposition is only occurring on the polished

side. It is likely the transfer ratios of above 30% are caused by deposition onto the rough sides.

2.4.6 Third deposition

It is best to allow a wait of at least 10 minutes before commencing the third deposition. Like the first deposition this dip involves drawing the substrate through and out of the monolayer. This deposition is usually an indicator of whether the previous two depositions are of good enough quality for reflectivity measurements. If they are of sufficient quality then the third deposition will give a transfer ratio of between 0.95 – 1 and good optical interference fringes. Interference fringes usually extend some distance above the meniscus, indicating that a substantial layer of water is being transferred along with the monolayer. This water layer thins with time to give the approximately 30Å thin layer in the final product. Fringes are one of the best indications of the quality of the film. They are able to show where the monolayer is depositing and whether there is dirt contamination in the deposited film.

2.4.7 Schaefer deposition

The Schaefer deposition is one of the hardest and crucial steps in the fabrication. A bad Schaefer deposition can remove significant amounts of previous depositions leading to lower bilayer coverage. Two factors were found vital for successful deposition, namely the level of horizontality and the use of the slowest speed possible (20 microns/second). This was not found to be possible with the standard computer controlled dipper, so a novel manual dipper was developed in-house with a rigid arm and micron height adjuster (Figure 2.2). It also had a horizontal level adjuster.

First the monolayer of the previous deposition was removed to allow the Teflon well part of the neutron cell (Figure 2.4) to be placed in the well of the trough. A new monolayer was then spread and compressed to 40mN/m. The substrate was mounted on the horizontal dipper and levelled initially with a spirit level. It was then lowered until it was within millimetres of the monolayer, whereupon the level was checked again using the spirit level. The substrate was then lowered closer. As the substrate approaches the monolayer its reflection in the water is used to align the level. With the manual dipper the substrate can be brought within microns of the monolayer and

still be adjusted. Only when the level is excellent the deposition should commence. The substrate is lowered at the very slow speed of approximately 2 microns per 10 seconds or less. When the substrate makes contact with the monolayer the surface pressure and area very slightly increases, remaining constant afterwards. The pressure and area increases are thought to be caused by removal of parts of the previous depositions, although this is not proven. Using the increase in values the transfer ratios can be calculated. With the area rise, it is simply the area increase divided by the surface area dipped. Although the transfer ratio can be calculated from the pressure rise, from experience a pressure rise below 3mN/m for the 8 x 5 x 2 substrates usually gives an excellent film. Between 5 – 10mN/m gives a good quality, whilst any value above 10mN/m gives a bad coverage film. The magnitude of the area increase is usually similar to the magnitude of the pressure increase. The quality of the Schaefer deposition does seem to be linked to the type of lipid as well, as phosphatidylethanolamines always gave lower pressure rises than phosphatidylcholines.

After the Schaefer deposition the substrate should remain at the height it touched the water for at least 2 minutes. It should then be lowered slowly until it makes contact with the Teflon reservoir well. The monolayer and water should then be removed completely. The surface tension of the water seals the substrate and well together. The sample is then transferred very carefully into the neutron cell (Figure 2.4). The neutron cell consists of the substrate and well sandwiched in between two aluminium heating plates. Care should be taken when using substrates of 1cm depth, as they are prone to cracking at the edges. The sample is then transferred to the reflectometer.

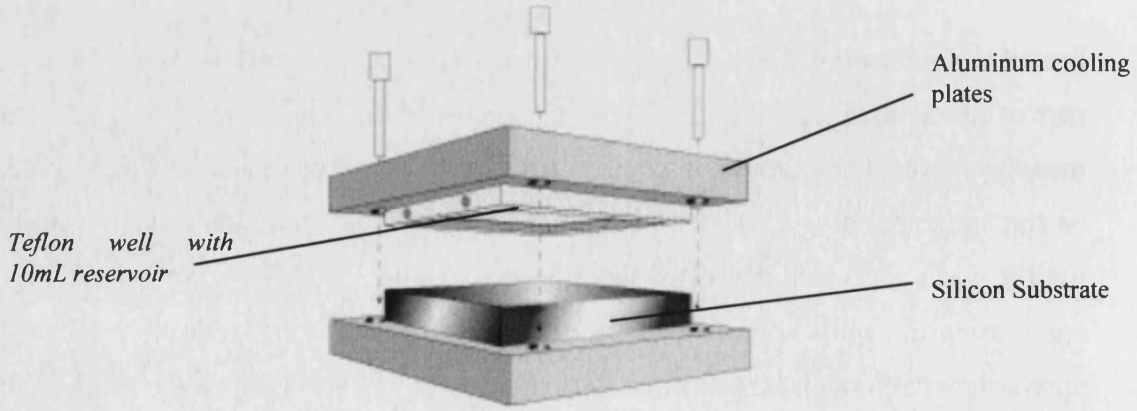

Figure 2.4 Neutron cell. *(Courtesy G. Fragneto)*

2.5 Principles of Neutron Reflectivity

2.5.1 Introduction

Neutron reflectivity is a non-destructive technique for studying structures and interfaces. Specular reflectivity provides composition and structural attributes perpendicular to plane to near angstrom precision. It can be used to measure the thickness of multiple layers within the sample and their roughness, composition and coverage. Reflectivity can be used to study air – solid, liquid – solid, air – liquid, liquid – liquid and solid – solid interfaces. It is possible to study a wide variety of different materials, from magnetic multilayers to biological systems at the solid – liquid interface. Examples include the kinetic adsorption of proteins onto hydrophobic surfaces (Fragneto 2000a), the study the physical structure of the light-emitting polymers (Webster 2002), the thermal fluctuations of orientated lipid membranes by non-specular neutron reflectometry (Salditt 2003) and the interaction of water with self-assembled monolayers (Schwendel 2003). Measurements can be performed at all types of solid, liquid and gas interfaces (Daillant 1999), including even liquid – liquid interfaces (Strutwolf 2000). The requirements of the sample are a planar geometry and a roughness no greater than the nanometer scale. It is preferable to have sample surface sizes of approximately $20cm^2$ or more, to reduce the counting time caused by the low flux of neutron sources.

In a reflection experiment, the elastic scattering (specular reflection) is determined as a function of the momentum transfer (q_z) perpendicular to the surface:

$$q_z = \frac{4\pi \sin\theta}{\lambda} = \frac{2\pi}{d_z} \tag{2.3}$$

where θ is the angle of incidence and λ is the wavelength of the neutrons.

In its most basic form a neutron scattering experiment consists of measuring the flux of scattered neutrons as a function of the momentum transfer with all of the sample's detailed structure and mechanics concealed in these two parameters. The scattering is proportional to the chemical composition and density perpendicular to the surface,

known as the scattering length density (SLD). Analysis of data usually involves fitting the reflectivity of a physical model to the experimental results, due to common phase problem, which arises because reflectivity depends on the square of the reflection coefficient, meaning that all phase information is lost (see data fitting section below). The structural parameters of the model are adjusted within realistic boundaries until the model reflectivity profile matches that of the experimental reflectivity.

2.5.2 Why use neutrons?

Neutron scattering has many advantages over other techniques such as x-rays and light scattering. The main advantage is that the scattering strength is not strongly related to the atomic number of atoms. In the case of x-rays and electrons, the scattering power of atoms increases in proportion to the number of electrons in the atom. There is no linear relationship like this present in neutrons as the scattering varies randomly from atom to atom. Even isotopes have substantially different scattering strengths. This means that neutrons are more sensitive to atoms such as hydrogen, carbon and nitrogen when in the presence of heavier atoms. Their presence is not obscured like in x-ray scattering. Neutrons are able to penetrate deep into samples, enabling the study of buried interfaces. They can even travel easily through centimetres of solid steel with only small losses due to absorption. Many analytical techniques of light and x-ray scattering have been applied to neutrons, such as small angle scattering, crystallography, and inelastic scattering.

2.5.3 Theoretical Principles

Neutron reflectivity has much in common with optical techniques, but with different refractive indices

2.5.4.1 Snell's Law

Neutrons passing from one medium to another medium with a different refractive index maybe reflected or transmitted according to the wavelength of the radiation, the angle of incidence and the difference in the refractive indices of the media. The interaction with the interfaces is described by an incidence wave (k_i), a reflected wave (k_r) and a transmitted wave (k_t) (Figure 2.5). In specular reflectivity k_i is equal to k_r

momentum transfer is perpendicular to the surface as $q_z = k_i - k_r$. Thus specular reflectivity gives information about the sample perpendicular to the surface

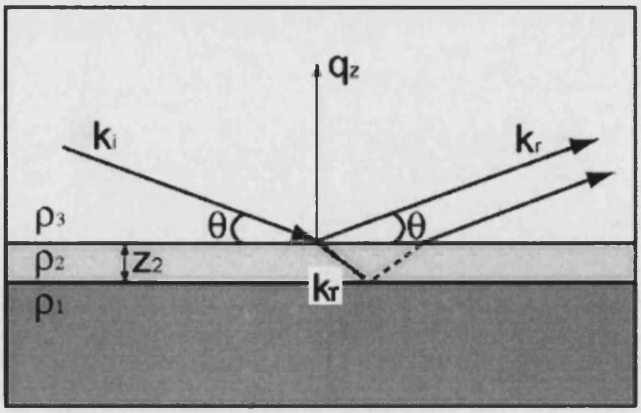

Figure 2.5 Reflection and transmission of a beam incident on an interface.

The relationship between the angle of transmitted (refracted) radiation (θ_r) relative to the angle of incident (θ_i) is described by Snell's law, which for radiation passing one medium, 0, with a refractive index of n_0 into a medium with a refractive index of n_1 can be defined as

$$n_0 \cos\theta_i = n_1 \cos\theta_r \tag{2.4}$$

According to Snell's law at a certain incidence angle there is no transmitted component and there is complete reflection of the incidence beam. This angle is known as the critical angle or known as the critical value when defined in q.

The ratio of refractive indices of the two media ($n = n_0/n_1$) is equal to

$$n = 1 - (\delta - i\beta) \tag{2.5}$$

The imaginary component β only occurs when the material is absorbing radiation. The real term is given by

$$\delta = \frac{\lambda^2}{2\pi} Nb \tag{2.6}$$

where N_b is the scattering length density and λ the wavelength. The refractive index is therefore related to the scattering length density by

$$n = 1 - \frac{\lambda^2}{2\pi}.Nb \tag{2.7}$$

The scattering length density is a measure of how strongly the radiation interacts with the material and for neutrons is given by

$$N = \Sigma b_i \rho_i = N_A \Sigma \frac{\rho_i}{A_i} b_i \tag{2.8}$$

where b_i is the neutron scattering length for the component i, with density ρ_i and atomic weight A_i. The scattering lengths of a range of commonly encountered elements are given in Table 2.1. Note the large difference in the scattering length of hydrogen and deuterium atoms and that the value for deuterium is higher than that of larger atoms like silicon.

Nucleus	b (10^{-4} Å)
1H	-0.374
2H	0.667
C	0.665
N	0.936
O	0.580
Si	0.415
P	0.513

Table 2.1 Neutron lengths of common elements for the most ambulant isotope.

Examples of scattering length densities of components used in this study are given in Table 2.2. The scattering length of the compound is simply the addition of the scattering length of the elements weighted by the stoichiometry.

Material	b (10^{-4} Å)	SLD (10^{-6} Å^{-2})
Si	0.42	2.07
SiO_2	1.59	3.41
H_2O	-0.17	-0.56
D_2O	1.91	6.35

Table 2.2 Scattering length and densities of bulk materials.

The critical angle (θ_c) is related to the difference in SLD between the bulk of a material, and the upper phase (usually air) by

$$\frac{\theta_c}{\lambda} = \sqrt{\frac{\Delta N b}{\pi}} \tag{2.9}$$

The value of the critical angle depends solely on the scattering length of the material (or more strictly the difference between the two media) and provides an excellent route to the determination of scattering length densities and hence the value of the scattering length b.

2.5.4.2 Fresnel Reflectivity

Calculation of the relative amounts of reflected to transmitted beam is calculated using the Fresnel equation

$$r = \left| \frac{n_1 \sin(\theta_1) - n_2 \sin(\theta_2)}{n_1 \sin(\theta_1) + n_2 \sin(\theta_2)} \right| \tag{2.10}$$

where r is the reflectance coefficient (can be imaginary), n_1 is the refractive index of medium 1, n_2 is the refractive index of medium 2, θ_1 is angle of the beam in medium 1 and θ_2 is the refracted beam from and thus the angle of the beam in medium 2. The Fresnel equation can also be written in terms of wave vector of each medium, where $k = 2\pi/\lambda$

$$r = \left| \frac{k_1 - k_2}{k_1 + k_2} \right| \tag{2.11}$$

The reflectivity, which is real, is then given by the product of r and its complex conjugate

$$R = r r^* \tag{2.12}$$

At angles below the critical angle, all neutrons are reflected the reflectivity is unity. At angles above the critical angle the reflectivity falls off sharply at approximately q^{-4}, which is referred to as Fresnel decay.

2.5.4.3 Surface roughness

Reflectivity is very sensitive to surface roughness on the atomic scale. Roughness shows up as a decrease in the reflected intensity which acts in a similar manner to a Debye – Waller factor (in crystallography, the Debye – Waller factor is applied to the diffracted intensity to account for the thermal displacement of atoms). Roughness greater than the nanometer scale is able to rapidly reduce the scattering length density profile to that of the background. This means that the surface of substrates have to be close to atom smoothness to be used in reflectivity. Silicon substrates commonly used in reflectivity are normally polished to a roughness of 3±2Å. Great care in the handling and the use usually retains this very low roughness. The roughness is modelled using an error function, whose sigma value corresponds to the roughness mean squared (RMS) of the surface.

2.5.4.4 Multilayer Reflection

One way of analysing the reflectivity from samples containing one or more layers is to apply the method known as the matrix formulation similar to that of Born and Wolf (Penfold 1994).

Reflectivity from a single film at the interface can be solved directly by calculating reflection coefficients for each interface using the Fresnel equation (equation 8) and then combining them together, taking into account the interference caused by reflection from the top and bottom of the thin layer

$$Ref = \frac{r_1 + r_2 . e^{ik_1 d}}{1 + r_1 . r_2 . e^{ik_1 d}} \qquad (2.14)$$

$$R = ref.ref^*$$

(2.13)

where r_1 and r_2 are reflectance coefficients of the two interfaces, k1 is the wave vector in the thin film and d its thickness. The reflectivity is given by the complex conjugate. The effect of the interference of the reflected beam is to introduce ripples onto the simple Fresnel decay (figure 2.6). The period of the ripples is equal to $2\pi/d$.

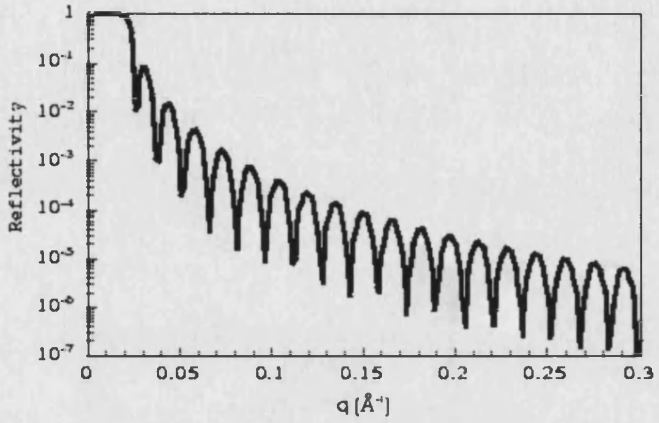

Figure 2.6 Interference of the reflected beams from the interfaces gives rise to ripples onto the simple Fresnel decay. The period of the ripples is proportional to the inverse thickness of the layers.

Roughness is brought into the calculation by multiplying each reflection coefficient by a Debye – Waller factor dependent on the sigma value for each interface. When more layers are introduced the calculation becomes too difficult. The reflectivity is therefore calculated in terms of a characteristic matrix, which is a function of layer density and thickness. Each layer has three terms associated with it, P_i, β_i and a roughness σ_i. The first is defined in terms of the refractive index and incident angle by

$$P_i = \left[n_i - n^2.\cos^2(\theta)\right]^{0.5}$$

(2.15)

and β including the thickness

$$\beta_i = \frac{2\pi}{\lambda}.d_i.P_i$$

(2.16)

where n and n_i are the refractive index of air (or bulk component) and layer i, and d_i is the layer thickness. The Fresnel reflectance, including the roughness, for each layer is then

$$r_i = \frac{P_i - P_{i+1}}{P_i + P_{i+1}} . e^{\frac{Q^2\sigma^2}{2}} \tag{2.17}$$

and the characteristic matrix for each layer

$$N_i = \begin{pmatrix} e^{i.\beta_{i-1}} & r_i . e^{-i.\beta_{i-1}} \\ r_i . e^{i.\beta_{i-1}} & e^{-i.\beta_{i-1}} \end{pmatrix} \tag{2.18}$$

The reflectivity is then calculated by multiplying all the matrices

$$M = \prod_i N_i$$

$$r = \frac{M_{1,0} . M^*_{1,0}}{M_{0,0} . M^*_{0,0}} \tag{2.19}$$

and finally calculating an overall reflectance by $R = r.r^*$

2.6 Analysis of Reflectivity Data

2.6.1 Introduction

Specular neutron reflectivity experiments are relatively straightforward in execution but the data analysis and interpretation is rather more difficult. There are three main problems associated with the analysis. The phase problem, the low momentum transfer available (q_z range) limiting the resolution and that an overall scattering length density profile is obtained from the analysis that may lead to ambiguities when assigning parts to individual section of the sample.

The phase problem is present in all scattering experiments. It arises because reflectivity depends on the square of the reflection coefficient, meaning that all phase information is lost (Reiss 1996). Knowledge of the phase in conjunction with the reflectivity is needed to obtain a unique determination of the density profile. Due to the phase problem a reflectivity measurement cannot usually be directly inverted to produce a single, unique scattering length density. Recent methods to overcome the phase problem have been developed (Majkrzak 1998, Aktosun 2000, Blaise 2003) but the most common and simplest way is to fit the reflectivity of a physical model to the experimental results (Lu 1996).

The available momentum transfer can be restricted by a number of factors. The main factor in solid-liquid samples is caused by background scattering from the liquid and hydrogenated components in the film. The highest q_z range is usually achieved when deuterated water is used, whilst water contains hydrogen atoms that increase incoherent background scattering. In the case of the profiles of double bilayers in D_2O, clear features are usually observed up to a maximum of $0.25Å^{-1}$, whilst in H_2O, the features are very subdued usually with a maximum of $0.15Å^{-1}$.

The ambiguity associated with the overall scattering length density can be reduced by use of realistic structural model parameters and by using chemically identical systems with different scattering length profiles. The latter method, known as contrast variation, involves substituting parts of the system for their deuterated or partially deuterated counterpart. This relies on the large difference in the scattering lengths of

hydrogen and deuterium atoms ($-0.38e^{-14}$m and $0.65e^{-14}$m respectively). The simplest method of contrast variation is to exchange the solvent for different D_2O/H_2O ratios. Another ways in bilayer studies are to use freely available deuterated lipids, but they do not always give the same structure as their hydrogenated counterparts.

Having recorded the reflectivity from a number of different contrasts, a unique solution of the structure is usually obtained by simultaneously fitting them with similar structural parameters, but with exchanged scattering length densities.

2.6.2 Methods of reflectivity data analysis

2.6.2.1 Box Model

The traditional way to treat neutron reflectivity data is to create a model of the sample, divide it into slabs characterised by thickness, scattering length density and roughness (Figure 2.7).

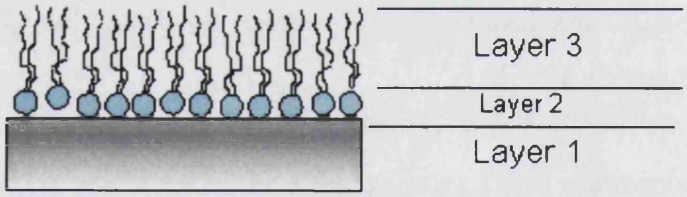

Figure 2.7 In the box model approach the sample is divided into layers

The scattering length density values are assumed not to vary significantly within the temperature range studied. They do however vary slightly with the hydration change that occurs with phase transitions. The layer thickness, roughness and level of solvation of the bilayers are the main variable parameters. Standard minimisation techniques are then used to vary these parameters until its calculated reflectivity unambiguously matches that of the real sample. This box model technique is successful for simple systems such as single bilayers but deteriorates for more complex systems, measured to higher momentum transfer and thus higher resolution (Schalke 2000, Hughes 2002b). A number of different programmes are available for

fitting the data this way. Two of the most popular are AFit (Thomas group, Oxford) and Parratt32 (Hahn Meitner Institut, Berlin).

2.6.2.2 Quasi-molecular approach

Recently a different method, the quasi-molecular approach (also known as distribution function method), has been employed to model reflectivity data of monolayers (Schalke 2000b) and hybrid double bilayers (Hughes 2002b). The method describes the bilayer fragments as distribution functions rather than slabs and was first developed by Wiener and White for the analysis of diffraction from multilamellar vesicles (Wiener 1991). A detailed account of the method applied to neutron reflectivity of lipid bilayers can be found in AV Hughes et al., (2002b). An overview will be given below.

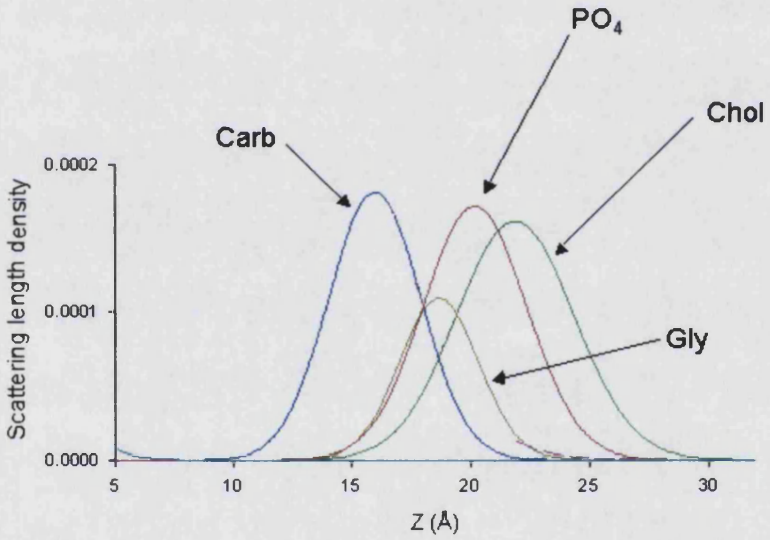

Figure 2.8 Each Gaussian represents the contribution of a particular molecular fragment to the overall SLD profile for a lipid head-group. The fragments are the choline, phospho, glycero and carbonyl.

With this method the scattering length density of the headgroups are described in terms of Gaussian distribution functions, where each Gaussian represents the contribution of a particular molecular fragment to the overall SLD profile (Figure 2.8). The head-group is divided into 4 fragments; the choline, phospho, glycero and carbonyl fragments, with each assigned a separate Gaussian. The centre of the Gaussian corresponds to the centre of mass of the fragment along the bilayer normal and the width accounting for thermal oscillations around the mean position. Its height

is the calculated scattering length contribution of the fragment. The Gaussian functions may vary within molecular considerations their centre position and half-widths along the bilayer normal representing the disorder present in bilayers. Figure 2.9 shows an example of the scattering length profile for a lipid bilayer. The alkyl chain region of each lipid leaflet is assumed to be a homogeneous region and is thus treated as a single alkyl layer. The methyl groups at the end of each chain region have a lower SLD so, are dealt with a separate Gaussian. The coverage of the bilayer is determined by scaling between a calculated 0% and 100% coverage until it fits the measured reflectivity profile (Hughes 2000b). The silicon oxide layer is described by single slab, with its thickness determined to be between 10 – 20Å (Fragneto 2000b). All unoccupied space in the headgroups, between the bilayers, and between the lower bilayer and silicon surface is assumed as occupied by water molecules. The total scattering length density of the sample is simply the sum of the Gaussian's, alkyl slab and silicon oxide slab.

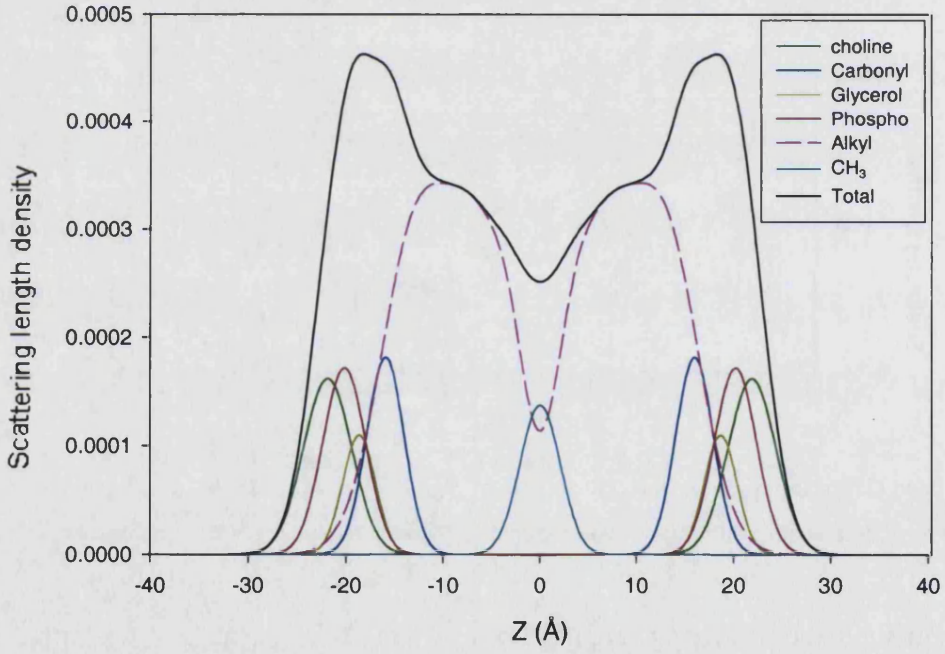

Figure 2.9 Scattering length density of a lipid bilayer

An example of the resulting scattering length density profile for a double bilayer in sample in D_2O is given in Figure 2.10. The profile reflects the scattering length density perpendicular to the surface. The silicon substrate (SLD of 2.07 x 10^{-6} $Å^{-2}$) can be seen on the far left, the thin water layer separating the lower bilayer from the substrate is seen next (6.35 x 10^{-6} $Å^{-2}$), followed by the bilayers (headgroups 1.74 x

10^{-6} Å^{-2} and chains –0.41 x 10^{-6} Å^{-2}) separated by a water layer. The bulk water is on the far right.

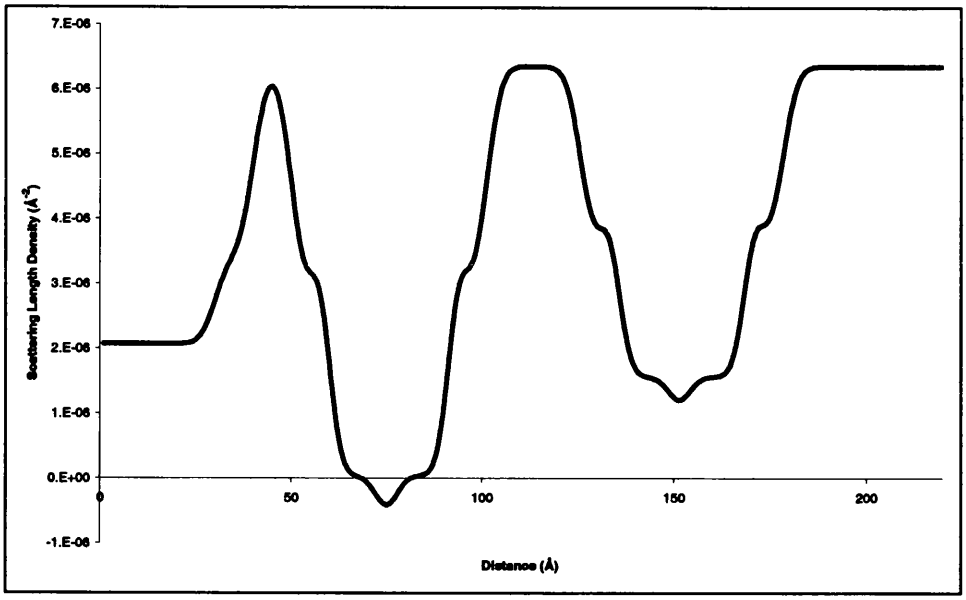

Figure 2.10 Scattering density of a double bilayer sample in D20.

The quasi-molecular approach is a more realistic representation of the bilayer constitution than the use of large slabs. It has successfully been used to fit synchrotron reflectivity of lipid monolayers to momentum transfer out to 0.8Å^{-1}, whilst box models were found to be rather inadequate to such momentum transfer. (Schalke 2000a)

The total number of variable parameters can be reduced down to 9 by the reliance of certain parameters on others and by defining the positions of fragments relative to the centre of the bilayer (Hughes 2000b). This means that each bilayer is described by an area per molecule, a position along the bilayer normal, an overall roughness and a coverage value. The scattering length density of each fragment is calculated from atomic scattering length tables using equation (2.5) and assumed not to vary over the temperature range measured. The thickness of the bilayer (D_B) can be obtained, as it is inversely proportional to the APM

$$D_B = \frac{2V_L}{APM_L} \qquad (2.20)$$

where V_L is the volume of the lipid fragment. Fragment volumes are available from molecular dynamics simulations and experimental results (Armen 1998). The thickness of the water layers was simply derived from the positions and thickness of the two bilayers. The silicon oxide is described by only one variable parameter, the thickness, as its roughness was characterised when polished and by reflectivity. It was found to have a RMS of 3±2Å² by AFM (ESRF optics laboratory, Grenoble and Charitat 1999).

The complete model was implemented in a *Matlab* environment, with the reflectivity profile calculated by use of the recursive Parratt algorithm (Parratt 1954). The programme calculates a range of acceptable fits from randomly starting points within realistic parameter boundary limits to minimise the chi-squared (χ^2) of the model and experimental profiles. The parameters are varied until χ^2 is unable to decrease by at least $10e^{-6}$.

2.7 Application of Reflectivity to Double Bilayers

Reflectivity studies of lipid systems are a reliable and an easy way of obtaining composition, structure, and kinetic and dynamic changes to near Å precision. Examples include the structural binding of divalent cations to monolayers of $DMPA^-$ (Schalke 2000), protein function in alkanethiol-tethered hybrid bilayer membranes (Plant 1999) and structural studies of polymer-cushioned lipid bilayers (Majewski 1998). Other examples can be found in the review of neutron reflection from interfaces with biological and biomimetic materials (Krueger 2001).

2.7.1 Advantages

Much of the work on lipid bilayers involves samples consisting of many of bilayers, which are necessary to enable several orders of Bragg reflections in diffraction studies. Whilst this is a very useful technique and has been greatly utilised (Lemmich 1996, Petrache 1998, Darkes 2000, Tristram-Nagle 2002), one issue is that the bilayer information is averaged over 100s of units, rather than being single bilayer specific information. Another issue is that higher quantities of biological compounds are needed which can be undesirable when very expensive proteins are being used. One of the main advantages of using neutron reflectivity on bilayers is the simplicity of sample needed. It can be used to study samples as thin as single monolayers on water to multiply stacked bilayers (Mennicke 2002). Only very small amounts of chemicals are needed and the sample can be contained in bulk water conditions. Another advantage is that it can yield information such as the modifications of bilayer induced by small proteins, which are too small to be seen by other techniques (Fragneto 2000b). Double bilayer samples have been used in a range of different studies with x-ray and neutron reflectivity from structural behaviour to protein orientation (Chapter 1)

2.7.2 Experimental Details

Solvent contrasts

The samples were usually measured in deuterated water, silicon-matched water (SMW), and 4-matched water (4MW) which has a SLD of 4×10^{-6} $Å^{-2}$. When deuterated lipids were used the sample was measured in pure water as well.

Deuterated water has a SLD of 6.35 x 10^{-6} $Å^{-2}$. Silicon-matched water consists of the molar ratio of 0.38 D_2O and 0.62 H_20 and has a scattering length density of 2.07 x 10^{-6} $Å^{-2}$. 4-matched water consists of the molar ratio of 0.66 D_2O and 0.34 H20 giving a SLD of 4.00 x 10^{-6} $Å^{-2}$. Ultra-pure water has a scattering length density of – 0.56 x 10^{-6} $Å^{-2}$.

Deuterated water gives no incoherent scattering and has a critical edge of ~ 0.014$Å^{-1}$. Reflectivity profiles in D_2O usually have large well-defined features. Silicon matched water usually has a higher background scattering from the incoherent scattering of the water present. It is not possible to see any critical edge, as there is no difference in the SLD of the two bulk mediums.

Contrast exchange procedure

The samples were usually fabricated in pure water. For accurate alignment of the sample it is better to exchange the solvent to D_2O. The Teflon well has two inlets for contrast exchange. Different types of techniques were evaluated. As the films are robust, it was found that the best and quickest way was to use a syringe with tubing protruding into the well. The capacity of Teflon well is approximately 10mL, so usually at least 60mL of solvent was pumped through at a rate of approximately 10mL per minute. In the case of exchanging the solvent for D_2O the position of the critical angle (θ_c) can be used to check whether it has been fully exchanged.

2.8 Double Bilayer Parameters

dw – thickness of water layer separating lower bilayer from substrate

lDb – total thickness of lower bilayer

lDc – thickness of chain region of lower bilayer

lAPM – average area per molecule of lower bilayer component

lRou – average roughness of lower bilayer

lCov – coverage of lower bilayer

Dw – thickness of water layer separating the two bilayers

uDb – total thickness of upper bilayer

uDc – thickness of chain region of upper bilayer

uAPM – average area per molecule of upper bilayer component

uRou – average roughness of upper bilayer

uCov – coverage of upper bilayer

2.9 The D17 Reflectometer at Institut Laue-Langevin

The measurements were performed on the high flux reflectometer D17 (Cubitt 2002) at the Institut Laue-Langevin, France, in time of flight mode (Figure 2.11). The basic features of a reflectometer is a radiation source (nuclear or spallation source), collimation and monochromators, the sample and the detection system. The main requirements for a reflectometer are high flux, flexible resolution, accurate collimation and precision neutron detection. D17 has all of these properties. The D17 reflectometer has the highest white beam flux at the sample position in the ILL of 9.6 x 10^9 n/s/cm 2 provided by the super-mirror-coated guide. The instrument has two modes of operation, time-of-flight (where the reflectivity is measured at a fixed angle and a pulsed wavelength band) and monochromatic (whether the wavelength is fixed and the angle varied), with the latter incorporating the polarised-neutron option.

The time-of-flight mode is realized by a double chopper system with variable phase and separation, giving a useful wavelength range of 2-20Å. The values of q are determined from the time of arrival of each neutron as a function of its wavelength. The advantage of time of flight mode is that it offers a greater flexibility of resolution and enables certain experiments like dynamics or fixed geometry to be carried out as an entire order of magnitude in q can be measured simultaneously in less than a minute. Time of flight mode is less efficient than the monochromatic mode in terms of the flux available at each q point as the flux at the extremes of usable wavelengths are much lower than the peak flux used in the monochromatic mode.

There are two options for the monochromic mode; one is a Fe/Si multilayer for polarised neutrons working at 6Å, the other a Ni/Ti multilayer producing a non-polarised beam at 5Å. Both have a resolution of 5%. Changing between time-of-flight and monochromatic modes of operation takes approximately 15 minutes so it is possible to utilise both modes in one experiment if required. The monochromatic beam is far easier for magnetic experiments (no q-dependent polarization efficiency).

Beam collimation is achieved by two slits before and after the super-mirror focusing guide. Background from the solvent in the sample usually limited the useful q-range to 0.25$Å^{-1}$. The large multi-detector is 250 x 500mm of the Helium 3 type and allows

the simultaneous measurement of background and off-specular scattering. The detector (^{3}He type) can be translated from 3.4 to 1m from the sample position

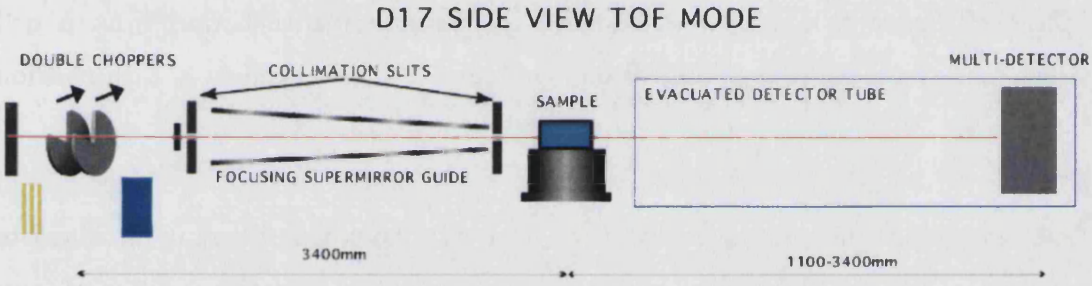

Figure 2.11 Image and schematic of the D17 Reflectometer at the Institut Laue-Langevein. (*Courtesy of R. Cubitt*)

D17 settings for Double bilayer measurements

The reflectivity of the double bilayer was measured at two angles (typically 0.7° and 4°) in time of flight mode. The first angle (a_1) had a chopper opening of 1.4 and slit openings of 0.8mm. The second angle (a_2) had a chopper opening of 5 and slit openings of 3.2mm. These chopper settings gave a spread of wavelengths between 2Å and 20Å.

The useful q range for double bilayers samples is 0.007 to 0.25 Å^{-1}, which was usually measured in 2 hours. Fast scans of only the first angle (q range 0.007 – 0.09) can be measured in 20 minutes.

2.9.1 D17 Data treatment

Background substitution

At high values of q the specular reflectivity is very small and the background scattering high. The source of this background scattering is related to the sample composition, sample environment and components of the reflectometer. The background substitution needs to be subtracted from the reflectivity profile. On D17 the background is usually subtracted by taking a mean of the strip either side of the specular scattering on the detector image and subtracting it. It is usually only necessary to fit the background if it is not very flat, but usually after dividing by the water (which measured for detector efficiency) it is flat.

Data collection

The D17 detector efficiency is tested by measuring the scattering from a cell containing water. Since the value of the scattering of water is known at each position of the detector, the measurements can then be corrected for any inefficiency.

The intensity of the neutron beam passing through the silicon block is measured in order to normalise the intensity of the reflected beam. The intensity is different from that of the incident beam by a factor related to loss of intensity from wide angle scattering or adsorption of neutrons by the solid substrate.

Once the sample is in place the sample is aligned in order to ensure that the neutron beam strikes exactly at the interface and not in the solid or liquid phases. This is simply done by scanning the position of around the interface until the highest reflectivity is measured. In a normal double bilayer experiment on the D17 reflectometer, the reflectivity is usually measured in time of flight mode at two angles. The angle is changed to obtain higher reflectivity at higher q. The reflectivity collected at the two angles is then joined to form the overall reflectivity profile. The measurement of the sample reflectivity is usually highly automated with the use of command files to enable temperature scan measurements. The alignment should be checked approximately every 20°C to account for any swelling of the Teflon well. It is not necessary to check the alignment after the solvent has been changed.

2.10 References

- Abeles F. (1950) *La determination de lindice et de lepaisseur des couches minces transparentes* J. Phys. Paris. 11, 310 – 314
- Aktosun T, Sacks P E. (2000) *Inversion of reflectivity data for non-decaying potentials.* J. Appl. Math. 60, 1340 –1356.
- Als-Nielsen J, Jacquemain D, Kjaer K. et al. (1994) *Principles and applications of grazing-incident x-ray and neutron-scattering from ordered molecular monolayers at the air-water interface* Phys. Rep. Rev. Sec. Phys. Lett. 246, 252 – 313
- Armen R S, Uitto O D, Feller S E. (1998) *Phospholipid component volumes: determination and application to bilayer structure calculations.* Biophys. J. 75, 734 – 744
- Bayer (2002) *Biology and Biotechnology* ESS – SAC/ENSA Workshop, ESS/SAC/Report/1/01
- Bengu E, Salud M, Marks L D. (2001) *Model-independent inversion of XR NR* data Phys. Rev. B, 63, 195414
- Blaise J K, Zheng S, Strzalka J. (2003) *Solutions Phase problem XR NR form thin films on lq surfaces* Phys. Rev. B, 67, 224201
- Bolze J, Takahasi M, Mizuki J, Baumgart T, Knoll W. (2002) *X-ray Reflectivity and Diffraction Studies on Lipid and Lipopolymer Langmuir-Blodgett Films under Controlled Humidity* J. Am. Chem. Soc. 124, 9412 - 9421
- Born and Wolf (1989) *Principles of optics*, Pergamon Press, Oxford.
- Brezesinski G, Mohwald H. (2003) *Langmuir monolayers to study interactions at model membrane surfaces* Adv. Coll. And interface Sci. 100-102 563-584
- Brinkhuis R H G, Schouten A J. (1991) *Thin-film behaviour of poly(methyl methacrylates) 1. Monolayers at the air –water interface* Macromolecules 24, 1487 - 1495
- Bucknall (1995) *SURF - A second generation neutron reflectometer* Proc ICANS XIII, PSI Proceedings 95-02 Vol 1, 123
- Carino S R, Tostmann H, Underhill R S. et al. (2001) *Real-Time Grazing Incidence X-ray Diffraction Studies of Polymerizing n-Octadecyltrimethoxysilane Langmuir Monolayers at the Air/Water Interface* J. Am. Chem. Soc. 123, 767 – 768
- Charitat T, Bellet-Amalric E, Fragneto G. et al. (1999) *Adsorbed and free lipid bilayers at the solid-liquid interface* Eur. Phys. J. B. 8, 583 – 593
- Cubitt R, Fragneto G. (2000) *D17: the new reflectometer at the ILL,* Appl. Phys. A 74, S329 – S331.
- Cubitt (2001) *Neutron Reflection: Principles and examples of applications.* Scattering (Pike and Sabatier)
- Daillant J. (1999) *X-ray and Neutron Reflectivity: Principles and Applications.* Springer-Verlag press, Heidelberg, Germany.
- Dalgliesh R. (2002) *Application of off-specular scattering XR NR to the study of soft matter* Curr. Opin. Coll. Inf. Sci 7 244-248
- Darkes M J M, Bradshaw J P. (2000) *Real-time swelling-series method improves the accuracy of lamellar neutron-diffraction data* Acta Cryst. D56, 48–54
- Ekelund K, Sparr E, Engblom J. et al. (1999) *An AFM study of lipid monolayers. 1. Pressure-induced phase behaviour of single and mixed fatty acids* Langmuir 15, 6946 – 6949
- Finnie K R, Haasch R, Nuzzo R G. (2000) *Formation and patterning of self-assembled monolayers derived from long-chain organosilicon amphiphiles and their use as templates in materials microfabrication* Langmuir 16, 6968 – 6976

- Flach C R, Dieudonne D, Bi X H. et al. (2000) *Biophysical studies of model stratum corneum lipid monolayers by infrared reflection-absorption spectroscopy and Brewster angle microscopy* J. Phys. Chem. B. 104, 2159-2165
- Fragneto G, Lu J R, McDermott D C. et al (1996) *Structure of monolayers of tetraethylene glycol monododecyl ether adsorbed on self-assembled monolayers on silicon: a neutron reflectivity study* Langmuir 12, 477 – 478
- Fragneto G, Su T J, Lu J R. et al. (2000a) *Adsorption of proteins from aqueous solutions on hydrophobic surfaces by neutron reflection* PCCP 2, 5214-5221
- Fragneto G, Graner F, Charitat T. et al. (2000b) *Interaction of the third helix of antennapedia homeodomain with a deposited phospholipid bilayer: a neutron reflectivity structural study* Langmuir 16, 4581-4588
- Fukuda K, Shibasaki Y, Nakahara H. (1981) *Polycondensation of long-chain esters of alpha-amino acides in monolayers at the air-water interface and in multilayers on solid surface* J. Macromolec. Sci. Chem. A15, 999 -1014
- Hatada M, Nishii M. (1977) *Polymerization induced by electron-beam irradiation of octadecylmethacrylate in form of a multilayer or monolayer* J. Polym. Sci., Polym. Chem. Ed. 15, 927 – 935
- Hughes A V, Roser S J, Gerstenberg M C. et al. (2002b) *Phase behaviour of DMPC free supported bilayers studied by neutron reflectivity* Langmuir 18, 8161 – 8171
- ILL Institut Laue Langevin, www.ill.fr
- Ikota H, Tomimitsu T, Motomura K. et al. (1998) *Miscibility and nonideality of mixing of heptanol and octylsulfinylethanol in the adsorbed film and micelle* Langmuir 1998, 14, 5347-5354
- Judeinstein P, Sanchez C. (1996) *Hybrid organic-inorganic materials: A land of multi-disciplinarity* J. Mater. Chem. 6, 511 - 525
- Koenig B W, Krueger S, Orts W J. et al. (1996) *Neutron reflectivity and atomic force microscopy studies of a lipid bilayer in water adsorbed to the surface of a silicon single crystal* Langmuir 12, 1343 – 1350
- Krueger S. (2001) *Neutron reflection from interfaces with biological and biomimetic materials* Curr. Opn. Coll. Inf. Sci. 6, 111 – 117
- Lawie (2000) *The structure of mixed monolayer films of DPPC and hexadecanol* Coll. Surf. A: Phys.chem Engin. Aspects 171, 217 – 224
- Lemmich J, Mortensen K, Ipsen J H. et al. (1996) *Small-angle neutron scattering from multilamellar lipid bilayers: Theory, model, and experiment* Phys. Rev. E. 53, 5169 –5180
- Leonard A, Escrive C, Laguerre M. et al. (2001) *Location of Cholesterol in DMPC Membranes. A Comparative Study by Neutron Diffraction and Molecular Mechanics Simulation†* Langmuir 17, 2019 -2030
- Lu J R, Lee E M, Thomas R K. (1996) *The Analysis and Interpretation of Neutron and X-ray Specular Reflection.* Acta Cryst. A. 52, 11-41
- Lu J R, Thomas R K. (1998) *Neutron Reflection from wet interfaces* J. Chem. Soc., Faraday Trans., 94, 995 – 1018
- Lu J R, Thomas R K, Penfold J. (2000) *Surfactant layers at the air-water interface: struc. & composition* Adv. Coll. Int. Sci., 84, 143-304
- Majewski J, Wong J Y, Park C K. et al. (1998) *Structural studies of polymer-cushioned lipid bilayers* Biophys. J. 75, 2363–2367
- Majkrzak C F, Berk N F. (1998) *Exact determination of the phase in neutron reflectometry by variation of the surrounding media.* Phys. Rev. B 58:15416 –15418.
- Matsuki H, Kanda T, Aratono M. et al. (1990) *Miscibility of 1-octanol and 2-(octylsulfinyl)ethanol in the absorbed film and micelle* Bull. Chem.Soc. Jpn. 1990, 63, 2159 – 2163

- McConlogue C W, Vanderlick T K. (1997) *Close Look at Domain Formation in DPPC Monolayers* Langmuir, 13, 7158-7164
- Mennicke U, Salditt T. (2002) *Preparation of solid supported lipid bilayers by spin coating* Langmuir 18, 8172 – 8177
- Miyashita T(1991) *Miscibility of 1-ocyanol and 2-(octylsulfinyl)ethanol in the adsorbed film and micelle* Chem. Lett. 1991, 969
- Miyashita T. (1993) *Recent studies on functional ultrathin polymer-films prepared by the Langmuir-Blodgett technique* Prog. Polm. Sci, 18, 263 – 294
- Motomura K, Matsukiyo H, Aratono M. (1986) *Phenomena in Mixed Surfactant Systems* ACS Symposium 311, American Chemical Society, 163
- Mumby S J, Swalen J D, Rabolt J F. (1986) *Orientation of poly(octadecyl methacrylate) and poly(octadecyl acrylate) in Langmuir-Blodgett monolayers investigated by polarized infrared spectroscopy* Macromolecules 19, 1054 – 1059
- Parratt L G. (1954) *Surface studies of solids by total ref. x-rays* Phys. Rev. 95, 359 - 369
- Penfold J, Thomas R K. (1990) *The application of the specular reflection of neutrons to the study of surfaces and interfaces J.* Phys. Con. Matt. 2, 1369 – 1412
- Penfold J, Thomas R K, Lu J R. et al. (1994) *The study of surfactant adsorption by specular neutron reflection* Physica B 198, 110 – 115
- Plant A L. (1999) *Supported hybrid bilayer membranes as rugged cell membrane mimics* Langmuir 15, 5128-5135
- Petrache H I, Goiliaev N, Tristram-Nagle S. et al. (1998) *Interbilayer interactions from high-resolution x-ray scattering* Phys. Rev. E. 57, 7014 – 7024
- Reiss G, Lipperheide R. (1996) *Inversion and the phase problem in specular reflection.* Phys. Rev. B. 53, 8157 - 8160
- Rivière-Cantin S, Henon S, Meunier J. (1996) *Phase transitions in Langmuir films of fatty acids* Phys. Rev. E 54, 1683 – 1686
- Salditt T, Munster C, Mennicke U. et al. (2003) *Thermal fluctuations of orientated lipid membranes by non-specular neutron reflectometry* Langmuir. 19, 7703 – 7711
- Sagiv J. (1980) *Organized monolayers by adsorption 1. formations and structure of oleophobic mixed monolayers on solid-surfaces* J. Am. Chem. Soc. 102, 92 – 98
- Schalke M, Losche M. (2000) *Structural models of lipid monolayers from x-ray and NR.* Adv. Coll. Int. Sci., 88, 243 - 274
- Schwartz D K, Knobler C M. (1993) *Direct observations of transitions between condensed Langmuir monolayer phases by polarised fluorescence microscopy* J. Phys. Chem 97, 8849 – 8851
- Schwendel D, Hayashi T, Dahint R. et al. (2003) *Interaction of water with self-assembled monolayers: Neutron reflectivity measurements of the water density in the interface region.* Langmuir, 19, 2284-2293
- Strutwolf J, Barker A L, Gonsalves M. et al. (2000) *Probing liquid vertical bar liquid interfaces using neutron reflection measurements and scanning electrochemical microscopy* J. Electroanal. Chem. 483, 163 – 173
- Swalen J, Allara D L, Andrade J D. et al. (1987) *Molecular monolayers and films. A panel report for the Materials Sciences Division of the Department of Energy* Langmuir 3, 932 – 950
- Teerenstra M N, Vorenkamp E J, Schouten A J. et al. (1992) *Langmuir-Blodgett films of poly(isocyanides) with different side chains 2 poly(3-cholesteryl-6-isocyanohexanoate)* Thin Solid Films 210, 496 – 499
- Tieke B, Lieser G, Wegner G. (1979) *Polymerization of diacetylenes in multilayers* J. Polym. Sci. Polym. Chem. 17, 1631 – 1644

- Tristram-Nagle S, Liu Y, Legleiter. et al. (2002) *Structure of gel phase DMPC determined by x-ray diffraction* Biophys. J. 83, 3324 – 3335
- Vig J R. (1985) *UV/Ozone cleaning of surfaces J. Vac. Sci. Technol. A,* 3, 1027 – 1034
- Yang L, Harroun T A, Heller W T. et al. (1998) *Neutron Off-Plane Scattering of Aligned Membranes.* Biophys. J. 75, 641 – 645
- Webster G R, Mitchell W J, Burn P L. et al. (2002) *Neutron reflection study on soluble and insoluble poly[2-(2'-ethylhexyloxy)-5-methoxy-1,4-phenylenevinylene)] films.* J. Appl. Phys., 91, 9066 – 9071
- Wen J Y, Wilkes G L. (1996) *Organic/inorganic hybrid network materials by the sol-gel approach* Chem. Mater. 8, 1667 – 1681
- Wu F, Corsico B, Flach C R. et al. (2001) *Deletion of the helical motif in the intestinal fatty acid-binding protein reduces its interactions with membrane monolayers: Brewster angle microscopy, IR reflection-absorption spectroscopy, and surface pressure studies.* Biochemistry 40, 1976-1983
- Zheng J, Zhu Z, Chen H. et al. (2000) *Nanopatterned assembling of colloidal gold nanoparticles on silicon* Langmuir 16, 4409 – 4412

3. Phase behaviour of dipalmitoylphosphatidylcholine double bilayers containing low amounts of cholesterol

3.1 Abstract

The phase behaviour of double bilayers containing different concentrations of cholesterol and DPPC (1,2-dipalmitoyl-sn-glycero-3-phosphocholine) was investigated by specular neutron reflectivity. The aim of the study was to assess the fabrication, stability and phase behaviour to assess their viability as biomembrane mimics. Fabrication of DPPC double bilayers with 0 – 10 mol% of cholesterol was investigated, especially with regards to very low concentrations (1 – 4 mol%), which are not possible via vesicle adsorption methods (*personal comms. Mouritsen, University of Southern Denmark*). Phosphatidylcholine vesicles containing very low amounts of cholesterol exhibit interesting structural phenomena near the main fluid – gel phase transition (Lemmich 1997), the reasons for which are still not fully understood.

Double bilayers of phosphatidylcholine have been observed to exhibit large swelling during the transition temperature range (Fragneto 2003). It is thought that the behaviour is connected. It was hoped that the addition of cholesterol to these double bilayers would also contribute to understanding the phenomena.

The fabrication and phase behaviour of double and single bilayers containing both hydrogenated chain DPPC and deuterated chain DPPC with cholesterol was also investigated. The aim was to develop a range of different deuterated versions, which were stable and exhibit full phase behaviour. This would aid greatly in biomembrane mimic studies as deuterated layers aid resolution of the structures and can be used to essentially highlight components in the bilayer.

3.2 Introduction

Cholesterol is one of the most important compounds in biological membranes. It has been found to regulate the fluidity of membranes, increasing the fluidity at low temperatures and reducing it at high temperatures (Yeagle 1986). The concentration varies from cell to cell. It is equimolar with phospholipids in membranes of the liver cells, erythrocytes and myelin while in the outermost layer of human epidermis it represents about 30 mol% of the lipid fraction. The ability of cholesterol to modulate the fluidity of membranes seems to be important in many biological processes, for example in cell fusion (Nakanishi 2001). It has also recently been found to influence the phase behaviour of lipid bilayers as a function of its concentration (Lemmich 1997). Cholesterol is oriented in the membrane such that its axis lies parallel to the lipid chains. This increases the order of the lipids in their upper part while decreases the packing constraints at the terminal methyl groups. The structure of cholesterol containing membranes has been probed by neutron and x-rays diffraction and small angle scattering (Wiener 1991, Knoll 1985, Mortensen 1988) using stacked bilayers and multilamellar systems. However the accurate vertical location in the membrane is still controversial (Leonard 2001).

The phase diagram of phospholipid bilayers has received much attention in the last decades and most of the work has concentrated on the three common phases, the gel ($L_{\beta'}$), ripple ($P_{\beta'}$) and fluid (L_{α}). While in the gel and ripple phases the acyl chains are conformationally ordered, in the fluid phase they are disordered. The incorporation of cholesterol into the phospholipid membrane usually broadens or eliminates the gel to liquid-crystalline (L_{α}) phase transition; it increases the orientational ordering of the hydrocarbons in the L_{α} phase of bilayers while decreasing it in the gel phase. At high concentrations it stabilises a liquid ordered (l_o) phase which is fluid from the point of view of lateral disorder and diffusion but at the same time the acyl chains in this phase have a high degree of conformational order (Vist 1990). The l_o phase is characterised by increased bilayer thickness and area compressibility modulus (Needham 1988; Trouard 1999). At low concentrations the molecule becomes interfacially active and promotes the formation of lipid domains (Mouritsen 1994). Phase behaviour studies have been classically carried out on either multilamellar phases or stacked bilayers.

Double bilayers of the phosphatidylcholine DPPC have been previously found to swell during the transition region (Fragneto 2001), which is likely due to the unique floating bilayer structure of this system. The results were interpreted in terms of a competition between the inter-bilayer potential and the membrane fluctuations and were used to estimate the bending rigidity of the bilayer. The large swelling of the floating bilayer around the main phase transition temperature was found to correspond to a minimum of the bending modulus in that region (Mecke 2003). It is not known if this is connected to the ripple phase observed in vesicles or is a particular behaviour of the double bilayer system.

In this chapter the effect of a range of different cholesterol molar ratios upon the phase behaviour of double bilayers of DPPC will be given (Figure 3.1). DPPC was chosen because of the abundant structural data and molecular dynamics simulations existing in literature, so is useful to validate the results. The aim was to characterise the full phase behaviour upon heating and cooling. It was found that the phase behaviour of pure DPPC double bilayers differs remarkably depending on whether the sample is being heated or cooled and the behaviour was found to be entirely reproducible during repeated temperature scans. This was also found to be the case for some of the concentrations of cholesterol. The full phase behaviour of DPPC will be given, followed by phase behaviour of very low amounts of cholesterol (1 – 4 mol% cholesterol) and then low amounts of cholesterol (6 – 10 mol% cholesterol). Unfortunately it was not possible to fabricate the biologically relevant concentration of 20 mol% cholesterol with DPPC. This range of cholesterol concentrations were chosen due to their effect on the phase equilibria (Vist 1990) and their effect on the phase transition behaviour (Lemmich 1997).

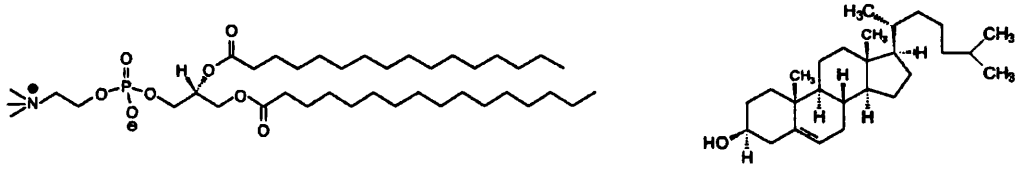

Figure 3.1 Chemical structures of DPPC (left) and cholesterol (right).

3.3 Fabrication Results

The fabrication of double bilayers containing ratios of cholesterol between 0 – 20 mol% was evaluated. The monolayers and depositions were fabricated according to the method detailed in the fabrication chapter. Monolayers of DPPC and cholesterol have been extensively studied in the past (McPhillips 1972, Yeagle 1985, McConnell 2003), so only the deposition results are given.

3.3.1 Depositions

DPPC with deuterated chains (d_{62}-DPPC) needs mild heating to dissolve in chloroform, whilst the hydrogenated version readily dissolves in cold chloroform. The transfer ratios and Schaefer deposition parameters are listed in Table 3.1.

Cholesterol ratio (mol%)	Tr1	Tr2	Tr3	Schaefer Deposition	
				Pressure	Area
0	1.04	0.43	1.00	7	5
0.5	1.01	0.37	0.99	9	6
1	1.01	0.37	1.00	7	5
2	1.02	0.34	1.01	8	5
4	1.00	0.21	0.98	16	13
6	1.04	0.50	1.05	8	6
8	1.03	0.29	1.07	6	
10	1.10	0.27	1.08	5	3
20					
d-DPPC 0 mol%	1.07	0.14	1.06	10	5
d-DPPC 10 mol%	1.11	0.27	1.09	20	10
h-DPPC 10 mol% single	1.11			12	9
d-DPPC 10 mol% single	1.07			7	4

Table 3.1 Average transfer ratios of DPPC with different molar ratios of cholesterol. Pressure is in mN/m and Area in cm^2. The ratios 0 – 20 mol% are with h-DPPC. Single denotes single bilayer.

No trend was observed in the transfer ratio versus cholesterol concentration. The transfer ratios of the first and third depositions were close to unity for all ratios, whilst the second deposition was consistently found to give a value below 0.5. It is likely that the monolayer is only transferring well onto the Angstrom roughness polished side (29% of the overall surface area), as when the reflectivity was fitted,

high coverage of the upper bilayer was always necessary for a good fit. Another indication of the quality of the deposition can be obtained from the optical fringes observed during the third deposition. Good depositions generally give straight fringes across the block. The presence of dirt or contamination is easily observable in the fringes.

All Schaefer depositions were good except for the 4 mol% of cholesterol sample which was higher as the block touched the sub phase at a higher speed than the others. It was therefore expected that the coverage of the upper bilayer would be lower for this sample.

The results show that it is possible to fabricate double bilayers containing very low amounts of cholesterol (0.5 – 2 mol%). This is a useful result as it is not possible to fabricate double bilayers containing very low amounts of cholesterol by vesicle adsorption (*personal communications with Mouritsen group, University of Southern Denmark*).

It was not possible to deposit 20 mol% cholesterol and DPPC. It likely that the cholesterol and DPPC are separating into domains, causing a heterogeneous monolayer that does not deposit well. The formation of rafts of cholesterol in membranes is a well-known phenomenon (Simons 1997, Subczynski 2003).

The deuterated samples generally gave bad transfer ratios for the second deposition. The first and third depositions were comparable to their hydrogenated counterparts. The addition of 10 mol% increased the second transfer ratio.

3.4 Modelling of DPPC – cholesterol Neutron Reflectivity

The reflectivity of the samples containing 0 –4 mol% was fitted using the layered model approach of the AFit programme due to the large behaviour (and suspected coexistence of two structures) observed upon cooling at transition phase temperatures. The samples containing 6 and 10 mol% were fitted using the quasi-molecular approach. Single bilayer data was fitted using the layered model approach.

The initial scattering lengths densities (SLD) used in the layered model approach are given in Table 3.2.

Material	SLD (10^{-6} Å^{-2})
Si	2.07
SiO_2	3.41
H_20	-0.56
D_20	6.35
Palmitoyl chain C_{30} H_{62}: Gel	-0.41
Fluid	-0.32
Deuterated Palmitoyl chain C_{30} D_{62}: Gel	7.66
PC head-group $C_{10}H_{18}O_8PN$	2.66
Cholesterol	0.22

Table 3.2 Scattering length densities used in DPPC and cholesterol bilayers. All values are from Fragneto (2000) except cholesterol from Deme (1997). The fluid phase chain value is calculated using volume of 1000Å^3, whilst gel used 800Å^3.

The low amounts of cholesterol of this study generally have little or no effect on the scattering length density of the chain region. Even the presence of 10% cholesterol only reduces the SLD of the chain region from –0.41 x 10^{-6}Å^{-2} to –0.36 x 10^{-6}Å^{-2}. An increase in the SLD of 0.05 x 10^{-6}Å^{-2} has practically no effect on the fit.

3.5 Phase behaviour of DPPC double bilayers

3.5.1 Introduction

The reflectivity of the DPPC double bilayer was measured in D_2O at various temperatures between 25°C and 48°C and down to 27°C. The thickness and roughness of the oxide was found to be a 8±1Å and 3±1Å respectively.

3.5.2 Gel Phase Structure

The reflectivity was measured initially in the gel phase temperatures of 25°C and 33°C, and then at 27.1°C after cooling down from the fluid phase. The fitted profiles are shown in Figure 3.2, with the parameters listed in Table 3.3.

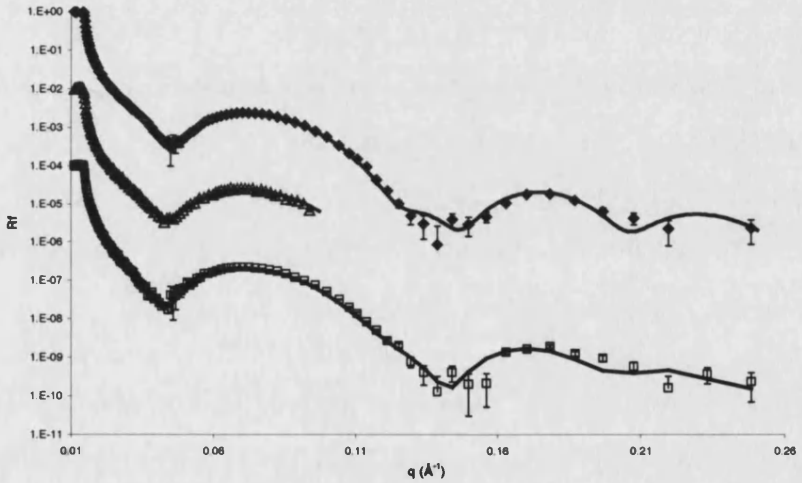

Figure 3.2 Fitted profiles of DPPC double bilayer at 25°C (♦) and 33°C (Δ), and 27.1°C after cooling from fluid phase (□).

	dw	lDb	lDc	lAPM	lRou	lCov	Dw	uDb	uDc	uAPM	uRou	uCov
25.0°C	12±1	50±2	35±1	46±2	3±1	100±2	27±1	49±2	34±1	47±2	5±2	93±4
33.0°C	12±1	50±2	35±1	46±2	3±1	100±2	29±1	49±2	34±1	47±2	5±2	92±4
27.1°C	12±1	50±2	35±1	46±2	3±1	100±2	29±1	49±2	34±1	47±2	9±2	80±4

Table 3.3 Fitted parameters of DPPC double bilayer at 25°C and 33°C, and then 27.1°C after cooling from fluid phase.

The upper and lower bilayers had similar thickness and roughness, but had different coverages, with the upper bilayer having a lower coverage. The difference was likely due to the use of the Schaefer deposition for the upper bilayer.

The gel structure after cooling from the fluid phase was similar to the initial structures, apart from its coverage and upper bilayer roughness. When the bilayers are heated to the fluid phase their coverage usually increases and then contracts when cooled back to the gel phase. The difference in coverages could be due to an annealing of the chains upon cooling from the fluid phase. The behaviour was also observed in the majority of the cholesterol containing samples.

The gel phase APM of the DPPC double bilayer of 47±2Å² was the same as the well defined value for vesicles of 47.9Å² (Nagle 2000). The thicknesses of the chain regions were also very similar to vesicle values of 35Å (Wiener 1989) and 34Å (Nagle 1996). They were slightly higher than those of adsorbed bilayers on silicon of 32Å (Koenig 1996), but were similar to deposited monolayers, which had a thickness of 22±4Å per leaflet including the head-groups (Kim 2001). The outer bilayer was therefore structurally similar to vesicles in solution and other deposited systems.

As the APM are similar to those of the vesicles, it is likely then that the chains are tilted like those in the vesicles (Banerjee 2002). Using a value of 41Å for the extended length of the acyl part of the DPPC bilayer (32 carbon atoms) and the chain region thicknesses, the upper bilayer had a chain tilt of 34° relative to the bilayer normal. The lower bilayer had a chain tilt of 31°. These were similar to those of literature, which vary around 30° (McIntosh 1980, Smith 1988, Sun 1994).

The three Langmuir-Blodgett depositions were deposited using monolayers with 49±1Å² and the Schaefer at 48±1Å². The bilayers had very similar APM to these. The structure of the monolayer is therefore not perturbed on deposition.

3.5.3 Fluid phase Behaviour

The reflectivity of the sample was measured at fluid phase temperatures between 41.8°C to 48.9°C and upon cooling back to 42.7°C. The fitted profiles at 41.9°C, 48.9°C and 42.7°C are shown in Figure 3.3 and the parameters listed in Table 3.4.

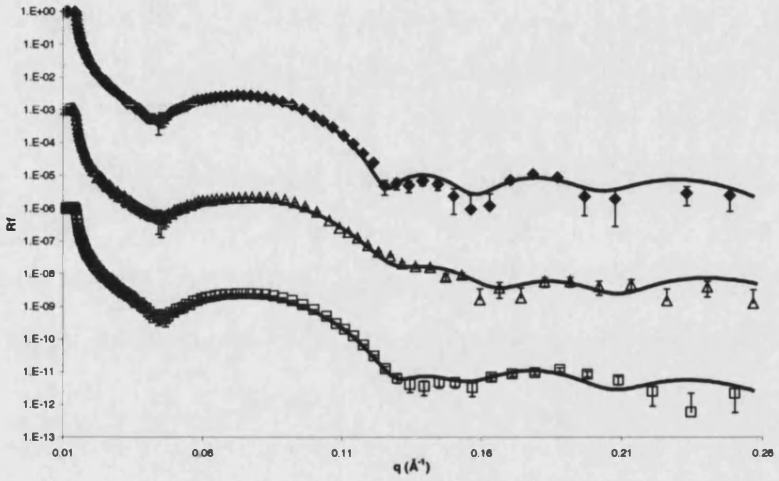

Figure 3.3 Fits of the reflectivity profiles of DPPC double bilayer at 41.9°C (♦), 48.9°C (Δ) and 42.7°C (□).

	dw	lDb	lDc	lAPM	lRou	lCov	Dw	uDb	uDc	uAPM	uRou	uCov
25.0°C	12±1	50±2	35±1	46±2	3±1	100±2	27±1	49±2	34±1	47±2	5±2	93±4
41.9°C	12±1	47±2	35±1	46±2	3±1	100±2	32±1	44±2	30±1	53±2	7±2	100±2
42.7°C	13±1	48±2	35±1	46±2	3±1	100±2	31±1	43±2	29±1	55±2	6±2	100±2
44.4°C	13±1	44±2	34±1	47±2	3±1	100±2	31±1	43±2	28±1	57±2	6±2	100±2
48.9°C	12±1	42±2	31±1	52±2	3±1	100±2	33±1	42±2	30±1	55±2	8±2	100±2
44.4°C	13±1	44±2	34±1	47±2	3±1	100±2	31±1	43±2	28±1	57±2	6±2	100±2
42.7°C	14±1	45±2	35±1	46±2	4±1	100±2	31±1	44±2	30±1	53±2	8±2	100±2

Table 3.4 Fitted parameters of fluid phase temperature DPPC double bilayer with increasing and decreasing temperature.

The upper bilayer exhibited parameters consistent with a fluid phase structure over the whole fluid phase temperature range. The transition to the fluid phase occurred between 40.3°C – 41.8°C, which was very close to that of 41.8°C of DPPC vesicles in solution (Racansky 1987). The lower bilayer however did not become fluid until 48.8°C. The lower bilayer therefore needed a temperature of 7°C higher than that of

the upper bilayer and of vesicles to become fluid. Similar behaviour was observed in DSPC double bilayers where a temperature of 10°C higher was needed for the lower bilayer to become fluid (Fragneto 2001). The likely reason for the difference in behaviour is that it is caused by a higher substrate restraining effect on the lower bilayer compared to the upper. Upon reducing the temperature to 44.4°C the lower bilayer returned to a gel like structure with parameters similar to the previous 44.4°C showing that the transition is completely reversible.

In literature the fluid phase APM of DPPC has a wide spread of values ranging from 56 – 72Å² (Nagle 2000). This is partly due to the presence of fluctuations in the bilayers and variations from the analytical method and sample type used. The APM of 57±3Å² lied within the range, whilst the lower bilayer value of 52Å² was just below the range. The thicknesses of the chain regions were similar to those of literature, where adsorbed bilayer thicknesses were 28Å (Koenig 1996), multilamellar vesicles 26Å (Lewis 1983) and 29Å (Nagle 1996) and unilamellar vesicles 26Å (Tristram-Nagle 1993).

The roughness of the upper bilayer increased slightly by 3Å, whereas the lower remained constant. The main water layer increased in thickness by 4 – 6Å. It then decreased back to 29Å when cooled to 25°C. This behaviour was not observed in any of the other samples, and it is unclear why it occurred. The upper bilayer coverage increased by 7% as expected from an increase in APM and is identical to the increase seen in OTS supported DMPC bilayers (Hughes 2002b).

3.5.4 Transition Phase Behaviour

The sample exhibited transitional behaviour upon heating between 35.9°C to 40.3°C and upon cooling between 39.9°C to 35.7°C. Different behaviour was observed depending on the direction of the gel – fluid phase change.

3.5.4.1 Behaviour between 35.9°C to 40.3°C

Three representative fits are shown in Figure 3.4 and the parameters are listed in Table 3.5, along with the gel phase 25°C and fluid phase 48.9°C.

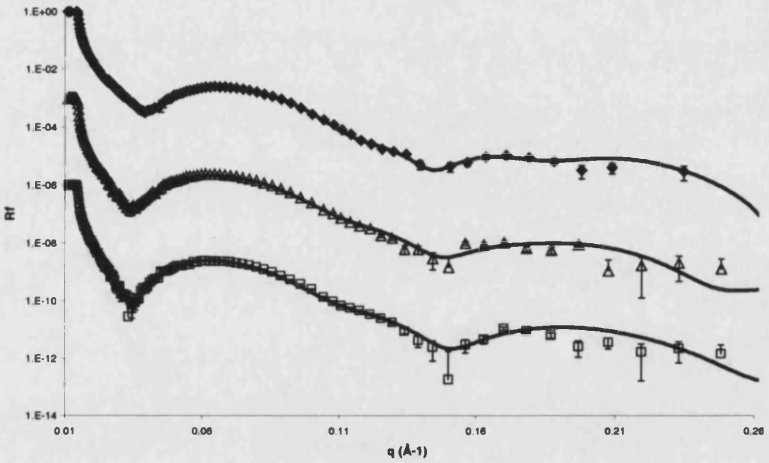

Figure 3.4 Fits of the reflectivity profiles of DPPC double bilayer at 35.9°C (♦), 37.7°C (Δ) and 39.5°C (□).

	dw	lDb	lDc	lAPM	lRou	lCov	Dw	uDb	uDc	uAPM	uRou	uCov
25.0°C	12±1	50±2	35±1	46±2	3±1	100±2	27±1	49±2	34±1	47±2	5±2	93±4
35.9°C	12±1	50±2	35±1	46±2	3±1	100±2	34±1	48±2	34±1	47±2	11±2	84±2
37.7°C	13±1	50±2	38±1	42±2	3±1	100±2	40±1	47±2	35±1	46±2	15±2	75±2
38.5°C	14±1	49±2	38±1	42±2	3±1	100±2	43±1	45±2	34±1	47±2	14±2	73±2
39.5°C	14±1	49±2	38±1	42±2	3±1	100±2	42±1	45±2	34±1	47±2	14±2	73±2
40.3°C	14±1	49±2	38±1	42±2	3±1	100±2	42±1	45±2	34±1	47±2	14±2	74±2
44.4°C	13±1	44±2	34±1	47±2	3±1	100±2	31±1	43±2	28±1	57±2	6±2	100±2
48.9°C	12±1	42±2	31±1	52±2	3±1	100±2	33±1	42±2	30±1	55±2	8±2	100±2

Table 3.5 Fitted parameters of transition phase region structures of DPPC double bilayer. The gel phase 25.0°C and fluid phase 44.4°C are given for comparison.

The structure of the lower bilayer and lower water layer retained a constant gel structure throughout the transitional temperature region. The thickness of the upper bilayer chain region also retained a gel phase thickness throughout, although the head-groups became slightly thinner, reducing the overall thickness of the bilayer. The main structural changes were increases in the thickness of the main water layer, in the roughness of the water layer – bilayer interface, in the solvation of the bilayer and in the bilayer roughness. The variation of these parameters between 25°C – 48.9°C are shown in Figure 3.5 and the maximum increases relative to the gel phase are listed in Table 3.6.

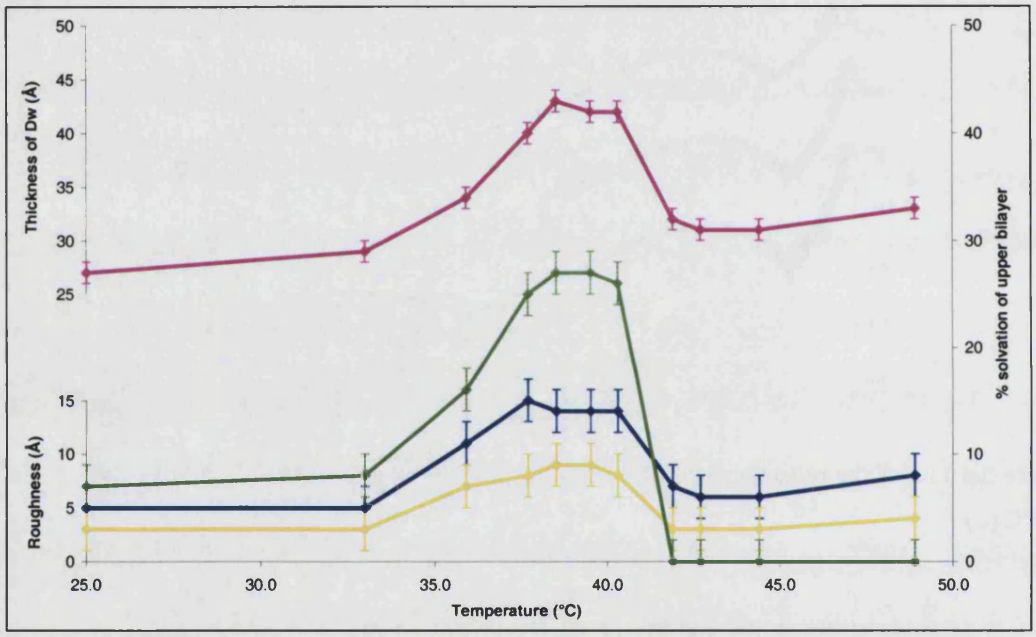

Figure 3.5 Upper bilayer and Dw parameters vs. temperature of DPPC double bilayer. Thickness main water layer (pink), roughness of water – bilayer interface (yellow), solvation of upper bilayer (green) and the average upper bilayer roughness (blue).

	Gel value (25°C)	Maximum transition phase value	Maximum increase
Water layer thickness	27Å	43Å	16Å
Water layer rougness	3Å	9Å	6Å
Upper bilayer rougness	5Å	15Å	10Å
Solvation of upper bilayer	7%	27%	20%

Table 3.6 Comparison of gel values and maximum transition values of DPPC double bilayer.

The water layer increased by a half its size and the roughness tripled in size. The bilayer roughness also tripled in size. DPPC vesicles exhibit pre-transitional behaviour starting at 35.7°C, which continues until the chain melting transition T_m of 41.8°C (Racansky 1987). Transition behaviour in the double bilayer matched this temperature range.

From the change in the parameters and the range of temperature over which they occurred, it is likely that the upper bilayer is displaying a ripple structure.

Interpretation of Behaviour

There is a striking similarity present between the upper bilayer roughness parameter value and literature values for the ripple amplitude of DPPC bilayers. The Mouritsen group measured the ripple amplitude of mica supported DPPC double bilayers formed by the adsorption of small unilamellar vesicles using AFM (Kaasgaard 2003). They estimated that the minimum value of the amplitude upon heating was 12Å. The roughness parameter of the upper bilayer of was determined to be 15Å by reflectivity. The similarities suggest that the roughness parameter is proportional to the amplitude of the ripple amplitude of the upper bilayer. The validity of this argument is whether the direct measurement of the ripple amplitude by AFM is the same as the roughness modelled in reflectivity using error functions. This needs considerably more work, which is beyond the scope of this thesis.

Another factor that needs to be considered concerning the upper bilayer roughness parameter is the wavelength of the ripple. Literature values for the ripple wavelength are well defined, with values normally between 100 – 150Å depending on the system (Woodward 1996 *and references therein*). The most recent measurement for DPPC was 150Å by the AFM measurements of Mouritsen group (Kaasgaard 2003). As the wavelength size is large compared to the ripple and the thickness of the bilayer itself, the periodicity would not be expected to significantly contribute to the roughness parameter. Changes in the roughness parameter would be expected to be predominantly determined by changes in the amplitude.

The increase in the solvation parameter of the upper bilayer is expected to occur for a dynamic rippling structure. This does not necessarily mean that the actual solvation of the bilayer has increased, only that there is increased solvent in the modelled layer due to the undulation nature of the bilayer.

In other systems the properties of the ripple phase is thought to progressively increase or decrease when changing temperature. This behaviour is not clear though, as the ripple periodicity of DMPC multilamellar vesicles was observed to decrease upon increasing the temperature (Matuoka 1990); whilst in other studies it did not change with temperature (Woodward 1996). In the latter study the ripple amplitude was observed to decrease upon decreasing temperature, becoming almost zero at the pre-transition temperature. Here however the behaviour varied with increasing temperature, with the parameters initially increasing, then remaining constant between 38.5°C to 40.3°C and then decreasing when approaching the transition temperature. This non-linear behaviour versus temperature was observed in all samples up to 10 mol% cholesterol. If the upper bilayer roughness and increase in the water layer are directly proportionally to the ripple structure, then the double bilayers is therefore behaving differently to that of vesicles.

3.5.4.2 Behaviour between 39.9°C – 35.8°C

It was not possible to fit the profiles using only one model. The profile shape changed remarkably upon cooling in the transition phase compared to the fluid phase profile. Figure 3.6 shows a comparison of the profiles at 42.7°C in the fluid phase and 37.3°C in the transition phase. The shape and position of the first fringe has dramatically changed. It is possible that the first fringe actually consists of two separate fringes from reflectivity from two coexisting structures (this is clearer in the 1 – 4 mol% profiles). The shift in the position of the first minimum to a lower q value indicates that the sample has become thicker, as its position in the gel and fluid phases is proportional to the overall sample thickness (Fragneto 2001). The sample can only become thicker by an increase in the thickness of the water layer or by an increase in the roughness of the upper bilayer, as the lower bilayer is usually static during the transition phase. Indeed the profile indicates that the lower bilayer has not

changed, as the second fringe is sensitive to the structure of the lower bilayer (Fragneto 2001); both profiles have the same second fringe structure at the fluid and transition temperature.

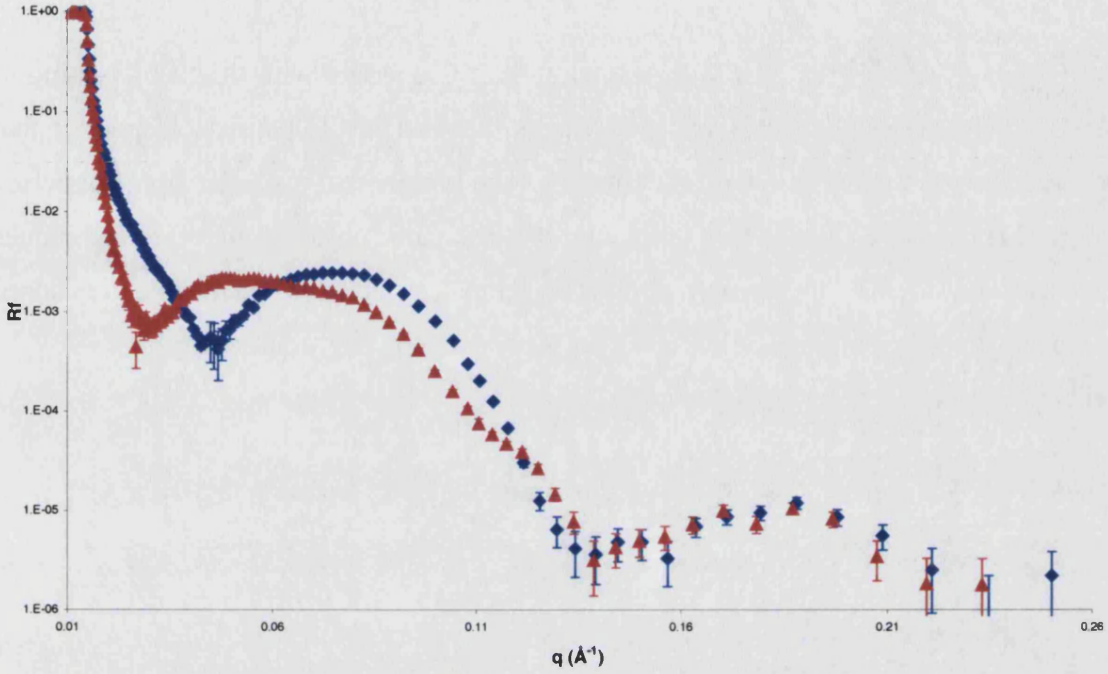

Figure 3.6 Comparison of the profiles at 42.7°C in the fluid phase (blue) and 37.3°C in the transition phase (red).

In multilamellar vesicles studies, the behaviour upon cooling in the transition phase has also been observed to be different from that observed upon heating (Matuoka 1993, Katsaras 2000). Upon heating, the ripple structure consisted of a population of asymmetric ripples with a short wavelength of 150Å and amplitude of 12Å. Upon cooling, coexistence of short and long ripple phases occurred. The short wavelength was similar to that present upon heating, whilst the long wavelength had almost double the wavelength of the short ripple phase. The Mouritsen group measured the minimum amplitude of the larger ripples as $\geq$ 50Å and wavelength of 280Å of mica supported DPPC double bilayers (Kaasgaard 2003). The d spacing was also observed to be 14Å thicker upon cooling. The DPPC sample used was almost identical to the sample here, except that the double bilayer was fabricated using the vesicle adsorption method and was upon mica. The behaviour of that sample and the sample here would therefore be expected to be very similar, if not identical, despite the use of different fabrication methods.

Fitting of profiles using two ripple models

The first fringe in the profiles of all the samples containing 0 – 4 mol% cholesterol appeared to consist of two superimposed fringes. The presence of the second bump on the first fringe is important and should not be ignored by the fit.

Figure 3.7 shows the profile measured at 37.3°C overlaid with the fit of heating to 37.7°C profile. The overlay clearly shows that the profile consists of part of that structure that was exhibited upon heating. The presence of a similar ripple structure to that observed in heating agrees with the behaviour observed by other techniques (Kaasgaard 2003). It is quite possible that the other features of the profile are caused by the presence of large amplitude ripples observed by the Mouritsen group.

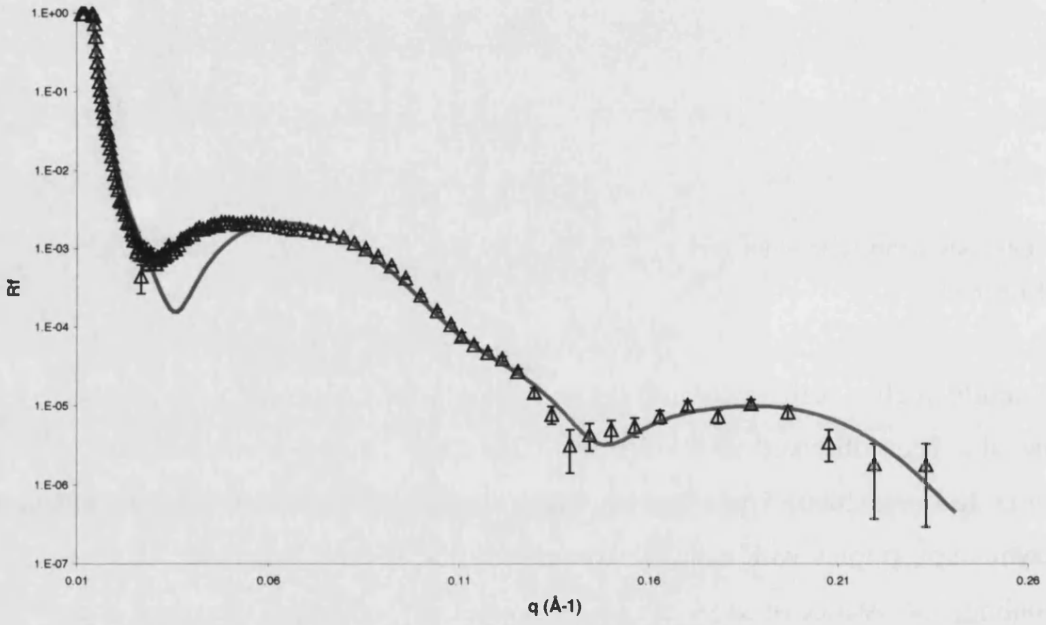

Figure 3.7 Reflectivity profile of cooling down to 37.3°C of DPPC double bilayer. Superimposed is the fit at 37.7°C upon heating.

One possible method of fitting the profiles is based on this expected co-existing ripple structures. The use of two separate models was evaluated. The reflectivity from two models was therefore used to fit different parts of the profile (it must be stated that this is not necessarily valid, further theoretical work is necessary). One model had an upper bilayer roughness and attributes similar to that exhibited upon heating in the transition phase. The other model had a much higher roughness, which

mimicked the large ripple structure observed by the Mouritsen group. Figure 3.8, 3.9 and 3.10 show the best fits of the profiles measured at 39.9°C, 37.3°C and 35.7°C using the separate reflectivity from the two ripple models. The green fits are the smaller ripple model and the red the large ripple phase model. It can be seen that when the two fits are overlaid on the profile they are able to account for all the features of the profile. The large ripple model fits the lower q features of the first fringe, whilst the smaller ripple model the higher q features. The fitted parameters of the models at the different temperatures are listed in Table 3.7.

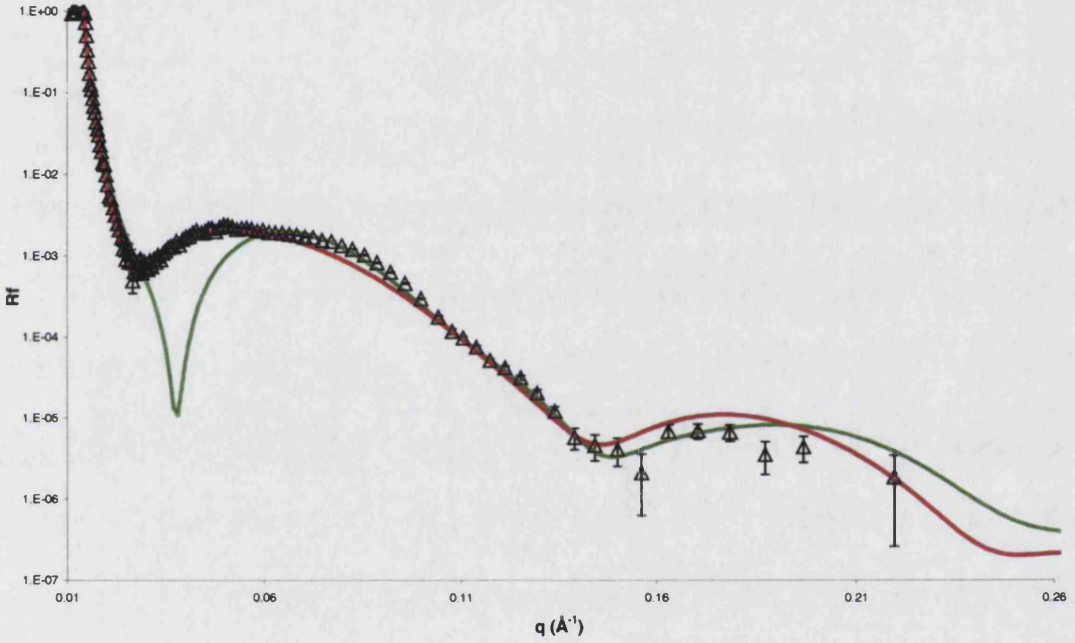

Figure 3.8 DPPC double bilayer profile upon cooling down to 39.9°C fitted using two ripple models. The green line is the small ripple phase, the red the large ripple phase.

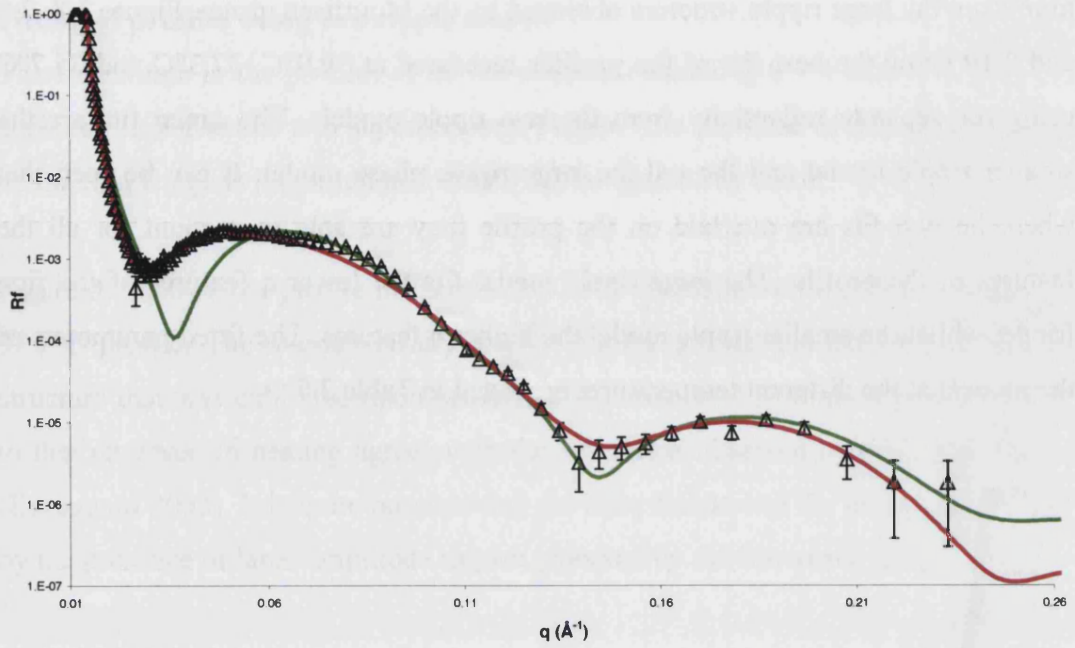

Figure 3.9 DPPC double bilayer profile upon cooling down to 37.3°C fitted using two ripple models. The green line is the small ripple phase, the red the large ripple phase.

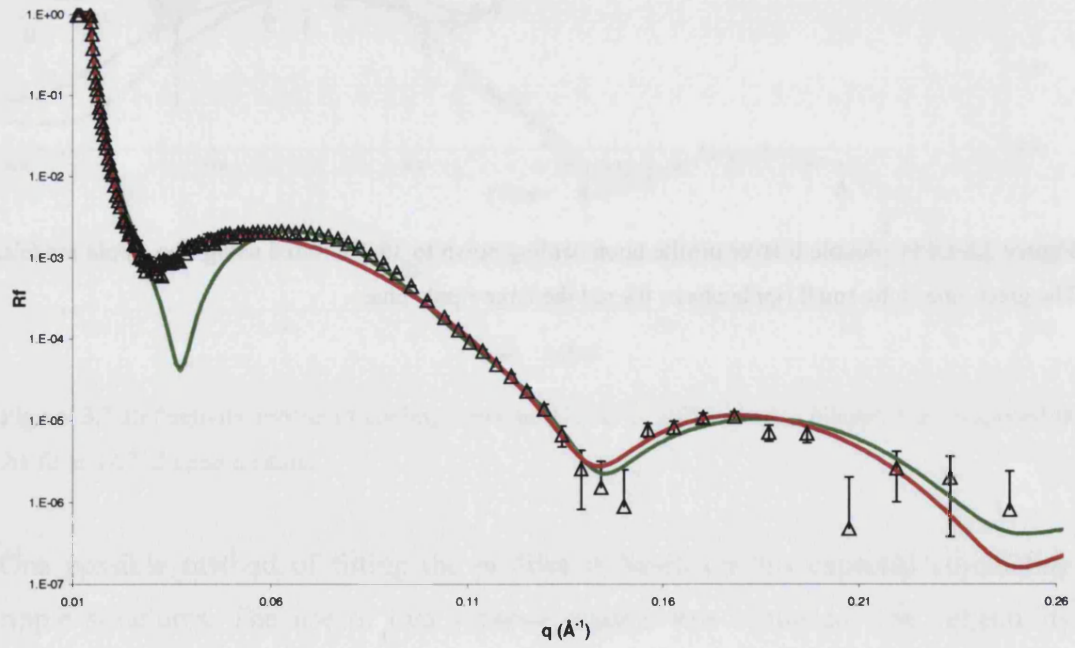

Figure 3.10 DPPC double bilayer profile upon cooling down to 35.7°C fitted using two ripple models. The green line is the small ripple phase, the red the large ripple phase.

		dw	lDb	lDc	lAPM	lRou	lCov	Dw	uDb	uDc	uAPM	uRou	uCov
39.9°C	small	18±1	47±2	37±1	43±2	4±1	96±2	39±1	48±2	34±1	47±2	16±2	63±4
	large	18±1	49±2	38±1	42±2	5±1	100±2	46±1	47±2	34±1	47±2	50±2	58±4
37.3°C	small	18±1	49±2	38±1	42±2	3±1	100±2	41±1	44±2	34±1	47±2	16±2	55±4
	large	18±1	49±2	38±1	42±2	5±1	100±2	44±1	45±2	34±1	47±2	52±2	56±4
35.7°C	small	18±1	48±2	37±1	43±2	4±1	100±2	40±1	45±2	34±1	47±2	15±2	57±4
	large	18±1	49±2	38±1	42±2	4±1	100±2	42±1	46±2	34±1	47±2	47±2	56±4

Table 3.7 Fitted parameters upon cooling DPPC double bilayer in transition phase. Two models were used to fit the profiles, a small ripple model and a large ripple model

Is the superimposition of two models justified?

The fact that it is possible to obtain good fits by the use of two models and obtain behaviour similar to those obtained on a very similar sample, seems to suggest that the use of two models is a possible way of interpreting the reflectivity data. However it is unlikely that the solution is as simple as just overlaying the two fits. It is more likely that a scaled average of the two fits is necessary. There could also be other issues to consider. The question is how the two sets of reflectivity should be combined? This is the crux of the problem, and determines whether the parameters given in Table 3.7 are valid. If the ripples in the sample were actually separate domains of small ripples and larger ripples, with domain sizes larger than the neutron coherence length, then it would be expected that the overall reflectivity of the profile would be a measured average of the reflectivity from the two types of domains. For example, if the ratio of large ripples to small ripples were 1:1, one would then multiply each fit by a half, and then sum to give the overall fit. This is shown in Figure 3.11 for the profile at 37.3°C. As expected, it can be seen that the ratio method is unable to fit satisfactory any of the features of the profile. If the ratio is increased in favour of one of the models then the fit decreases for the other features taken into account by the other model. The only way for this ratio method to work successfully would be for the two models to be fitted so that they are above the features of the profile, and then scaled down to the profile by the ratios. This is simply not a viable method of fitting and it increases the uncertainty by inclusion of an unknown ratio factor.

It is unlikely however that the two ripple structures exist as large domains. In the AFM studies of the Mouritsen group on DPPC double bilayers they found that large ripples coexisted within small ripple domains (Kaasgaard 2003). The domains were not homogeneous.

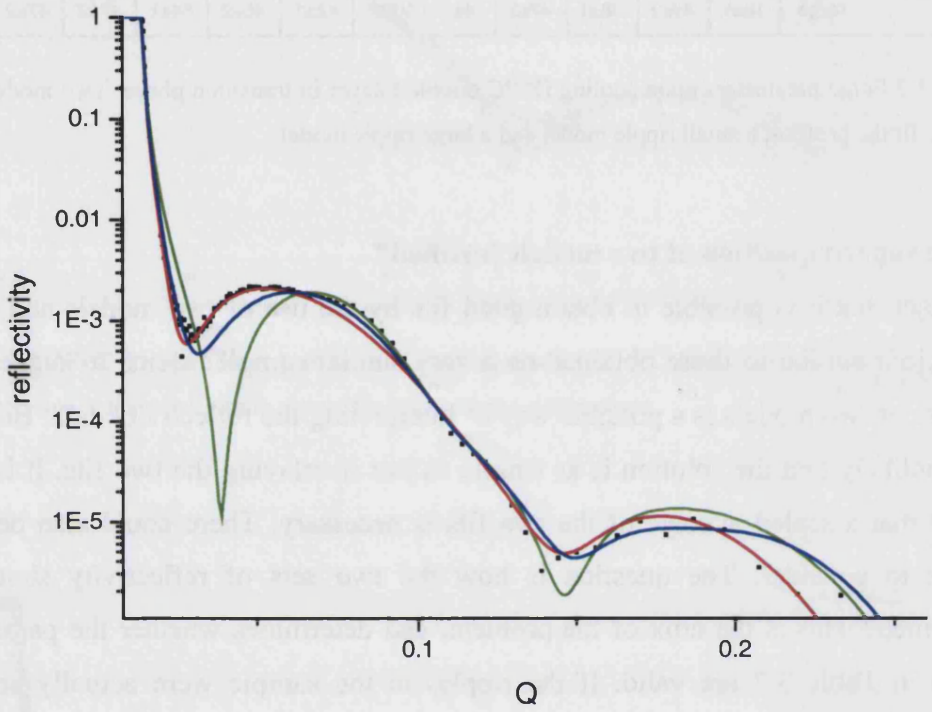

Figure 3.11 Reflectivity profile at 37.3°C (black dots). The large roughness model is red, low roughness model green. The blue line is a 1:1 average of the two fits.

If the size of the domains of large and small ripples were smaller than the neutron coherence length or if there was coexistence within the domains, then the analysis of the data is much more complex (Goldar 2002, Goldar PhD Thesis 2002, University of Bath) and beyond the scope of this thesis. It is likely that the profiles here fall into this category, due to the coexistence of large ripples within smaller ripple domains observed by the AFM measurements.

As the two superimposed fits give similar results to those of the Mouritsen group, what follows is a discussion of the two models based on the proposed link. This is an

approximation, and source for further work. The likely existence of two high roughness ripple structures poses interesting work for theorists.

Small ripple model results

The best fits using the small ripple model have an upper bilayer roughness of 16±2Å and water layer thickness of 40±1Å. Compared to the fluid phase structure at 42.7°C, this is an increase of 8±2Å in the roughness and 9±1Å in the water layer thickness. If the upper bilayer roughness is actually a direct measurement of the ripple amplitude, this would mean that the amplitude of the upper bilayer is slightly higher than that measured by AFM of 12Å (Kaasgaard 2003). However, the measurement of the amplitude by AFM study gave the minimal possible value, since the size of the AFM tip was comparable to the size of the ripples. It was therefore unlikely that the tips were able to reach the bottom of the ripple valleys, leading to an underestimate. This was found to be particularly true in the case of the small ripples, where the underestimate of the amplitude is most pronounced. It is likely therefore that the difference between the two values is insignificant, and that the value of 16±2Å could be a good representation of the small ripple phase amplitude.

Large ripple model results

The best fits using the large ripple model have an upper bilayer roughness of 50±2Å and water layer thickness of 44±1Å. This gives an increase of 42±2Å in the roughness and 13±1Å in the water layer thickness in comparison to the fluid phase. The average roughness of the upper bilayer was the same value as the minimum amplitude of the large ripple phase measured by AFM. In comparison to the small ripple phase, the underestimation of the amplitude is less pronounced due to the larger amplitude and wavelength of this ripple phase. Therefore the average value of 50±2Å could be a good representation of the large ripple phase amplitude.

Lower bilayer and water layer structure

The both ripple models give almost identical parameters for the structure of the lower bilayer and the lower water layer. This similarity suggests the validity of the use of two ripple models to fit this data. The thickness of the chain region is similar to that

observed in the transition region when heating, which was slightly higher than the gel phase values. The lower water layer has swelled during the transition region. Whilst swelling was also observed upon heating, it was not as large as this. The swelling of the lower water layer could be due to the decrease in confinement of the lower bilayer by the rippling upper bilayer causing the main water layer to increase. The roughness of the lower bilayer did not increase, indicating that the lower bilayer is not exhibiting ripple behaviour.

Trends in parameters as a function of temperature

Unlike upon heating, there the thickness of the water layer did not vary as a function of temperature in the small ripple model. The upper bilayer roughness also remained relatively constant. If the small ripple structure is similar to that observed upon heating, then it is behaving differently upon cooling. There is however a similarity between the maximum value of the upper bilayer roughness observed upon heating and the constant value observed upon cooling. The presence of the large ripple phase could be enabling the small ripple phase to reach its maximum amplitude across the whole temperature range, rather than reach a maximum in the middle of the temperature range.

In the large ripple model the water layer thickness was found to decrease progressively as the temperature was lowered, whilst the upper bilayer roughness had a maximum at value 37.3°C. It is possible therefore that the large ripple phase has a maximum amplitude in the middle of the transition temperature range, whilst the smaller ripple amplitude remains relatively constant throughout.

3.6 Phase behaviour of 1 mol% Cholesterol 99 mol% DPPC

3.6.1 Introduction

The phase behaviour of 1 mol% cholesterol 99 mol% DPPC double bilayer sample was investigated at temperatures between 25°C and 43°C and down to 25°C in D_2O. The reflectivity of the gel and fluid phases was also measured in a number of solvent contrasts to aid the resolution of the structure. The thickness and the roughness of the oxide at all temperatures were 8±1Å and 3±1Å respectively.

3.6.2 Gel Phase Structure

The sample was measured initially in the gel phase at 25.0°C and 30.5°C, then at 25.2°C after cooling from the fluid phase. The fitted profiles are shown in Figure 3.12 and parameters in Table 3.8.

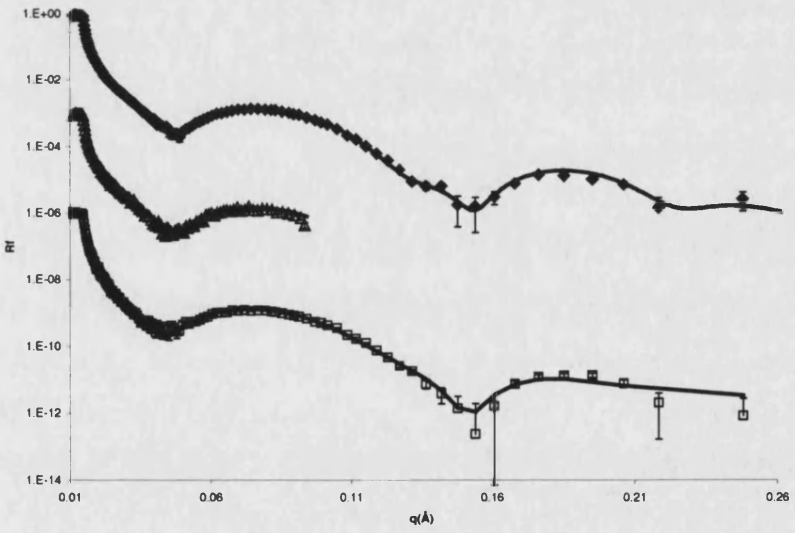

Figure 3.12 Fitted profiles of 1 mol% cholesterol 99 mol% DPPC double bilayer at 25.0°C (♦) and 30.5°C (Δ), and 25.2°C after cooling from fluid phase (□).

	dw	lDb	lDc	lAPM	lRou	lCov	Dw	uDb	uDc	uAPM	uRou	uCov
25.0°C	9±1	49±2	34±1	47±2	5±1	97±2	22±1	48±2	35±1	46±2	7±2	86±2
30.5°C	9±1	49±2	34±1	47±2	5±1	100±2	23±1	48±2	35±1	46±2	7±2	86±2
25.2	10±1	46±2	35±1	46±2	3±1	95±2	28±1	48±2	34±1	47±2	10±2	88±4

Table 3.8 Fitted parameters of 1 mol% cholesterol 99 mol% DPPC double bilayer at 25.0°C and 30.5°C, and then 25.2°C after cooling from fluid phase

The gel phase structure after the fluid phase was similar to that of the initial bilayers, except for an increase in the main water layer. It is likely that the thickness is equilibrated during the temperature scan. Similar behaviour was observed in the 2 mol% sample. This is discussed more fully in section 3.13.2.

The upper and lower bilayers had similar structures, except that the upper bilayer had a slightly higher roughness and a lower coverage. The thickness and area per molecule of the 1 mol% sample were very similar to those of the DPPC sample (Table 3.3) it is likely that the presence of this ratio of cholesterol is not interfering with the structure and the tilt of the DPPC.

The scattering density profiles of the 1 mol% sample and the DPPC samples at 25°C are shown in Figure 3.13. The main differences are in the thickness of the main water layer (5Å) and in the lower water layer (3Å). The structures of the bilayers however are similar, with both samples having a bilayer thickness of 34 – 35Å and similar coverage. The upper bilayer of the 1% sample had a slightly higher roughness than the pure DPPC sample.

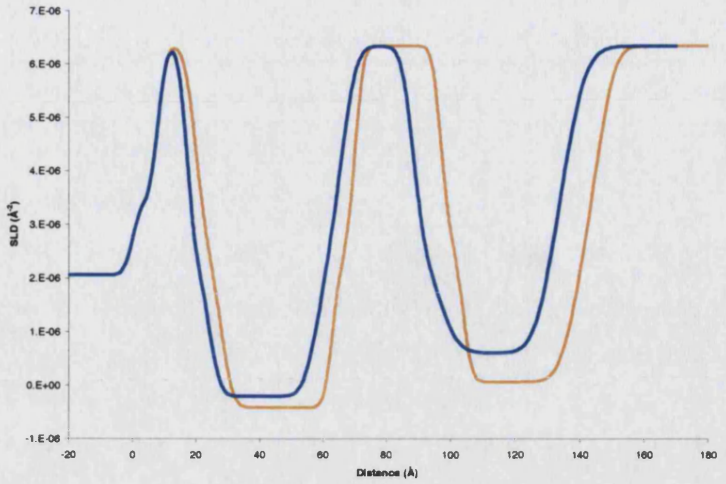

Figure 3.13 Scattering density profiles of 1% cholesterol 99% DPPC double bilayer (blue) and pure DPPC sample (orange) at 25°C.

3.6.3 Fluid phase Structures

The reflectivity of the sample in D_2O was measured at fluid phase temperatures between 43.2°C to 47.3°C and to 43.9°C. The fitted profiles at 43.2°C, 47.3°C and 43.9°C are shown in Figure 3.14 and the fitted parameters are listed in Table 3.9.

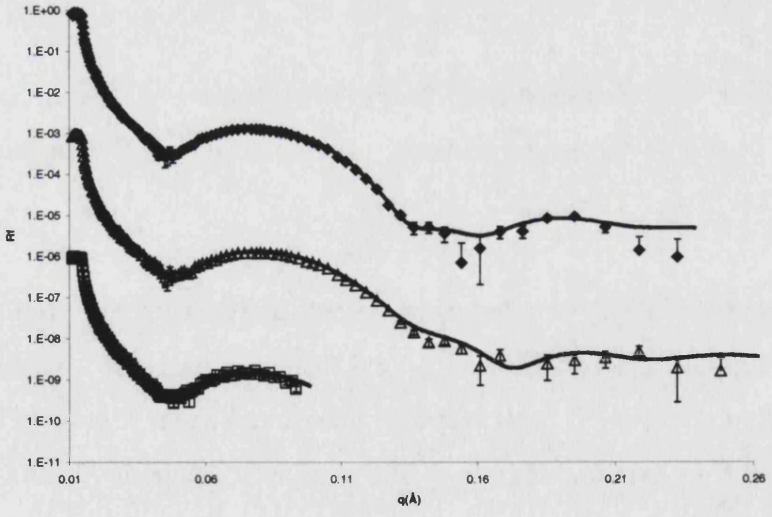

Figure 3.14 Fits of the reflectivity profiles of 1 mol% cholesterol 99 mol% DPPC double bilayer at 43.2°C (♦), 47.3°C (Δ) and 43.9°C (□).

	dw	lDb	lDc	lAPM	lRou	lCov	Dw	uDb	uDc	uAPM	uRou	uCov
25.0°C	9±1	49±2	34±1	47±2	5±1	97±2	22±1	48±2	35±1	46±2	7±2	86±2
43.2°C	10±1	45±2	34±1	47±2	3±1	97±2	29±1	42±2	28±1	57±2	9±2	95±4
47.3°C	10±1	41±2	30±1	53±2	3±1	100±2	29±1	42±2	28±1	57±2	9±2	95±4
43.9°C	8±1	45±2	34±1	47±2	3±1	97±2	28±1	44±2	30±1	53±2	9±2	95±4

Table 3.9 Fitted parameters of fluid phase structure 1 mol% cholesterol 99 mol% DPPC double bilayer at various temperatures

The main transition to the fluid phase (Tm) occurred between 42.1°C to 43.2°C, which was just slightly higher than of the transition observed in DPPC vesicles (41.8°C). This is different to the effect of very low amounts of cholesterol previously observed in DMPC vesicles, where it caused a minute depression of Tm (Lemmich 1997).

The lower bilayer behaved similar to the DPPC sample as it needed a temperature of 5°C higher than that of the upper bilayer to become fluid. When the temperature was reduced to 43.6°C the lower bilayer became gel like again with identical parameters to that of the previous 43.2°C. The difference in behaviour between the two bilayers is likely due to higher restraining effect by the substrate on the lower bilayer.

The main water layer increased from 23Å in the gel phase to 29Å in the fluid phase, whilst that of the lower water remained did not change. The increase was also observed in the 2 mol% sample.

The changes in the bilayer parameters of the 1% sample were very similar to those in the DPPC sample, in that the chain region thickness decreased by 4Å, whilst the roughness did not change. The areas per molecule and chain region thicknesses were similar to the fluid phase APM range of 56 – 72Å^2 (Nagle 2000) and thickness of 29Å (Nagle 1996).

3.6.3.1 Fluid Phase Contrast Exchange Structures at 47°C

The sample was measured in D_2O, SMW and 4MW at 47°C. The fitted profiles are shown in Figure 3.15 and the parameters are listed in Table 3.10. With the SMW it was necessary to use a scattering length density of 3.07 x $10^{-6}Å^{-2}$ instead of the calculated value of 2.07 x $10^{-6}Å^{-2}$. This was consistently found to be the case for a wide range of samples and is thought to be due to incomplete exchange of solvent.

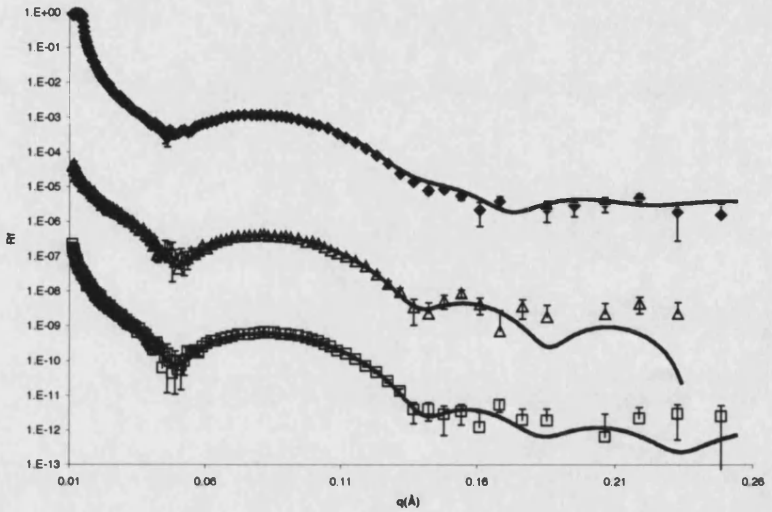

Figure 3.15 Fitted profile of 1 mol% cholesterol 99 mol% DPPC double bilayer at 47°C in D_2O (♦), SMW (Δ) and 4MW (□).

	dw	lDb	lDc	lAPM	lRou	lCov	Dw	uDb	uDc	uAPM	uRou	uCov
D_2O 47.3°C	10±1	41±2	30±1	53±2	3±1	100±2	29±1	42±2	28±1	57±2	9±2	95±2
SMW 47.7°C	8±1	38±2	28±1	57±2	4±1	100±2	25±1	45±2	31±1	52±2	5±2	100±2
4MW 47.4°C	8±1	40±2	29±1	55±2	4±1	100±2	28±1	39±2	29±1	55±2	7±2	100±2
Average	9±1	40±2	29±1	55±2	4±1	100±2	27±2	42±3	29±2	55±3	7±2	98±3

Table 3.10 Fitted parameters of different contrasts 1 mol% cholesterol 99 mol% DPPC double bilayer at 47°C and the average of the values. SMW is silicon matched water and 4MW is 4-matched water.

The thicknesses of both chain regions were all similar. The main variations were in the thickness of the water layer, with SMW having the largest difference, and the upper bilayer roughness. Overall, the average of the parameters gave a good compromise structure with most contrast parameters within ± 2 of the average.

3.6.4 Transition Phase Structures and Behaviour

The sample exhibited transitional behaviour between 33.1°C to 42.1°C and between 41.4°C to 31.0°C. Different behaviour was observed depending on the direction of the temperature change.

3.6.4.1 Structural behaviour between 33.1°C – 42.1°C

Three fits during the transition phase temperatures are shown in Figure 3.16. The parameters are given in Table 3.11, along with the gel phase 25.0°C and fluid phase 47.3°C for comparison.

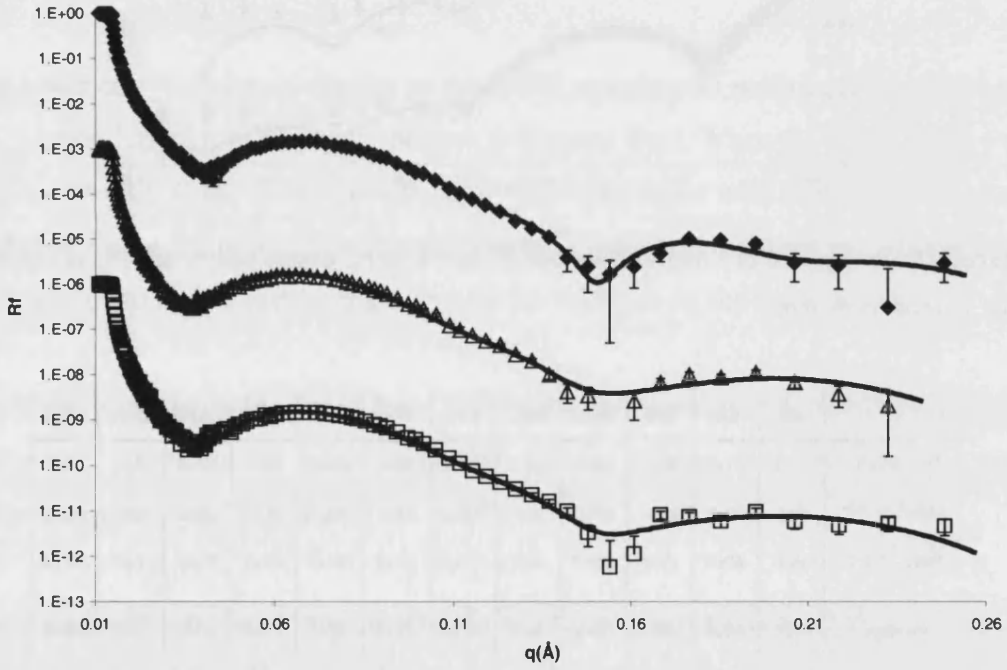

Figure 3.16 Fitted reflectivity profiles of 1 mol% cholesterol 99 mol% DPPC double bilayer at 33.8°C (♦), 35.9°C (Δ) and 41.3°C (□).

	dw	lDb	lDc	lAPM	lRou	lCov	Dw	uDb	uDc	uAPM	uRou	uCov
25.0°C	9±1	49±2	34±1	47±2	5±1	97±2	22±1	48±2	35±1	46±2	7±2	86±4
33.1°C	8±1	49±2	34±1	47±2	5±1	100±2	26±1	48±2	35±1	46±2	7±2	86±3
33.8°C	9±1	47±2	34±1	47±2	5±1	100±2	30±1	51±2	35±1	46±2	12±2	78±3
34.8°C	10±1	46±2	35±1	46±2	5±1	98±2	35±1	49±2	34±1	47±2	16±2	78±3
35.9°C	10±1	46±2	35±1	46±2	5±1	98±2	36±1	49±2	34±1	47±2	16±2	78±3
37.1°C	10±1	46±2	35±1	46±2	5±1	98±2	36±1	49±2	34±1	47±2	16±2	78±3
37.5°C	10±1	46±2	35±1	46±2	5±1	98±2	37±1	49±2	34±1	47±2	16±2	78±3
38.4°C	10±1	46±2	35±1	46±2	5±1	98±2	36±1	49±2	34±1	47±2	16±2	78±3
39.3°C	10±1	46±2	35±1	46±2	5±1	98±2	36±1	49±2	34±1	47±2	16±2	78±3
40.3°C	10±1	46±2	35±1	46±2	5±1	98±2	36±1	49±2	34±1	47±2	16±2	78±3
41.3°C	10±1	46±2	35±1	46±2	5±1	98±2	34±1	49±2	34±1	47±2	15±2	78±3
42.1°C	10±1	46±2	35±1	46±2	5±1	98±2	32±1	49±2	34±1	47±2	12±2	78±3
47.3°C	10±1	41±2	30±1	53±2	3±1	100±2	29±1	42±2	28±1	57±2	9±2	95±2

Table 3.11 Fitted parameters at transition phase temperatures of 1 mol% cholesterol 99 mol% DPPC double bilayer. The gel phase 25.0°C and fluid phase 47.3°C are given for comparison.

The structure of the lower bilayer and lower water layer remained static throughout, retaining the gel phase structure. The thickness of the upper bilayer also remained constant. The main changes were increases in the thickness of the main water layer, upper bilayer roughness and solvation. The change in the parameters as a function of temperature 25.0°C – 47.3°C are shown in Figure 3.17. The maximum increase, along with those of the DPPC sample values are listed in Table 3.12. The maximum increase was reached 2°C above the initial increase. The values then remained relatively constant until 41.3°C when they decreased. This differed from the behaviour of the DPPC sample, which had a symmetrical increase and decrease either side of the maximum values at 39°C.

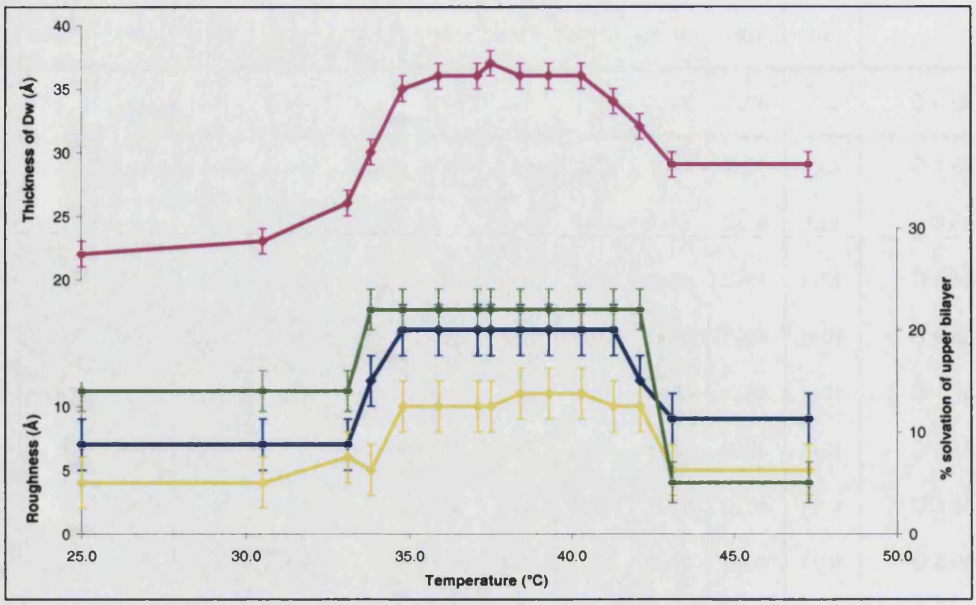

Figure 3.17 Upper bilayer and Dw parameters vs. temperature of 1 mol% cholesterol 99 mol% DPPC double bilayer. Water layer thickness (pink), roughness of water – bilayer interface (yellow), solvation of upper bilayer (green) and the average upper bilayer roughness (blue).

	Gel value (25°C)		Maximum transition phase value		Maximum increase	
	DPPC	1 mol%	DPPC	1 mol%	DPPC	1 mol%
Dw	27Å	22Å	43Å	37Å	16Å	15Å
WRou	3Å	4Å	9Å	10Å	6Å	6Å
Urou	5Å	7Å	15Å	16Å	10Å	9Å
uSolv	7%	14%	27%	22%	20%	8%

Table 3.12 Comparison of the gel phase and maximum transition phase values of 1 mol% cholesterol 99 mol% DPPC double bilayer with DPPC double bilayer.

The maximum increase of the parameters was similar to those of the pure DPPC sample, except for the solvation of the upper bilayer. The parameters suggest that the 1 mol% sample is exhibiting a similar ripple structure to that present in the DPPC sample. The non-linear behaviour versus temperature was similar to the DPPC sample, meaning that its behaviour differed from that observed in other systems (Matuoka 1990, Woodward 1996). A comparison and discussion of the effect of

cholesterol on the ripple structure of the double bilayers upon heating is given in section 3.13.3.

3.6.4.1 Structural behaviour between 41.4°C – 31.0°C

As in the case of the DPPC double bilayer, the 2 mol% sample and the 4 mol% sample, the reflectivity profiles observed upon cooling were complex, especially the shape of the first fringe. It looked to consist of two fringes. This is clearer in these profiles than it was for the DPPC profiles. It was not possible to fit the profiles using only one model. However unlike the DPPC sample, it is not possible to overlay the fit when heated to 36°C on the profile when cooled to 36°C and obtain a fit of part of the profile (Figure 3.18).

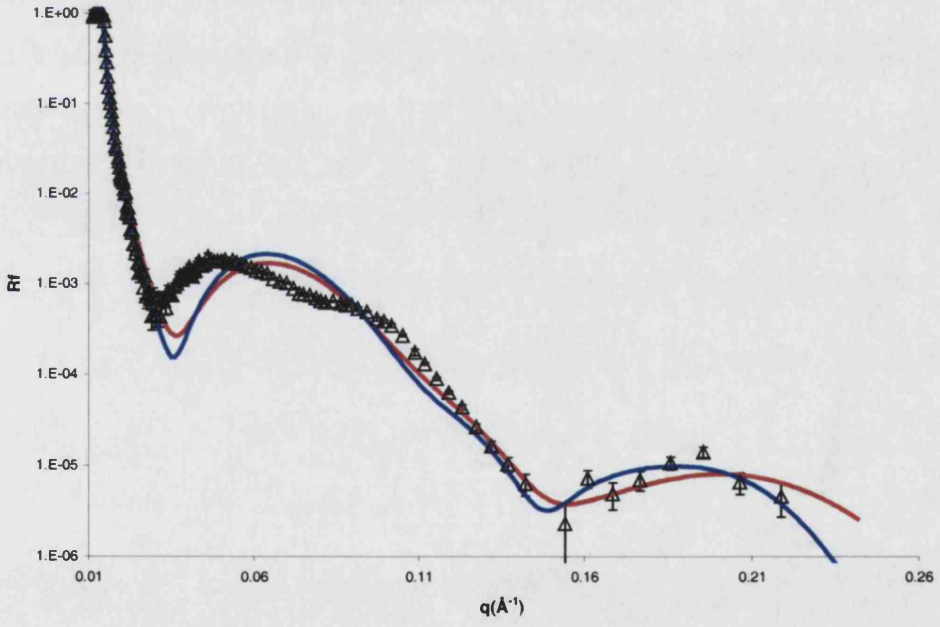

Figure 3.18 1 mol% sample profile when cooled from fluid phase to 36.0°C. Red line is 36°C fit when heated from gel phase. Blue line is DPPC double bilayer best fit when heated to 37.7°C.

The second feature on the first fringe has been shifted to higher q by the presence of 1 mol% cholesterol in the sample. The q position of the minimum of the first fringe is proportional to the overall thickness of the sample for the gel and fluid phases (Fragneto 2001). A shift to higher q indicates a decrease in the sample thickness. If the first fringe does consist of two fringes, then this could suggest that the structure

causing the second fringe at 0.09Å^{-1} is thinner than that present in the DPPC sample and in the 1 mol% sample when heating in the transition temperature range.

If the upper bilayer is exhibiting coexisting large ripple and small ripple structures, like those observed on mica supported DPPC double bilayers (Kaasgaard 2003), then the presence of 1 mol% cholesterol could be reducing the structural features of the smaller ripple structure. When two models are used to fit different parts of the profile, they suggest that this is the case. (The validity of using two models to fit different parts of the profile is not proven, but seems to give close results to that observed by in the mica supported DPPC double bilayers). Figure 3.19, 3.20 and 3.21 show the fits of the profiles measured at 41.4°C, 36.0°C and 34.1°C using the two models. The parameters are listed in Table 3.13. One model consists of a high upper bilayer roughness and large water layer, and the other a lower upper bilayer roughness and smaller water layer. The large roughness model enables the feature on the left of the first fringe to be fitted (red line); the lower roughness model enables the feature on the right of the first fringe to be fitted (green line). The large roughness model models the large amplitude ripple and the smaller roughness model the smaller amplitude ripple phase.

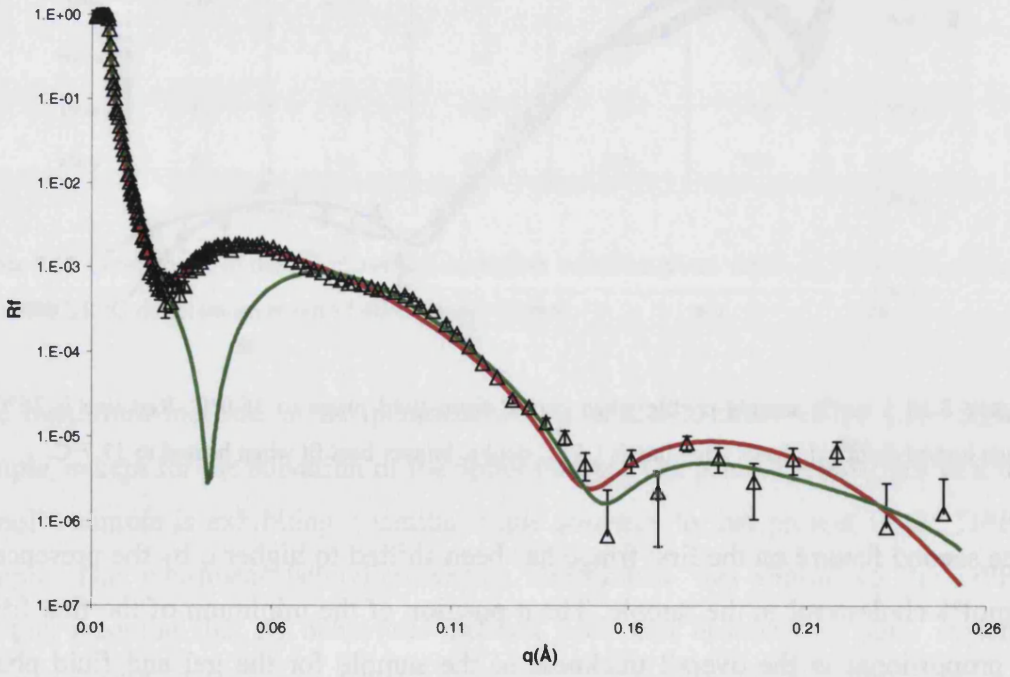

Figure 3.19 1 mol% sample profile at 41.4°C. Large roughness model (red), small roughness model (green)

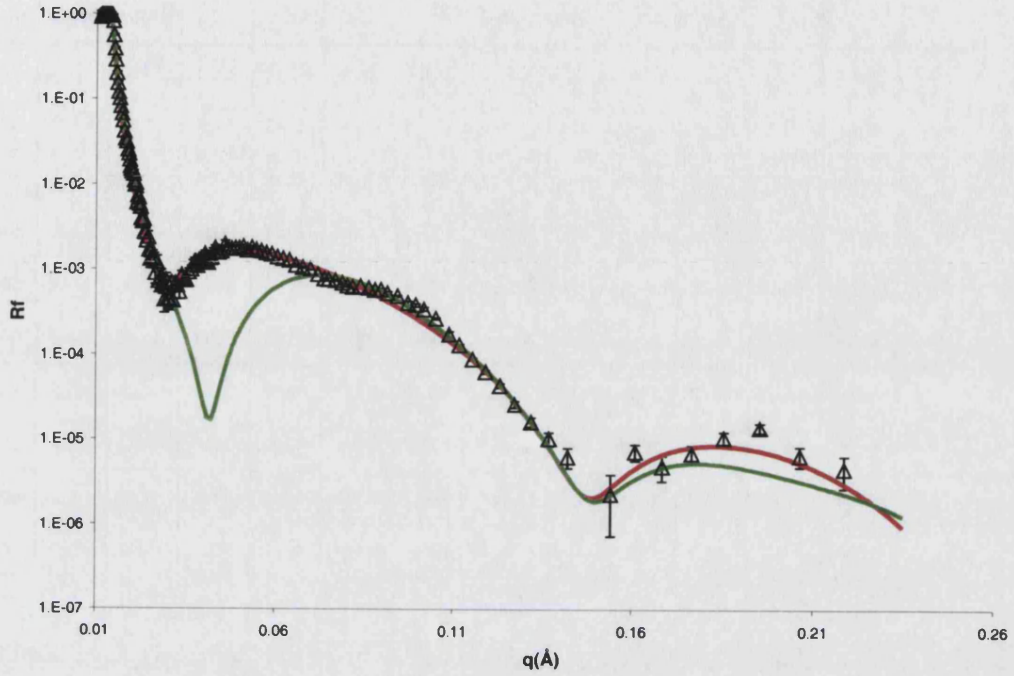

Figure 3.20 1 mol% sample profile at 36.0°C. Large roughness model (red), small roughness model (green)

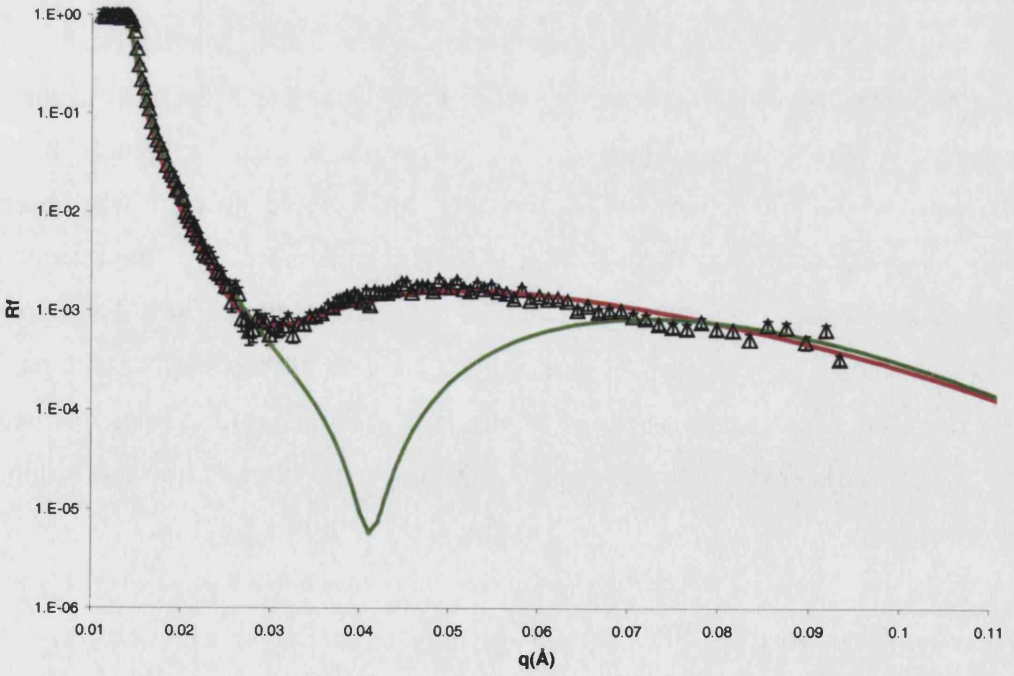

Figure 3.21 1 mol% sample profile at 34.1°C. Large roughness model (red), small roughness model (green)

		dw	lDb	lDc	lAPM	lRou	lCov	Dw	uDb	uDc	uAPM	uRou	uCov
41.4°C	small	14±1	44±2	34±1	47±2	6±1	93±2	29±1	47±2	35±1	46±2	17±2	53±4
	large	16±1	48±2	36±1	44±2	4±1	100±2	41±1	47±2	36±1	44±2	44±2	57±4
38.6°C	small	14±1	44±2	34±1	47±2	7±1	92±2	30±1	46±2	34±1	47±2	17±2	50±4
	large	16±1	48±2	36±1	44±2	4±1	100±2	41±1	47±2	36±1	44±2	44±2	57±4
36.0°C	small	14±1	45±2	35±1	46±2	6±1	92±2	30±1	47±2	34±1	47±2	17±2	50±4
	large	16±1	48±2	36±1	44±2	5±1	100±2	42±1	47±2	36±1	44±2	44±2	54±4
34.1°C	small	14±1	44±2	34±1	47±2	7±1	92±2	31±1	46±2	34±1	47±2	17±2	50±4
	large	16±1	48±2	36±1	44±2	4±1	100±2	42±1	47±2	36±1	44±2	45±2	56±4
31.0°C	small	14±1	44±2	34±1	47±2	7±1	92±2	31±1	46±2	34±1	47±2	16±2	50±4
	large	14±1	48±2	36±1	44±2	4±1	100±2	41±1	47±2	36±1	44±2	45±2	56±4

Table 3.13 1 mol% sample fitted parameters using two models. Small is smaller roughness model, representing small amplitude ripple. Large is high roughness model, representing large amplitude ripple.

Small ripple model

The upper bilayer roughness is the same as that observed upon heating, but the water layer is thinner by 6±2Å. The thinner water layer agrees with the shift in the first minimum in the profile (Figure 3.18). This suggests that the sample behaves differently to the AFM study, where the same small ripple structure was observed upon heating and cooling (Kaasgaard 2003). The structure of the small roughness structure could be affected by presence of the high roughness structure. The coverage of upper bilayer is very low (it was not possible to fit the profile without low coverage). This is expected when use of planar layered model for a rippled structure. The water would feature in the curved structure of the bilayer, but not within the bilayer itself.

When compared to the DPPC sample structure at similar temperatures, the small model had the same upper bilayer roughness parameter, but the water layer thickness was thinner by 10Å. The difference in water layer thickness could be linked to the

thinner gel and fluid phase water layer observed in the 1 mol% and 2 mol% samples compared to the DPPC sample.

If the use of two models is valid, then this indicates that the presence of 1 mol% reduces the change in the structural parameters compared to the DPPC sample. This was indicated by the shift in positions of some of the features of the profile to higher q position (Figure 3.18). This effect is similar to the effect on the behaviour upon heating, where the increase in the structural parameters was less than that of the DPPC sample.

Large ripple model

The upper bilayer roughness was lower by 5Å than that of the DPPC sample. The water layer was also thinner by 5Å. The use of this large model seems to suggest that the presence of 1 mol% cholesterol decreases the level of structural change observed compared to the DPPC sample. It is therefore possible that the 1 mol% decreases the structure of the large amplitude ripple.

Lower bilayer and water layer structure

The parameters for the lower water layer and bilayer vary slightly between the two models. The larger model has a thicker water layer and bilayer compared to the smaller roughness model. The differences are not large though and are close to the error in the values.

Trends in parameters versus temperatures

Unlike the transition behaviour upon heating, once they have increased, the upper bilayer roughness and water layer thickness remained constant. There is no evidence of a maximum in any of the parameters as a function of temperature. This is the same behaviour as observed in the DPPC sample. The constant behaviour is clear when the profile shapes are compared as a function of temperature (Figure 3.22).

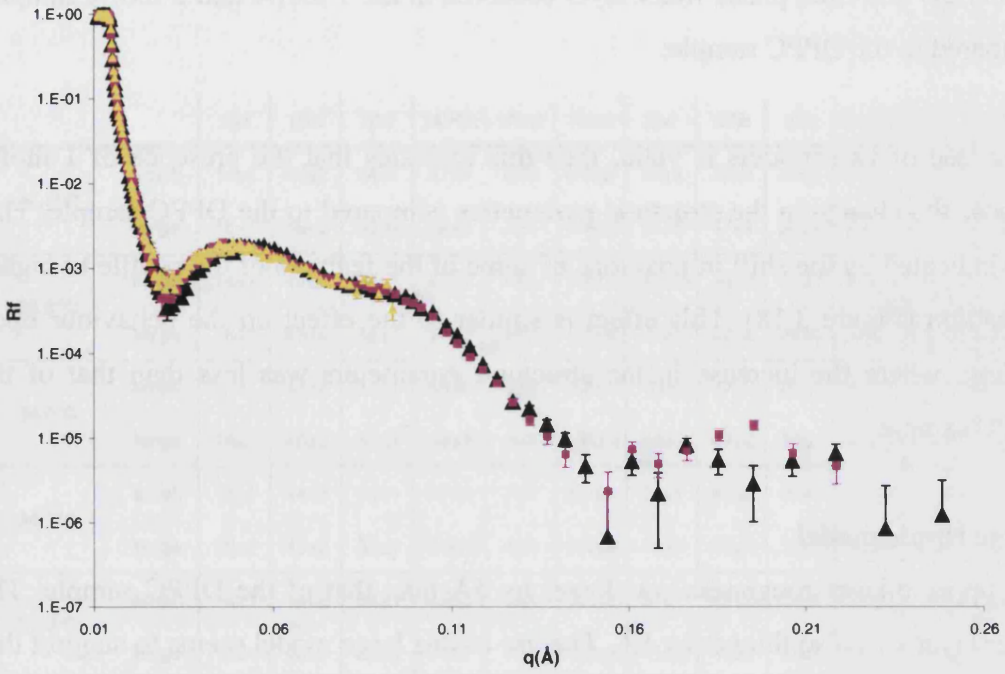

Figure 3.22 Comparison profiles of 1 mol% sample at 41.1°C, 36.0°C and 34.1°C.

If the use of two superimposed models is valid, then 1 mol% reduces the level of structural change observed during the transition region upon cooling. It is interpreted as reducing the size of the large ripple and small ripple structures.

3.7 Phase behaviour of 2mol% Cholesterol 98mol% DPPC

3.7.1 Introduction

The reflectivity of the 2 mol% Cholesterol 98 mol% DPPC sample was measured in D_2O at temperatures between 26.4°C and 48.0°C and down to 26.1°C. The gel and fluid phase structures were also measured in D_2O and silicon matched water (SMW). The thickness and the roughness of the oxide were 8±1Å and 3±1Å respectively.

3.7.2 Gel Phase Structure

The reflectivity of the sample was measured initially in the gel phase at 26.4°C and 31.5°C and then 26.1°C after cooling from the fluid phase. The fitted profiles are shown in Figure 3.23 and the parameters in Table 3.14.

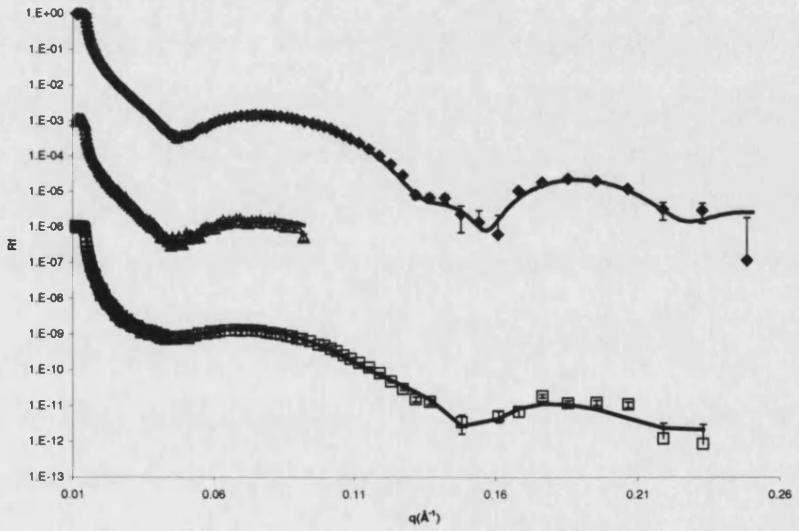

Figure 3.23 Fitted profiles of 2 mol% cholesterol 98 mol% DPPC double bilayer at 26.4°C (♦), 31.5°C (Δ), and 26.1°C after cooling from fluid phase (□).

The bilayer structures after cooling was similar to that of the initial structures. Like the 1 mol% sample the structure after cooling had a considerably thicker water layer. It is likely that the thickness is equilibrated during the temperature scan. This is discussed more fully in the section 3.13.2. Gel phase thickness of water layers as a function of cholesterol. Also, like the 1 mol% sample, the upper bilayer coverage was lower and roughness higher after cooling.

	dw	lDb	lDc	lAPM	lRou	lCov	Dw	uDb	uDc	uAPM	uRou	uCov
26.4°C	10±1	48±2	34±1	47±2	3±1	100±2	23±1	46±2	34±1	47±2	6±2	95±2
31.5°C	10±1	49±2	34±1	47±2	3±1	100±2	24±1	46±2	34±1	47±2	6±2	95±2
26.1°C	9±1	44±2	33±1	48±2	5±1	100±2	28±1	52±2	34±1	47±2	11±2	90±2

Table 3.14 Fitted parameters of 2 mol% cholesterol 98 mol% DPPC double bilayer at 26.4°C and 31.5°C, and then 26.1°C after cooling from fluid phase

The thicknesses of the chain regions of the upper and lower bilayers were identical, and the coverage and roughness very similar. The thicknesses of the chain regions were very similar to those of the DPPC sample and the 1 mol% cholesterol sample. They were also very similar to those of DPPC vesicles of 35Å (Weiner 1989) and 34Å (Nagle 2000). The APM values were also very similar to those of DPPC literature of 47.9Å (Nagle 2000). These similarities differ to the effect of 2 mol% cholesterol on vesicles of deuterated chain DMPC, which increased the overall thickness of the bilayer (Mortensen 1988). But in that study it was unclear whether the cholesterol increased the bilayer thickness or the water layer thickness.

The thickness of the water layer was different compared to the DPPC sample. This difference was not an issue though, as like in the case of the 1 mol% cholesterol sample, once it was heated to the fluid phase it increased to a value similar to that of the pure DPPC sample. After which it remained constant when decreasing the temperature back to the gel phase. The thickness of the main water layer was equilibrated over the temperature scan.

The overall structure of the 2 mol% sample was very similar to that of the 1 mol% sample. The only significant differences were the bilayer coverages, with the 1% being higher. This was likely due to differences in the fabrication process.

3.7.3 Fluid Phase Structures

The reflectivity of the sample was measured at fluid phase temperatures between 41.6°C and 48.0°C and then down to 41.8°C. The fitted profiles are given in Figure 3.24 and the parameters listed in Table 3.15.

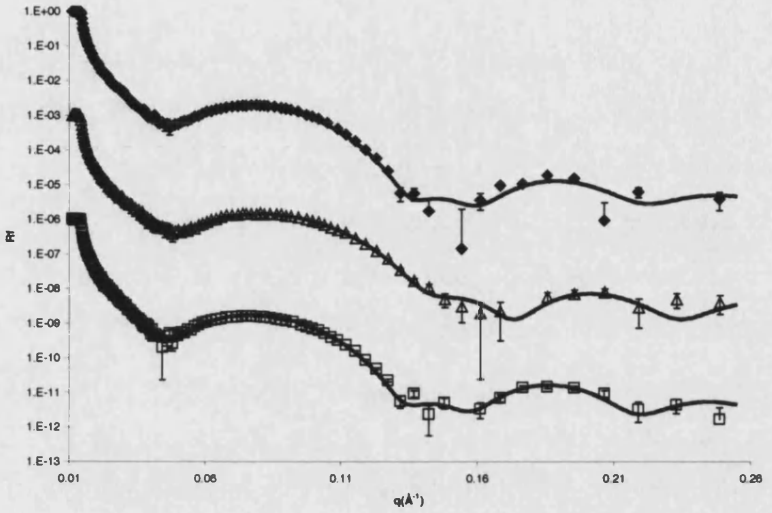

Figure 3.24 Fits of the reflectivity profiles of 2 mol% cholesterol 99 mol% DPPC double bilayer at 41.6°C (♦), 48.0°C (Δ) and 41.8°C (□).

	dw	lDb	lDc	lAPM	lRou	lCov	Dw	uDb	uDc	uAPM	uRou	uCov
26.4°C	10±1	48±2	34±1	47±2	3±1	100±2	23±1	46±2	34±1	47±2	6±2	95±2
41.6°C	10±1	45±2	34±1	47±2	3±1	100±2	27±1	45±2	30±1	53±2	6±2	100±4
42.6°C	10±1	45±2	34±1	47±2	3±1	100±2	27±1	45±2	30±1	53±2	6±2	100±4
43.5°C	8±1	43±2	32±1	50±2	3±1	100±2	26±1	41±2	28±1	57±2	6±2	100±4
48.0°C	9±1	41±2	30±1	53±2	3±1	100±2	27±1	42±2	29±1	55±2	5±2	100±4
43.6°C	9±1	45±2	34±1	47±2	3±1	100±2	27±1	42±2	29±1	55±2	5±2	100±4
41.8°C	11±1	46±2	34±1	47±2	3±1	100±2	27±1	44±2	31±1	52±2	6±2	93±4

Table 3.15 Parameters of fluid phase structure of 2 mol% cholesterol 98 mol% DPPC double bilayer.

The upper bilayer exhibited parameters consistent with a fluid phase structure over the temperature range measured. The transition to the fluid phase (T_m) occurred between 40.8°C – 41.6°C, which was slightly lower than that of DPPC vesicles of 41.8°C (Racansky 1987). This minute depression of the T_m has previously been observed for DMPC vesicles with low amounts of cholesterol (Lemmich 1997).

The lower bilayer did not become fluid until 48.0°C, so required a temperature 7°C higher than the upper bilayer. Upon reducing the temperature back to 43.6°C, the lower bilayer went back to the gel phase again, showing that the transition is reversible. This behaviour parallels that of the DPPC sample and 1 mol% sample.

The thickness of the main water layer increased by 4Å compared to the gel phase. After which it remained constant when the temperature was lowered to the gel phase. It is therefore likely that the water layer became equilibrated by the temperature scan. The thickness however was still 6Å less than in the DPPC sample. The lower water thickness remained constant throughout, indicating it is controlled predominantly by forces between the substrate and lower bilayer.

The bilayer parameters and changes were similar to those of the DPPC sample and the 1 mol% sample and therefore similar to DPPC vesicles (Nagle 2000).

3.7.3.1 Fluid Phase Contrast Exchange Structures at 48°C

The sample was also measured in SMW at 48°C. The fitted profile in SMW is shown in Figure 3.25. The fitted parameters are listed in Table 3.16. A SLD of 3.0 x 10^{-6}Å^{-2} was used for the SMW contrast.

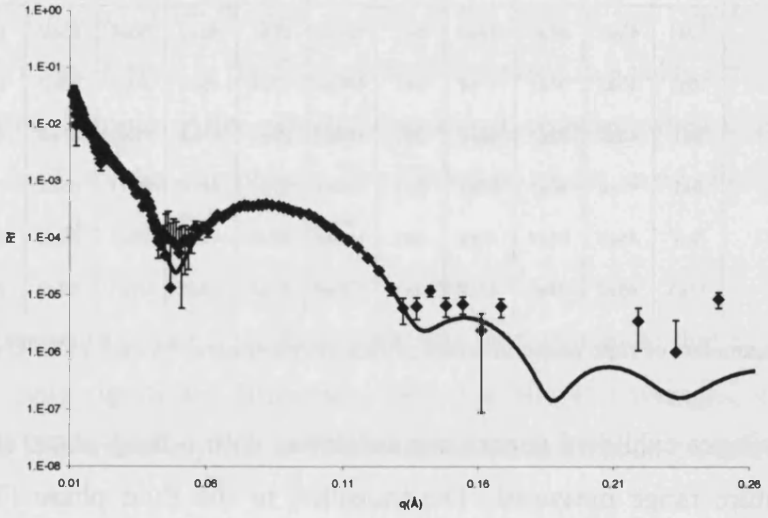

Figure 3.25 Fitted profile of 2 mol% cholesterol 98 mol% DPPC double bilayer at 48.2°C in SMW.

	dw	lDb	lDc	lAPM	lRou	lCov	Dw	uDb	uDc	uAPM	uRou	uCov
D_2O 48.0°C	9±1	41±2	30±1	53±2	3±1	100±2	27±1	42±2	29±1	55±2	5±2	100±4
SMW 48.2°C	10±1	39±2	29±1	55±2	3±1	100±2	25±1	45±2	29±1	55±2	5±2	100±4
Average	10±1	40±2	30±1	54±2	3±1	100±2	26±1	44±2	29±2	55±3	5±2	100±4

Table 3.16 Fitted parameters of different contrasts 2 mol% cholesterol 98 mol% DPPC double bilayer at 47°C and the average of the values. SMW is silicon matched water. The error bars of the average row indicate the spread of the values.

The structural parameters of the two contrasts show good agreement, with the differences being within the error margins. The similarities are clearly visible in the scattering length density profiles shown in Figure 3.26.

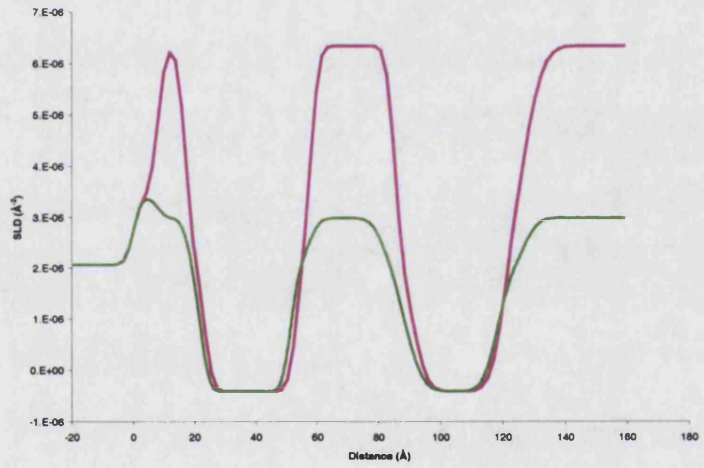

Figure 3.26 Scattering length density profiles of 2 mol% cholesterol 98 mol% DPPC double bilayer at 48°C in different contrasts. D_2O (pink) and SMW (green).

Therefore the 2 mol% cholesterol 98 mol% DPPC double bilayer sample at 48°C had a well defined structure of an upper bilayer chain region thickness of 29Å and main water layer Dw of 26Å. The structure of the fluid phase was very similar to the 1 mol% cholesterol sample, and quite similar to the DPPC double bilayer. The presence of 2 mol% cholesterol does not significantly modify the structure.

3.7.4 Transition Phase Structures and Behaviour

The sample exhibited transitional behaviour between 34.1°C to 40.8°C and upon cooling between 39.2°C to 32.2°C. Different behaviour was observed depending on the direction of the temperature change.

3.7.4.1 Structural behaviour between 34.1°C – 40.8°C

The fits of three representative temperatures in the transition phase are shown in Figure 3.27 and the parameters are listed in Table 3.17.

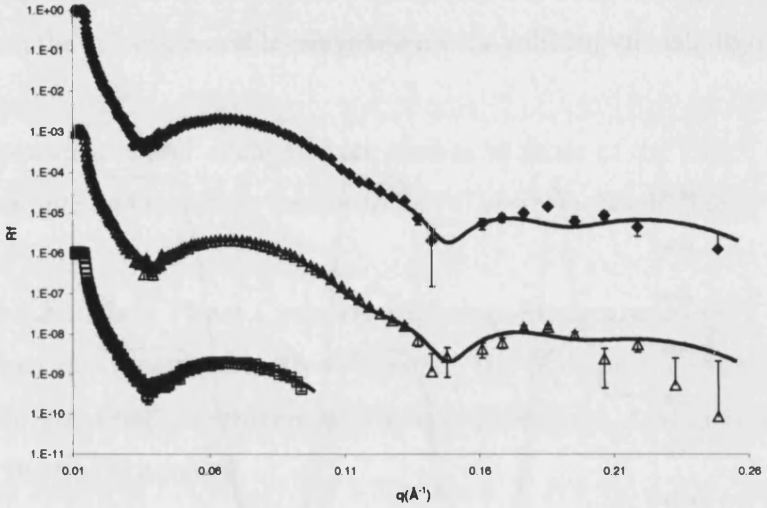

Figure 3.27 Fits of the reflectivity profiles of 2 mol% cholesterol 98 mol% DPPC double bilayer at 34.9°C (♦), 36.6°C (Δ) and 39.1°C (□).

The structure of the lower bilayer and lower water retained its gel phase structure throughout. The upper bilayer also retained its gel phase thickness throughout. As in the case of the DPPC sample, the main changes were an increase in the thickness of the main water layer, an increase in the upper bilayer roughness and an increase in the solvation of the upper bilayer.

	dw	lDb	lDc	lAPM	lRou	lCov	Dw	uDb	uDc	uAPM	uRou	uCov
26.4°C	10±1	48±2	34±1	47±2	3±1	100±2	23±1	46±2	34±1	47±2	6±2	95±2
34.1°C	10±1	47±2	34±1	47±2	3±1	100±2	29±1	51±2	35±1	46±2	13±2	80±4
34.9°C	8±1	48±2	34±1	47±2	3±1	98±2	33±1	50±2	35±1	46±2	12±2	83±4
35.8°C	8±1	48±2	34±1	47±2	3±1	98±2	33±1	50±2	34±1	46±2	12±2	83±4
36.6°C	10±1	48±2	35±1	46±2	3±1	100±2	31±1	51±2	34±1	46±2	11±2	87±4
37.4°C	9±1	47±2	35±1	46±2	3±1	100±2	32±1	51±2	34±1	46±2	11±2	86±4
38.3°C	9±1	47±2	35±1	46±2	3±1	100±2	32±1	51±2	34±1	46±2	11±2	86±4
39.1°C	9±1	47±2	35±1	46±2	3±1	100±2	32±1	51±2	34±1	46±2	11±2	86±4
40°C	9±1	47±2	35±1	46±2	3±1	100±2	32±1	51±2	34±1	46±2	11±2	86±4
40.8°C	9±1	48±2	35±1	46±2	3±1	100±2	30±1	51±2	34±1	46±2	11±2	88±4
48.0°C	9±1	41±2	30±1	53±2	3±1	100±2	27±1	42±2	29±1	55±2	5±2	100±4

Table 3.17 Fitted parameters at transition phase temperatures of 2 mol% cholesterol 98 mol% DPPC double bilayer. The gel phase 26.4°C and fluid phase 48.0°C parameters are given for comparison.

The change in the parameters as a function of temperature is shown in Figure 3.28 and the maximum values are listed in Table 3.18 along with the DPPC values.

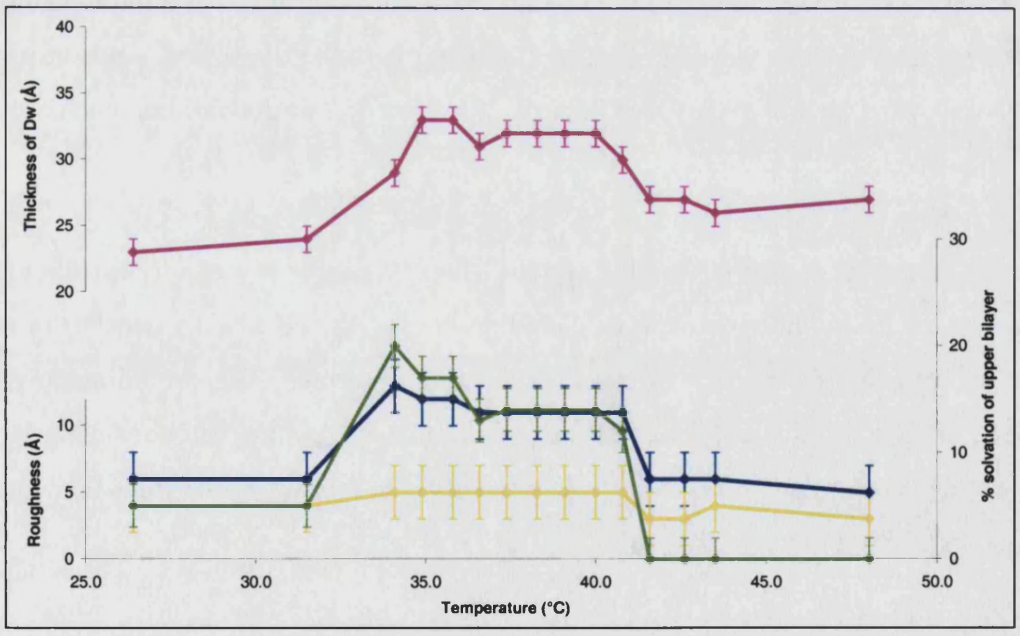

Figure 3.28 Upper bilayer and Dw parameters vs. temperature of 2 mol% cholesterol 98 mol% DPPC double bilayer. Thickness main water layer (pink), roughness of water – bilayer interface (yellow), solvation of upper bilayer (green) and the average upper bilayer roughness (blue).

	Gel value at 25°C		Maximum transition phase value		Maximum increase	
	DPPC	2 mol%	DPPC	2 mol%	DPPC	2 mol%
Dw	27±1Å	23±1Å	43±1Å	33±1Å	16±1Å	10±1Å
WRou	3±2Å	4±2Å	9±2Å	5±2Å	6±2Å	1±2Å
Urou	5±2Å	6±2Å	15±2Å	13±2Å	10±2Å	7±2Å
uSolv	7±4%	5±4%	27±4%	20±4%	20±4%	15±4%

Table 3.18 Comparison of the gel phase and maximum transition phase values of 2 mol% cholesterol 98 mol% DPPC double bilayer with DPPC double bilayer.

The behaviour of this sample as a function of temperature was similar to the DPPC sample; however the maximum values were less. The largest differences were in the thickness of the water layer (by 6Å) and the roughness of the water layer. A full comparison and discussion of the effect of cholesterol on the ripple structure of the double bilayers upon heating is given in section 3.13.3.

3.7.4.2 Structural behaviour between 39.2°C – 32.2°C

The behaviour of the 2 mol% sample was very similar to that of the 1 mol% sample. The profile at 36°C is shown in Figure 3.29 along with the fit of 36°C when heating. It can be seen that unlike the DPPC sample, the behaviour is not similar upon cooling as upon heating.

As in the case of the DPPC sample and the 1 mol% sample it was not possible to fit the profiles using only one fit. It is likely that the first fringe actually consists of two fringes from the reflectivity from two coexisting structures. This would agree with the behaviour of mica supported DPPC double bilayers, which had coexisting large amplitude ripples and small amplitude ripples upon cooling in the transition phase (Kaasgaard 2003).

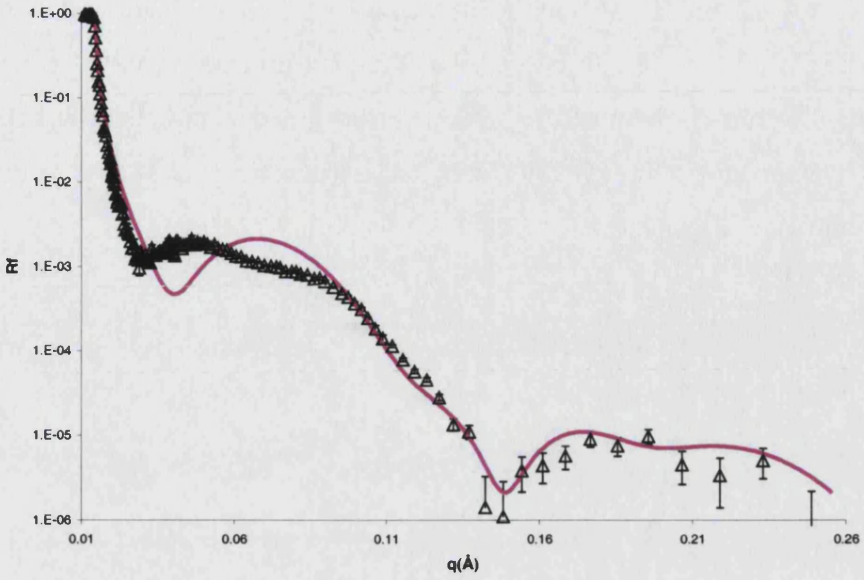

Figure 3.29 2 mol% profile when cooled from fluid phase to 36.5°C. The pink line is the 36.6°C fit when heated from gel phase.

A comparison of the profiles of the DPPC, 1 mol% and 2 mol% samples at 36°C is given in Figure 3.30. The profiles indicate that the behaviour of the 1 mol% and 2 mol% samples is similar, but differs compared to the DPPC sample. The 1 mol% and 2 mol% samples were also found to have similar structural behaviour in the gel and fluid phases.

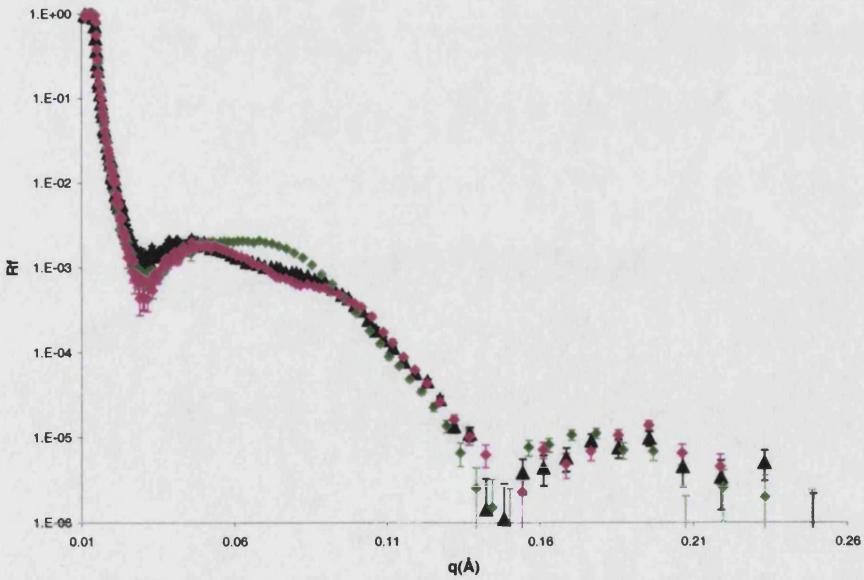

Figure 3.30 Profiles at 36°C of DPPC sample (green), 1 mol% sample (pink) and 2 mol% sample (black)

Figure 3.32, 3.33 and 3.34 show the fits of 39.2°C, 36.5°C and 34.8°C using two models. The parameters are listed in Table 3.19. Unfortunately at 39.2°C and 34.8°C only a small q range was measured due to beam time constraints. The behaviour at these two temperatures thought was likely to be the same as at 36.5°C as the profiles were all similar (Figure 3.31).

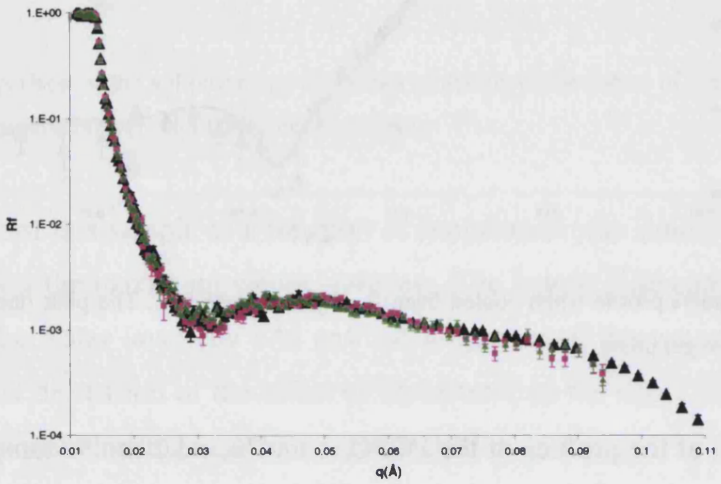

Figure 3.31 Profiles of 2 mol% sample at 39.2°C (pink), 36.5°C (black) and 34.8°C (green). All the profiles are similar.

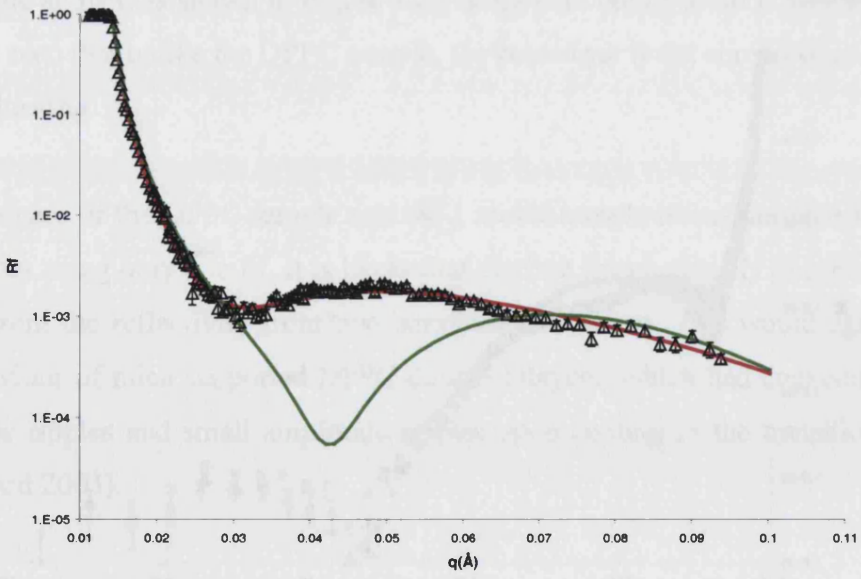

Figure 3.32 Fit of 2 mol% profile at 39.2°C using two superimposed models.

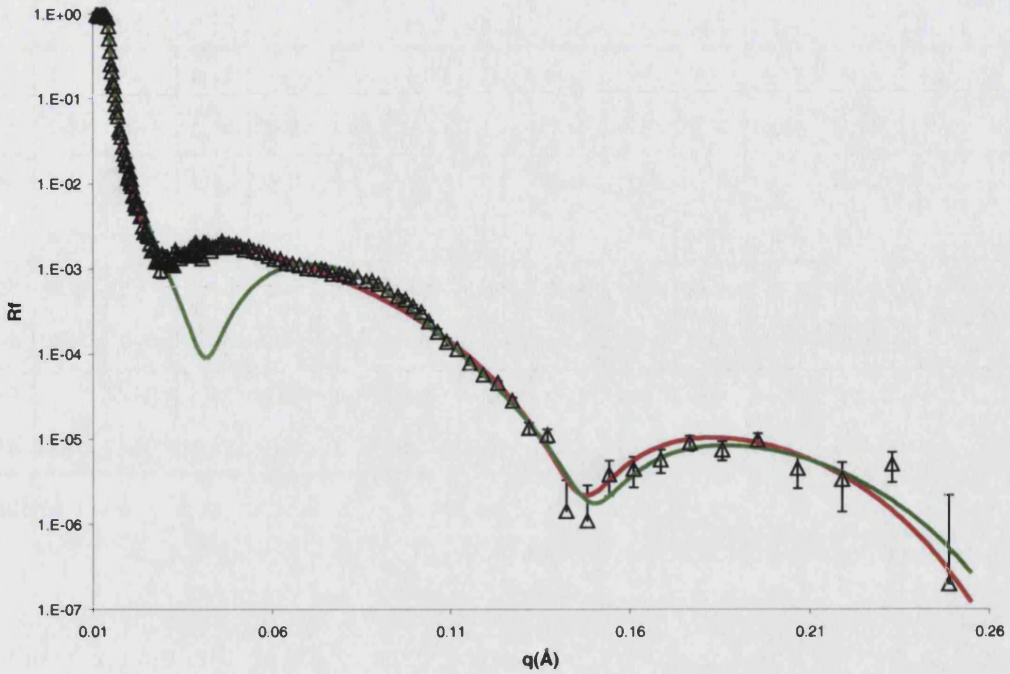

Figure 3.33 Fit of 2 mol% profile at 36.5°C using two superimposed models.

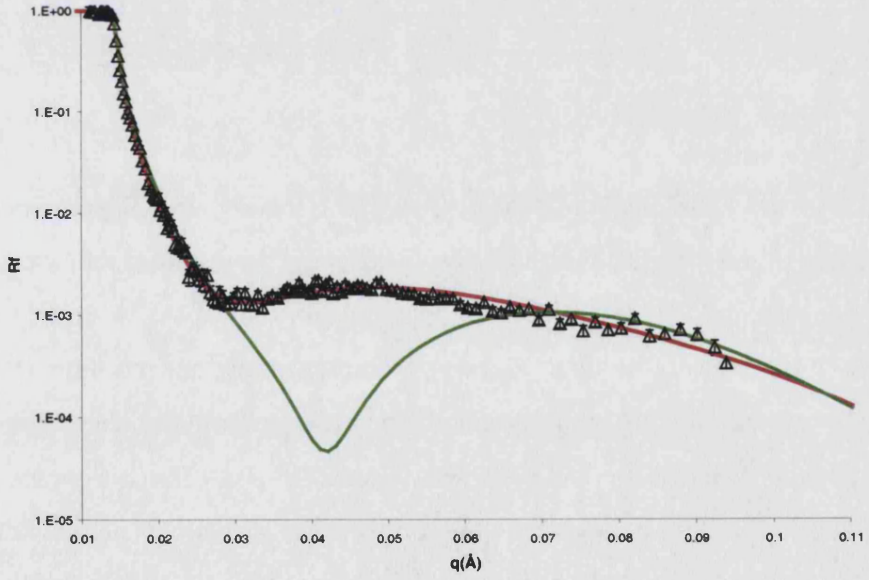

Figure 3.34 Fit of 2 mol% profile at 34.8°C using two superimposed models.

		dw	lDb	lDc	lAPM	lRou	lCov	Dw	uDb	uDc	uAPM	uRou	uCov
39.2°C	small	15±1	46±2	36±1	44±2	6±1	95±2	30±1	45±2	33±1	46±2	15±2	53±4
	large	16±1	48±2	36±1	44±2	4±1	100±2	46±1	46±2	35±1	44±2	45±2	47±4
36.5°C	small	14±1	48±2	36±1	44±2	4±1	97±2	30±1	45±2	33±1	47±2	16±2	54±4
	large	16±1	48±2	36±1	44±2	4±1	100±2	45±1	46±2	35±1	44±2	45±2	47±4
34.8°C	small	15±1	46±2	36±1	44±2	6±1	95±2	31±1	45±2	33±1	47±2	15±2	53±4
	large	14±1	49±2	37±1	43±2	4±1	100±2	46±1	45±2	34±1	44±2	46±2	47±4
32.2°C	small	15±1	46±2	36±1	44±2	6±1	95±2	31±1	46±2	33±1	47±2	16±2	53±4
	large	14±1	49±2	37±1	43±2	4±1	100±2	46±1	45±2	34±1	44±2	46±2	57±4

Table 3.19 2 mol% sample fitted parameters using two models. Small represents small amplitude ripple. Large represents large amplitude ripple structure.

Based on the use of two models to fit different parts of the profile, the upper bilayer consisted of two constant coexisting ripple structures. The large model structure had a constant roughness of 45±2Å over the transitional temperature range. Likewise the roughness of the low roughness structure (16±2Å) did not vary as a function of temperature. The structural behaviour is very similar to that exhibited by the 1 mol% sample.

Small ripple model

Compared to the behaviour upon heating in the transition the phase upper bilayer roughness is slightly higher than that observed upon heating and the water layer is slightly thinner. This suggests different behaviour to that of AFM study, where the same small ripple structure was observed upon heating and cooling (Kaasgaard 2003). The model had the same upper bilayer roughness parameter as the DPPC sample, but the water layer thickness was thinner by 10Å. The difference in water layer thickness could be linked to the thinner gel and fluid phase water layer observed in the 1 mol% and 2 mol% samples compared to the DPPC sample.

Larger ripple model

The upper bilayer roughness was less (by 5Å) than in the DPPC sample. The water layer thickness was similar though. The use of the large roughness model indicates that the presence of 2 mol% cholesterol in the bilayers decreases the level of

structural change in comparison to that observed in the DPPC sample. This could be interpreted as the presence of the 2 mol% cholesterol reduces the large amplitude ripple, as the upper bilayer roughness is likely to be proportional to the ripple amplitude.

Lower bilayer and lower water layer structure

The two models give similar parameters for the structure of the lower water layer and lower bilayer. The water layer thickness swelled compared to the fluid and gel phases. This behaviour was also observed in the DPPC sample and the 1 mol% sample. It is likely connected to the increased environment space of the lower bilayer by the rippling upper bilayer.

Trends in the parameters as a function of temperatures

Unlike the transition behaviour upon heating, once the upper bilayer roughness and water layer thickness had increased they remained constant as a function of temperature. This is also clear in the comparison of the profiles in Figure 3.31. This constant structure versus temperature was also observed for the DPPC sample and the 1 mol% sample.

Transition phase conclusion

If the use of two models is valid, 2 mol% cholesterol reduces the level of structural change during the transition region upon cooling compared to the DPPC sample. It is therefore likely that it reduces the size of the structures of the large ripple and the small ripple.

3.8 Phase behaviour of 4 mol% Cholesterol 96 mol% DPPC

3.8.1 Introduction

The phase behaviour of the 4 mol% Cholesterol 96 mol% DPPC sample was measured in D_2O between 25.1°C and 47.6°C and then down to 25.4°C. The D_2O was not exchanged completely, so its scattering length density was actually 5.89 x 10^{-6}Å^{-2}. The oxide was found to have a thickness of 8±1Å and roughness of 3±1.

3.8.2 Gel Phase Structure

The reflectivity of the sample was measured in the gel phase initially at 25.1°C, 27.3°C, 29.4°C, 30.3°C and 31.5°C, and then at 25.4°C after cooling. The fitted profiles of 25.1°C and 31.5°C are shown in Figure 3.35 and the parameters listed in Table 3.20.

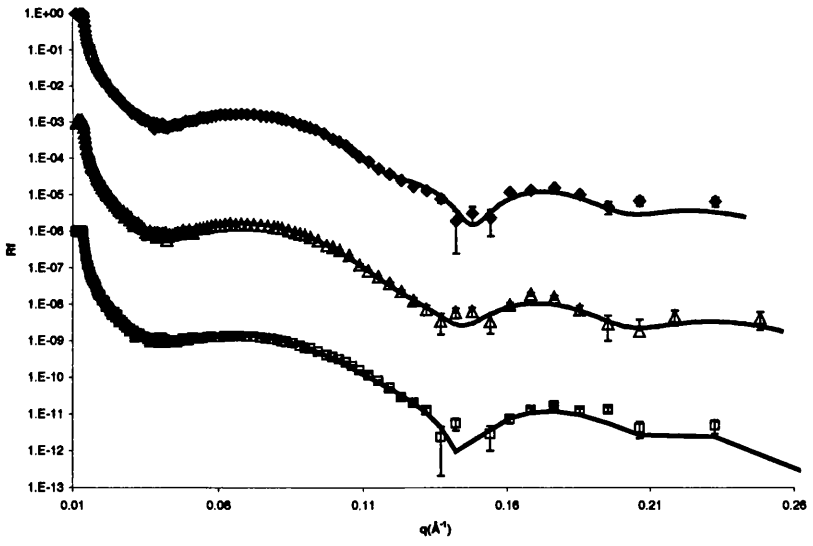

Figure 3.35 Fitted profiles of 4 mol% cholesterol 96 mol% DPPC double bilayer at 25.1°C (♦), 31.5°C (Δ) and 25.4°C after cooling from fluid phase (□).

	dw	lDb	lDc	lAPM	lRou	lCov	Dw	uDb	uDc	uAPM	uRou	uCov
25.1°C	9±1	48±2	34±1	47±2	5±1	100±2	29±1	52±2	36±1	44±2	9±2	89±2
27.3°C	8±1	47±2	34±1	47±2	5±1	100±2	29±1	53±2	35±1	46±2	9±2	88±2
29.4°C	8±1	47±2	34±1	47±2	5±1	100±2	29±1	53±2	35±1	46±2	9±2	88±2
30.3°C	8±1	47±2	34±1	47±2	5±1	100±2	29±1	53±2	35±1	46±2	9±2	88±2
31.5°C	9±1	47±2	34±1	47±2	5±1	96±2	30±1	51±2	35±1	46±2	10±2	91±2
25.4°C	8±1	49±2	34±1	47±2	3±1	94±2	27±1	55±2	37±1	43±2	11±2	91±2

Table 3.20 Fitted parameters of 4 mol% cholesterol 96 mol% DPPC double bilayer at gel phase temperatures, including after cooling down from fluid phase (25.4°C).

The structure after cooling was similar structure to the initial structure. The upper and lower bilayer had similar chain region thicknesses, but different head-groups thickness and bilayer roughness values. Like the 1 mol% and 2 mol% samples, the thickness of the chain region was identical to that of the DPPC sample. This is expected; as the low ratio of cholesterol would not be expected significantly interfere with the packing of the DPPC chains. The dimension of the chains was therefore similar to that of literature values for DPPC vesicles of 35Å (Weiner 1989) and 34Å (Nagle 2000) and the APM were also similar to DPPC in literature of 47.9Å (Nagle 2000).

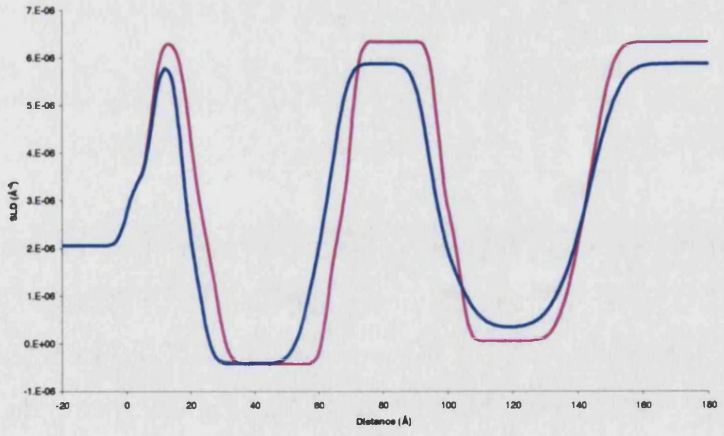

Figure 3.36 Scattering density profiles of 4 mol% cholesterol 96 mol% DPPC double bilayer (blue) and pure DPPC sample (pink) at 25°C.

Even though the 4 mol% sample had similar chain thickness parameters to that of the DPPC structure, the overall sample varied (Figure 3.36). The DPPC sample had

thicker water layers, a lower roughness and a thicker oxide. The difference in the water layers thicknesses could be due to fabrication aspects or to modification of the Helfrich forces that determine the mean separation of the bilayers (Helfrich 1977). The higher bilayer roughness could be due to fabrication aspects as the Schaefer parameters were worse for the 4 mol% sample.

3.8.3 Fluid Phase Behaviour

The reflectivity of the sample was measured at fluid phase temperatures between 41.3°C to 47.6°C and then down to 44.4°C. The fitted profiles at 41.3°C, 47.6°C and 44.4°C are shown in Figure 3.37 and parameters listed in Table 3.21.

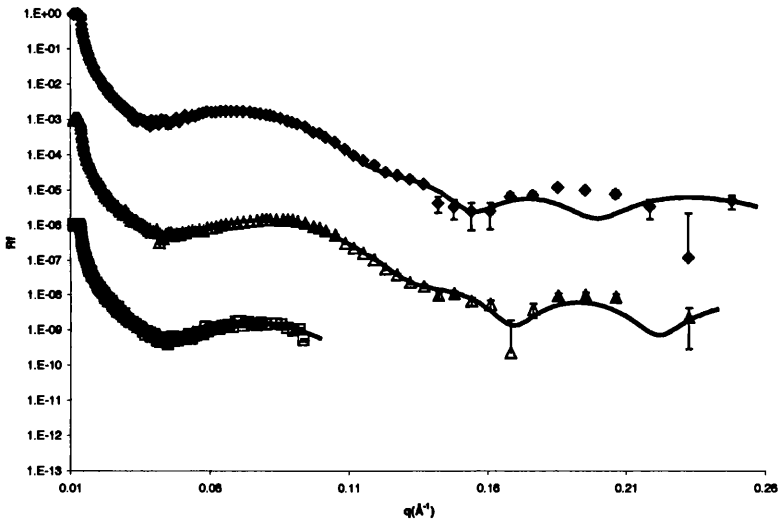

Figure 3.37 Fits of the reflectivity profiles of 4 mol% cholesterol 96 mol% DPPC double bilayer at 41.3°C (♦), 47.6°C (Δ) and 44.4°C (□).

The transition of the upper bilayer to the fluid phase structure occurred between 40.2°C – 41.3°C. This was slightly lower than that of DPPC of 41.8°C (Racansky 1987) and is consistent with the minute depression of T_m in DMPC vesicles by cholesterol (Lemmich 1997). This behaviour was also observed in the 2 mol% and 6 mol% samples.

	dw	lDb	lDc	lAPM	lRou	lCov	Dw	uDb	uDc	uAPM	uRou	uCov
25.1°C	9±1	48±2	34±1	47±2	5±1	100±2	29±1	52±2	36±1	44±2	9±2	89±2
41.3°C	9±1	43±2	33±1	48±2	4±1	98±2	34±1	49±2	33±1	48±2	9±2	91±4
42.4°C	10±1	43±2	33±1	48±2	3±1	100±2	33±1	45±2	29±1	55±2	9±2	97±4
43.5°C	10±1	43±2	33±1	48±2	3±1	100±2	32±1	46±2	30±1	53±2	7±2	97±4
44.5°C	10±1	42±2	32±1	50±2	3±1	100±2	29±1	46±2	30±1	53±2	6±2	97±4
47.6°C	10±1	40±2	30±1	53±2	3±1	100±2	30±1	44±2	30±1	53±2	7±2	93±4
44.4°C	10±1	43±2	33±1	48±2	3±1	100±2	31±1	46±2	30±1	53±2	7±2	97±4

Table 3.21 Fitted parameters of fluid phase structure of 4 mol% cholesterol 96 mol% DPPC double bilayer at various temperatures.

The difference between the thickness of the chain regions of the gel phase and fluid phase was 6Å, whilst the area per molecule increased by 9Å^2. The coverage increased by 8% as expected from the increase in APM. The bilayer roughness decreased slightly, but not significantly. As in the case of the behaviour of the DPPC, 1 mol% and 2 mol% samples, the lower bilayer required a temperature 6°C higher than that of the upper bilayer to transform to a fluid bilayer. The thickness of the chain region started decreasing at 44.5Å and become fluid at 47.6°C. It decreased by 4Å relative to the gel phase. Its thickness was the same as the upper bilayer. Upon decreasing the temperature the lower bilayer became gel like at 44.5°C. 4 mol% of cholesterol did not alter the phase behaviour of the lower bilayer.

The thickness of the water layer gradually decreased during the fluid phase temperature scan, becoming a constant value at 44.5°C. After which it remained relatively constant upon decreasing the temperature. It is likely that the thickness of the water was equilibrated by the temperature scan.

The scattering length density profiles of the 4 mol% sample and the DPPC sample are shown in Figure 3.38. The 4 mol% sample had a higher upper bilayer roughness and lower coverage. The water layer was also thinner. This differs from multilamellar vesicles, were the water layer in the fluid phase was not changed by the incorporation of cholesterol (Rand 1980).

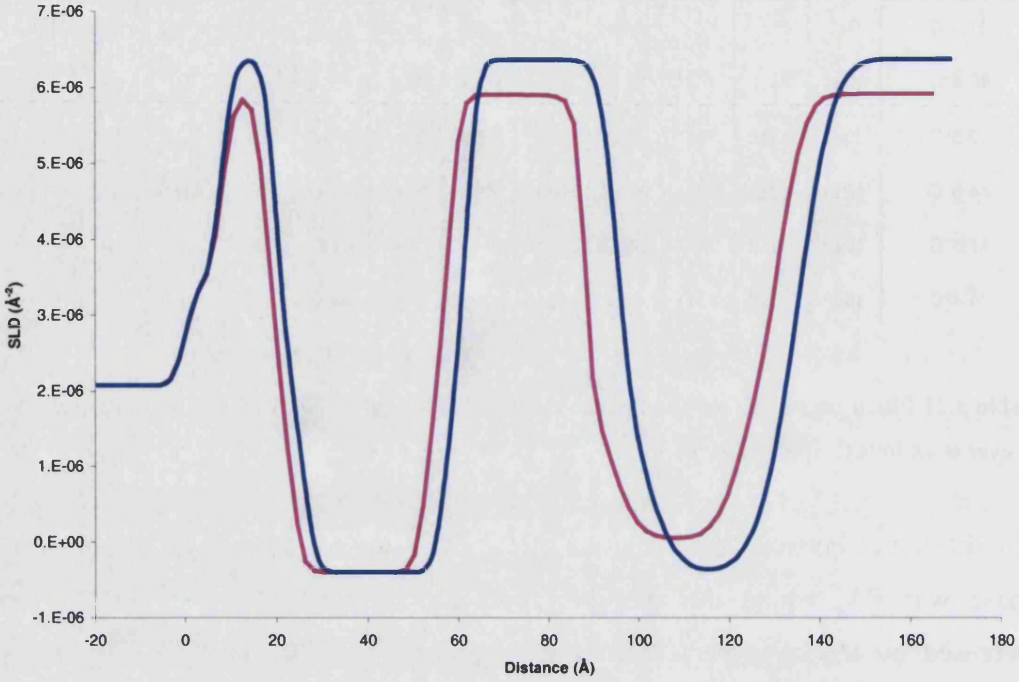

Figure 3.38 Scattering length density profiles of 4 mol% cholesterol 96 mol% DPPC double bilayer (pink) and DPPC double bilayer (blue) at 48°C.

3.8.4 Transition Phase Structures and Behaviour

The sample exhibited transitional behaviour between 32.0°C to 40.2°C and between 41.4°C to 31.2°C. Different behaviour was observed depending on the direction of the temperature change.

3.8.4.1 Structural behaviour between 32.0°C – 40.2°C

Three representative fits at 34.4°C, 36.7°C and 40.2°C are shown in Figure 3.39 and parameters listed in Table 3.22.

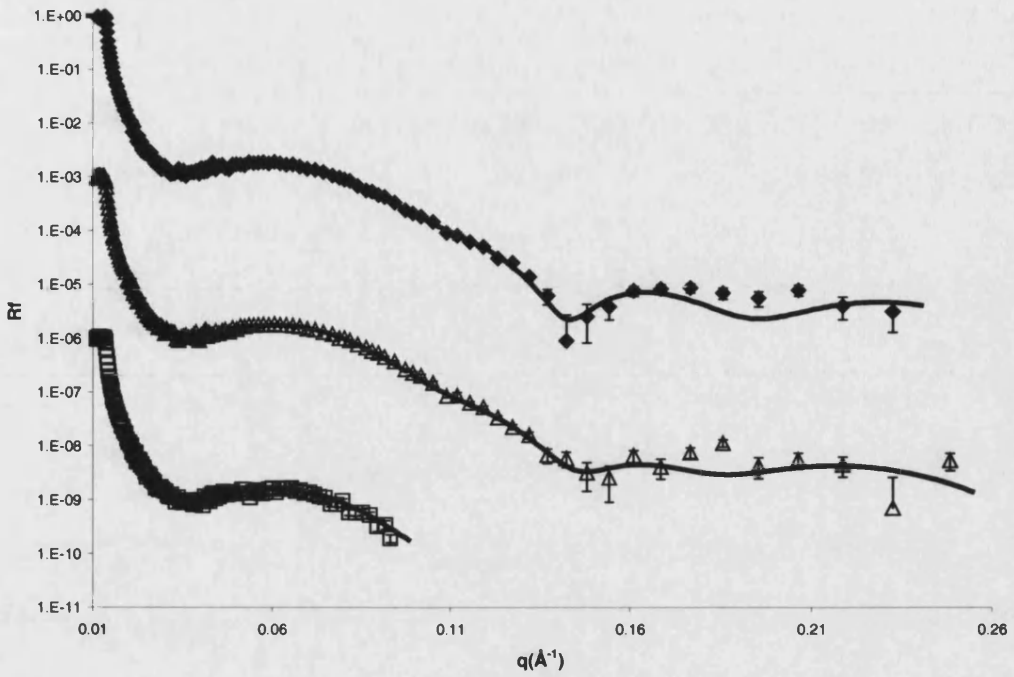

Figure 3.39 Fits of the reflectivity profiles of 4 mol% cholesterol 96 mol% DPPC double bilayer at 34.4°C (♦), 36.7°C (Δ) and 40.2°C (□).

	dw	lDb	lDc	lAPM	lRou	lCov	Dw	uDb	uDc	uAPM	uRou	uCov
25.1°C	9±1	48±2	34±1	47±2	5±1	100±2	29±1	52±2	36±1	44±2	9±2	89±2
32.0°C	8±1	46±2	33±1	48±2	6±1	96±2	33±1	51±2	35±2	46±2	10±2	88±4
33.3°C	7±1	44±2	32±1	50±2	6±1	96±2	36±1	53±2	36±2	44±2	10±2	88±4
34.4°C	8±1	46±2	34±1	47±2	5±1	97±2	34±1	57±2	39±2	41±2	14±2	86±4
35.2°C	8±1	46±2	34±1	47±2	5±1	97±2	35±1	57±2	39±2	41±2	14±2	86±4
36.7°C	9±1	45±2	34±1	47±2	6±1	96±2	35±1	55±2	37±2	43±2	14±2	88±4
37.2°C	9±1	45±2	34±1	47±2	6±1	96±2	37±1	55±2	37±2	43±2	14±2	88±4
38.1°C	8±1	45±2	34±1	47±2	6±1	96±2	36±1	55±2	37±2	43±2	14±2	88±4
38.5°C	8±1	45±2	34±1	47±2	7±1	96±2	37±1	55±2	37±2	43±2	14±2	88±4
39.4°C	8±1	45±2	34±1	47±2	7±1	96±2	37±1	55±2	37±2	43±2	14±2	88±4
40.2°C	8±1	45±2	34±1	47±2	7±1	96±2	35±1	55±2	37±2	43±2	14±2	88±4
47.6°C	10±1	40±2	30±1	53±2	3±1	100±2	30±1	44±2	30±1	53±2	7±2	93±4

Table 3.22 Fitted parameters at transition phase temperatures of 4 mol% cholesterol 96 mol% DPPC double bilayer. The gel phase 25.1°C and fluid phase 47.6°C are given for comparison.

The lower bilayer and lower water layer remained constant throughout. As in the 0 – 2 mol% samples, the main structural changes were in the main water layer thickness, the roughness of the upper bilayer and the solvation of the upper bilayer. The changes in these parameters over the temperature 25.1°C – 47.6°C are shown in Figure 3.40 and a comparison of the gel phase values and maximum transition phase values, along with the values of the DPPC sample are listed in Table 3.23

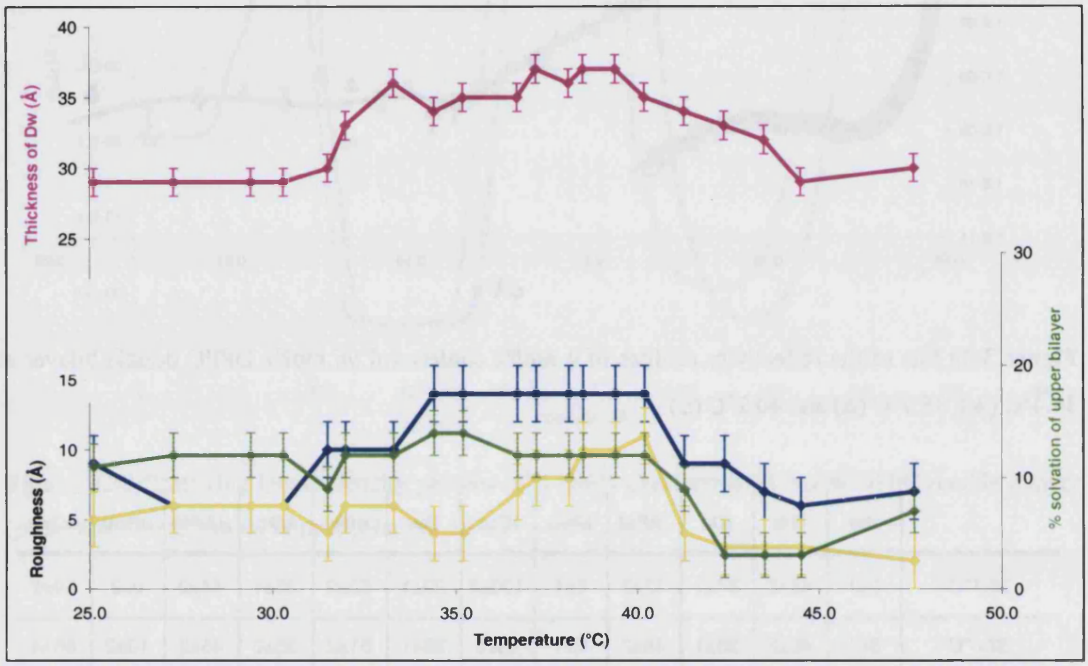

Figure 3.40 Upper bilayer and Dw parameters vs. temperature of 4 mol% cholesterol 96 mol% DPPC double bilayer. Thickness main water layer (pink), roughness of water – bilayer interface (yellow), solvation of upper bilayer (green) and the average upper bilayer roughness (blue).

	Gel value at 25°C		Maximum transition phase value		Maximum increase	
	DPPC	4 mol%	DPPC	4 mol%	DPPC	4 mol%
Dw	27±1Å	29±1Å	43±1Å	37±1Å	16±1Å	8±1Å
WRou	3±2Å	5±2Å	9±2Å	11±2Å	6±2Å	6±2Å
Urou	5±2Å	9±2Å	15±2Å	14±2Å	10±2Å	5±2Å
uSolv	7±4%	11±4%	27±4%	14±4%	20±4%	3±4%

Table 3.23 Comparison of the gel phase and maximum transition phase values of 4 mol% cholesterol 96 mol% DPPC double bilayer with DPPC double bilayer.

The increase in the bilayer roughness and water layer thickness are consistent with the formation of a ripple phase structure. However the maximum increase these parameters were less than in the DPPC sample. The difference in the increase in the water layer thickness was almost a half, whilst the roughness of the water layer and upper bilayer were slightly lower. It is quite possible that the higher presence of 4 mol% is restricting the transition behaviour of the DPPC. A full comparison and discussion of the effect of cholesterol on the ripple structure of the double bilayers upon heating is given in section 3.13.3.

The scattering length density profiles at 25.1°C and 36.7°C are shown in Figure 3.41. The water layer thickness increased, as did the roughness of the water layer and upper bilayer. The static structure of the lower bilayer is clearly visible as well.

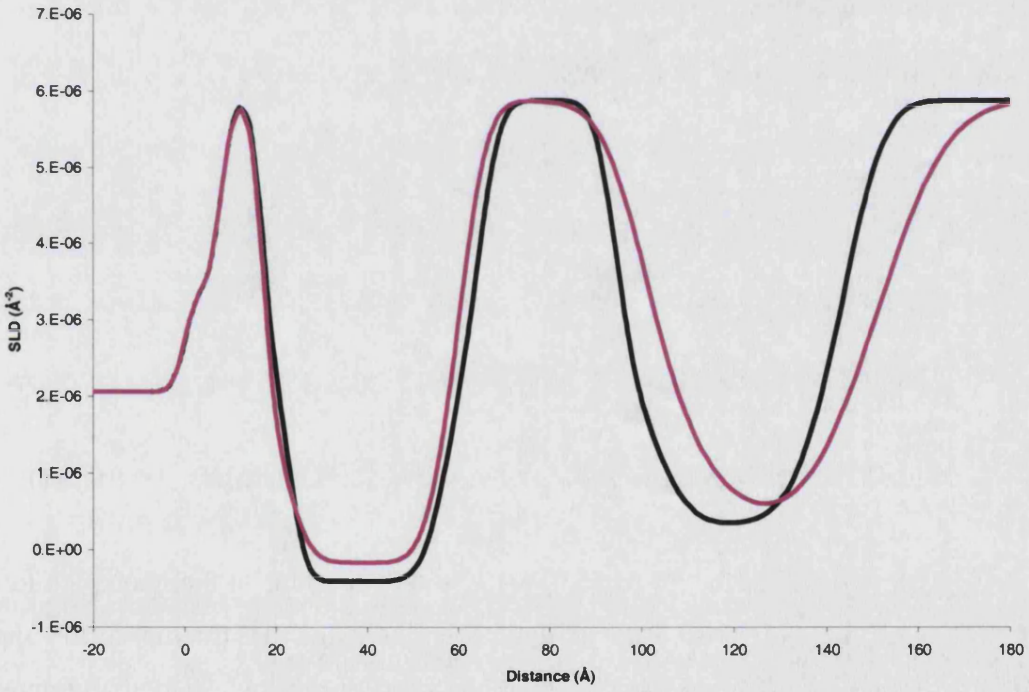

Figure 3.41 Scattering length density profile of 4 mol% cholesterol 96 mol% DPPC double bilayer at 25.1°C (black) and 36.7°C (pink).

3.8.4.2 Structural behaviour between 41.4°C to 31.2°C

The 4 mol% sample behaved differently to the 0 – 2 mol% samples. The shape of the profile as a function of temperature was different. Between 41.4°C and 36.4°C a shift occurs in the first fringe (Figure 3.42). The first minimum is raised to a higher intensity. It continues to shift higher between 36.4°C and 34.6°C. For the 0 – 2 mol% the profiles did not change over the transition temperature range.

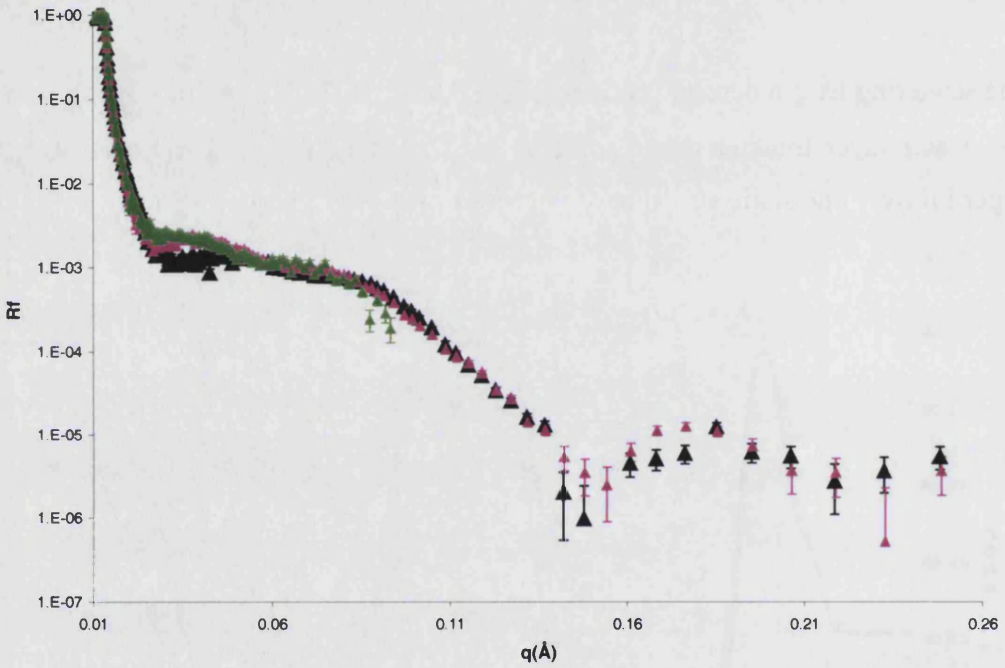

Figure 3.42 Profiles of 4 mol% sample at 41.4°C (black), 36.4°C (pink) and 34.6°C (green).

It was not possible to fit the profiles at 36.4°C and 34.6°C due to their complex form. The fitting of this sample is on going work. It is likely that the structure of the upper bilayer consists of two rippling phases, as the profiles resemble two superimposed profiles. Figure 3.43 shows the 4 mol% profile at 36.4°C and the 2 mol% at 36.5°C. The differences are visible. If the 4 mol% sample was exhibiting two coexisting ripple structures, then one or both of the ripple structures is strongly altered by the presence of 4 mol%, compared to 2 mol%.

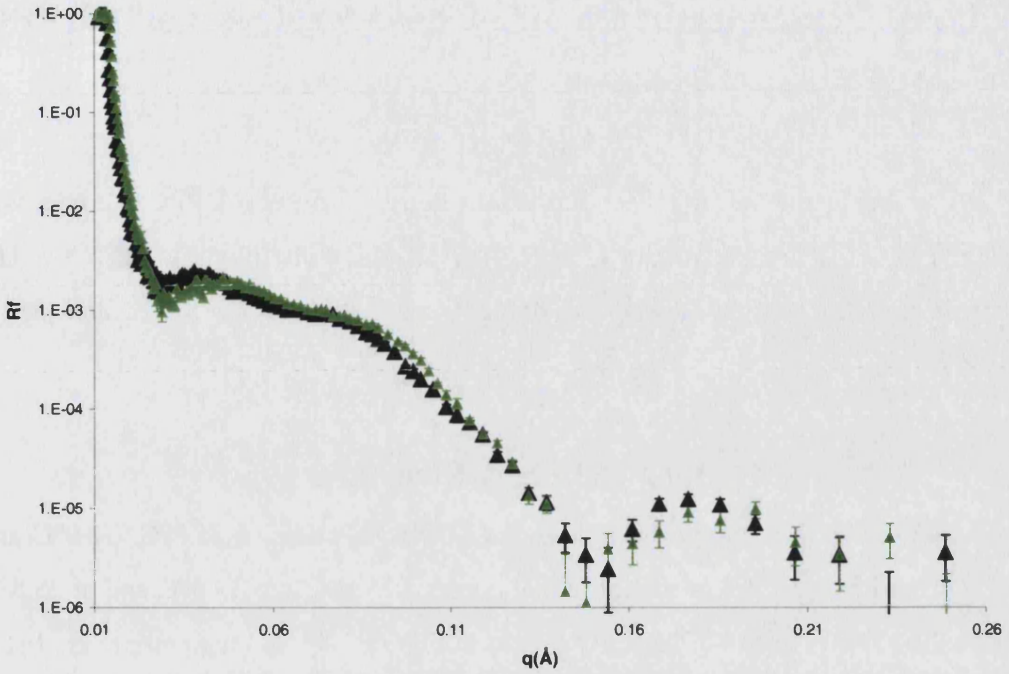

Figure 3.43 Profiles of 4 mol% sample at 36.4°C (black) and 2 mol% sample at 36.5°C (green).

The analysis of the 4 mol% cholesterol sample is on going work. It would be useful to probe the in-plane bilayer structure with AFM.

3.9 Phase behaviour of 6 mol% Cholesterol 94 mol% DPPC

3.9.1 Introduction

The phase behaviour of the 6 mol% Cholesterol 94 mol% DPPC sample was measured in D_2O between 25.8°C and 48.0°C and then down to 25.8°C. The thickness and the roughness of the oxide were found to be 8±1Å and 3±1Å respectively.

3.9.2 Gel Phase Structure

The reflectivity of the sample was measured in the gel phase at 25.8°C, 31.0°C and 33.0°C. The fitted profiles of the initial gel phase at 25.8°C and 33.0°C and at 25.8°C after cooling from the fluid phase are shown in Figure 3.44 and the parameters listed in Table 3.24.

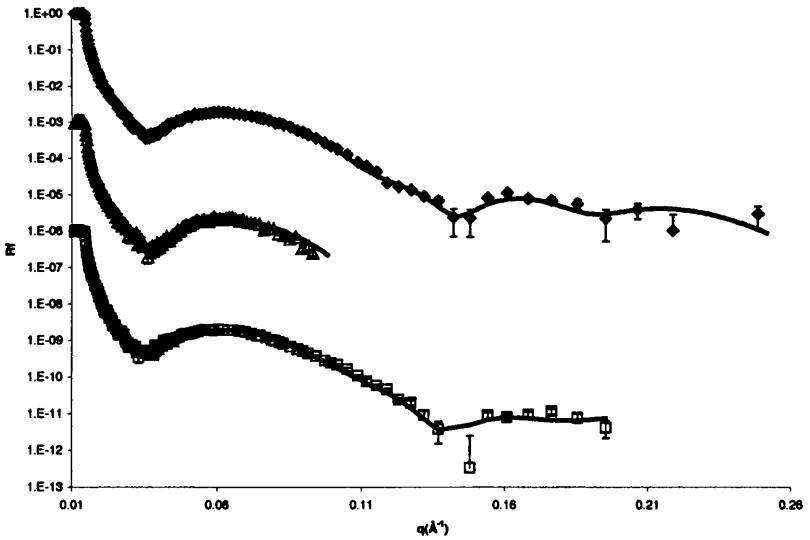

Figure 3.44 Fits of the reflectivity profiles of 6 mol% cholesterol 94 mol% DPPC double bilayer at 25.8°C (♦) and 33.0°C (Δ), and 25.8°C after cooling from fluid phase (□)

	dw	lDb	lDc	lAPM	lRou	lCov	Dw	uDb	uDc	uAPM	uRou	uCov
25.8°C	7±1	50±2	35±1	46±2	6±1	94±2	33±1	52±2	38±1	42±2	10±2	75±2
31.0°C	7±1	50±2	35±1	46±2	6±1	94±2	35±1	53±2	38±1	42±2	10±2	73±2
33.0°C	8±1	51±2	36±1	44±2	6±1	94±2	34±1	51±2	37±1	43±2	10±2	73±2
25.8°C	9±1	50±2	37±1	43±2	4±1	93±2	35±1	55±2	38±1	42±2	13±2	70±2

Table 3.24 Fitted parameters of 6 mol% cholesterol 94 mol% DPPC double bilayer at gel phase temperatures, including after cooling down from fluid phase (25.8°C).

The lower bilayer had a chain region thickness similar to DPPC vesicles of 35Å (Weiner 1989) and 34Å (Nagle 2000), whilst the upper bilayer was thicker. The upper bilayer thickness of 38Å gives a chain tilt of 22° relative to the bilayer normal, which is considerably less than that of the DPPC upper bilayer of 31°. 6 mol% of cholesterol interferes with the tilt of the DPPC chains.

The roughness of both of the bilayers was higher than that of the 0 – 2 mol% bilayers. The coverages of both bilayers were also lower than those samples, with the upper bilayer having a particularly low coverage of 73±2Å. The scattering length density profiles of the 6 mol% sample and DPPC sample are given in Figure 3.45. The higher thickness and roughness of the 6 mol% upper bilayer is visible, as is the lower coverage. The differences in the thickness of both water layers is also visible

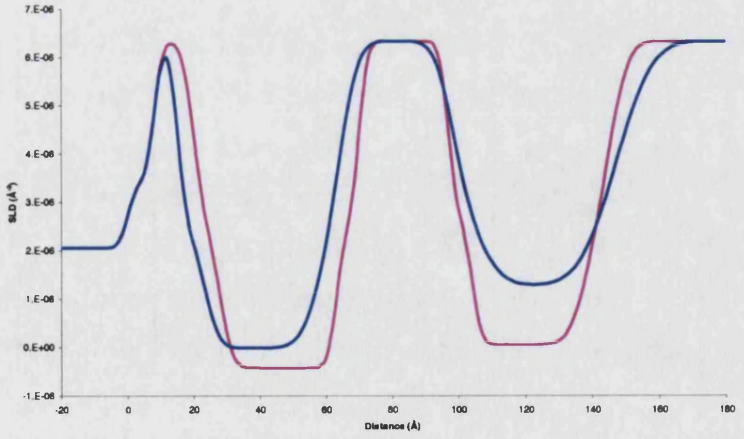

Figure 3.45 Scattering length density profiles of 6 mol% cholesterol 94 mol% DPPC double bilayer (blue) and pure DPPC sample (pink) at 25°C.

3.9.3 Fluid Phase Behaviour

The sample was measured at fluid phase temperatures between 41.7°C to 48.0°C and down to 41.6°C. The fitted profiles at 45.3°C, 48.0°C and 41.6°C are shown in Figure 3.46 and the parameters listed in Table 3.25.

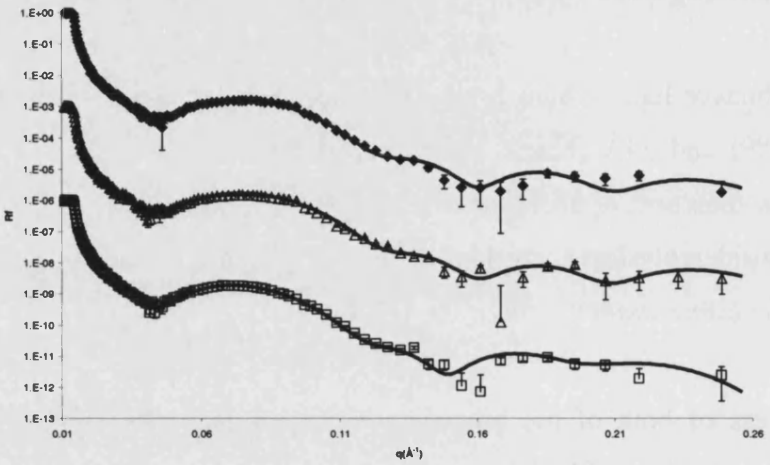

Figure 3.46 Fits of the reflectivity profiles of 6 mol% cholesterol 94 mol% DPPC double bilayer at 45.3°C (♦), 48.0°C (Δ) and 41.6°C (□).

	dw	lDb	lDc	lAPM	lRou	lCov	Dw	uDb	uDc	uAPM	uRou	uCov
25.8°C	7±1	50±2	35±1	46±2	6±1	94±2	33±1	52±2	38±1	42±2	10±2	75±2
41.7°C	12±1	47±2	34±1	47±2	4±1	96±2	33±1	48±2	32±1	50±2	9±2	81±4
42.6°C	12±1	46±2	32±1	50±2	4±1	96±2	32±1	46±2	31±1	52±2	6±2	81±4
43.5°C	12±1	45±2	31±1	52±2	4±1	96±2	32±1	45±2	30±1	53±2	6±2	81±4
45.3°C	11±1	45±2	30±1	53±2	4±1	96±2	31±1	48±2	31±1	52±2	7±2	79±4
48.0°C	11±1	44±2	31±1	52±2	4±1	96±2	31±1	47±2	31±1	52±2	7±2	81±4
45.3°C	11±1	44±2	31±1	52±2	4±1	96±2	31±1	47±2	31±1	52±2	7±2	81±4
43.5°C	11±1	44±2	31±1	52±2	4±1	96±2	31±1	47±2	31±1	52±2	7±2	81±4
41.6°C	12±1	49±2	34±1	47±2	3±1	94±2	30±1	50±2	34±1	47±2	8±2	80±4

Table 3.25 Parameters of fluid phase structure of 6 mol% cholesterol 94 mol% DPPC double bilayer.

The transition of the upper bilayer to a fluid phase structure occurred between 40.8°C – 41.7°C, which was just slightly lower than that of pure DPPC vesicles of 41.8°C

and is consistent with literature (Lemmich 1997). The lower bilayer became fluid between 41.7°C to 42.6°C, which was slightly higher than the T_m of the upper bilayer. This differs to the 0 – 4 mol% samples, which required a temperature of 6°C higher than that of the upper bilayer. The cholesterol is able to increase the fluidity of the lower bilayer at lower temperatures, overcoming the suspected constraining force from the substrate. This is consistent with the effect of cholesterol in membranes, where it increases the fluidity at lower temperatures and restricts it at higher temperatures (Yeagle 1985). The lower bilayer became a gel structure again at 41.6°C. The effect of the cholesterol was therefore fully reversible. The thickness of both chain regions and the increase in area per molecule were comparable to that of DPPC sample and to DPPC vesicles (Nagle 1996, 2000).

The roughness of both the upper and lower bilayers decreased upon going to the fluid phase. If the DPPC and 6 mol% of cholesterol were immiscible then the roughness would have been expected to increase, to account for differences in the height of the domains. It is unlikely that domain formation is occurring as it has only been observed at ratios of 14 mol% in DMPC vesicles (Knoll 1985).

Other changes that occurred were a slight decrease in the thickness of the main water layer. The coverage of the upper bilayer increased, as expected from the increase in APM) whilst that of the lower bilayer remained the constant.

3.9.4 Transition Phase Behaviour

The reflectivity of the sample was measured in the transitional temperature between 34.4°C to 40.8°C and between 38.9°C to 34.3°C. Fitted profiles upon increasing and decreasing the temperature are shown in Figure 3.47 and the parameters listed in Table 3.26.

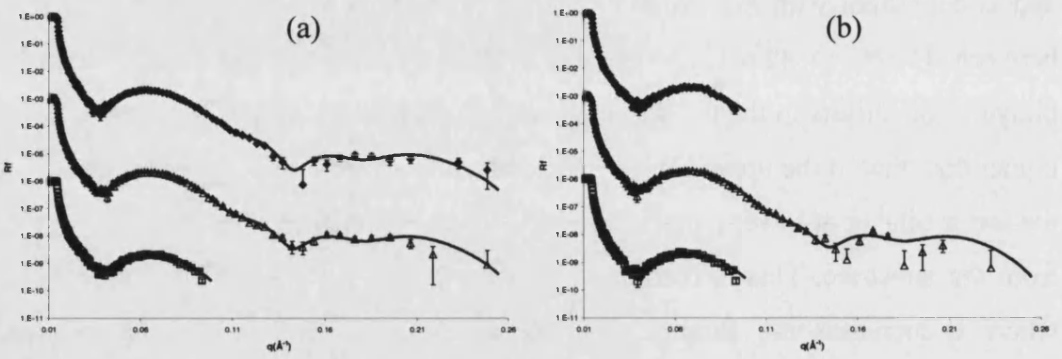

Figure 3.47 Fits of 6 mol% cholesterol 94 mol% DPPC double bilayer of (a) increasing temperature 34.4°C (♦), 36.5°C (Δ) and 39.1°C (□) and (b) decreasing at 38.9°C (♦), 36.0°C (Δ) and 34.3°C (□).

	dw	lDb	lDc	lAPM	lRou	lCov	Dw	uDb	uDc	uAPM	uRou	uCov
25.8°C	7±1	50±2	35±1	46±2	6±1	94±2	33±1	52±2	38±1	42±2	10±2	75±2
34.4°C	10±1	50±2	36±1	44±2	4±1	93±2	36±1	52±2	38±1	42±2	11±2	88±4
35.6°C	11±1	51±2	36±1	44±2	4±1	93±2	37±1	52±2	38±1	42±2	11±2	86±4
36.5°C	11±1	50±2	36±1	44±2	4±1	93±2	36±1	52±2	38±1	42±2	10±2	86±4
37.3°C	11±1	51±2	36±1	44±2	4±1	93±2	36±1	52±2	38±1	42±2	11±2	88±4
38.2°C	11±1	51±2	36±1	44±2	4±1	93±2	36±1	52±2	38±1	42±2	11±2	88±4
39.1°C	12±1	51±2	36±1	44±2	4±1	93±2	36±1	52±2	38±1	42±2	9±2	88±4
39.9°C	11±1	51±2	36±1	44±2	4±1	93±2	33±1	53±2	38±1	42±2	8±2	88±4
40.8°C	12±1	51±2	36±1	44±2	4±1	92±2	31±1	53±2	38±1	42±2	6±2	88±4
48.0°C	11±1	44±2	31±1	52±2	4±1	96±2	31±1	47±2	31±1	52±2	7±2	81±4
38.9°C	11±1	49±2	35±1	46±2	4±1	93±2	34±1	52±2	38±1	9±2	11±2	72±4
36.0°C	11±1	50±2	35±1	46±2	4±1	93±2	35±1	51±2	38±1	9±2	11±2	72±4
34.3°C	11±1	50±2	35±1	46±2	4±1	93±2	35±1	51±2	38±1	9±2	11±2	72±4
31.9°C	8±1	52±2	37±1	43±2	4±1	93±2	33±1	53±2	38±1	9±2	10±2	71±4
25.8°C	8±1	49±2	36±1	44±2	4±1	93±2	34±1	56±2	38±1	12±2	11±2	70±4

Table 3.26 Fitted parameters of 6 mol% cholesterol 94 mol% DPPC double bilayer transition phase structures upon increasing and decreasing the temperature. The gel phases before and after the temperature scan 25.8°C and the fluid phase 48.0°C are given for comparison.

The behaviour in the transition phase was less than that observed in the 0 – 4 mol% samples. Figure 3.48 shows the change in the thickness of the main water layer,

upper bilayer roughness and solvation parameters as a function of temperature. Table 3.27 lists the maximum increases in these parameters along with those of the DPPC sample. The maximum increase values are relative to gel phase upon increasing temperature and to fluid phase upon decreasing it. The increase in the parameters observed is lower upon decreasing the temperature.

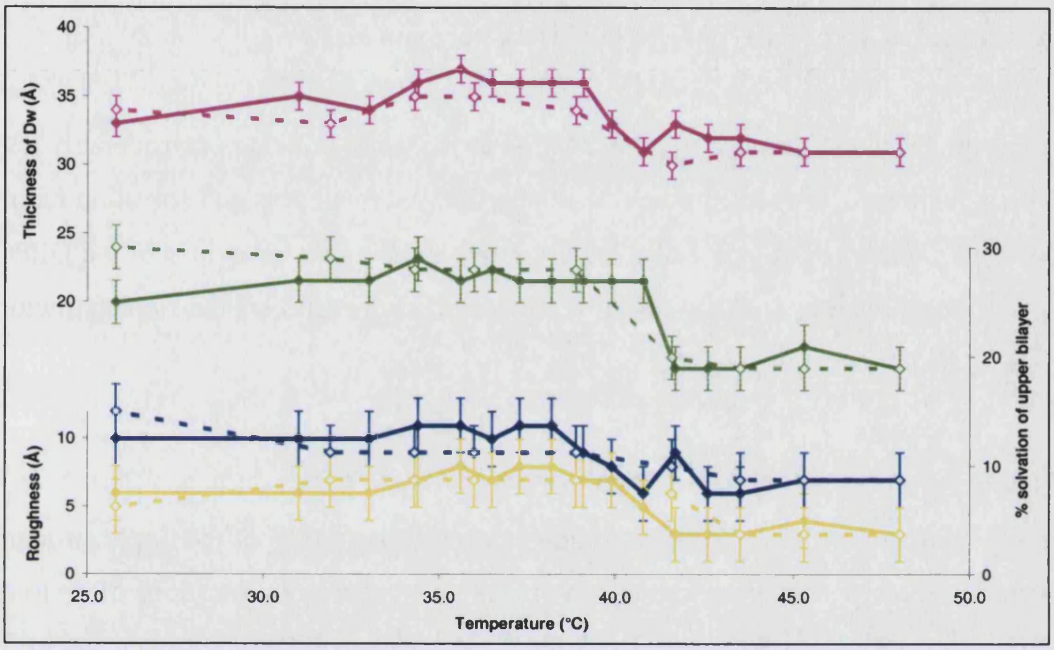

Figure 3.48 Thickness main water layer (pink), roughness of water – bilayer interface (yellow), solvation of upper bilayer (green) and the average upper bilayer roughness (blue) of 6 mol% cholesterol 94 mol% DPPC double bilayer. The bold lines are increasing temperature and dashed decreasing temperature.

	Gel value at 25°C		Fluid 48°C	Maximum transition phase value			Maximum increase		
	DPPC	6 mol%	6 mol%	DPPC	6 mol% up	6 mol% down	DPPC	6 mol% up	6 mol% down
Dw	27±1Å	33±1Å	31±1Å	43±1Å	37±1Å	35±1	16±1Å	4±1Å	4±1Å
WRou	3±2Å	6±2Å	3±2Å	9±2Å	8±2Å	7±2Å	6±2Å	2±2Å	4±2Å
Urou	5±2Å	10±2Å	7±2Å	15±2Å	11±2Å	9±2Å	10±2Å	1±2Å	2±2Å
uSolv	7±4%	25±4%	19±4%	27±4%	29±4%	28±4%	20±4%	4±4%	9±4%

Table 3.27 Comparison of the gel phase and the fluid phase with the maximum transition phase values upon increasing and decreasing the temperature of 6 mol% cholesterol 94 mol% DPPC double bilayer with DPPC double bilayer.

As in the case of the other 0 – 4 mol% samples, the structure of the lower bilayer layer remained constant throughout the transition temperature range.

The 6 mol% sample had different behaviour to the 0 – 4 mol% samples in that very similar behaviour was observed upon heating and cooling. The same increase in the thickness of the water layer was observed, whilst the increases in the roughness of the water layer and upper bilayer parameters were similar.

Compared to the DPPC sample, the increase in the water layer was considerably less, with a quarter of the size, although the upper bilayer roughness and solvation hardly changed. 6 mol% of cholesterol therefore reduces the phase behaviour of the DPPC. A full comparison and discussion of the effect of cholesterol on the ripple structure of the double bilayers upon heating is given in section 3.13.3.

Interpretation

In literature the cholesterol concentration at which elimination of the ripple structure occurs is unclear. Ripple structures have been observed at concentrations of up to 14 mol% cholesterol (Adachi 1995), 15 mol% (Karmakar 2003), and even up to 20 mol% (Copeland 1980, Mortensen 1988). Other studies have said that cholesterol concentrations as low as 7 mol% suppresses the ripple structure (Vist 1990). From these varied studies it would be expected that the 6 mol% sample still exhibits ripple behaviour.

Another structural phenomenon occurring in bilayers that has a similar increase in the water layer is that of anomalous swelling. This behaviour appears when cooling in the fluid phase close to the fluid – gel transition temperature. The bilayer repeat unit swells between 2 – 4Å (Hønger 1994, Richter 1999, Mason 2000, Pabst 2003). The swelling is thought to be largely due to a swelling of the water layer, but also maybe partially due to a slight increase in the bilayer thickness (Mason 2000). It is thought to be caused by a softening of the bilayer near the transition, which lowers the bending rigidity of the bilayer (Lemmich 1997). Anomalous swelling is thought to have a critical point just below T_m, but is obscured by the events of the transition (Richter 1999). The cholesterol concentrations up to 15 mol% have been observed to

enhance the anomalous swelling. Inclusion of 10 mol% of cholesterol into DMPC vesicles was observed to increase the swelling to 4.2Å from the 2.4Å observed for DMPC vesicles (Richter 1999). The increase of 4 Å in the water layer of the 6 mol% cholesterol double bilayer is very similar to this. The increase in the water layer could be connected to anomalous swelling, but is questionable as the behaviour is usually only observed only upon cooling in the fluid phase above the main transition. But the suspected presence of the critical point below the main transition could suggest a connection.

3.10 Phase behaviour of 10 mol% Cholesterol 90 mol% DPPC

3.10.1 Introduction

The phase behaviour of the 10 mol% Cholesterol 90 mol% DPPC sample was measured in D_2O between 25.1°C and 47.2°C and then down to 25.2°C. The thickness and the roughness of the oxide were found to be 11±1Å and 3±1Å respectively.

3.10.2 Gel Phase Structure

The reflectivity of the sample was measured in the gel phase at 25.1°C, 31.2°C and 34.7°C. The fitted profiles measured at 25.1°C and 34.7°C, and at 25.2°C after cooling from the fluid phase are shown in Figure 3.49 and the parameters listed in Table 3.28.

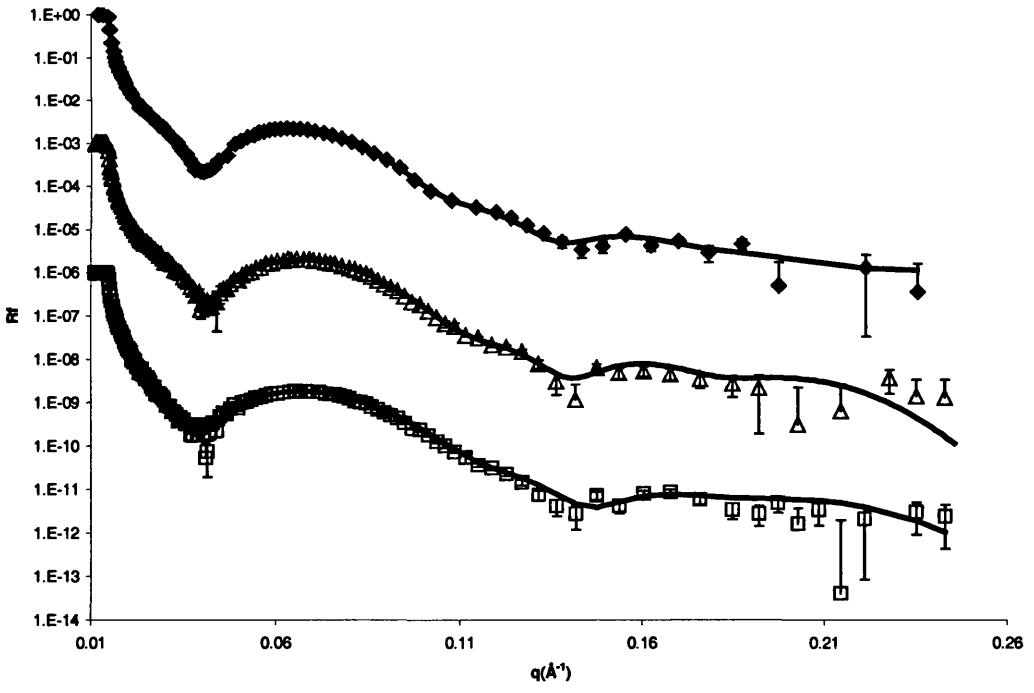

Figure 3.49 Fits of the reflectivity profiles of 10 mol% cholesterol 90 mol% DPPC double bilayer at 25.1°C (♦) and 34.7 °C (Δ), and 25.2°C after cooling from the fluid phase (□).

	dw	lDb	lDc	lAPM	lRou	lCov	Dw	uDb	uDc	uAPM	uRou	uCov
25.1°C	14±1	51±2	35±1	45±2	12±1	100±4	36±1	53±2	37±1	43±2	16±2	75±4
31.2°C	15±1	49±2	35±1	46±2	10±1	96±4	36±1	53±2	37±1	43±2	14±2	71±4
34.7°C	12±1	49±2	34±1	47±2	8±1	95±4	34±1	52±2	36±1	44±2	13±2	72±4
25.2°C	10±1	51±2	34±1	47±2	4±2	95±4	32±1	51±2	36±1	44±2	11±2	70±4

Table 3.28 Fitted parameters of 10 mol% cholesterol 90 mol% DPPC double bilayer at gel phase temperatures, including after cooling down from fluid phase (25.2°C).

The structure after cooling down from the fluid phase differed from the initial structures in a number of ways. The differences are discussed in the fluid phase section because they are connected to the fluid phase behaviour

The lower bilayer had a chain region thickness similar to DPPC sample and vesicles of 35Å (Weiner 1989) and 34Å (Nagle 2000), whilst that of the upper bilayer was thicker at 37±1Å. This was similar to the structure of the 6 mol% sample. It is likely that the cholesterol reduces the tilt of the chains. These chains have an average tilt of 25.5° relative to the normal to the plane of the bilayer, which is slightly lower than literature values for DPPC bilayers which range around 30° (McIntosh 1980, Smith 1988, Sun 1994). It is also considerably lower than the upper bilayer of the DPPC sample which had a tilt angle of 34°.

The roughness of both bilayers was considerable higher than that of the DPPC sample which had roughnesses of 3Å and 5Å. The roughness of both bilayers decreased by 4Å over the 25.1 – 34.7°C temperature range. This is discussed fully in the fluid phase section. Both water layers were also considerable thicker than in the DPPC sample, with a difference of 3±1Å in the lower water layer and 8Å in the main water layer. It could be that 10 mol% of cholesterol is modifying the Helfrich forces which determine the mean separation of the bilayers.

The coverage of the upper bilayer was much lower than that of the DPPC sample. Increasing amounts of cholesterol was found to progressively decrease the coverage of the upper bilayer.

3.10.3 Fluid Phase Structures

The sample was measured at fluid phase temperatures between 41.8°C to 47.2°C and then down to 42.8°C. The fitted profiles 45.5°C, 47.2°C and 42.8°C are shown in Figure 3.50 and the parameters listed in Table 3.29.

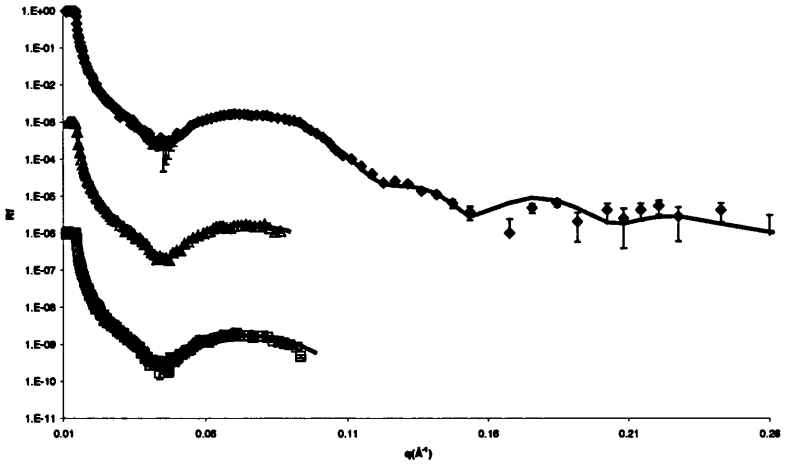

Figure 3.50 Fits of the reflectivity profiles of 10 mol% cholesterol 90 mol% DPPC double bilayer at 45.3°C (♦), 47.2°C (Δ) and 42.8°C (□).

	dw	lDb	lDc	lAPM	lRou	lCov	Dw	uDb	uDc	uAPM	uRou	uCov
25.1°C	15±1	51±2	35±1	46±2	12±1	100±4	36±1	53±2	37±1	43±2	16±2	75±4
41.8°C	11±1	45±2	31±1	51±2	5±1	95±2	35±1	49±2	34±1	47±2	4±2	70±4
42.6°C	11±1	45±2	32±1	51±2	3±1	96±2	34±1	48±2	33±1	48±2	3±2	73±4
43.5°C	10±1	43±2	30±1	53±2	3±1	95±2	35±1	46±2	32±1	50±2	3±2	73±4
44.4°C	10±1	43±2	30±1	53±2	3±1	96±2	34±1	47±2	33±1	48±2	2±2	72±4
45.4°C	11±1	45±2	31±1	51±2	3±1	95±2	32±1	47±2	33±1	48±2	3±2	72±4
47.2°C	11±1	45±2	31±1	51±2	3±1	95±2	31±1	45±2	32±1	50±2	3±2	72±4
42.8°C	11±1	46±2	31±1	51±2	3±1	95±2	31±1	46±2	33±1	48±2	3±2	74±4

Table 3.29 Parameters of fluid phase structure of 10 mol% cholesterol 90 mol% DPPC double bilayer.

The change in the thickness of the chain regions as a function of temperature is shown in Figure 3.51. The thickness remained relatively constant until between

39.1°C – 39.9°C, after which it decreasing, finally reaching a constant value around 42.6°C. The two bilayers therefore had the same phase behaviour. The transition temperature was different to that of the DPPC sample, which had a transition between 40.3°C – 41.9°C for the upper bilayer and 44.4°C – 48.9°C for the lower bilayer. The presence of 10 mol% cholesterol lowers the transition temperature of both bilayers, lowering it considerably for the lower bilayer. It also broadens the temperature range over which it occurs. This behaviour was similar to that of the 6 mol% sample.

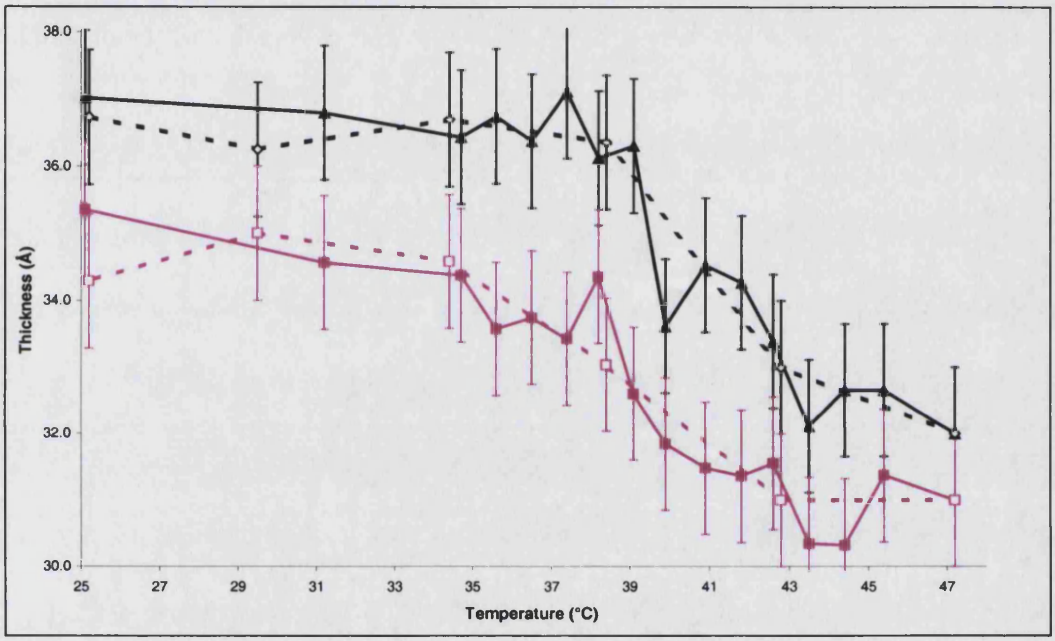

Figure 3.51 Variation of thickness of chain regions as a function of temperature of 10 mol% cholesterol 90 mol% DPPC double bilayer. The black line is the upper bilayer, the pink line the lower bilayer. Bold lines are heating, dashed are cooling.

The phase transitions were reversible, occurring at almost the same temperature upon heating as upon cooling. The thickness of the chain regions of both the bilayers decreased by 5Å. This was comparable to the DPPC sample. Although the decrease was the same, the upper bilayer was 3Å thicker than the DPPC sample. The gel phase was also thicker by this amount. It is likely that this level of cholesterol is increasing the chain order in the fluid phase. This is in agreement with literature data that indicate that the net effect of cholesterol is to increase the lipid bilayer thickness by 3-4 Å independently of temperature (Leonard 2001).

The change in the roughness of both bilayers as a function of temperature is shown in Figure 3.52. The change in the bilayer roughness behaved differently to the DPPC sample and to the 1 – 6 mol% samples. The initial gel phase roughness at 25°C was 11Å higher than the DPPC sample and 6Å higher than the 6 mol% sample. The upper bilayer roughness steadily decreased up to 39.9°C after which it rapidly decreased to 3Å at 42.6°C. The lower bilayer behaved in a similar fashion. Upon decreasing the temperature in the fluid phase and then in the gel phase the roughness of the upper bilayer increased, whilst that of the lower bilayer remained constant. The roughness of the upper bilayer of 9Å at 25°C was less than that of the original of 16Å at 25°C.

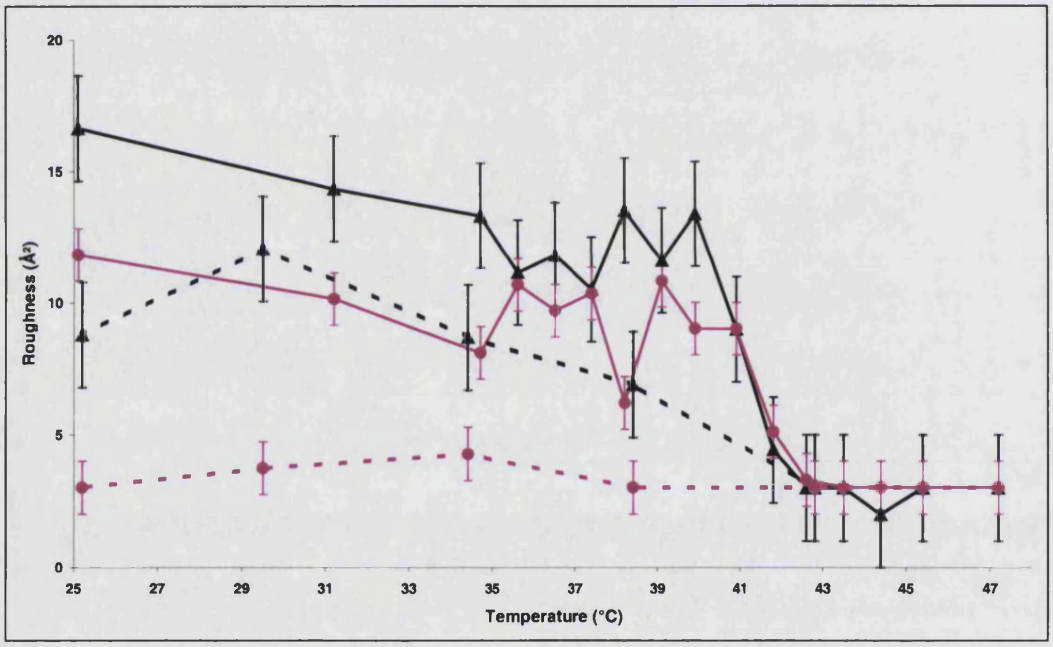

Figure 3.52 Variation of bilayer roughness as a function of temperature of 10 mol% cholesterol 90 mol% DPPC double bilayer. The black line is the upper bilayer, the pink line the lower bilayer. Bold lines are heating, dashed are cooling.

The phenomenon of very high roughness in the gel phase and low roughness in fluid phase, and the irreversible nature, was unexpected and differed from that of the 0 – 6 mol% samples. It can be rationalised by the cholesterol interfering with the packing of the DPPC chains. Molecular dynamic simulations have shown that at very high cholesterol concentrations (50 mol%) DPPC bilayers have higher roughness than

pure DPPC, due to the shorter cholesterol molecules (Smondyrev and Berkowitz, 1999). No information on the roughness of 10 mol% cholesterol bilayers could be found in the literature. The most likely explanation for the high roughness in the gel phase is related to miscibility issues. It has been observed in vesicles containing cholesterol concentrations between 8 – 24 mol% that two coexisting phases are observed (Knoll 1985). One consists of a tilted phase resembling that of a pure DPPC bilayer and the other a non-tilted mixture containing 24 mol% of cholesterol. The figure of 24 mol% corresponds to reconciling the concepts of phase separation and complex formation. The same group established that there was complete miscibility in the fluid phase in vesicles up to ratios of 14 mol%, with strong evidence that it was the case up to 45 mol%. Complete miscibility in the 10 mol% sample here would be expected to have lower roughness than the phases occurring in the gel phase. The different behaviour observed with the lower bilayer close to the silicon might be related to substrate effects.

The thickness of the water layer decreased progressively during the fluid phase temperatures. Swelling of the water layer was observed upon heating during the transition region and was expected to occur upon cooling in the transition region.

The thickness of the sample cooled to 25.8°C water layer was 32Å and thus was similar to those of the high fluid phase temperature structures. Larger amounts of cholesterol between 20 – 50 mol% have been observed to slightly increase the Van der Waals forces between bilayers (Simon 1991), which would decrease the water layer thickness. However why this would only start to occur in the fluid phase of this sample is unclear.

3.10.4 Transition Phase Behaviour

The sample was measured in the transitional temperature range between 35.6°C to 40.9°C and between 38.4°C to 34.4°C. Fitted profiles upon increasing and decreasing the temperature are shown in Figure 3.53 and the parameters listed in Table 3.30. Unfortunately upon cooling, only two temperatures were measured in the transition phase (38.4°C and 34.4°C). It is therefore not possible to give a complete picture of this phase upon cooling.

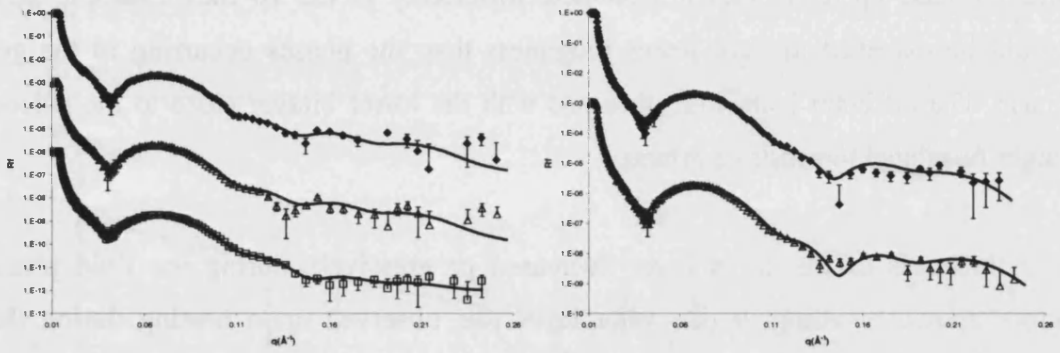

Figure 3.53 Fits of 10 mol% cholesterol 90 mol% DPPC double bilayer of (a) increasing temperature 35.6°C (♦), 37.4°C (Δ) and 39.9°C (□) and (b) decreasing at 38.4°C (♦) and 34.4°C (Δ).

Figure 3.54 shows the change in the thickness of the water layer and the roughness and solvation of the upper bilayer as a function of temperature. The roughness of the upper bilayer remained relatively constant during both heating and cooling in the transition phase. The water layer however swelled upon heating. The swelling occurred over the range 37.4 – 42.6°C, with a maximum at 39.9°C and magnitude of 5 Å (Figure 3.55). It started just before the melting of the chains and finished just before the end of them and was symmetrical either side of the maximum. It was not possible to ascertain whether it occurred upon cooling as the two temperatures measured upon cooling, 38.4°C and 34.4°C, are either side of where it occurred upon heating. As the behaviour is similar to the 6 mol% sample upon heating, it is likely that the 10 mol% sample exhibited similar swelling upon cooling.

	dw	lDb	lDc	lAPM	lRou	lCov	Dw	uDb	uDc	uAPM	uRou	uCov
25.1°C	15±2	51±2	35±1	46±2	12±1	100±4	36±1	53±2	37±1	43±2	16±2	75±4
35.6°C	14±2	49±2	34±1	47±2	10±1	98±4	34±1	52±2	37±1	43±2	11±2	72±4
36.5°C	13±2	48±2	34±1	47±2	10±1	97±4	35±1	52±2	36±1	44±2	12±2	70±4
37.4°C	14±2	49±2	34±1	47±2	10±1	99±4	34±1	53±2	36±1	44±2	11±2	72±4
38.2°C	11±2	49±2	34±1	47±2	9±1	94±4	35±1	52±2	36±1	44±2	14±2	71±4
39.1°C	12±2	47±2	33±1	49±2	11±1	99±4	36±1	52±2	36±1	44±2	12±2	68±4
39.9°C	13±2	46±2	32±1	50±2	9±1	98±4	38±1	48±2	34±1	48±2	13±2	72±4
40.9°C	14±2	45±2	32±1	51±2	9±1	100±4	36±1	49±2	35±1	46±2	9±2	73±4
47.2°C	11±1	45±2	31±1	51±2	3±1	95±2	31±1	45±2	32±1	50±2	3±2	72±4
38.4°C	10±2	50±2	34±1	47±2	3±1	98±4	34±1	49±2	35±1	46±2	8±2	72±4
34.4°C	10±2	52±2	34±1	47±2	4±1	98±4	32±1	51±2	35±1	46±2	10±2	72±4
25.8°C	10±1	51±2	34±1	47±2	4±1	95±4	32±1	51±2	36±1	44±2	11±2	70±4

Table 3.30 Fitted parameters of 10 mol% cholesterol 90 mol% DPPC double bilayer transition phase structures upon increasing and decreasing the temperature. The gel phases before and after the temperature scan 25.8°C and the fluid phase 48.0°C are given for comparison.

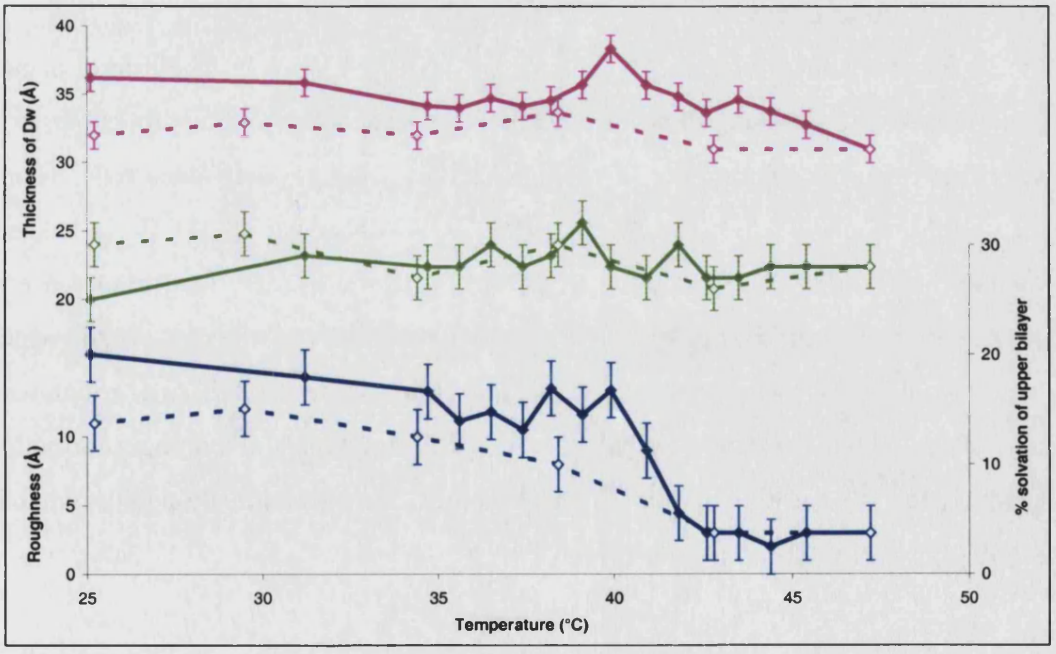

Figure 3.54 Thickness main water layer (pink), solvation of upper bilayer (green) and the average upper bilayer roughness (blue) of 10 mol% cholesterol 90 mol% DPPC double bilayer. The bold lines are increasing temperature and dashed decreasing temperature.

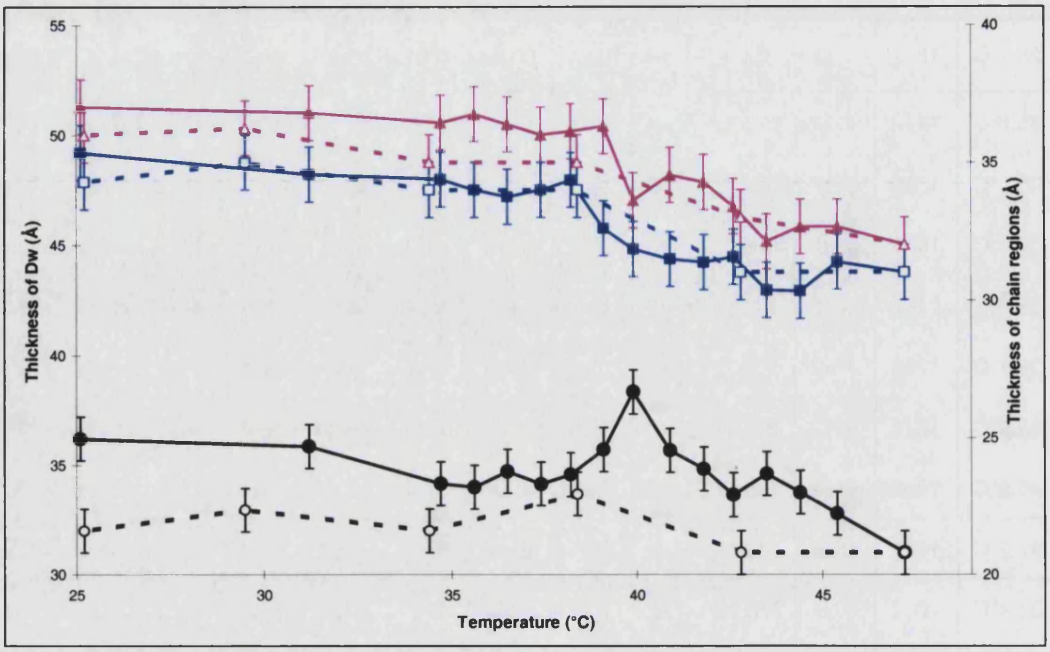

Figure 3.55 Thickness of upper chain region (pink) and lower chain region (blue), and thickness of main water layer (black) of 10 mol% cholesterol 90 mol% DPPC double bilayer. The bold lines are increasing temperature and dashed decreasing temperature.

Interpretation of behaviour

The concentration at which the suppression of the ripple phase by cholesterol occurs is slightly ambiguous as ripple structures have been observed up to cholesterol concentrations of 20 mol%. In recent studies, suppression occurred around concentrations of 14 – 15 mol% (Adachi 1995, Karmakar 2003). It is unclear whether the 10 mol% sample exhibited a ripple structure as there was no increase in roughness. The sample already had very high roughness in the gel phase, which suggested domain formation, whilst in the fluid phase it had low roughness, suggesting complete miscibility. The high gel phase roughness and domain formation could hinder the formation of a ripple structure. The question though is what is causing the swelling of the water layer.

The level of swelling is similar to that observed in the phenomenon of anomalous swelling mentioned for the 6 mol% sample. It is observed when cooling in the fluid phase near to the main transition temperature T_m. A small swelling of 2 – 4Å has

been observed for phosphatidylcholine bilayers (Hønger 1994, Richter 1999, Mason 2000, Pabst 2003). The swelling is has been observed with cholesterol concentrations up to 15 mol% (Richter 1999). The similar increases in the water layer could suggest a connection of the swelling of the 10 mol% sample with anomalous swelling. However anomalous swelling is usually only observed upon cooling.

3.11 Deuterated DPPC double bilayers

3.11.1 Introduction

The fabrication of double bilayers using DPPC lipids with deuterated chains (d_{62}-DPPC) has not previously been successful. The fabrication was assessed again and the resulting structure measured by reflectivity. Deuterated double bilayers of DSPC (the chains each have 2 more carbon units than DPPC) have been fabricated and the phase behaviour studied (Fragneto 2003).

The fabrication results were given in the fabrication results section (Table 3.1). It can be seen that whilst the first and third depositions were excellent and were comparable to the hydrogenated version, the second deposition was very poor. It had a transfer ratio of 0.14 and bad fringes were observed. Given that the ratio of polished to unpolished of blocks is 29% and if the deposition occurred only on the polished side, the maximum coverage for that deposition would be 48%.

The deuterated double bilayer was measured in H_2O only at 25°C due to the very poor quality of sample.

3.11.2 Gel phase structure

The profile was fitted using a double bilayer model. The profile resembles somewhat the profile of a single bilayer, but it was not possible to fit it with a single bilayer model.

The fitted profile at 25.1°C is given in Figure 3.56. The parameters used are listed in Table 3.31 along with those of the hydrogenated version. The double bilayer had a very low coverage for the lower bilayer, as expected from the low transfer ratio. This is why the reflectivity profile does not have the expected double bilayer shape.

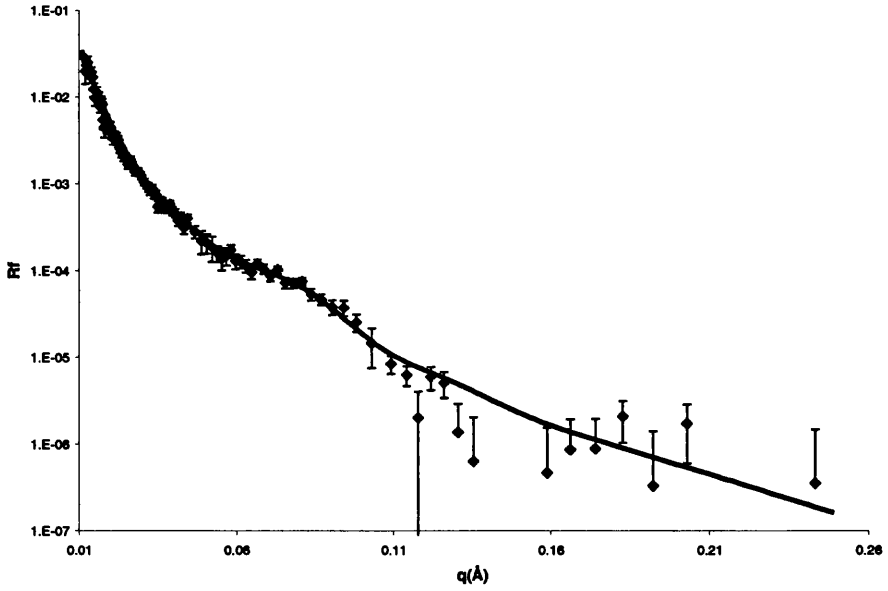

Figure 3.56 Fitted profile of deuterated DPPC double bilayer at 25.1°C (♦)

	dw	lDb	lDc	lAPM	lRou	lCov	Dw	uDb	uDc	uAPM	uRou	uCov
d-DPPC 25.1°C	11±1	51±2	37±1	43±2	18±1	48±2	27±1	52±2	38±1	42±2	24±2	70±2
h-DPPC 25.0°C	12±1	50±2	35±1	46±2	3±1	100±2	27±1	49±2	34±1	47±2	5±2	93±2

Table 3.31 Fitted parameters of deuterated DPPC double bilayer and the hydrogenated DPPC double bilayer at 25°C

The structure of the deuterated double bilayer was very different from the hydrogenated version. As expected from the low second transfer ratio, the coverage of the lower bilayer was very low. The upper bilayer coverage was also low. Both bilayers had very high roughness, which is probably a due to patches of bilayers and holes. The thickness of the chains was larger than that of the hydrogenated version. The fact that the chain thickness is large, and thus the chains more vertical, indicates that the molecules are probably form domains. The larger thickness also indicates that the deuterated chains are also less tilted than their hydrogenated counterparts. It is unclear why this is the case.

3.11.3 Interpretation

It has not been possible to make high quality d_{62}-DPPC double bilayers despite repeated efforts. The main problem is the second deposition, which normally tends to be the most sensitive deposition. The reason for the fabrication differences between the hydrogenated and deuterated samples is unclear. Monolayers of hydrogenated and deuterated DPPC have previously been found to have different surface pressures when measured at the same APM. This was attributed to either reduced Van der Waals interactions between the deuterated chains or due to an increase in local disorder introduced by a higher chain kink order or enhanced vibrational mode or a combination of both (Vaknin 1991).

The monolayer structures were found to be similar when measured by x-ray and neutron reflectivity measurements high above the transition to the highly condensed phase. Substrate supported bilayers containing 51 mol% d-DMPC and 49 mol% h-DMPC have previously been formed by vesicle adsorption, but the degree of coverage was not mentioned (Johnson 1991). In other more complicated systems, involving depositions of deuterated DPPC onto polymer films, the monolayer was found to have a coverage as low as 40% (Perez 2003).

It is not clear why a deuterated version of DPPC does not deposit. It could be connected to contamination in the components, but this is unlikely as would it would show up in the analytical tests by the company.

3.12 Single bilayers of d-DPPC and h-DPPC containing 10 mol% cholesterol

Single bilayers of hydrogenated and deuterated chain DPPC with 10 mol% cholesterol were successfully fabricated. Their phase behaviour was compared to the double bilayer versions to assess whether there are significant differences in the phase behaviour of the isotopic variants. An understanding of the phase behaviour of the deuterated single bilayer aids its applicability as a biomembrane, especially in light of the fabrication problems of double bilayers of d_{62}-DPPC

No significant differences or trends were observed between the two versions in the fabrication. The fabrication results were given in the fabrication section of this chapter.

3.12.1 h-DPPC and 10 mol% cholesterol

The sample was measured at 25.2°C and 48.4°C in a range of different solvent contrasts. The oxide thickness of 18Å was large and was likely due to an older silicon substrate being used. Its roughness was 3Å and thus comparable to the other substrates. The fitted profiles at the two temperatures in the different solvent contrasts are shown in Figure 3.57 and the parameters listed in Table 3.32.

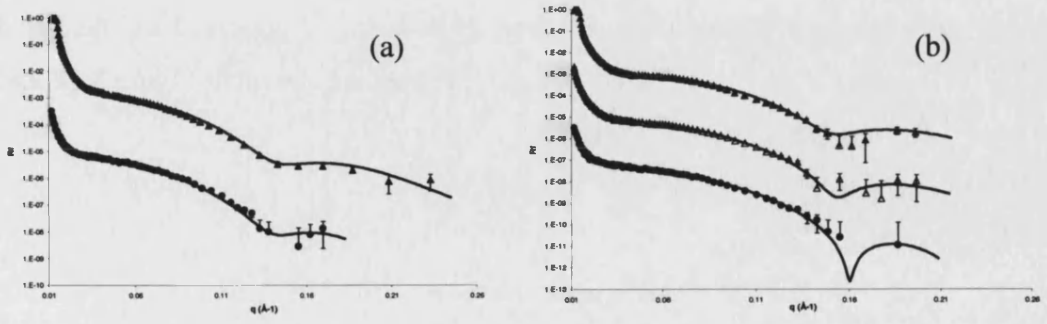

Figure 3.57 Fitted profiles of single bilayer of h-DPPC containing 10 mol% cholesterol at 25.2°C (a) in D_2O (▲) and SMW (●), and at 48.4°C in D2O (▲), 4MW (Δ) and SMW (●).

		dw	Db	Dc	APM	Rou	Cov
25.2°C	D_2O	9±1	54±2	36±1	44±2	6±1	82±4
	SMW	8±1	52±2	34±1	47±2	5±1	74±4
48.4°C	D_2O	9±1	50±2	31±1	52±2	4±1	80±4
	4MW	9±1	50±2	31±1	52±2	4±1	80±4
	SMW	9±1	48±2	29±1	55±2	4±1	80±4

Table 3.32 Fitted parameters of single bilayer of hydrogenated DPPC containing 10 mol% cholesterol

The single bilayer exhibited gel and fluid phases, with a difference in the chain region thickness of 5Å. The chain region thickness and roughness of the bilayer in both phases is very similar to the lower bilayer of the 10 mol% double bilayer. The water layer though was slightly thinner than that of double bilayer and the coverage lower. This could be due to the use of the Schaefer deposition.

The single bilayer is therefore similar to that of the lower bilayer of the double bilayer, even though different fabrication techniques were used.

3.12.2 d- DPPC and 10 mol% cholesterol

The deuterated sample was measured at 25.7°C and 47.9°C in a range of different solvent contrasts. The oxide thickness was 8Å and its roughness 3Å. The fitted profiles at the two temperatures in the different contrast are shown in Figure 3.58 and the parameters are listed in Table 3.33.

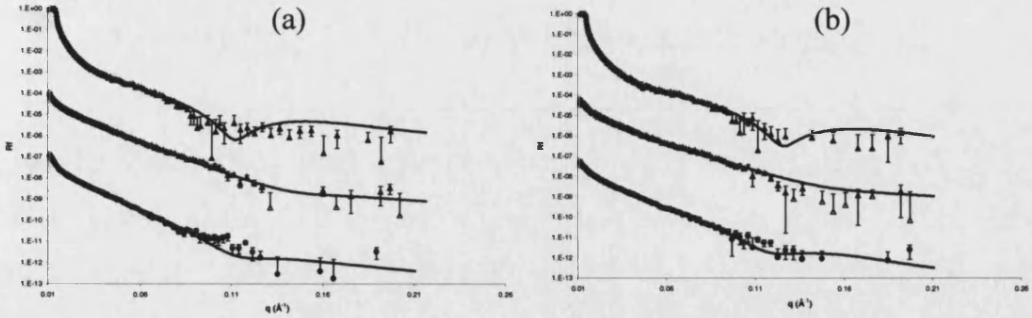

Figure 3.58 Fitted profiles of single bilayer of h-DPPC containing 10 mol% cholesterol at 25.7°C (a) in D_2O (▲), H_2O (Δ) and SMW (●), and at 47.9°C in D2O (▲), H_2O (Δ) and SMW (●).

		dw	Db	Dc	APM	Rou	Cov
25.2°C	D_2O	6±1	57±2	35±1	46±2	16±1	98±4
	H_2O	6±1	57±2	35±1	46±2	16±1	98±4
	SMW	6±1	59±2	38±1	42±2	15±1	82±4
	D_2O	6±1	50±2	28±1	57±2	15±1	94±4
48.4°C	H_2O	6±1	50±2	28±1	57±2	15±1	94±4
	SMW	6±1	50±2	28±1	57±2	14±1	94±4

Table 3.33 Fitted parameters of single bilayer of deuterated DPPC containing 10 mol% cholesterol

Unlike the double bilayer version, the single bilayer had good coverage. Like the hydrogenated single and double bilayers it exhibited both gel and fluid phase structures, with a decrease in the chain thickness of 7Å. The roughness was much higher than these samples though and resembled that present in the lower bilayer of deuterated double bilayer.

3.13 Comparison of double bilayer parameters

3.13.1 Gel phase chain region thickness as a function of cholesterol

Cholesterol is known to have a condensing effect on the area per molecule of phosphatidylcholine molecules in bilayers (Smondryev 1999, Radhakrishnan 2000, Chiu 2002). A condensing of the area per molecule would be expected to increase in the thickness of the chain region as it would reduce the tilt of the chains. Table 3.34 shows the thickness of the chain region versus cholesterol content.

	Initial		Equilibriated	
mol%	dc	Dc	dc	Dc
0	35±1	34±1	35±1	34±1
1	34±1	35±1	35±1	34±1
2	34±1	34±1	33±1	34±1
4	34±1	36±1	34±1	37±1
6	35±1	38±1	36±1	38±1
10	35±1	37±1	34±1	36±1

Table 3.34 Gel phase initial and equilibrated thickness of chain region versus cholesterol content of lower (dc) and upper bilayer (Dc)

The presence of 4 – 10 mol% cholesterol in the gel phase increased the upper bilayer thickness by 3 – 4Å before and after the temperature scan compared to the DPPC thickness. Below 4 mol% the thickness was identical to DPPC. The thickness of the lower bilayer chain region was not affected by the presence of cholesterol contents even up to 10 mol%. The difference in the behaviour between the upper and lower bilayers could be due to the substrate exerting a stronger restraining force on the lower bilayer.

There was no trend presence in the thickness of the fluid phase chain regions as a function of cholesterol content. This is expected as the chains are not higher ordered or tilted in the fluid phase (Nagle 2000). Cholesterol would not be expected to influence the thickness.

3.13.2 Water layer thickness as a function of cholesterol

The gel phase thickness of the water layers as a function of cholesterol content before and after the temperature scans are shown in Table 3.35. The initial thickness of the lower water layers varied without a trend. The thickness was likely determined by differences in the fabrication. After cooling from the fluid phase it is likely that the thickness is equilibrated and predominantly determined by the strength of the interaction between the substrate and lower bilayer. The majority of the samples had a similar lower water layer thickness of 9±1Å, so it is unlikely that cholesterol effects this interaction.

25°C	Intial thickness (Å)		Equilibrated thickness (Å)	
Molar ratio of cholesterol (mol%)	dw	Dw	dw	Dw
0	12±1	27±1	12±1	29±1
1	9±1	22±1	10±1	29±1
2	10±1	23±1	9±1	28±1
4	9±1	29±1	8±1	27±1
6	7±1	33±1	9±1	35±1
10	14±1	37±1	9±1	31±1

Table 3.35 Comparison of thickness of water layers in gel phase at 25°C before and after temperature scans.

The initial thickness of the main water layer varies significantly, with a difference of 15Å between the 1 mol% and 10 mol% samples. The thickness of the water layers after the temperature scan seems to have been equilibrated, as apart from the 6 mol% sample, they all have a thickness within 29±2Å with no trend present. The reason for the larger value of the 6 mol% sample is unclear, although when measured in SMW, the contrast gave a value of 32Å. This behaviour differs from previous literature studies, where the presence of small concentrations of cholesterol was been found to dramatically increase the fluid separation in gel phase DPPC vesicles (Rand 1980, Simon 1991). Incorporation concentrations of cholesterol between 3 – 10 mol% were observed to increase the thickness by 15 – 25Å. The increase was due to the cholesterol inducing large periodic ripples in the plane of the bilayer that increased the entopic repulsion between the bilayers. The reason for the difference in the

behaviour of the double bilayer could be linked to the difference in confinement of the bilayers.

The thickness of the main water layer in the fluid phase at 47°C is plotted as a function of cholesterol content in Figure 3.59.

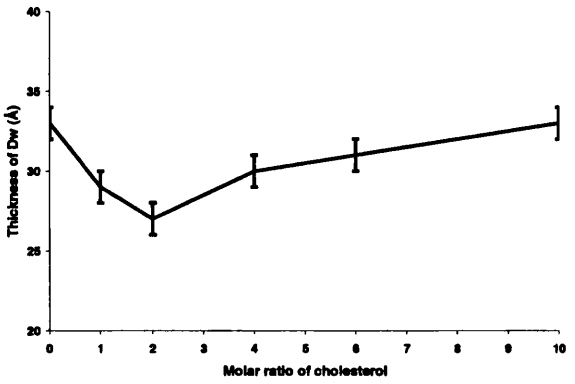

Figure 3.59 Fluid phase thickness of main water layer of double bilayers at 47°C as a function of cholesterol content.

In previous studies using vesicles, the water layer did not appreciatively increase with small amounts of cholesterol, and was almost independent of cholesterol content (Hui 1983, Simon 1991). In the case of the double bilayer there is a small trend present, where very low amounts of cholesterol (1 – 2 mol%) decrease the water layer thickness. When the cholesterol level was increased the thickness then progressively returned back to the DPPC sample thickness.

The very low concentrations of cholesterol are influencing the interactions between the two bilayers and thus the changing the distance between the two bilayers. The main interactions between the two bilayers are attractive Van der Waals forces and repulsive undulations, with the addition of the influence of substrate forces here (Chapter 1). It would be expected that the cholesterol could reduce the fluctuations, due to its influence on the fluctuations in the transition region (i.e. ripples). But a reduction in the fluid phase fluctuations (repulsive forces) would be expected to bring the two bilayers closer. Unlike the effect of cholesterol on the transition phase behaviour, increasing the cholesterol concentration does not have a linear effect on the thickness of the water layer. However, previously very low amounts of

cholesterol have been observed to have a different effect on the bilayer behaviour in comparison to higher amounts, in that case it was anomalous swelling (Lemmich 1997). It could therefore be the same situation for the thickness of the water layer in the fluid phase.

3.13.3 Effect of cholesterol upon heating in the transition phase

The similarities between the values of the upper bilayer roughness of the DPPC double bilayer and the value of the ripple amplitude of a very similar system (Kaasgaard 2003) suggest that the roughness parameter is proportional to the amplitude of the ripple structure. The possibility of a link between the two values is very interesting as only very limited and scattered data on ripple amplitudes have previously been reported.

Maximum increase in parameters versus cholesterol content

Table 3.36 shows the maximum increase in the water thickness and upper bilayer roughness parameters of the 0 – 6 mol% ratios of cholesterol in the transition region. The 10 mol% sample behaved differently so is not discussed here. It can be seen that the maximum increase of the parameters successively decreases as the concentration of cholesterol is increased. The behaviour of the 1 mol% sample only slightly differed from the DPPC sample with the 15Å amplitude, but by 2 mol% the difference is larger. The 4 mol% cholesterol parameters indicate that a rippling structure is still present, whilst by 6 mol% it is not possible to determine whether one is present as the difference in the upper bilayer roughness between the gel and transition phase is so low. Only a swelling of the water layer is observed. This was also the case in the 10 mol%. It is likely therefore that the incorporation of cholesterol progressively decreases the amplitude of the ripple phase, until a ratio of 6 mol%, where it cannot be discerned.

	Gel value (25°C)					Maximum transition phase value					Maximum increase				
	0 mol%	1 mol%	2 mol%	4 mol%	6 mol%	0 mol%	1 mol%	2 mol%	4 mol%	6 mol%	0 mol%	1 mol%	2 mol%	4 mol%	6 mol%
Dw	27±1Å	22±1Å	23±1Å	29±1Å	33±1Å	43±1Å	37±1Å	33±1Å	37±1Å	37±1Å	16±1Å	15±1Å	10±1Å	8±1Å	4±1Å
Urou	5±2Å	7±2Å	6±2Å	9±2Å	10±2Å	15±2Å	16±2Å	13±2Å	14±2Å	11±2Å	10±2Å	9±2Å	7±2Å	5±2Å	1±2Å
uSolv	7±4%	14±4%	5±4%	11±4%	25±4%	27±4%	22±4%	20±4%	14±4%	29±4%	20±4%	8±4%	15±4%	3±4%	4±4%

Table 3.36 The gel phase values, maximum values and maximum increase in values of the parameters during the transition phase of the different ratios of cholesterol with DPPC.

The maximum increase in the upper bilayer roughness versus the maximum increase in the water layer is plotted in Figure 3.60. When the error bars are taken into account it can be seen that the decrease in both parameters is almost proportional. This is expected for a rippling structures as the larger the ripple the larger the average water thickness.

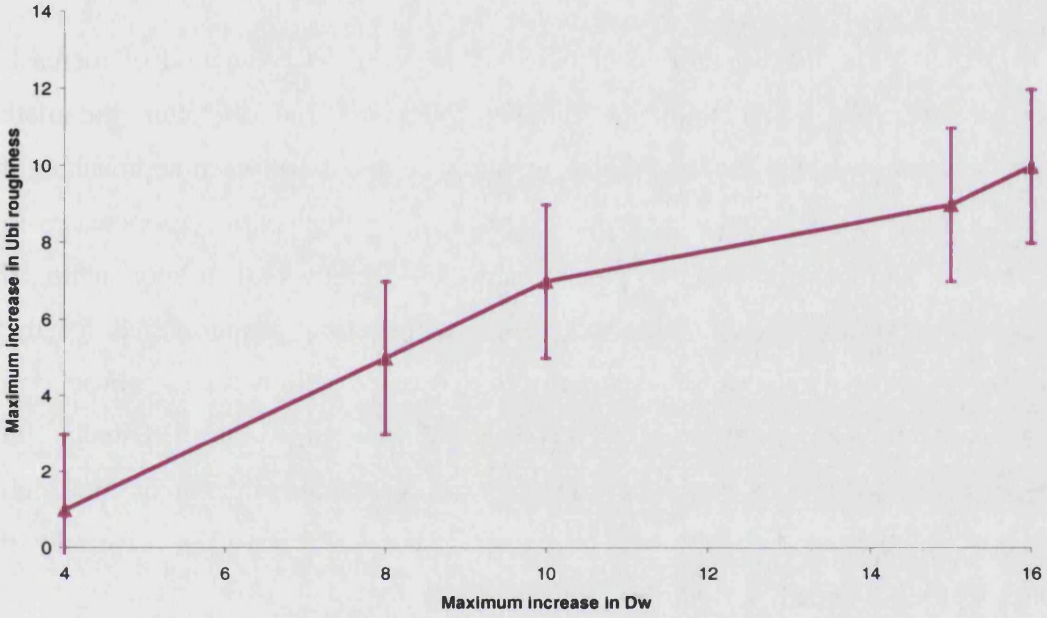

Figure 3.60 Maximum increases in the upper bilayer roughness versus the maximum increase in the water layer.

It was not possible to find literature on the change in ripple amplitude as a function of cholesterol in phosphatidylcholine systems. In one study the introduction of cholesterol into DMPC vesicles was been observed to increase the periodicity of the ripple (Mortensen 1988). However, cholesterol also gave rise to a marked temperature dependence of the periodicity. The relationship between periodicity and cholesterol is therefore not trivial. The effect of the introduction of the cholesterol on the amplitude cannot be inferred from the effect on the wavelength, as the relationship between the ripple periodicity and amplitude is not clear in literature. The two properties could be connected, as in the case of the two ripple structures observed when cooling in the transition phase, which consisted of a long wavelength

ripple with large amplitude and a short wavelength with small amplitude (Kaasgaard 2003). Other studies though suggest that they are not related, as when the ripple amplitude was observed to decrease with decreasing temperature, but the wavelength remained constant (Woodward 1996). It is therefore not possible to say whether decreases in the ripple amplitude are accompanied by decreases in the wavelength. In the double bilayer study it can only be said that increasing amounts of cholesterol is probably decreasing the ripple amplitude.

The ratios 0 – 4 mol% exhibited the same behaviour as a function of increasing temperature. The water thickness, bilayer roughness and solvation parameters initially increased, then reached a plateau, and then decreased when approaching the main transition. The behaviour would suggest that the ripple structure increases to a maximum amplitude during the plateau and then decreases when approaching the main transition. No linear behaviour versus temperature was observed for these ratios. This behaviour would differ to that observed with vesicles whose ripple amplitude and wavelength progressively changed with temperature (Matuoka 1993, Woodward 1996). This could be due to the different containment of the double bilayer where one side of the bilayer is open to the reservoir, when in vesicles the bilayers are contained between two bilayers.

The thickness of the main water layer at 25°C varied for the different ratios. The increase in the water layer observed in the transition phase was related to the initial gel phase thicknesses. The thickness of the water layer versus temperature is shown in Figure 3.61. The data has been shifted so that all the water layer thicknesses of all the samples at 25°C are the same as the DPPC sample, allowing direct comparison of the increase.

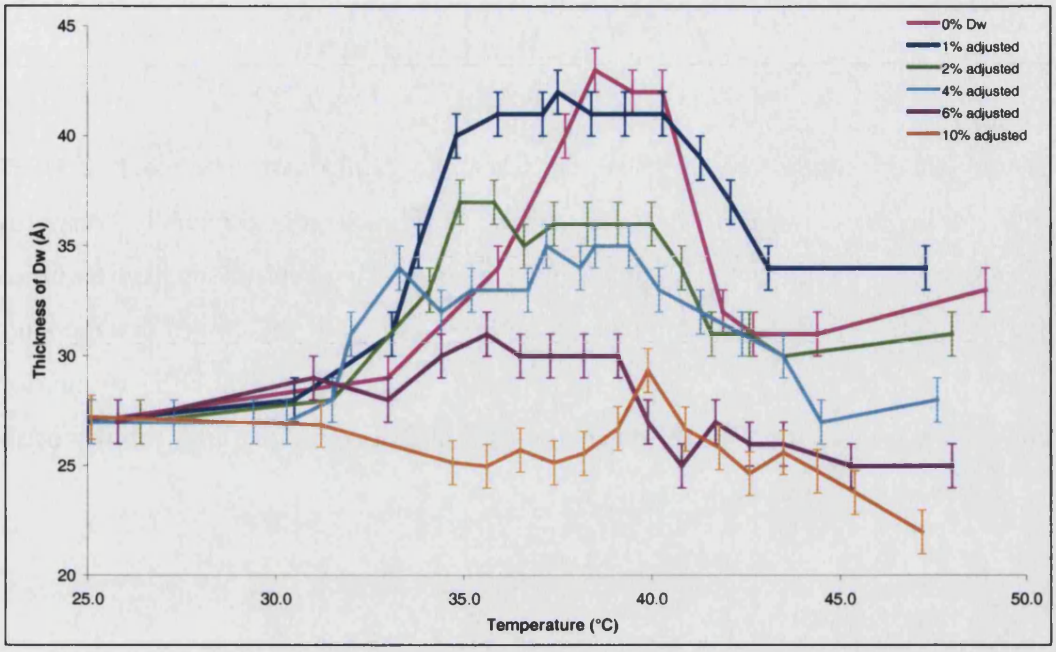

Figure 3.61 Change in the main water layer (Dw) thickness as a function of temperature. The plots have been shifted vertically so that they all have the same water layer thickness at 25°C.

The progressive decrease in the maximum values of the water layer as a function of cholesterol is clearly visible. The addition of 1 – 4 mol% cholesterol also progressively broadens the temperature range over which the increase occurs. The addition of 10 mol% causes the sample to behave differently to the lower ratios. This is probably due domain formation, which occurs in samples with cholesterol ratios above 8 mol% (Knoll 1985) and was discussed more fully in the 10 mol% section. The increase of the water layer is proportional to the bilayer roughness (Figure 3.60) and probably the ripple structure. The increase is caused by an increase in the bilayer separation, which would be effected by the ripple structure (Mecke 2003).

Conclusion

Increasing the cholesterol concentrations progressively decreases the level of structural change observed upon heating the double bilayers in the transition region. With 0 – 4 mol% the ripple structure is still present due to the increase in bilayer roughness. By 6 – 10 mol% it is not possible to clearly determine the ripple structure. Increasing the cholesterol concentration progressively decreases the size of the increase in the water layer thickness.

3.14 Overall Conclusion

The aim of this study was to assess the fabrication and phase behaviour of DPPC double bilayers containing 0 – 10 mol% of cholesterol, especially very low concentrations (1 – 4 mol%). Vesicle studies of similar concentrations have exhibited interesting phase behaviour which is not fully understood. It was hoped that the study of the phase behaviour of the double bilayer system would aid the discussion, providing relevant biophysical information and also increase the applicability of the systems as biomembrane mimics.

Fabrication conclusions

The results have shown that with the Langmuir-Blodgett-Schaefer technique it is possible to fabricate stable DPPC double bilayers containing between 0 – 10 mol% cholesterol. It is not possible to fabricate double bilayers with very low concentrations of cholesterol (1 – 2 mol%) by vesicle adsorption. Langmuir-Blodgett techniques are able to overcome the problem. It was not possible to fabricate high coverage double bilayers containing 20 mol%. It is likely that with high concentrations, domain formation of cholesterol rich regions and poor regions occurs (Knoll 1985). There could also be deposition problems with the liquid-ordered state that cholesterol forms a these concentrations (Vist 1990).

Unfortunately it was not possible to fabricate high coverage double bilayers of deuterated chain DPPC (d_{62}-DPPC), although it was possible to fabricate high coverage single bilayers of d_{62}-DPPC with 10 mol% cholesterol. The reason for the difference in fabrication behaviour between the hydrogenated DPPC and deuterated DPPC are being investigated. It may be necessary to apply different fabrication techniques for the deuterated lipid bilayers.

DPPC cholesterol phase behaviour conclusions

All samples containing between 0 – 10 mol% cholesterol exhibited fully stable and reversible gel, transition and fluid phases.

The thickness of the gel phase bilayers was found to increase with increasing cholesterol concentration. The presence of cholesterol therefore reduces the tilt of the DPPC chains. There was no correlation in the thickness of the fluid phase bilayer versus cholesterol concentration. This is expected as the chains are disordered in the fluid phase.

No trend was observed in the gel phase thickness of the main water layer separating the bilayers as a function of cholesterol content. However, in the fluid phase the water layer thickness decreased for very low concentrations (1 – 2 mol%), then increased back to that of the DPPC sample thickness with increasing cholesterol concentration.

Upon heating in the transition region the samples containing 0 – 4 mol% exhibited large increases in the upper bilayer roughness and water layer thickness parameters. This was interpreted as the observation of a rippling structure. The addition of 1 – 4 mol% cholesterol progressively broadened the temperature range over which the increase in parameters occurred. Increasing the cholesterol concentrations from 1 – 10 mol% progressively reduced the level of increase in these parameters observed in the transition region. With 0 – 4 mol% the ripple structure was still visible by the increases in the bilayer roughness, but by 6 – 10 mol% it was not possible to determine whether a ripple structure was present as only a swelling of the water layer was observed.

Upon cooling in the transition phase the reflectivity profiles of the 0 – 4 mol% samples were different to those measured during heating. The first fringe looked to consist of two overlapping fringes; especially the samples contained 1 – 4 mol%. It was not possible to fit these profiles successfully using only one model. Literature studies on similar samples suggest the presence of two coexisting rippling structures upon cooling. One ripple structure had parameters similar to the ripple observed upon heating and the other ripple had larger amplitude and wavelength parameters. It is likely that the profiles observed for the 0 – 4 mol% samples are due to a

combination of the reflectivity from the two distinct rippling structures. It was possible to fit parts of the profiles using two separate models representing two ripple structures. These gave results that were similar to those observed in other studies. The use of two models to fit different parts is only a simple approximation. Further work needs to be undertaken to understand the effect of two high roughness coexisting ripple structures on the reflectivity profiles. This is beyond the scope of this thesis.

What can be inferred for the 1 – 4 mol% profiles is that the presence of cholesterol alters the structure of one of the ripple structures present in the DPPC sample. The feature observed on the right side of the first fringe in the profile shifted to a higher q with 1 – 4 mol% cholesterol. It is possible that the cholesterol is reducing the size of the smaller ripple structure.

Upon cooling in the transition region the samples containing 6 – 10 mol% behaved differently to those containing 0 – 4 mol% cholesterol. They exhibited similar behaviour upon heating and cooling. Only a small increase in the water layer thickness was observed. It was not possible to say confidently whether 6 – 10 mol% of cholesterol eliminates the ripple structure, only that it likely reduces it. The different behaviour of the higher cholesterol concentrations could be caused by the formation of cholesterol rich and poor domains (Knoll 1985) that could be hindering the formation of ripples.

Phase behaviour of deuterate chain DPPC bilayers

As it was not possible to fabricate high coverage double bilayers of deuterated chain DPPC the phase behaviour of this system was not investigated. The phase behaviour of single bilayers of DPPC and d_{62}-DPPC containing 10 mol% was studied. The phase behaviour of the single bilayer of DPPC and 10 mol% cholesterol exhibited similar structural behaviour to the double bilayer version. The single bilayer of d_{62}-DPPC and 10 mol% cholesterol had a similar gel and fluid phase bilayer thickness to the hydrogenated DPPC single bilayer. Its roughness however was much higher.

3.15 References

- Adachi T, Takahashi H, Hatta I. (1995) *Cholesterol effects on ripple structure studied by small-angle neutron and x-ray diffraction* Physica B, 213&214, 760 – 762
- Banerjee S. (2002) *Exploring the ripple phase of biomembranes* Physica A 308, 89 – 100
- Chiu S W, Jakobsson E, Mashl R. et al. (2002) *Cholesterol-induced modifications in lipid bilayers: a simulation study* Biophys. J. 83, 1842–1853
- Copeland B R, McConnel H M. (1980) *The rippled structure in bilayer membranes of phosphatidylcholine and binary mixtures of phosphatidylcholine and cholesterol* Biochim. Biophys. Acta 599, 95 - 109
- Cunningham B, Brown A D, Wolfe D H, Williams WP, Brain A. (1998) *Ripple phase PC Effect chain length, position, and unsaturation* Phys. Rev. E. 58, 3662 –3672
- Deme B, Lee L T. (1997) *Adsorption of a hydrophobically modified polysaccharide at the air-water interface: kinetics and structure* J. Phys. Chem. B. 101, 8250 – 8258
- Dixon G S, Black S G, Butler C T. et al. (1982) *A differential AC calorimeter for biophysical studies* Analytical Biochemistry 121, 55 – 61
- Fragneto G, Graner F, Charitat T. et al. (2000b) *Interaction of the third helix of antennapedia homeodomain with a deposited phospholipid bilayer: a neutron reflectivity structural study* Langmuir 16, 4581-4588
- Fragneto G, Charitat T, Graner F. et al. (2001) *A fluid floating bilayer* Europhys. Lett. 53, 100 – 106
- Goldar A, Roser S J, Hughes A. et al. (2002) *The effect of surface texture on total reflection of neutrons and X-rays from modified interfaces* Phys. Chem. Chem. Phys. 4, 2379 – 2386
- Helfrich W. (1977) *Steric interaction of fluid membranes in multilayer systems* Z. Naturforsch 33a, 305 – 315
- Hughes A V, Goldar A, Gerstenberg M C. et al. (2002a) *Hybrid SAM phospholipid approach to fabricating free supported lipid bilayer* PCCP 4, 2371 –2378
- Hughes A V, Roser S J, Gerstenberg M C. et al. (2002b) *Phase behaviour of DMPC free supported bilayers studied by neutron reflectivity* Langmuir 18, 8161 – 8171
- Hui S W, He N B. (1983) *Molecular organisation in cholesterol-lecithin bilayers by x-ray and electron diffraction measurements* Biochemistry 22, 1159 – 1164
- Kaasgaard T, Leidy C, Crowe J H. et al. (2003) *Temperature-controlled structure and kinetics of ripple phases in one- and two-component supported lipid bilayers* Biophys. J. 85, 350 – 360
- Kaizuka Y, Groves J T.(2004) *Structure and dynamics of supported intermembrane junctions* Biophys. J. 86, 905 – 912
- Karmakar S, Raghunathan V A. (2003) *Chol. Induced Modulated Phase in Phospholipid Membranes* Phys. R. Lett. 91, 9, 098102
- Katsaras J, Tristram-Nagle S, Liu Y. et al. (2000) *Clarification of the ripple phase of lecithin bilayers using fully hydrated, aligned samples* Phys. Rev. E. 61, 5668 – 5677
- Kim K, Kim C, Byun Y. (2001) *Preparation of a dipalmitoyl-phosphatidylcholine/cholesterol Langmuir-Blodgett monolayer that suppresses protein adsorption* Langmuir 17, 5066 – 5070
- Knoll W, Schmidt G, Ibel K. et al. (1985). *Small-Angle Neutron Scattering Study of Lateral Phase Separation in Dimyristoylphosphatidylcholine-Cholesterol Mixed Membranes.* Biochemistry. 24, 5240 – 5246.

- Koenig B W, Krueger S, Orts W J. et al. (1996) *Neutron reflectivity and atomic force microscopy studies of a lipid bilayer in water adsorbed to the surface of a silicon single crystal* Langmuir 12, 1343 – 1350
- Lemmich J, Mortensen K, Ipsen J H. et al. (1997) *The effect of cholesterol in small amounts on lipid-bilayer softness in the region of the main phase transition* Eur. Biophys. 25, 293 – 304
- Leonard A, Escrive C, Laguerre M. et al. (2001) *Location of Cholesterol in DMPC Membranes. A Comparative Study by Neutron Diffraction and Molecular Mechanics Simulation†* Langmuir 17, 2019 -2030
- Lewis B A, Engelman D M. (1983) *Lipid bilayer thickness varies linearly with acyl chain length in fluid phosphatidylcholine vesicles* J. Mole. Bio. 166, 211 – 217
- McConnell H M, Radhakrishnan A. (2003) *Condensed complexes of cholesterol and phospholipids* (Review) BBA 1610, 159 – 173
- MacIntosh T J. (1980) *Differences in hydrocarbon chain tilt between hydrated phosphatidylethanolamine and phosphatidylcholine bilayers. A molecular packing model.* Biophys. J. 29, 237 – 245
- McPhillips (1972) Progress in Surface and Membrane Science 5, Academic Press, New York,
- Mason P C, Gaulin B D, Epand R M. et al. (2000) *Critical swelling in single phospholipid bilayers* Phys. Rev. E. 61, 5634 – 5639
- Matuoka S, Kato S, Akiyama M. et al. (1990) *Temperature dependence of the ripple structure in dimyristoylphosphatidylcholine studied by synchrotron X-ray small-angle diffraction* Biochim. Biophys. 1028, 103 – 109
- Matuoka S, Yao H, Hatta I. (1993) *Condition for the appearance of the metastable P beta' phase in fully hydrated phosphatidylcholines as studied by small-angle x-ray diffraction* Biophys. J. 64, 1456 – 1460
- Matuoka S, Kato S, Hatta I. (1994) *Temperature change of the ripple structure in fully hydrated DMPC/cholesterol multilayers* Biophys. J. 67, 728 – 736
- Mecke K R, Charitat T, Graner F. (2003) *Fluctuating lipid bilayer in an arbitrary potential: theory and experimental determination of bending rigidity* Langmuir 19, 2080 – 2087
- Mortensen K, Pfeiffer W, Sackmann E. et al. (1988) *Structural properties of a phosphatidylcholine-cholesterol system as studied by small-angle neutron scattering: ripple structure and phase diagram* Biochem. Biophys. Acta 945, 221 – 245
- Mouritsen O G, Jorgensen K. (1994) *Dynamical order and disorder in lipid bilayers* Chem. Phys. Lipids. 73, 3 – 25
- Nagle J F, Zhang R, Tristram-Nagle S. et al. (1996) *X-ray structure determination of fully hydrated L alpha phase dipalmitoyl-phosphatidylcholine bilayers* Biophys.J. 70, 1419 – 1431
- Nagle J F, Tristram-Nagle S. (2000) *Structure of lipid bilayers* Biochim. Biophys. Acta 1469 159 – 195
- Nakanishi M, Hirayama E, Kim J. (2001) *Characterisation of myogenic cell membrane: II. Dynamic changes in membrane lipids during the differentiation of mouse C2 myoblast cells* Cell Biol. Int. 25, 971 – 979
- Needham D, McIntosh T J, Evans E. (1988) *Thermomechanical and transition properties of Dimyristoylphosphatidylcholine / cholesterol bilayers* Biochemistry 27, 4668 – 4673.
- Pace R J, Chan S I. (1982) *Molecular motions in lipid bilayers. 1. Statistical mechanical model of acyl chain motion* J. Chem. Phys. 76, 4217 – 4227.
- Perez U A, Faucher K M, Majkrzak C F. et al. (2003) *Characterisation of a Biomimetic Polymeric Lipid Bilayer by Phase Sensitive Neutron Reflectometry* Langmuir 19, 7688 – 7694

- Prestegard J H, Wilkinson A. (1974) *Proton relaxation studies of water in concentrated dimyristoyllecithin—water systems* Biochim. Biophys. Acta 345, 439 – 447
- Racansky (1987) *A study of the phase-transitions in phosphatidylcholine and phosphatidylethanolamine model membranes using polarizing microscopy* Acta Physica Slovaca 37, 166 - 176
- Radhakrishnan A, Anderson T G, McConnell H M. (2000) *Condensed complexes, rafts, and the chemical activity of cholesterol in membranes* Proc. Natl. Acad. Sci. 97, 12422 – 12427
- Rand R P, Parsegian V A, Henry J A C. et al. (1980) *The effect of cholesterol on measured interaction and compressibility of dipalmitoylphophatidylcholine bilayers* Can. J. Biochem. 37, 959 – 968
- Simon S A, McIntosh T J. (1991) *Surface ripples cause the large fluid spaces between gel phase bilayers containing small amounts of cholesterol* Biochim. Biophys. Acta 1064, 69 – 74
- Simons K, Ikonen E (1997) *Functional rafts in cell membranes* Nature 387, 569-572
- Smith G S, Sirota E B, Safinya C R. et al. (1988) *Structure of the L-beta phases in a hydrated phosphatidylcholine multimembrane.* Phys. Rev. Lett. 60, 813 – 816.
- Smondryev AM, Berkowitz M L. (1999) *Structure of DPPC/cholesterol bilayer at low and high cholesterol concentrations: molecular dynamics simulation* Biophys. J. 77, 2075 – 2089.
- Subczynski W K, Kusumi A. (2003) *Dynamics of raft molecules in the cell and artificial membranes: approaches by pulse EPR spin labelling and single molecule optical microscopy* Biochim. Biophys Acta 1610, 231 – 243
- Sun W J, Suter M A, Worthington C R. et al. (1994) *Order and disorder in fully hydrated unorientated bilayers of gel phase DPPC* Phys. Rev. E. 49, 4665 – 4676
- Tristram-Nagle S, Zhang R, Suter RM. et al. (1993) *Measurement of chain tilt angle in fully hydrated bilayers of gel phase lecithins* Biophysical J. 64, 1097 – 1109
- Trouard T P, Nevzorov A A, Alam T M. et al. (1999) *Influence of cholesterol on dynamics of dimyristoylphosphatidylcholine bilayers as studied by deuterium NMR relaxation.* J. Chem. Phys. 110, 8802 – 8818.
- Vist M R, Davis J H. (1990) *Phase equilibria of cholesterol / dipalmitoylphosphatidylcholine mixtures: 2H nuclear magnetic resonance and differential scanning calorimetry* Biochemistry 29, 451 – 464.
- Watts A, Harlos K, Maschke W. et al. (1978) *Control of the structure and fluidity of phosphatidylglycerol bilayers by pH titration* Biochim. Biophys. Acta 510, 63 - 74
- Wiener M C, Suter RM, Nagle J F. (1989) *Structure of the fully hydrated gel phase of dipalmitoyl-phosphatidylcholine* Biophys. J. 55, 315 – 325
- Wiener M C, White S H. (1991) *Fluid bilayer structure determination by the combined use of x-ray and neutron-diffraction. 2. Composition-space refinement method.* Biophys. J. 59, 162 – 173.
- Woodward J T, Zasadzinski J A. (1996) *Amplitude, wave form, and temperature dependence of bilayer ripples in the Pbeta' phase* Phys. Rev. E. 53, R3044
- Yeagle P L. (1985) *Cholesterol and the cell membrane.* Biochim. Biophys. Acta. Rev. Biomem. 822, 267 – 287
- Zasadzinski J, Schneir J, Gurley J. et al. (1988) *Scanning tunnelling microscopy of freeze-fracture replicas of biomembranes* Science 239, 1013 – 1015

4. Phase behaviour of DPPE bilayers with and without Cholesterol

4.1 Introduction

Single and double bilayers of DPPE with and without cholesterol were studied by neutron reflectivity. The aim was to assess the stability and phase behaviour of the DPPE bilayers for use as biomembrane mimics. Cholesterol was incorporated to increase the realism of the sample and to compare its behaviour to that of DPPC and cholesterol double bilayers.

4.1.1 Introduction to Phosphoethanolamines

Phosphatidylethanolamines are one of the most abundant lipids in membranes, often accounting for up to a third of the total percentage of lipids present, as in the case of human and the rat erythrocyte plasma membranes (Datta 1987). They are frequently the main lipid component of microbial membranes such as *E. coli.* The phosphatidylethanolamine used is this study was 1,2-dipalmitoyl-phosphoethanolamine (DPPE) (Figure 4.1). The structure is almost identical to that of the phosphatidylcholine DPPC except that it has an amine group instead of the choline $[N(CH_3)_3]^+$ head-group of DPPC. This smaller head group enables them to form strong hydrogen bonds between the phosphate and the primary amine. This ability distinguishes phosphatidylethanolamines from phosphatidylcholines. The smaller head-group combined with the large chain area gives DPPE a conical shape structure.

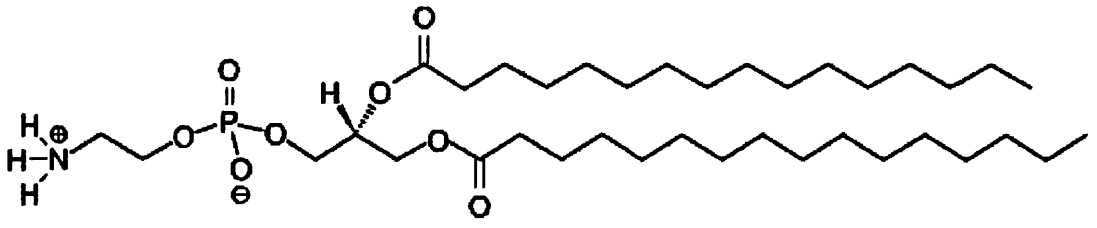

Figure 4.1 Chemical structure of 1,2-dipalmitoyl-phosphoethanolamine

Phosphatidylethanolamines are asymmetrically distributed in membranes, often located in the inner leaflet facing the cytoplasm. As well as being one of the major building blocks of membranes, they have a specific involvement in supporting active transport by the lactose permease. They are also thought to act as a 'chaperone' during the assembly of membrane proteins, guiding the folding path for the proteins and aiding in its transition from the cytoplasmic to the membrane environment (Lipid Analysis Unit website, UK).

Despite their predominance in membranes, phosphatidylethanolamines have not received as much attention as phosphatidylcholines. For example, the total number of publications listed in the *Web of Science* with the word phosphatidylethanolamines in is just over 300, whilst the number for phosphatidylcholines is over 1400. This difference is also reflected in Lipidat (Ohio) a web-based database of thermodynamic and associated information, the number of records for PE is only 2 722 compared to 11 583 for PC.

4.1.2 DPPE phase behaviour

In solution, phosphatidylethanolamines exhibit lamellar gel and liquid phases and a range of non-lamellar phases. For certain PE lipids, a transition from the lamellar liquid phase to a non-lamellar inverted hexagonal phase is observed (Seddon 1983, Harper 2001).

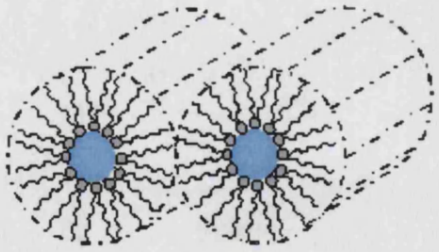

Figure 4.2 Schematic of inverted hexagonal phase. The rods are hexagonally packed.

Inverted hexagonal phases are long rods aligned in hexagonal stacks (Figure 4.2). The rods contain water channels inside and lipids on the outside orientated with their head-group inwards and the chains outwards (Hamley 2000). The water core is circular up to a certain radius limit, above which it is deformed due to packing difficulties (Turner 1992). The inverted hexagonal phase accommodates best the

packing of the small head-group and larger chains. In contrast phosphatidylcholines are not known to form hexagonal phases, unless in a mixture of non-similar lipids (Lipidat, Ohio). Non-lamellar phases have been found in vital cell tasks, such as in cell division where a non-lamellar phase forms around the area in the membrane where the cell is splitting with another cell. A similar effect occurs in cell fusion (Seddon 1991).

The fluid – inverted hexagonal transition normally happens at significantly higher temperatures than the main gel – liquid transition T_m. For example, DSPE (C_{18}) has a T_m of 75.5°C (Harlos 1981) and a fluid – inverted hexagonal temperature (T_H) of 109.5°C. For DPPE it is likely that the T_H occurs at 118.0°C, with a T_m of 64.5°C (Harlos 1981). It has been found for DOPE that the observed T_H is dependent upon the rate at which the temperature is changed (Toombes 2002). The temperature of T_H is also dependent on chain length. Contrary to the trend that an increase in chain length increases the value of T_m, T_H actually decreases with increasing chain length (Harlos 1981). The inclusion of alkanes such as dodecane reduces T_H, presumably by a reduction in the hydrocarbon packing stress.

The T_m temperatures of phosphatidylethanolamines are generally higher than those for similar chain length phosphatidylcholines. DPPE has a T_m of 64.5°C whereas DPPC has a T_m of 41.8°C, even though they have the same chain length. This is due to the ability of the PE head-group amine protons to form hydrogen bonds with the neighbouring phosphate oxygens (Bloom 1980).

The phase behaviour of dispersed vesicles of phosphatidylethanolamines in solution is abundant, whilst literature on the behaviour of stacked multilamellar bilayers is rather more limited in number. Lamellar stacks of phosphatidylethanolamines have been found to be unstable in the planar structure, forming inverted hexagonal structures at the T_m (J. P. Bradshaw et al., *unpublished results*).

4.1.3 DPPE and Cholesterol studies

The phase behaviour and organisation of DPPC and cholesterol has been the subject of extensive study. Conversely, studies of phosphatidylethanolamines and cholesterol mixtures have been rather limited in number despite the abundance of phosphatidylethanolamines in membranes (McMullen 1999). Previous studies have shown cholesterol to have a greater effect on transition temperatures of phosphatidylethanolamines compared to phosphatidylcholines. Addition of cholesterol to DPPE vesicles leads to a continuous decrease and broadening of T_m, whilst concentrations of 50 mol% of cholesterol showed no detectable T_m in calorimetric studies. The transition enthalpy also decreases almost linearly with increasing mol% (Blume 1980). Inclusion of 30 mol% cholesterol to DOPE lowered the lamellar – hexagonal transition T_H by ~ 30°C (Marinov 1995) The reduction in T_m and T_H with the addition of cholesterol is likely due to the cholesterol molecules interfering with the H-bonding of the phosphatidylethanolamines head-groups.

Phosphatidylethanolamines have also been observed to form cubic phases (Shalaev 1999). The formation of the cubic phase was found to be induced by cholesterol in POPE (Wang 2002), as well as formation of liquid-ordered phase in POPE at certain concentrations (Pare 1998). It is not possible to generalise the effect of cholesterol on the behaviour of phosphatidylethanolamines as it varies appreciatively with the structure of the head-group and the chain structure and length (McMullen 1996).

Supported single bilayers and monolayers of phosphatidylethanolamines have been used in a limited number of studies; examples include the interaction of key proteins involved in cell division with supported bilayers of DPPE (Alexandre 2002), studies of the interactions of antimicrobial peptides with DPPE monolayers (Gidalevitz 2003). AFM studies have been used to map the adhesive forces between deposited DMPE monolayers and surfaces (Berger 1995).

4.2 Fabrication of DPPE bilayers

4.2.1 Overview

The purpose of this part of the study was to evaluate the fabrication of double bilayers of DPPE. Once it was found that the double bilayers were partially unstable upon heating past the T_m, the deposition of DPPE with a range of different cholesterol ratios between 5 – 30 mol% was also evaluated. Single bilayers of DPPE were also deposited to compare their phase behaviour with that of the double bilayer and to aid in understanding the phase behaviour of the double bilayer.

The different isotherms are shown first, followed by the results of the depositions. The isotherms are shown only for reference purposes as isotherms of phospholipids in with cholesterol have been greatly studied in the past (Gaines 1966, Roberts 1990).

4.2.2 Isotherms

The monolayers were fabricated using the method detailed in the fabrication chapter. One problem encountered with all solutions containing DPPE was that DPPE is only mildly soluble in chloroform at room temperature. Gentle heating (~ 40°C) was necessary to dissolve the DPPE prior to spreading as a monolayer. Care has to be taken not to overheat the solution, as this was found to give bad monolayers that subsequently did not deposit well. It was found impossible to dissolve the deuterated chain DPPE, even when small amounts of methanol were added to the chloroform (this method, recommended by the supplier, works for problematic lipids like phosphatidylserines). It was therefore not possible to measure isotherms of d-DPPE or to deposit them. It is unclear why it fails to dissolve, it could be due to the differences in hydrogen bonding between the hydrogen and deuterium atoms.

Representative examples of isotherms of DPPE with 0 mol%, 5 mol% and 30 mol% molar ratios of cholesterol are shown in Figure 4.3. As the solutions were heated to dissolve the DPPE, it is not possible to calculate an accurate area per molecule for the isotherms, as the volume of chloroform increases even with mild heating and it is therefore difficult to evaluate the lipid concentration. The position of the isotherms

on the x-axis should be treated as arbitrary and not an indication of the effect of cholesterol on the area per molecule of DPPE. At room temperature DPPE has a small transition in gradient at a surface pressure of 36mN/m and unlike isotherms of DPPC it has no plateau. It is sufficient here to say that all isotherms were stable over the time measured, with no area loss when held at a constant surface pressure. The different monolayers were therefore deemed suitable for depositions.

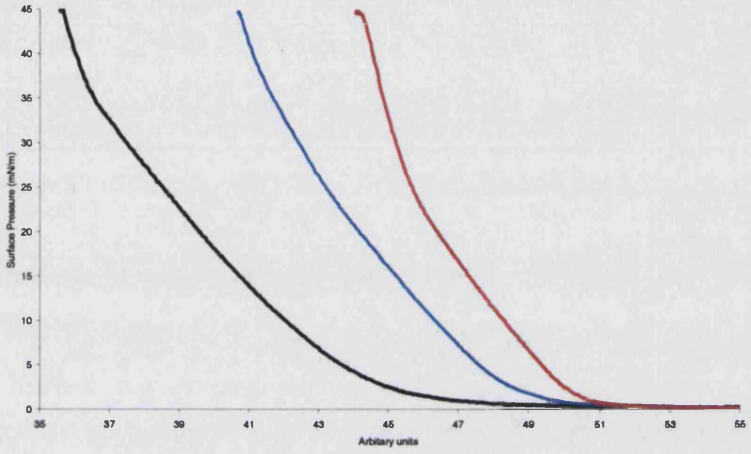

Figure 4.3 Left to right: representative isotherms of DPPE, 5 mol% cholesterol 95 mol% DPPE, 30 mol% cholesterol 70 mol% DPPE

4.2.3 Depositions

Langmuir – Blodgett depositions of 0 mol%, 5 mol%, 10 mol% and 30 mol% were evaluated to assess their fabrication. The averages of the transfer ratios are shown in Table 4.1.

	Cholesterol (mol%)	Tr1	Tr2	Tr3
DPPE	0	1.04	0.80	1.00
	5	1.03	0.98	1.02
	10	1.07	1.05	1.05
	30	1.06	1.07	0.97

Table 4.1 Average transfer ratios of range of cholesterol – DPPE ratios

DPPE consistently gave higher transfer ratios for the second deposition (average Tr2 of 0.80) than DPPC (average Tr2 of 0.43, chapter 3). As only a 29% of the 8 x 5 x 2 cm^2 silicon substrates is polished, and double bilayers are formed only on the polished side with high coverages, its is likely that DPPE deposits more readily on the rougher sides of the substrate than DPPC.

It was not possible to ascertain whether the first and third transfer ratios are affected by the inclusion of cholesterol, as they all were unity. However there is a clear trend present in the second transfer ratio with the inclusion of cholesterol. The transfer ratio increases to unity with only the addition of very small cholesterol ratio of 5 mol%. A slight rise in its value is seen with increased ratios. The 10 mol% ratio of cholesterol was chosen to evaluate its stabilisation effect on the double bilayer. In the monolayer phase separation of DPPE and cholesterol is not expected as previously phase separation has only been observed at concentrations of 35 – 40 mol% cholesterol (Cheetham 1989).

4.2.3.1 Reflectivity Samples

Table 4.2 lists the fabrication results of the DPPE single bilayer, DPPE double bilayer and the 10 mol% Cholesterol 90 mol% DPPE double bilayer. All were fabricated as detailed above and in the fabrication chapter. The only difference was that the Schaefer deposition of the DPPE double bilayer was done in a D_2O sub-phase instead of H_2O. This was the method used in the past, but was discontinued

due to the very high cost of D_2O. Interestingly much lower values for the pressure and area rise were observed with a D_2O sub-phase.

	Tr1	Tr2	Tr3	Schaefer Deposition Pressure	Area
DPPE single bilayer	1.02	-	-	4.0	4.5
DPPE double bilayer *	1.03	0.86	1.04	0.8	0.8
10% cholesterol DPPE double bilayer	1.07	1.05	1.05	12.0	1.5

Table 4.2 Transfer ratios and Schaefer pressure and area rise for samples used in reflectivity studies. Pressure is in mN/m and area in cm^2. (* Schaefer deposition performed in D_2O rather than H_2O)

The transfer ratios and Schaefer pressure and area rises were excellent for the DPPE single and double bilayers. Whilst the transfer ratios were excellent for the 10 mol% ratio, the Schaefer pressure rise was somewhat high, even though the area rise was excellent. It was therefore likely that the substrate made contact quite fast with the sub-phase, causing the large pressure rise, without being detrimental to the quality of the film. If the area had risen higher, then this would have indicated better the removal of previous layers, however the reflectivity results for this sample indicated high coverage.

4.3 Modelling of DPPE neutron reflectivity

The reflectivity profiles in this chapter were fitted with AFit (University of Oxford). The Bragg peak of the DPPE double bilayer was fitted using the Parratt (HMI, Berlin) programme.

The scattering lengths are listed in Table 4.3. They were kept constant when fitting. The thickness, roughness and solvent content were the variable parameters. All sample temperatures had an error of ±0.1°C.

Material	SLD (10^{-6} Å^{-2})
Si	2.07
SiO_2	3.41
H_2O	-0.56
D_2O	6.35
Palmititoyl chain $C_{30}H_{62}$	-0.41
PE head-group $C_7H_9O_8PN$	2.66
Cholesterol	0.22

Table 4.3 Scattering length densities used in modelling of DPPE bilayer samples. All values from Fragneto (2000) except PE head-group from Kuhl (1998) and cholesterol from Deme (1997).

4.4 DPPE double bilayer

4.4.1 Introduction

To evaluate the phase behaviour and stability of DPPE double bilayer membrane mimics, the reflectivity of the sample was measured at a range of temperatures between 25 – 84°C. The sample was then measured upon cooling to assess the reversibility. The sample was measured only in D_2O. The reflectivity was measured using the D17 reflectometer of the Institut Laue-Langevin. The profiles were fitted using the *AFit* programme. The silicon oxide was found to have a constant thickness of 11Å and roughness of 3Å at all temperatures. The results section is divided into two parts, the gel phase temperature behaviour and the fluid phase temperature behaviour.

4.4.2 Gel phase structure

Within the gel phase temperature range the structure did not change significantly despite the large temperature range measured (25.2°C – 62.9°C). The reflectivity was measured at 13 intermediate temperatures. Fits of three representative temperatures (25.2°C, 47.3°C and 62.9°C) are shown in Figure 4.4. The average values of the structural parameters at all the temperatures measured are given in Table 4.4.

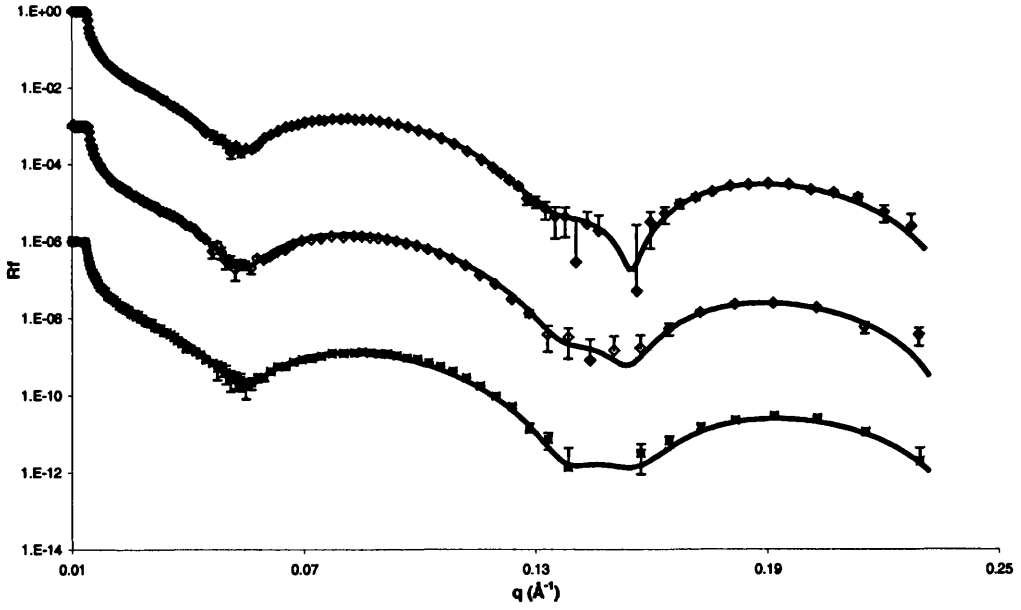

Figure 4.4 Fitted reflectivity profiles of DPPE double bilayers at 25.2°C (◆), 47.3°C (◊) and 62.5°C (■).

The head-groups were found to have an average thickness of 7±1 at all gel phase temperatures. The solvent content of the bilayers remained constant throughout. The coverage of the lower bilayer was found to be excellent at 98±2% and 99±1% for the upper bilayer, which agreed with the high transfer ratios of the depositions.

	dw	lDb	lDc	lRou	lCov	Dw	uDb	uDc	uRou	uCov
Gel temperatures	13±1	49±2	36±1	3±1	98±2	16±2	51±2	37±1	5±2	100±1%

Table 4.4 Average parameters of gel phase temperature structures of DPPE double bilayers.

The scattering length density profile of the structure at 25.2°C is shown in Figure 4.5. The two minima correspond to the two alkyl chain regions (hydrogenated so SLD close to –0.41 x 10^{-6} Å^{-2}), whilst the higher parts correspond to the water layers (deuterated so closer to 6.35 x 10^{-6} Å^{-2}). The low roughness and similarities between the two bilayers can clearly be seen, as can the well-defined water layer separating the lower bilayer from silicon oxide.

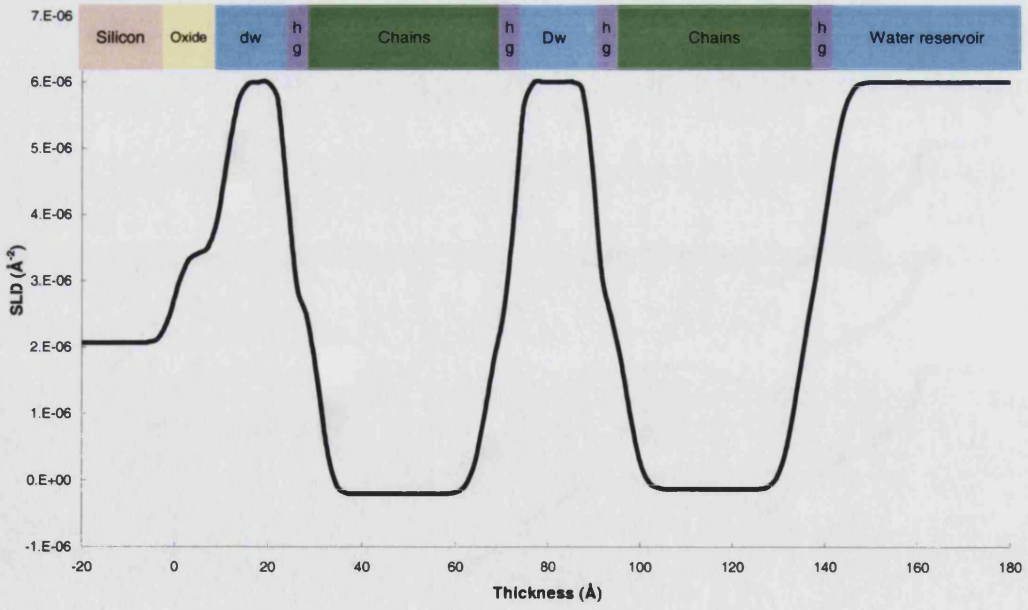

Figure 4.5 Scattering length density profile at 25.2°C. The structure of a double bilayer can clearly be seen in the form of two hydrogenated head-group and chain regions separated by a deuterated water region. The thin water layer between the silicon oxide and lower bilayer is also clearly visible.

Discussion

The stability of the bilayer over the measured gel phase temperature range is reassuring, but not totally unexpected, as the chains of the bilayer are immobile in the gel phase.

Deposited monolayers of DPPE have been found to have a thickness of 27±2Å by X-ray photoelectron spectroscopy (Solletti 1996), which is slightly higher than half the bilayer thickness of the lower and upper bilayers (25Å and 25.5Å respectively). Monolayers of DPPE on a water sub-phase have been found by ellipsometry and X-ray reflectivity to have a chain thickness of 19Å, head-group thickness of 6.5Å and bilayer roughness of 4Å at 20°C at a surface pressure of 40mN/m (Thoma 1996). If the lower and upper bilayer chain regions of the double bilayer sample are divided into leaflets, then their thickness of 18Å and 18.5Å are slightly lower than that of the monolayer on water. The maximum extension of DPPE chains has been calculated to be 19.1Å (Thoma 1996). A comparison of these suggests that the chains in the double bilayers are close to full extension, are not tilted in any way and have little or no interdigitation. The similarities of the bilayer and head-group thickness to those of the monolayers suggest that the monolayer structure does not change significantly on deposition. This is likely due to the high deposition coverage. The similarities in the roughness of the monolayer on water and those of the bilayers also suggest that the roughness of the monolayers is conserved on deposition. No additional roughness has been added by the deposition procedure, even by the Schaefer deposition procedure.

The bilayer thickness was higher than that of DPPC bilayers, which had a thickness of 34±1Å in the double bilayers (chapter 3.4). The difference is due to the lack of molecular tilt of phosphatidylethanolamines that is present in the gel phase of phosphatidylcholines (McIntosh 1980).

4.4.3 Transition phase behaviour

Unlike phosphatidylcholines, in general phosphatidylethanolamines do not exhibit large transition phase behaviour, usually only exhibiting gel – fluid transition. Vesicles of DPPE in solution have a gel – fluid transition at 64°C (Racansky 1987). In this study the transition of the upper bilayer occurred between 62.9 – 64.1°C and continued until 69.5°C. The lower bilayer transition occurred between 67.4 – 69.5°C. The fitted parameters are shown in Table 4.5. Both chain regions continued to thin slowly until becoming constant at 74.4°C. The reduction was also accompanied by a decrease in the thickness of the lower water layer (dw). As expected for phosphatidylethanolamines no additional phase behaviour (i.e. ripple phase) is observed at the transition.

Temperature (°C)	dw	lDb	lDc	lRou	lCov	Dw	uDb	uDc	uRou	uCov
62.5	13±1	51±2	36±1	3±1	96±2	14±2	50±2	37±1	4±2	100±3%
62.9	13±1	51±2	36±1	3±1	96±2	14±2	50±2	37±1	4±2	100±3%
64.1	12±1	49±2	35±1	3±1	93±2	14±2	49±2	34±1	6±2	100±3%
67.4	12±1	47±2	35±1	3±1	93±2	14±2	49±2	34±1	6±2	100±3%
69.5	10±1	47±2	31±1	5±1	94±2	13±2	44±2	30±1	6±2	100±3%
70.2	10±1	45±2	31±1	6±1	94±2	14±2	44±2	30±1	6±2	100±3%
74.4	10±1	42±2	28±1	5±1	94±2	14±2	41±2	27±1	6±2	100±3%

Table 4.5 Structural parameters of the DPPE double bilayer around the literature gel – liquid transition temperature of 64°C. All values are in Å. The transition in the double bilayers occurs at a similar temperature range of 62.9 – 69.5°C.

The structural change was consistent with a gel – fluid phase transition. As the transition temperature of the upper bilayer started to occur at the same temperature of vesicle dispersions, it is likely that the upper bilayer is generally unhindered by the substrate, with similar behaviour to that of vesicles. The difference in the transition temperature for the upper and lower bilayer is probably due to higher influence of the substrate on the lower bilayer. A difference in the behaviour of the two bilayers has previously been observed in DPPC double bilayers (Fragneto 2001).

Structural changes in the sample can often be directly inferred from changes in the reflectivity profiles. The first minimum has previously been found to be sensitive to the thickness of the overall sample (Fragneto 2001). A shift to higher q usually indicates a reduction in the overall thickness as $q \propto d^{-1}$ and indeed a shift to higher q can be seen in the DPPE sample either side of the T_m (Figure 4.6).

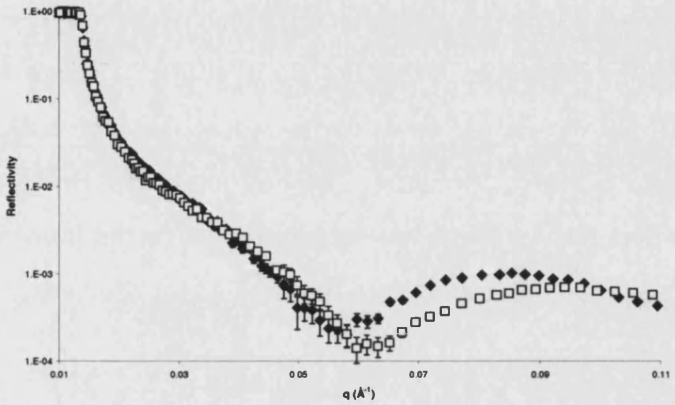

Figure 4.6 The reduction in the thickness of the sample is observed by a shift in the position of the first minimum to higher q with temperature. 64.1°C (◆), 69.5°C (□).

4.4.4 Fluid phase behaviour

4.4.4.1 Introduction

The reflectivity was measured at fluid phase temperatures from 64.1°C to 84.0°C and then down to 67°C. The gel – fluid transition between 64.1 – 69.5°C was accompanied surprisingly by a partial structural rearrangement into a structure that gave rise to a Bragg peak. The Bragg peak is clearly present at 69.5°C at a q of 0.12Å^{-1} and could be present at 64.1°C at a q of 0.11Å^{-1} (Figure 4.7). The overall form of the reflectivity profile however indicates that the bulk of the sample remained as a double bilayer structure. The position of the Bragg peak shifts with temperature and remains present even on cooling below the transition temperature. This indicates the formation of an irreversible repeat unit structure.

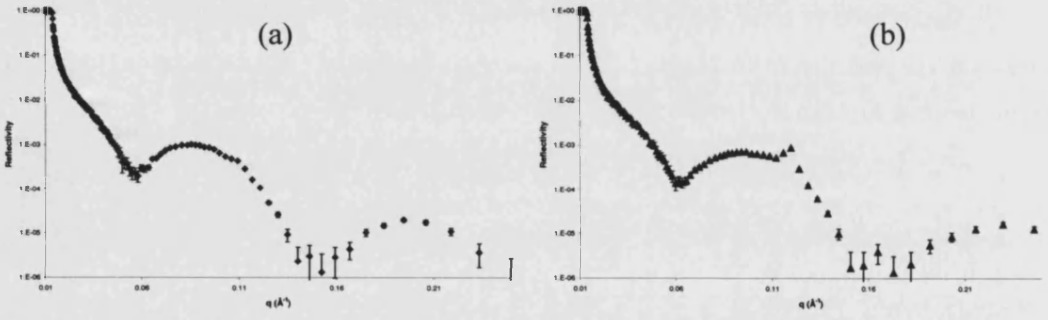

Figure 4.7 Presence of a Bragg peak in the reflectivity of DPPE double bilayers above T_m. (a) 64.1°C, (b) 69.5°C

The data was analysed by two methods. Initially the data was fitted without consideration of the Bragg peak using the normal double bilayer model. The Bragg peak was then analysed separately.

4.4.4.2 Analysis of data using double bilayer model

The shape and strength of the reflectivity profiles indicates that the sample was predominantly a double bilayer structure. The data was therefore initially fitted using the double bilayer model without consideration of the Bragg peak. The fitted parameters for the fluid phase temperatures upon heating and cooling are shown in Table 4.6 along with the average of the values for the gel phase. Due to beam-time constrains and the desire to study the behaviour of the Bragg peak with temperature, only the q range 0.05 – 0.25 was measured for 80.3°C and 84.0°C – 70.3°C measurements. Three fits are shown in Figure 4.8.

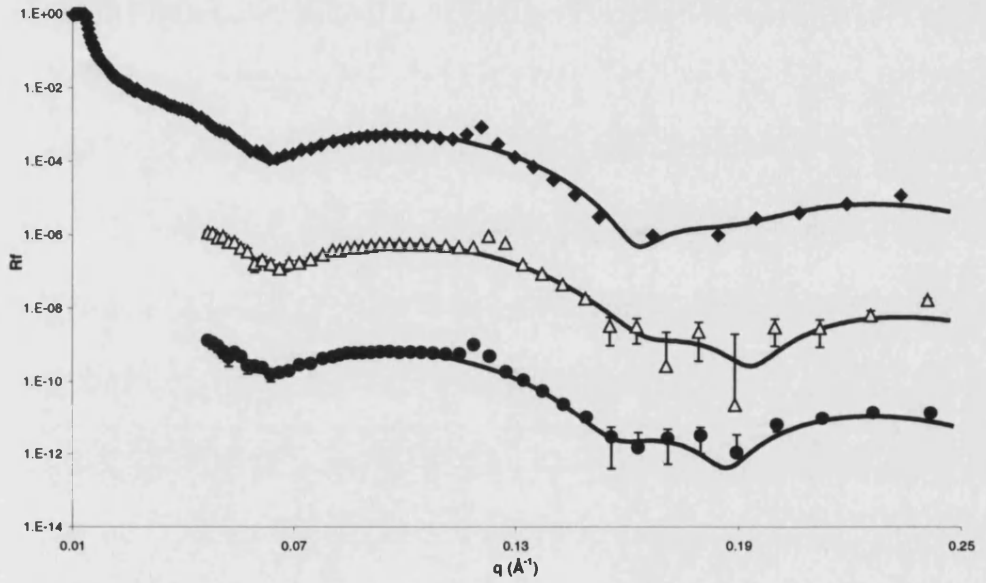

Figure 4.8 Fits of DPPE double bilayer at fluid phase temperatures using a double bilayer model. 74.4°C (◆), 84.0°C (△) and cooled 70.3°C (●).

Temperature (°C)	dw	lDb	lDc	lRou	lCov	Dw	uDb	uDc	uRou	uCov
Gel	13±1	49±2	36±1	3±1	98±2	16±2	51±2	37±1	5±2	100±1%
69.5	10±1	47±2	31±1	5±1	94±2	13±2	44±2	30±1	6±2	100±3%
70.2	10±1	45±2	31±1	6±1	94±2	14±2	44±2	30±1	6±2	100±3%
74.4	10±1	42±2	28±1	5±1	94±2	14±2	41±2	27±1	6±2	100±3%
80.3	10±1	42±2	28±1	3±1	93±2	14±2	42±2	27±1	5±2	100±3%
84.0	10±1	41±2	27±1	3±1	93±2	14±2	41±2	26±1	5±2	100±3%
76.5	10±1	41±2	28±1	4±1	97±2	14±2	44±2	30±1	4±2	100±3%
74.1	11±1	41±2	28±1	5±1	96±2	14±2	43±2	29±1	6±2	100±3%
70.3	10±1	41±2	28±1	5±1	97±2	14±2	44±2	30±1	4±2	100±3%

Table 4.6 Fitted parameters for fluid phase temperatures and the average of the gel phase parameters. All values are in Å.

Figure 4.9 shows the thickness of the chain regions versus temperature. The constant thickness at gel phase temperatures and the behaviour at the transition region of between 64.1°C – 69.5°C can clearly be seen. Above the T_m of 64°C the chain region thickness continued to decrease very slowly until becoming constant at 74.1°C. The 9Å decrease in the chain region between the gel and fluid phase temperatures was of an expected magnitude and was slightly larger than the 6Å decrease observed in DPPC lipids (Nagle 1996). No change was observed in the roughness of the upper bilayer between the gel and fluid phase. It is possible that the roughness of the lower bilayer increased slightly, but the values fluctuate somewhat. The coverage of the upper bilayer remained constant, whilst the values for the lower bilayer fluctuate.

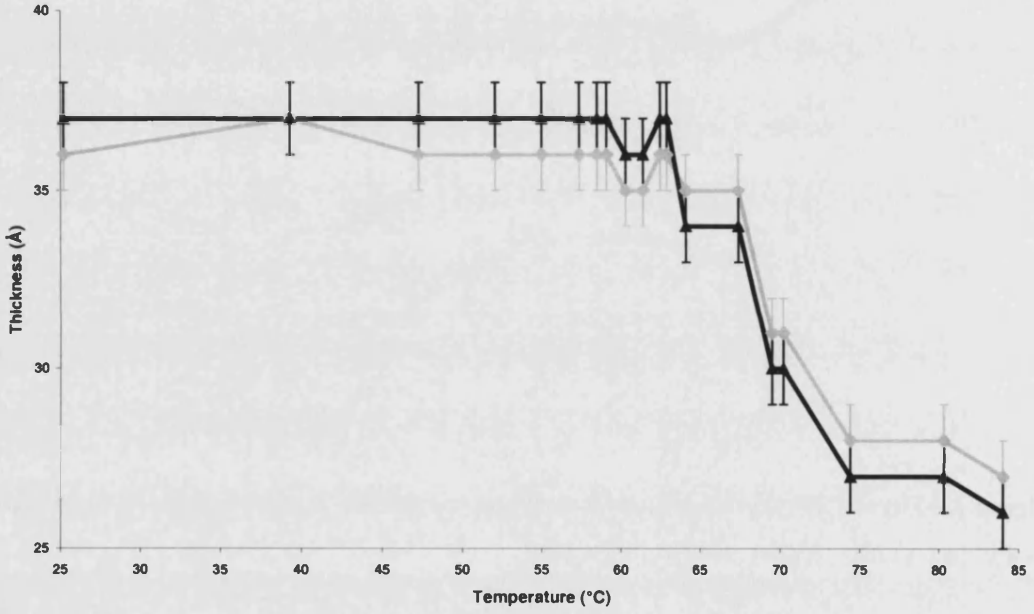

Figure 4.9 Thickness of chain regions vs. temperature. Upper bilayer is the black line and lower bilayer is the grey line. The constant thickness of the gel phase, transition phase between 64.1 – 69.5°C and the fluid phase can clearly be seen.

The fitted parameters are similar to those found in literature for multilamellar vesicles (MLV). Small angle x-ray scattering (SAXS) of DPPE at 75°C gave a bilayer thickness of 46Å, a chain thickness of 30Å and a thin water layer of 5Å (Pabst 2000). Liposomes of POPE were found to have a chain region length of 29Å by SAXS (Rappolt 2003). The thickness of the water layer was also found to be similar to other phosphoethanolamine MLV, where a range of different chain lengths gave a constant thickness of 13±1Å for a range of temperatures (Seddon 1984,

Harper 2001). Given the similarities between the results and literature it is therefore likely that the majority of the sample is behaving similar to a liquid phase of multilamellar vesicles and is therefore not inhibited strongly by the substrate.

Figure 4.10 shows the scattering length density profiles of the sample at 25.2°C in the gel phase and at 74.1°C in the fluid phase. The thinning of the chains and water layers is clearly visible as well as the shift of the bilayers closer to the substrate. As the solvent was not exchanged completely, the water regions have a SLD of 6.0 x 10^{-6} $Å^{-2}$ rather than the D_2O value of 6.35 x 10^{-6} $Å^{-2}$.

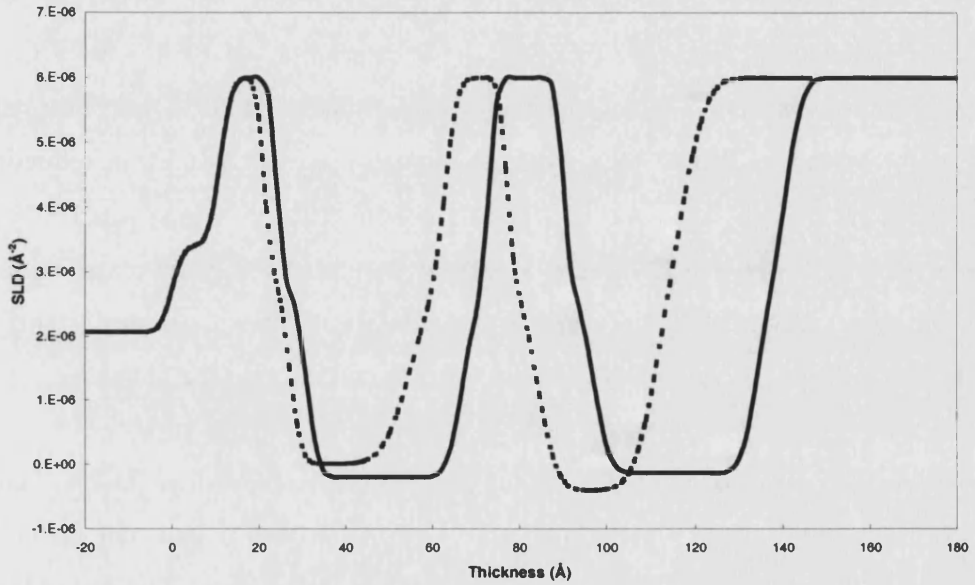

Figure 4.10 Scattering length densities of DPPE double bilayer at 25.2°C (bold line) and 74.1°C (dotted).

Structure on reducing temperature

The fitted parameters of the gel phase upon cooling are shown in Table 4.7, along with the original gel phase values and two fluid phase structures upon heating.

Temperature (°C)	dw	lDb	lDc	lRou	lCov	Dw	uDb	uDc	uRou	uCov
Ave. Gel heating	13±1	49±2	36±1	3±1	98±2	16±2	51±2	37±1	5±2	100±3%
Fluid 70.3	10±1	41±2	28±1	5±1	97±2	14±2	44±2	30±1	4±2	100±3%
Fluid 67.4	10±1	43±2	30±1	4±1	97±2	14±2	45±2	31±1	4±2	100±3%
Gel 64.5	11±1	47±2	34±1	3±1	90±2	14±2	50±2	34±1	6±2	100±3%
Gel 61.3	11±1	50±2	35±1	4±1	92±2	14±2	52±2	38±1	3±2	100±3%
Gel 29.0	11±1	50±2	37±1	3±1	93±2	16±2	53±2	38±1	3±2	100±3%

Table 4.7 Fitted parameters for cooled gel phase temperatures. Fluid phase values and the original gel phase parameters are shown for comparison. All values are in Å.

The cooled gel phase values are very similar to the original gel phase values, except for the coverage of the lower bilayer, which is 5±2% lower. This difference is also observed when going through the fluid – gel transition of 67.4 – 64.5°C. The decrease in coverage is expected upon changing from the fluid to gel phase and is similar to that seen in DMPC hybrid double bilayers (Hughes 2002). The reduction is not seen in the upper bilayer because the original gel phase coverage was 100%. It is unclear why the gel phase coverage differs though, as the coverage remained constant when heating in the original gel and fluid phase. It may signify an equilibrating of the packing of the molecules upon cooling into the gel phase.

The scattering length density profiles of the sample at the initial 25.2°C and the 29.0°C after cooling are shown in Figure 4.11. There are only small differences between the two structures when fitted without the Bragg peak. The lower bilayer has shifted slightly towards the substrate and the coverage differs.

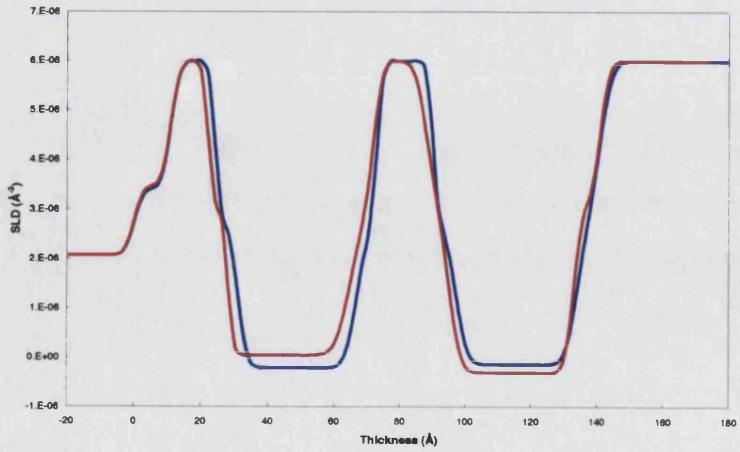

Figure 4.11 Scattering length density profiles of the sample of initial 25.2°C (blue) and 29.0°C (red) on reducing the temperature. The structure has only slightly changed overall.

4.4.4.3 Discussion of Bragg peak

Bragg diffraction occurs when Bragg's law, $n\lambda = 2d \sin\theta$ is satisfied (where d is the repeat unit, θ the angle of incidence and λ the wavelength of incidence). The height of Bragg peaks is dependent on the scattering length density (SLD) difference between the interfaces and the roughness of the boundary between the layers. A large difference in SLD will give a higher peak than a smaller difference. If the interface is rough, then the interference will be less constructive and the peak smaller. The width of Bragg peak is proportional to number of repeat units. For the purpose of data analysis it was assumed that there are two structures present, that of the double bilayer and that of the repeat unit giving rise to the Bragg peak. The reflectivity profile is assumed to be superposition of the individual reflectivity curves.

Bragg peak behaviour with temperature

The Bragg peak was first observed at 69.5°C but may have been present at 64.1°C. It remained at all temperatures, even when the temperature was reduced to 29.0°C. The q position, d spacing and fitted thickness of chain regions versus temperature are all shown in Table 4.8.

Temperature (°C)	q Bragg peak ($Å^{-1}$)	d spacing	lDb	uDb
69	0.120	52	47±1	49±1
74	0.121	52	42±1	41±1
80	0.123	51	42±1	42±1
84	0.123	51	41±1	41±1
76	0.122	52	41±1	44±1
74	0.123	51	41±1	43±1
70	0.119	53	41±1	44±1
67	0.119	53	43±1	45±1
64	0.104	60	47±1	49±1
61	0.102	62	50±1	52±1
64	0.104	60	50±1	51±1
29	0.100	63	50±1	53±1

Table 4.8 Bragg peak position, d spacing and thickness of upper (uDb) and lower (lDb) bilayer with temperature. UDb and lDb were obtained by fitting the profile whilst ignoring the Bragg peak. Error in Bragg peak position is ±0.01.

The position and magnitude of the Bragg peak between 69.5 – 84.0°C – 67.4°C remained constant, with a d spacing of 52±1Å. However, upon cooling close to the

fluid – gel transition of 64°C the Bragg peak shifted to a lower q value. Between 67.4°C – 64.5°C the d spacing increased from 53 to 60Å. The magnitude of the Bragg peak decreased as well (Figure 4.12). Below 64.5°C the d spacing and magnitude of the peak remains constant at all temperatures down to 29.0°C.

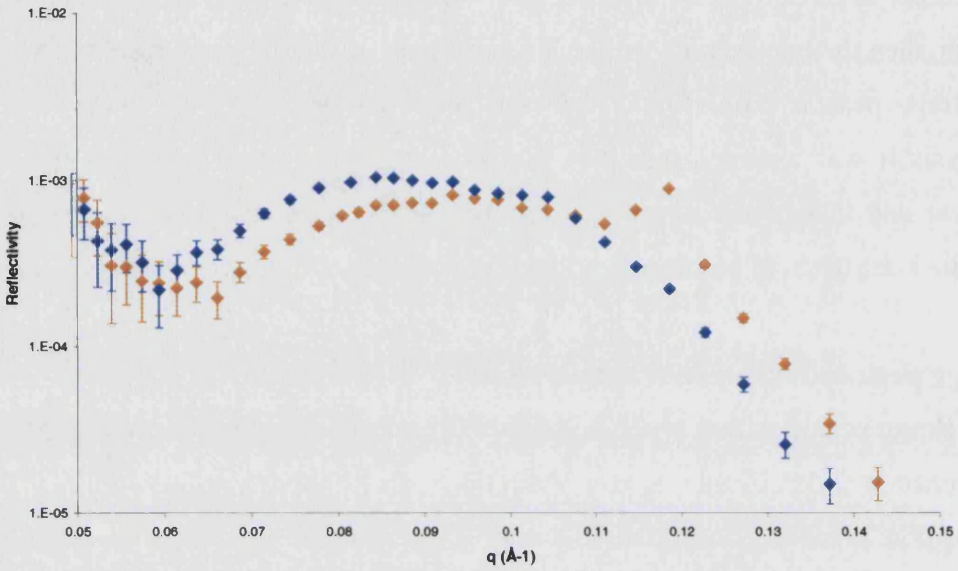

Figure 4.12 Reflectivity profiles of 67.4°C and 64.5°C. The shift in the position of the Bragg peak can be seen.

Discussion of d spacing

Normally the d spacing quoted for multilamellar vesicles consists of the bilayer and one of the water layers separating the bilayers. The fitting of the fluid phase temperatures without consideration of the Bragg peak gave an average upper bilayer thickness of 42±2Å and gel phase thickness of 52±1. The average thickness of the main water layer for the fluid phase was 14±2Å and 16±2 for the gel phase. These equate to a d spacing of 56Å for the fluid phase and 68Å for the gel phase and. The Bragg peak gives an average d spacing for the fluid phase of 52±1 and 62±1 for the gel phase.

Between the fluid and gel phases the d spacing obtained form the Bragg peak increased by 10Å. This would suggest either an increase in the thickness of the chain region or a swelling of the water layer in the repeat unit. As the increase in d spacing occurred so close to the T_m of DPPE, it would be expected to be due to an increase in

chain thickness rather than swelling of the water. The increase is also very similar to that seen in the double bilayer upon the gel – fluid transition (8Å).

Overall, in both the gel and the fluid phase the d spacing obtained without consideration of the Bragg peak was 4±1Å greater than the d spacing calculated from the Bragg peaks. If the repeating structure was a lamellar bilayer, it is likely then that the water layer in the repeat structure is 11Å rather than the 15Å in the double bilayer. The chain region in both the gel and fluid would not be expected to reduce by this amount. The repeat unit that gives rise to the Bragg peak is not necessarily a repeat planar lamellar bilayer. A possible repeat structure is of layers of inverted hexagonal rods above the double bilayers. Planar multilamellar bilayers of DOPE have previously been found to form inverted hexagonal rods (J. P. Bradshaw, Edinburgh, *unpublished results*). Inverted hexagonal rod structure consists of water filled rod like miscelles arranged into a hexagonal lattice (Figure 4.13). The lipids are orientated in the rods with their head-groups towards the internal water channels and tails outwards.

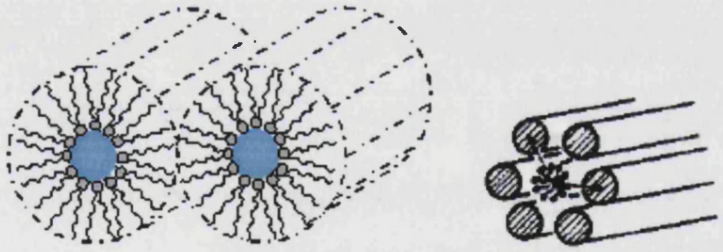

Figure 4.13 Schematics of inverted hexagonal phase

4.4.4.4 Analysis of Bragg peak

The Bragg peak was fitted using the multiple layers mode of the *Parratt 3.2* reflectivity fitting programme. The aim was not just to fit the Bragg peak, but to obtain a close fit for the whole profile as well.

As the profile showed such a well defined double bilayer form, it is likely that the structure was predominantly a double bilayer, with only a small amount of the total lipids present forming the repeat structure. The models used here therefore consisted of a double bilayer as a support, with a repeat structural above it. The parameters of the double bilayer used were those obtained from fitting the fluid phase temperatures without the Bragg peak. The coverage was allowed to vary, whilst the thickness and roughness was held constant. The d spacing from the Bragg peak was used to define the overall thickness of the repeat unit. The fact that most of the sample remained as a double bilayer means that the repeat units must have low coverage. It is likely therefore that the repeat structure is only occupying a small part of the area above the double bilayer.

The intention was to evaluate two models for obtaining the repeat structure, consisting of a planar multilamellar repeat structure and an inverted hexagonal repeat structure, but complications arose when trying to create a model that realistically modelled the inverted hexagonal structure. Coverage issues also arose with the planar multilamellar structure.

Inverted hexagonal model discussion

It is unlikely that an inverted hexagonal structure has been formed, as the d spacing (52±1 for the fluid phase and 62±1 for the gel phase) is closer to that of a planar bilayer structure rather than inverted hexagonal. Inverted hexagonal structures tend to have large structures due to the large diameter of the initial water channel, which has been found to be 25Å for DDPE (di-C_{12}), 44Å for DAPE (di-C_{20}) (Seddon 1984) and 30Å for POPE (Rappolt 2003) in aqueous dispersions. The transition temperature of the fluid planar structure to the hexagonal is often considerably higher than that of the gel – fluid planar transition (Harper 2001, Toombes 2002, Rapport 2003).

From a modelling point of view it is difficult to form a realistic model of rods of inverted hexagonal structures along the surface. The rods cannot be clearly divided into planar layers. It was therefore not possible to model an inverted hexagonal repeat unit. The main features of the inverted hexagonal structure are all in the plane of the bilayer due to their spherical nature. However with specular reflectivity the structure normal to the surface is obtained, with the in-plane features averaged. It would be more useful to measure the off-specular reflectivity to obtain a clearer idea of whether an inverted hexagonal structure is formed.

Planar lamellar model

Unlike the inverted hexagonal structure, a model could easily be constructed for the planar lamellar structure. It consisted of a repeat unit consisting of four layers, which were a head-group layer, chain region layer, head-group layer and a water layer. The bilayer of the repeat unit contained a high solvation content to account for the expected low coverage of each layer. The overall thickness of the repeat unit was fixed to that of the d spacing obtained from the Bragg peak. Roughness values similar to those found in the double bilayer were used for the repeat unit, as high roughness would have given a much broader Bragg peak.

The main difficulty with this model was one of bilayer coverage. For Bragg peaks to occur with this model there needs to be a significantly large difference in the scattering length density between the chain region and head-group interface, or between the head-group and water layer interface. As the head-groups are generally 10% more hydrated that of the chain region (Fragneto 2001) and the bilayer coverage very low per repeat unit, it is likely that the head-group scattering length density will be closer to that of the solvent. This would mean that the main difference in SLD would have to be between the chain region and the head-group.

One issue concerning the formation of a repeat planar lamellar model is why part of the upper bilayer would preferably rearrange from the double bilayer into a repeat stacking unit. One reason could be that the lipids prefer a multilamellar type arrangement, where the lipid head-groups of one bilayer face the head-groups of

another layer, rather than facing the open reservoir. The conical shape of the DPPE lipid may aid the rearrangement from the double bilayer to the repeat lamellar structure. Another possible reason for the formation of a repeat lamellar structure is a space issue. When a bilayer becomes fluid its area per molecule increases leading to an increase in the coverage of the bilayer (Hughes 2002). Unlike the DPPC upper bilayer which had a gel phase coverage of 93% and a fluid phase coverage of 100% (Chapter 3), the upper bilayer of the DPPE double bilayer already had a coverage of 100% in the gel phase. The expansion in the DPPE area per molecule upon becoming fluid could then force part of the bilayer to buckle and then rearrange to form a repeat multilamellar structure. The conical shape of the DPPE lipid would also aid this rearrangement from the planar bilayer.

Best fit using planar lamellar model

Two assumptions were used when developing a model for the planar lamellar repeat unit. First it is assumed that the best fit is likely only to be an approximation of the actual structure, as in reality it likely to be more complex than the model. The second assumption is that the repeating unit is only located in one area of the bilayer and consists of a finite number of repeats. In reality however, it could be the case that there are many different areas where the repeat unit is located consisting of different numbers of repeats.

There were two requirements for the acceptability of the fit. Firstly the fit of the Bragg peak had to match both the height and thickness. The second requirement was that the overall fit had to fit or lie below that of the rest of the profile.

The best fit of the sample at 74°C with the model is shown in Figure 4.14. Unfortunately this fit is completely unrealistic as the total percentage of lipids required to cause the appearance of the Bragg structure is higher than that present in the double bilayer before appearance of the Bragg peak. Each bilayer of the repeat unit needed a coverage of at least 15% to create a sufficient difference in the scattering length density between the bilayer and water to cause the Bragg peak. It was also necessary to have a minimum number of repeat units of 12 to fit the Bragg

peak. The overall fit also required the upper bilayer of the double bilayer to have a high coverage.

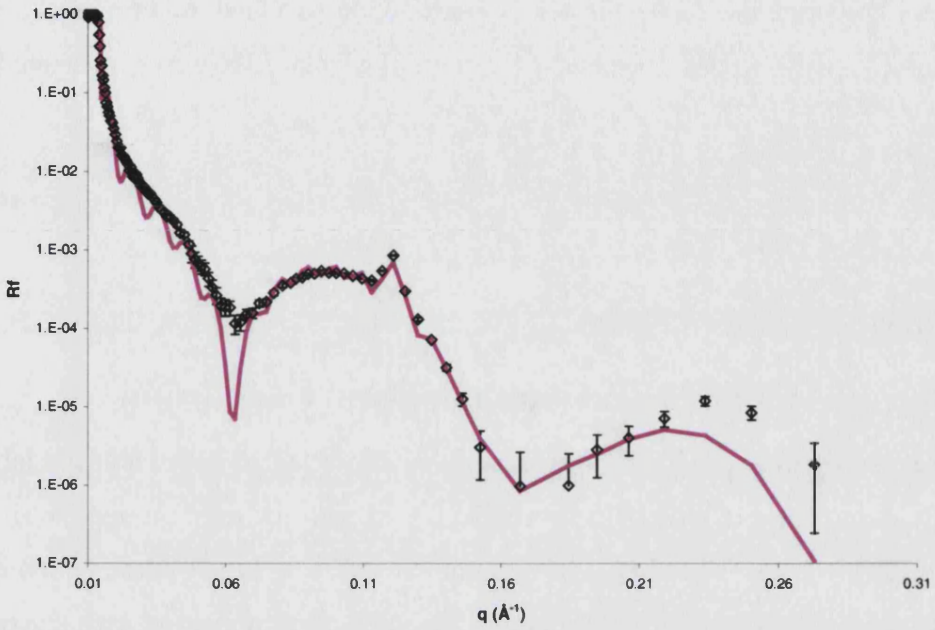

Figure 4.14 Best fit of profile containing Bragg peak. The parameters of the fit however are impossible due to the need to use a higher total percentage of lipids than that present in sample.

It was simply not possible to obtain a good fit of the Bragg peak using the repeat planar model whilst still satisfying the other structural requirements. It is possible that the Bragg is being caused by a non-lamellar type repeat structure or that the repeating structure is not uniform in coverage and number of repeat units. Given the conical shape of the DPPE lipid it would be expected to be some form of spherical structure. The fitting of the Bragg peak is on-going work.

Bragg peak conclusions

The two models proposed to elucidate the repeat structure are insufficient and are not able to describe the repeat structure realistically. It is likely that the repeat unit is more complex than purely a repeat lamellar structure or inverted hexagonal structure or the sample is not uniform. Further experiments would be needed to obtain structural information on the repeat unit. One useful type of measurement would be off-specular reflectivity, which would enable the in-plane structure to be probed. X-ray measurements are better than neutrons due to their higher flux, which leads to a

detectable signal from the off-specular scattering. AFM measurements would also give useful in-plane information.

It is unlikely that the lower bilayer is contributing to the formation of the repeat structure. To confirm this, the phase behaviour of a single bilayer was measured.

4.4.5 DPPE Double bilayer Conclusion

The results of the reflectivity measurements show that it is possible to fabricate DPPE double bilayers with high coverage aligned bilayers, even though the shape of the DPPE molecule is conical. The structure is stable at all gel phase temperatures. However at a temperature of 5°C above the gel – fluid transition a Bragg peak is clearly present in the reflectivity profile, signifying that part of the double bilayer has become unstable and formed a repeat structure above the double bilayer. Despite the appearance of the Bragg peak, the majority of the reflectivity profile remained unchanged and was unmistakeably due to the presence of a high coverage double bilayer structure. Two models were proposed to understand the repeating structure. They were both however unable to fit the profile with realistic parameters. The fitting of the Bragg peak is on-going work. Further experiments are needed to understand the structure, especially ones that probe the in-plane bilayer structure. A greater understanding of the repeat unit structure could suggest ways of stabilising the double bilayer structure in the fluid phase.

4.5 DPPE single bilayer

The reflectivity of the single bilayer of DPPE was measured at temperatures below and above the vesicle gel – fluid transition at 64°C of DPPE. The purpose of this study was to investigate the phase behaviour of DPPE close to the substrate and investigate whether a repeat structure occurred like that in the double bilayer. The sample was measured in D_2O on SURF at ISIS, England. The profiles were fitted with the AFit program using a 5-layer model consisting of an oxide, water layer, head-group, chain region and head-group.

The reflectivity was measured at 25°C, 47°C, 61°C, 65°C, 74°C, and 79°C. The shape of the profiles was consistent with the presence of a single bilayer. The profiles were identical up to 65°C whereupon a slight shift of the first fringe occurred between 65 – 74°C and then a larger shift between 74 – 79°C. The difference in the profiles at 25°C and 79°C profiles is shown in Figure 4.15. The difference is similar to that observed in other single bilayers samples like the 10 mol% cholesterol 90 mol% DPPC bilayer (See DPPC cholesterol chapter) where the first fringe lowers slightly and first minimum shifts to higher q. This difference in the profile has been found previously in other samples to indicate a transition between a gel and fluid phase.

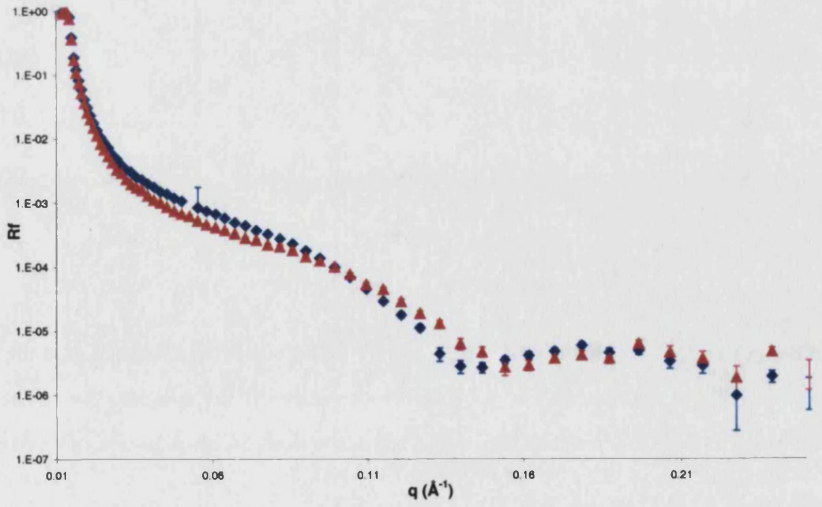

Figure 4.15 Difference in the reflectivity profiles of single bilayers of DPPE at 25°C (blue) and 79°C (red).

Fitted profiles at 25°C, 65°C, 74°C and 79°C are shown in Figure 4.16. Fitted parameters for all the temperatures are listed in Table 4.9.

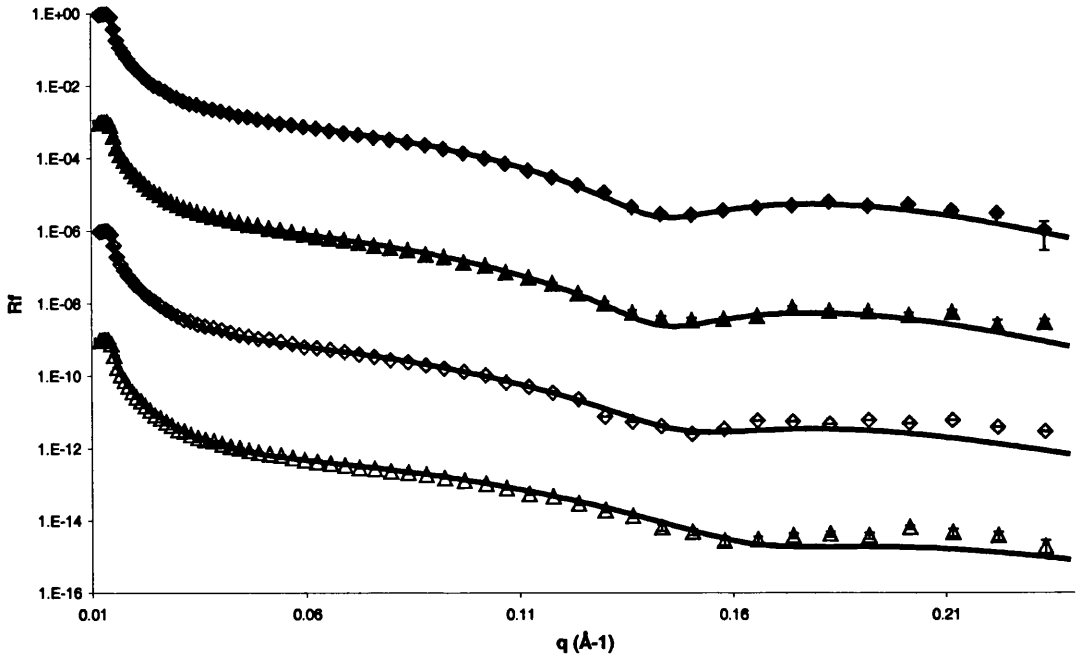

Figure 4.16 Fits of the reflectivity of a single DPPE bilayer at 25 (◆), 65 (▲), 74 (◊), 79°C (△)

Temperature (°C)	dw	Db	Dc	Rou	Cov
25	6±1	54±2	39±2	7±2	88%±2
47	6±1	53±2	39±2	8±2	86%±2
61	6±1	54±2	39±2	7±2	90%±2
65	6±1	54±2	39±2	7±2	91%±2
74	5±1	52±2	36±2	8±2	90%±2
79	5±1	46±2	31±2	8±2	89%±2

Table 4.9 Fitted parameters of DPPE single bilayer. Db is the bilayer thickness, Dc is the chain region thickness, Rou is bilayer roughness and Cov is the coverage of the bilayer. dw is the water layer separating the lower bilayer from the silicon substrate. All values are in Å unless otherwise specified.

4.5.1 Phase behaviour

The DPPE single bilayer was stable over all temperatures measured, even up to 15°C above the T_m. A clear gel – fluid transition was observed between 65°C – 74°C, which was slightly higher than that observed in the upper bilayer of the double bilayer and of vesicles in solution of 64°C (Racansky 1987). The value of the transition temperature was closer to that observed in the lower bilayer of the double bilayer of between 67 – 74°C. The scattering length density profiles of the sample at 25°C, 65°C, 74°C and 79°C are shown in Figure 4.17. The constant thickness of the water layer and the reduction in the thickness of the bilayer with the transition are clearly visible. The reduction is progressive.

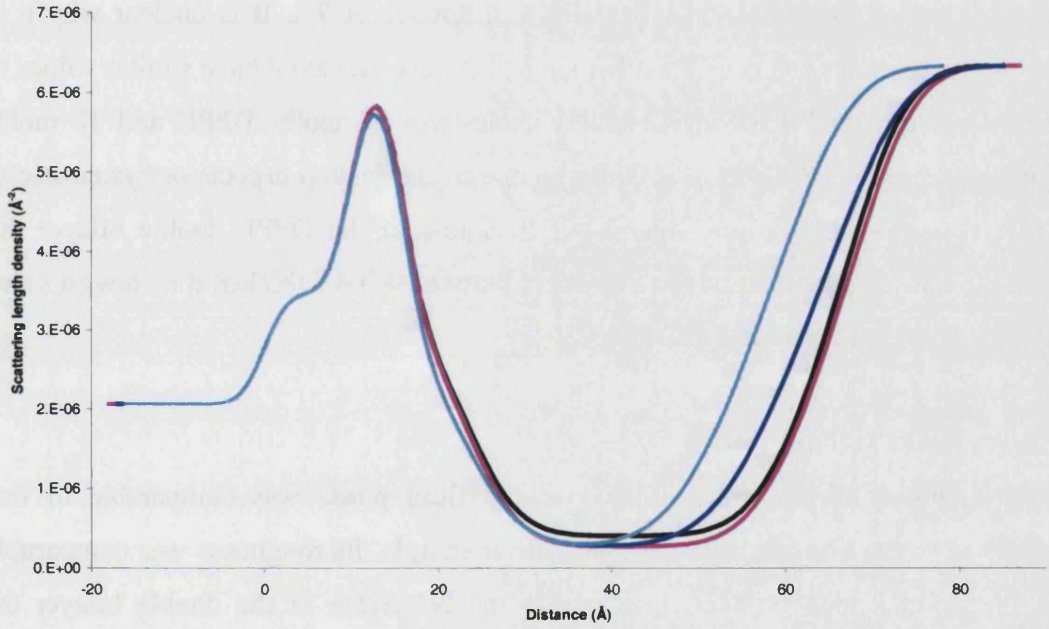

Figure 4.17 Scattering length density profile of DPPE single bilayer at 25°C (black), 65°C (pink) 74°C (blue) and 79°C (light blue).

The thickness of the bilayer is comparable to that of the lower leaflet of the double bilayer sample.

4.5.2 Comparison with double bilayer structure

Gel phase comparison

The gel phase single bilayer was 2 – 3Å thicker than either of the bilayers of the double bilayer sample. This difference though is insignificant once the error in the parameters is taken into account. The single bilayer roughness was approximately 4Å higher than that of the lower bilayer of the double bilayer, but comparable to that of the upper bilayer. This could be due to the fact that the Schaefer deposition was used for both, leading to a higher roughness. The single bilayer coverage was less than that of either of the lower or upper bilayers. It is likely due to differences in the fabrication. The lower water layer of the single bilayer was considerably thinner than that present in the double bilayer, with a difference of 7Å. It is unclear why it is lower, as the water layers of the other single bilayers measured have similar values to their double bilayer versions (2 mol% cholesterol 98 mol% DPPC and 10 mol% cholesterol 90 mol% DPPC). It could be due to fabrication aspects or systematic to DPPE samples. The lower water layer thickness of the DPPE double bilayer did reduce with temperature and the transition, but was still 4Å thicker at its lowest value of 10Å observed between 74°C - 84°C.

Fluid phase comparison

The thickness of the single bilayer in the fluid phase was comparable to that observed in the bilayers of the double bilayer sample. Its roughness was comparable to that of the upper bilayer. Contrary to the behaviour of the double bilayer the roughness of the single bilayer did not vary with temperature. The roughness of the single bilayer remained high throughout. This could be due to the closer proximity of the single bilayer to the substrate, which leads to a greater restraining effect on the bilayer. Even though the single bilayer exhibits fluid like behaviour in its thickness, it may not have complete fluidity. This is also reflected in the fact that the coverage does not increase in the fluid phase, unlike that of the double bilayer.

4.5.3 Single bilayer Conclusion

The DPPE single bilayer exhibited similar phase behaviour to that of lower bilayer of double bilayer. This shows that the behaviour of single bilayers is not affected by use of a different fabrication technique for the outer leaflet. No Bragg peak was observed in the reflectivity profile, even up temperatures of 15°C above the gel – fluid transition temperature. In the double bilayer the Bragg peak was observed at 5°C above the gel – fluid transition temperature. The results of the single bilayer show that the formation of the repeat structure in the double bilayer is likely to be solely caused by instability in the upper bilayer.

4.6 DPPE and 10 mol% cholesterol double bilayer

4.6.1 Introduction

The aim of this study was to assess the ability of cholesterol to stabilise the double bilayer. It was hoped that the addition of cholesterol would stabilise the DPPE double bilayers, enabling it to be used as a membrane mimic. Cholesterol is known to have a stabilising effect on membranes, increasing their fluidity at low temperature and restricting it at higher temperatures (Yeagle 1985).

DPPE double bilayers containing 10 mol% cholesterol were prepared and the reflectivity measured over a range of temperatures. The ratio of cholesterol used was chosen on the basis of the known interactions between DPPC bilayers and cholesterol. Very low and high ratios of cholesterol are known to affect the phase behaviour, whilst intermediate ratios affect it to a lesser extent (Lemmich 1997).

4.6.2 Methods

The reflectivity was measured between 25.3 to 61.6°C and down from 61.6 to 25.2°C. The sample was not measured at fluid phase temperatures because it was more important to measure a second scan between 25.2°C to 51.5°C due to sample stability issues. The sample was measured in D_2O on the D17 reflectometer. All the reflectivity profiles were fitted using the AFit programme, using the 9-layer model previously used for the DPPE double bilayer. The scattering length density of the chain region of the bilayers was adjusted from -0.41 x 10^{-6} Å^{-2} to -0.36 x 10^{-6} Å^{-2} to compensate for the effect of 10 mol% ratio and the size difference of the cholesterol on the chains (cholesterol has a scattering length density of 0.22 x 10^{-6} Å^{-2} (Deme 1997)). [The volume of cholesterol is 685Å^3 (calculated from a density of 1.067g/cm^{-3}) and the volume of two palmitoyl chains of DPPE is 800Å^3 (Fragneto 2000)]. The SLD of the head-groups was not compensated as cholesterol has been found to predominately locate in the chain region of DPPC bilayers, with only the hydroxyl group close to the head-groups (Leonard 1999, Smondyrev 2001). It was assumed that cholesterol located in the same way in DPPE bilayers.

4.6.3 Phase behaviour

Upon heating the reflectivity profile underwent a drastic change between 52 – 56.1°C (Figure 4.18). The profile lost its small fringe structure to form a wide fringe with no real minima. After this the profile structure remained relatively constant for all temperatures, including when cooling back to 25°C. Only minor changes occurred with heating and cooling.

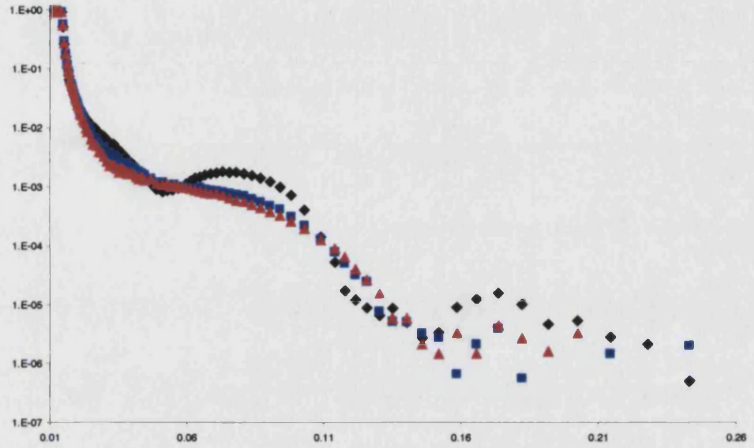

Figure 4.18 Reflectivity profiles of DPPE double bilayer with 10 mol% cholesterol at of 25.3°C (black), 56.1°C (blue) and 61.6°C (red).

Fit of the reflectivity profiles at 25.3°C, 56.1°C, 61.6°C and 25.2°C are shown in Figure 4.19 and the parameters listed in Table 4.10.

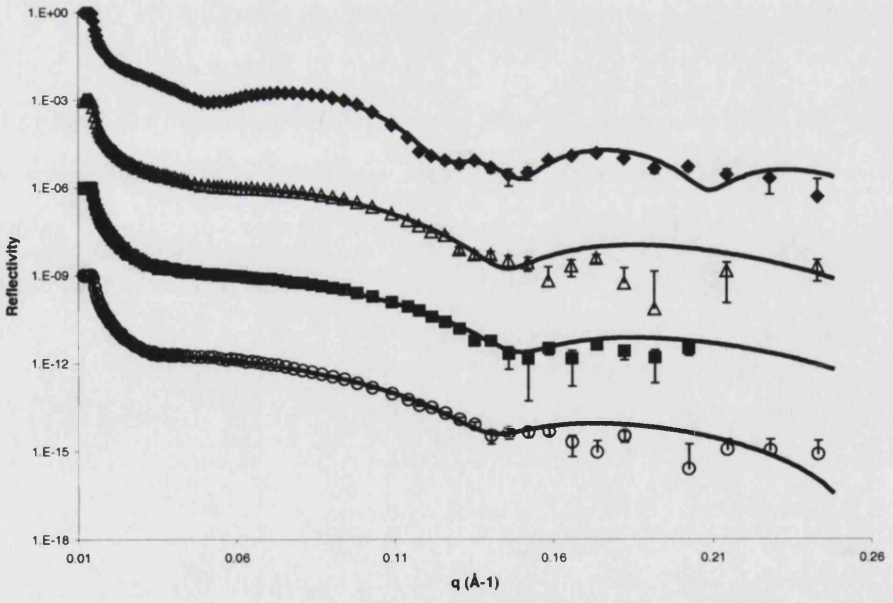

Figure 4.19 Fitted reflectivity profiles at 25.3°C (◆), 56.1°C (Δ), 61.6°C (■) and 25.2°C cooled (O)

Temperature (°C)	dw	lDb	lDc	lRou	lCov	Dw	uDb	uDc	uRou	uCov
25.3	12±1	51±2	37±1	5±2	87±2	23±1	47±2	37±1	5±2	100±2
34.4	11±1	51±2	37±1	3±2	89±2	22±1	52±2	37±1	5±2	100±2
43.6	11±1	50±2	36±1	3±2	90±2	21±1	51±2	37±1	5±2	100±2
47.1	11±1	50±2	36±1	5±2	89±2	22±1	49±2	37±1	6±2	100±2
52.2	9±1	49±2	35±1	7±2	88±2	22±1	51±2	36±1	7±2	100±2
56.4	11±2	52±2	38±1	3±2	95±2	18±9	50±9	35±7	6±12	7±5
61.6	12±1	51±2	37±1	4±2	90±2					
56.1	12±1	53±2	37±1	5±2	91±2					
52.4	13±1	52±2	37±1	4±2	93±2					
47.3	13±1	53±2	38±1	3±2	91±2					
43.5	14±1	54±2	39±1	4±2	91±2					
34.4	14±1	53±2	38±1	5±2	91±2					
25.2	14±1	53±2	38±1	5±2	92±2					
34.4	15±1	51±2	37±1	7±2	92±2					
43.4	15±1	51±2	37±1	7±2	92±2					
47.2	15±1	51±2	37±1	7±2	92±2					
52.5	15±1	51±2	37±1	7±2	91±2					

Table 4.10 Fitted parameters of reflectivity of DPPE double bilayers with 10 mol% cholesterol. All values are in Å, except for the coverages, which are in %.

The structure at 25.3°C was found to be consistent with a gel phase structure and similar to that of the DPPE double bilayer. The double bilayer retained the same structure up to 47.1°C. The scattering length density profiles of the DPPE double bilayers with and without cholesterol are shown in Figure 4.20. The bilayer chain thickness and first water layer are both similar, whilst the roughness is slightly higher in the presence of cholesterol. The thickness of the main water layer was also different, with a 7Å larger thickness in the cholesterol-containing sample. This maybe due to a modification by cholesterol of the Helfrich forces that determine the separation distance of the bilayers (Helfrich 1977).

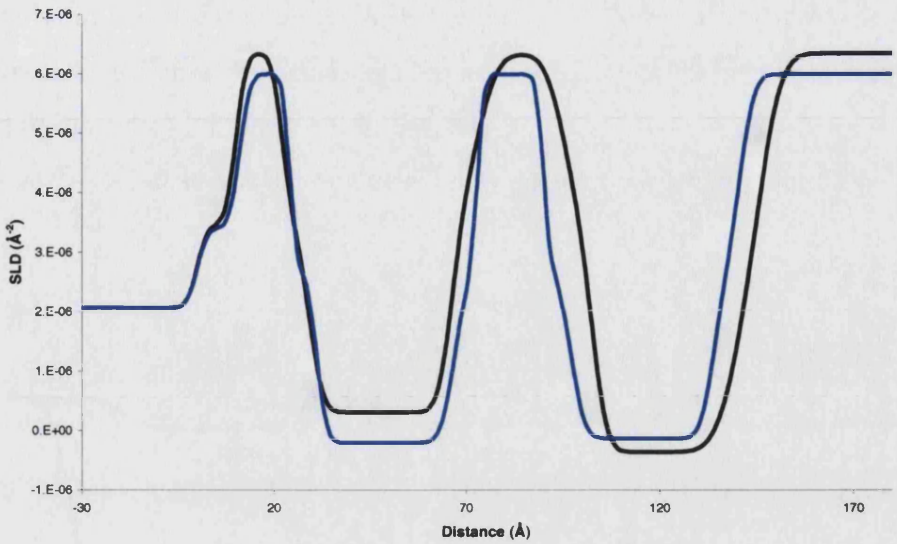

Figure 4.20 Scattering length densities of double bilayer of DPPE and 10mol% cholesterol (black) and double bilayer of pure DPPE (blue) at 25°C.

Between 52.2 – 56.4°C the structure of the reflectivity profiles drastically changed. It went from a profile structure commonly observed for a double bilayer to one commonly observed for a single bilayer. In fact between 52.2 – 56.4°C, 93% of the upper bilayer was removed and by 61.6°C the sample consisted only of a single bilayer. It was not possible to get an excellent fit of the 56.4°C profile above a q of $0.16Å^{-1}$. This is likely due to the disorder of system caused by the partial removal of the upper bilayer. Therefore the coverage value of the upper bilayer at this temperature should be interpreted with some caution. The unbinding occurred approximately 7°C below the gel – fluid transition temperature of DPPE. There was no indication in the structure at lower temperatures that the upper bilayer would unbind as the structure of the lower bilayer remains unchanged throughout the unbinding, retaining its gel-like structure. There was also no indication that either bilayer has undergone a phase transition.

The structure at the highest temperature measured (61.6°C) consists of a single bilayer with an identical structure to that of the initial lower bilayer at 25.3°C.

The sample was then measured at a range of temperatures upon cooling to 25.2°C. As shown in Table 4.10, the only structural change was a slight increase in the lower water layer upon returning to 25.2°C. The scattering length density profiles at

25.3°C, 56.4°C, 61.6°C and 25.2°C are shown in Figure 4.21. The similarities in the lower bilayer over all temperatures measured can clearly be seen. The extremely low coverage at 56.4°C is observed as an increase of the upper bilayer scattering length density to almost that of the solvent value. The similarities of the 25°C before and after heating can also be seen.

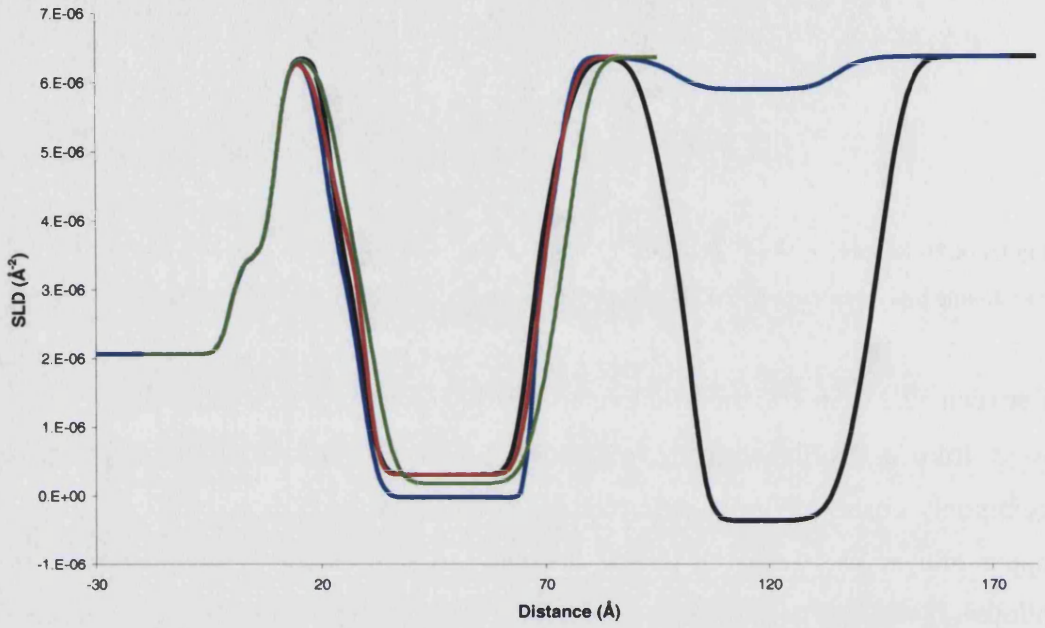

Figure 4.21 Scattering length density profiles at 25.3°C (black), 56.1°C (blue), 61.6°C (red) and 25.3°C (green).

No change was seen upon heating the sample up to 52.5°C again. The lower bilayer remained constant.

The chain thickness throughout the temperature scans was very similar to that found in vesicles and the DPPE double bilayer. The presence of 10 mol% cholesterol does not alter it. This is expected, as phosphatidylethanolamines molecules are not tilted like phosphatidylcholines are and thus the thickness is less affected by cholesterol. Phosphatidylethanolamines chains are often close to full extension in the gel phase; cholesterol would therefore not be expected to alter the lateral dimension in any way. It would alter the lipid area per molecule slightly though.

4.6.4 Interpretation

Although the presence of 10 mol% cholesterol does not significantly change the structure of the double bilayer, it completely destabilises the floating bilayer when near fluid phase temperatures. This might be related to the fact that the affinity between cholesterol and phosphatidylethanolamines is less than that of phosphatidylcholines and cholesterol (Van Dijck 1979). Recent research has shown that the interaction of cholesterol with lipids varies appreciably with the structure of the head-group and the structure and length of the hydrocarbon chains (McMullen 1996).

4.6.4.1 Effect on transition temperature

The unbinding of the upper bilayer occurred 7°C lower than the main gel – fluid transition temperature (T_m) of pure DPPE vesicles and that of the transition in the upper bilayer of the pure DPPE double bilayer. The incorporation of cholesterol has been found to progressively reduce the T_m of phosphatidylethanolamines vesicles up to molar concentrations of 20 mol% (McMullen 1997, 1999). 10 mol% cholesterol has been found to lower the T_m of DSPE by 4°C. Cholesterol has also been observed to lower the lamellar – inverted hexagonal transition temperature T_H for certain unsaturated phosphatidylethanolamines (Ohvo 2002). If the gel – fluid transition temperature of the upper bilayer has been lowered by 10 mol% cholesterol, then it could well be that the upper bilayer is becoming fluid at 56.1°C, enabling the molecules to have sufficient freedom to unbind. But this cannot be ascertained from the results here. The lower bilayer remained gel like throughout.

4.6.4.2 Molecular shape of DPPE

The unbinding of the upper bilayer by the presence of cholesterol would not have been expected, due to the favourable interaction of similar lipids and cholesterol. But although the DPPE molecule is very similar to DPPC, the behaviour of phosphatidylcholines and cholesterol cannot be used as a basis for the behaviour phosphatidylethanolamines and cholesterol (McMullen 1996). The bulk shape that a lipid prefers under a given set of conditions can be rationalised by considering the geometric packing of the lipids, which in turn can be described by the shape factor

characteristic of the lipid molecule under these conditions (Lewis 2000). The most likely reason therefore that the unbinding occurs in DPPE rather than DPPC is the shape of the DPPE molecule. DPPE is conical, whilst DPPC is cylindrical. The conical shape obviously would favour a spherical sample over a planar sample. The presence of cholesterol located in the chain region would be expected to increase the conical shape of the DPPE, further destabilising it as a planar structure.

4.6.4.3 Miscibility issues

When considering the mechanical effect of cholesterol on the DPPE bilayer, the miscibility of the binary sample needs to be taken into account. It has been empirically found that miscibility of cholesterol with any lipid is inversely related to the characteristic degree of order or tightness of packing of the phospholipid at a given temperature and phase state. Phosphatidylethanolamines head-groups have strong attractive electrostatic and hydrogen bonding, which is reflected in their high transition temperatures (McMullen 1997, 1999). Phospholipids with strong intermolecular interactions tend to exclude cholesterol from the bilayer above certain concentrations. In vesicles of phosphatidylethanolamines – cholesterol bilayers, the strong lipid inter-head-group electrostatic and hydrogen bonding interactions favour PE-PE interactions over PE-chol interactions (Ohvo 2002). However, domains of cholesterol have been only found to occur at concentrations of 35 mol% or above (Cheetham 1989). Cholesterol has also been found to exhibit a reduced miscibility in gel phase compared to fluid phase (McMullen 1997, 1999). It is likely therefore that the cholesterol has limited miscibility in the gel phase of the double bilayer. But the low molar concentration of cholesterol used in the double bilayer would suggest that whilst having limited miscibility, it is still mixing and would not be expected to form domains. One theory on why the incorporation of cholesterol caused the unbinding is based on the vertical location of the cholesterol in the bilayer. It is known that the cholesterol is predominantly located in chain region of the lipids, with only the hydroxyl group towards the lipid head-group. This is observed for phosphatidylcholine bilayers (Smondyrev 2001) and given the predominately hydrophobic nature of cholesterol it is likely the case in phosphatidylethanolamines. The presence of the cholesterol molecule in the chain region of the lipid would

therefore increase the relative chain – tail size ratio. The conical shape of DPPE would be increased, adding to the instability of the planar sample. This theory obviously rests on the two components having at least limited miscibility, which for this low cholesterol ratio is expected.

4.6.4.4 Unbinding due to fluctuations

The unbinding of a bilayer from a substrate, or another membrane or a substrate has been predicted to be driven predominantly by thermally excited fluctuations (Lipowsky 1986, Seifert 1993). Small vesicles unbind by thermal activation, whilst larger vesicles unbind via shape fluctuations. The fluctuations are able to overcome the attractive Van de Waals and electrostatic forces holding the bilayer to the interface. The same balance of forces in multilamellar vesicles are thought also to be the main forces present in double bilayer samples (Hughes 2002). Double bilayers of DPPC have been heated to temperatures 40°C above their T_m without unbinding occurring (Fragneto 2003). The in-plane fluctuations and swelling of the water layer around the main transition of double bilayers are currently being investigated (J. Daillant et al.). The effect of cholesterol on the fluctuations of phosphatidylethanolamines bilayers is unclear in literature. In the case of phosphatidylcholines, the inclusion of 8 – 14 mol% of cholesterol in DMPC has been found to sustain some fluctuations of the transition region down to temperatures 10°C lower than T_m (Mortensen 1988). The stabilising effect of cholesterol in membranes, which increases the fluidity of systems at low temperatures, and decreases it at higher temperatures (Yeagle 1985) would be expected to limit the fluctuations. The results here show no indication of an increase in fluctuations of either bilayer around the unbinding temperature. If the fluctuations had increased with the inclusion of 10 mol% of cholesterol then the roughness of the sample and thickness of water would have been expected to increase. The parameters of the upper bilayer however remained constant until the unbinding temperature range of 52.2°C to 56.4°C. The parameters of the lower bilayer also remained constant throughout. Increased fluctuations would be expected to increase the off-specular scattering present on the two-dimensional D17 detector image. However there was no indication of increased fluctuations on those images. It is therefore likely that cholesterol is not increasing the fluctuations. The main factor in the unbinding of the

DPPE – cholesterol bilayer is therefore more likely due to structural driving forces rather than fluctuations. However, it may be the case that the fluctuations occur at the actual unbinding temperature, leading to the immediate removal of the bilayer and are thus not possible to observe over the measurement time.

4.6.4.5 Influence of substrate on lower bilayer

The fact that the thickness of the lower water layer, that separates the lower bilayer from the substrate, remained constant after the loss of the upper bilayer indicates that the presence of upper bilayer is not a significant factor on determining the thickness. It is therefore likely that that the thickness is controlled predominantly by the interaction of the bilayer and the substrate only, in these uncharged systems. The difference in the T_m of the upper and lower bilayers in the pure DPPE sample are most likely caused by a greater influence of the substrate on the lower bilayer than on the upper. The fact that the upper bilayer is completely removed whilst none of the lower bilayer detaches indicates the greater level of freedom of the upper bilayer and also the restricting force of the substrate on the lower bilayer.

It is likely that the removal of upper bilayer is largely instantaneous, as partial removal of bilayer would leave domains of bilayer that would need to rearrange their structure to protect their edges from exposure to the water. In solution it would be expected that lipids from the upper bilayer are forming a vesicle structure.

4.6.4.6 Comparison with DPPE single and double bilayer structures

The structure of the cholesterol containing lower bilayer was similar to that of the DPPE single bilayer. The thickness, roughness and coverage were all similar. However, the lower water layer was thicker than that present in the single bilayer, having a thickness more similar to that in the DPPE double bilayer. It could be then that the double bilayer structure intrinsically results in a thicker lower water layer.

Although the double bilayers of pure DPPE and with 10 mol% cholesterol have similar structures at gel phase temperatures, the behaviour around the fluid phase temperatures is different, although it is probably related to the same causes. Whilst

the upper bilayer with cholesterol is completely removed, the pure DPPE system forms a repeat structure. The inherent planar instability of the upper bilayer of DPPE is therefore increased by the cholesterol, and its effect is to remove the bilayer rather than rearrange the structure. DPPE alone is not sufficient to unbind from the surface, even up to 20°C above its T_m.

4.6.5 Conclusions

The presence of 10 mol% cholesterol destabilised the upper bilayer rather than stabilised it. It is likely that the cholesterol, which is located predominantly in the chain region, increases the conical shape of the DPPE molecule and thus renders it less favourable as a planar structure. Other compounds should be assessed to see whether they are able to stabilise the upper bilayer of DPPE double bilayers, preferably those compounds that locate in the head-group region of the molecule. Also the planar stability of other types of phosphatidylethanolamines should be investigated.

The behaviour of this sample remarkable differed from that of the phosphatidylcholine DPPC double bilayer containing 10 mol% cholesterol, which was found to be completely stable overall all temperatures measured, including the fluid phase.

4.7 Overall conclusions of DPPE samples

The aim of this study was to develop a stable DPPE double bilayer that exhibited phase behaviour similar to that of DPPE vesicles in solution. It was hoped that this would allow the use of the system as a bio-membrane mimic for protein studies.

It was found possible to fabricate high quality samples of DPPE double bilayers, single bilayers and also double bilayers containing 10 mol% cholesterol.

When the phase behaviour of DPPE double bilayers was studied with neutron reflectivity it was found that part of the upper bilayer became unstable at a temperature just above the gel – fluid transition. A Bragg peak appeared in the reflectivity profile indicating the formation of an irreversible repeat unit structure. However the profile still indicated the presence of a high coverage double bilayer, even up to temperatures 10°C above the transition temperature. Two different types of models were proposed to elucidate the structure of the repeat unit. It was hoped that an understanding of the structure would enable methods to be undertaken to stop the formation of the repeat unit and thus obtain a stable DPPE double bilayer for use as a biomembrane mimic. Unfortunately neither of the models was able to give a satisfactory fit of the Bragg peak using realistic parameters. It is likely that the repeat structure is more complex than can be modelled with a layered structure. The fitting of the Bragg peak is thus on-going work. Future experiments are needed to understand the behaviour, especially ones that probe the in-plane structure of the bilayer. When the profile of the double bilayer was fitted without consideration of the Bragg peak, the results indicate that the double bilayer became fluid with parameters similar to those of DPPE vesicles. It also showed a transition back to the gel phase, giving similar gel phase parameters to those of the initial gel phase structure.

The phase behaviour of a single bilayer of DPPE was studied to assess the possible of its use as a biomembrane mimic, and to understand whether a repeat unit structure is formed from single bilayer structures. Unlike the double bilayer, the single bilayer was found to be completely stable over all temperatures measured, even up to 15°C above the gel – fluid transition temperature. The single bilayer exhibited similar

phase behaviour to the lower bilayer of the double bilayer, exhibiting stable gel and fluid phases. These results show that the formation of the repeat structure in the double bilayer is solely caused by upper bilayer. The stability and phase behaviour of the single bilayer sample indicate that it could be used in biomembrane studies.

The phase behaviour of a double bilayer consisting of 90 mol% DPPE and 10 mol% cholesterol was investigated to ascertain whether cholesterol stabilises the fluid phase of the upper bilayer. Unfortunately the presence of the cholesterol had completely the opposite effect. When the temperature of the sample was increased, the upper bilayer was found to completely detach below the gel – fluid transition temperature. Since it is known that the cholesterol is predominately located in the chain region of the DPPE molecule, this would essentially increase the conical shape of the DPPE molecule making the planar structure highly unfavourable at higher temperatures. The behaviour of the sample remarkably differed compared to the phosphatidylcholine DPPC double bilayer with 10 mol% cholesterol which was found to be completely stable overall all temperatures measured, including the fluid phase.

Future perspectives are the incorporation of DPPE into mixed component double bilayers, in the hope that it would be stabilised as planar structure by presence of other lipids. Another future perspective is to study the formation of the repeat unit with other techniques such as AFM to probe the in-plane bilayer structure. A full understanding of structure of repeat unit could lead to new methods to stabilise the upper bilayer in the fluid phase.

4.8 References

- Berger C E H, Van der Werf K O, Kooyman R P H. et al. (1995) *Functional Group Imaging by Adhesion AFM of Lipid Monolayers* Langmuir 11, 4188 - 4192
- Blume A. (1980) *Thermotropic behaviour of phosphatidylethanolamine-cholesterol and phosphatidylethanolamine-phosphatidylcholine-cholesterol mixtures* Biochemistry, 19, 4908 – 4913
- Cheetham J J, Wachtel E, Bach D. et al. (1989) *Role of the stereochemistry of the hydroxyl group of cholesterol and the formation of non-bilayer structures in phosphatidylethanolamines* Biochemistry 28, 8928 – 8934
- Dalgliesh R. (2002) *Application of off-specular scattering XR NR to the study of soft matter* Curr. Opin. Coll. Inf. Sci 7 244-248
- Datta (1987) *A comprehensive introduction to membrane biochemistry* Floral Publishing, Madison
- Deme B, Lee L T. (1997) *Adsorption of a hydrophobically modified polysaccharide at the air-water interface: kinetics and structure* J. Phys. Chem. B. 101, 8250 – 8258
- Demel R A, Jansen J W C M, Van dijch P W M. (1977) *Preferential interaction of cholesterol with different classes of phopholipids* Biochim. Biophys. Acta 1, 1 – 10
- Du H, Chandaroy P, Hui S W. (1997) *Polyethylene glycol with PE on lipid surfaces inhibits protein ads. and cell adh.* Biochim. Biophys. Acta 1326 236–248
- Fragneto G, Graner F, Charitat T. et al. (2000b) *Interaction of the third helix of antennapedia homeodomain with a deposited phospholipid bilayer: a neutron reflectivity structural study* Langmuir 16, 4581-4588
- Fragneto G, Charitat T, Graner F. et al. (2001) *A fluid floating bilayer* Europhys. Lett. 53, 100 – 106
- Fragneto G, Charitat T, Bellet-Amalric E. et al. (2003) *Swelling of phospholipid floating bilayers: the effect of chain length* Langmuir 19, 7695 – 7702
- Gaines (1966) *Insoluble monolayers at gas – liquid interfaces*, Interscience, New York,
- Gidalevitz D, Ishitsuka Y, Muresan A S. et al. (2003) *Interaction of antimicrobial peptide protegrin with biomembranes* PNAS 100, 6302 – 6307
- Harlos K, Eibl H. (1981) *Hexagonal phases in phospholipids with saturated chains: phosphatidylethanolamines and phosphatidic acids* Biochemistry 20, 2888 – 2892
- Hamley (2000) *Introduction to soft matter*, John Wiley and Sons Ltd, England.
- Harper P E, Mannock D A, Lewis R N A H. et al. (2001) *x-ray diff of various PE lamellar and inverted hexagonal phases* Biophys. J. 81, 2693–2706
- Hayter J B, Highfield R R, Pullman B J. et al. (1981) *Critical reflection of Neutrons – a mew technique for investigating interfacial phenomena* J. Chem. Soc., Faraday Trans. 1, 77, 1437-1448
- Helfrich W. (1977) *Steric interaction of fluid membranes in multilayer systems* Z. Naturforsch 33a, 305 – 315
- Hughes A V, Roser S J, Gerstenberg M C. et al. (2002b) *Phase behaviour of DMPC free supported bilayers studied by neutron reflectivity* Langmuir 18, 8161 – 8171
- Koenig B W, Krueger S, Orts W J. et al. (1996) *Neutron reflectivity and atomic force microscopy studies of a lipid bilayer in water adsorbed to the surface of a silicon single crystal* Langmuir 12, 1343 – 1350
- Kuhl T L, Majewski J, Wong J Y. et al. (1998) *A neutron reflectivity study of polymer-modified phospholipid monolayers at the solid-solution interface: polyethylene glycol-lipids on silane-modified substrates* Biophys. J. 2352 – 2362
- Lemmich J, Mortensen K, Ipsen J H. et al. (1997) *The effect of cholesterol in small amounts on lipid-bilayer softness in the region of the main phase transition* Eur. Biophys. 25, 293 – 304

- Leonard A, Escrive C, Laguerre M. et al. (2001) *Location of Cholesterol in DMPC Membranes. A Comparative Study by Neutron Diffraction and Molecular Mechanics Simulation†* Langmuir 17, 2019 -2030
- Lewis R N A H, McElhaney R N. (2000) *Surface charge markedly attenuates the nonlamellar phase-forming propensities of lipid bilayer membranes: calorimetric and 31P-nuclear magnetic resonance studies of mixtures of cationic, anionic, and zwitterionic lipids* Biophys. J. 79, 1455 – 1464
- Lipid Analysis Unit, University of St Andrews, UK
- Lipowsky R, Leibler S. (1986) *Unbinding transitions of interacting membranes* Phys. Rev. Lett. 56, 2541 – 2544
- Lipowsky R. (1991) *The conformation of membranes* Nature 349, 475 – 481
- Marinov R, Dufourc E J. (1995) *Cholesterol stabilises the hexagonal type II phase of 1-palmitoyl-2-oleoyl sn glycero-3-phosphoethanolamine. A solid state 2H and 31P NMR study* J. Chim. Phys. 92, 1727 – 1731
- McIntosh T J. (1980) *Differences in hydrocarbon chain tilt between hydrated phosphatidylethanolamine and phosphatidylcholine bilayers. A molecular packing model.* Biophys. J. 29, 237 – 245
- McMullen T P W, McElhaney R N. (1997) *Differential scanning calorimetric studies of the interaction of cholesterol with distearoyl and dielaidoyl molecular species of phosphatidylcholine, phosphatidylethanolamine, and phosphatidylserine* Biochem. 36, 4979 – 4986
- McMullen T P W, Lewis R N A H, McElhaney R N. (1999) *Calorimetric and spectroscopic studies of the effects of cholesterol on the thermotropic phase behaviour and organisation of a homologous series of linear saturated phosphatidylethanolamine bilayers* Biochim. Biophys. Acta 1416, 119 – 134
- Mortensen K, Pfeiffer W, Sackmann E. et al. (1988) *Structural properties of a phosphatidylcholine-cholesterol system as studied by small-angle neutron scattering: ripple structure and phase diagram* Biochem. Biophys. Acta 945, 221 – 245
- Nagle J F, Zhang R, Tristram-Nagle S. et al. (1996) *X-ray structure determination of fully hydrated L alpha phase dipalmitoyl-phosphatidylcholine bilayers* Biophys.J. 70, 1419 – 1431
- Nagle J F, Tristram-Nagle S. (2000) *Structure of lipid bilayers* Biochim. Biophys. Acta 1469 159 – 195
- Pabst G, Rappolt M, Ameritsch H. et al. (2000) *Struc. info MLV: Full q-range fitting with high quality x-ray data* Phys. Rev. E. 62 4000 - 4009
- Pitman M C, Suits F, Feller S E. (2004) *Molecular dynamics investigation of the structural properties of phosphatidylethanolamine lipid bilayers* IBM Research report, Jan 2004.
- Racansky (1987) *A study of phase transitions in phosphatidylcholine and phosphatidylethanolamine model membranes using polarised microscopy* Acta physica Slovaca 37, 166 – 176
- Rappolt M, Hickel A, Bringezu F. et al. (2003) *Mechanism of the lamellar/inverse hexagonal phase transition examined by high resolution x-ray diffraction* Biophys. J. 84, 3111 – 3122
- Roberts (1990) *Langmuir – Blodgett films*, Plenum Press, New York and London
- Seddon J M, Cevc G, Marsh D. (1983) *Calorimetric studies of the gel-fluid (L,-L,) and lamellar-inverted hexagonal (L,-HII) phase transitions in dialkyl- and diacylphosphatidylethanolaminest* Biochemistry 22, 1280 – 1289
- Seddon J M, Cevc G, Kaye R D. et al. (1984) *X-ray diffraction study of polymorphism of hydrated diacyl- and dialkyl-phosphatidylethanolamines* Biochemistry 23, 2634 – 2644
- Seddon J M. (1991) *Liquid crystals and the living cell* New Scientist 1769, 45-49.
- Seifert (1993) *Adhesion and unbinding of vesicles* Dynamical phenomenon at surfaces, interfaces and membranes, Nova Science Publishers, Commack.
- Shalaev E Y, Steponkus P L. (1999) *Phase diagram of DOPE: water systems at subzero temperatures and at low water contents* Biochim. Biophys. Acta 1419, 229 – 247

- Solletti J M, Botreau M, Sommer F. et al. (1996) *Elaboration and Characterisation of Phospholipid Langmuir-Blodgett Films.* Langmuir 12, 5379-5386
- Smondyrev A M, Berkowitz M L. (2001) *Molecular dynamics simulation of the structure of dimyristoylphosphatidylcholine bilayers with cholesterol.* Biophys. J. 80, 1649 – 1658.
- Takahashi H, Sinoda K, Hatta I. (1996) *Effects of the lamellar and the inverted hexagonal phases of DEPE* Biochem. Biophys. Acta, 1289, 209 – 216
- Takahashi H, Aoki H, Kodama M. et al. (1997) *Transformation from metastable gel phase to stable crystalline phase of DMPE* Chem. Phys. Lip. 89 83–89
- Thoma M, Schwendler M, Baltes H. (1996) *Ellips. XR on PE PC monolayers in n-Dodecane, n-Hexadecane, and Bicyclohexyl* Langmuir 12, 1722-1728
- Thurmond R L, Dodd S W, Brown M F. (1991) *Molecular areas of phospholipids as determined by 2H NMR spectroscopy* Biophys. J. 59, 108 – 113
- Toombes G E S, Finnefrock A C, Tate M W. et al. (2002) *Determination of La – HII phase transition temperature for 1,2-dioleoyl-sn-glycero-3-phosphatidylethanolamine* Biophys. J. 82, 2504 – 2510
- Turner D C, Gruner S M. (1992) *X-ray diffraction reconstruction of the inverted hexagonal (HII) phase in lipid water systems* Biochemistry 31, 1340 – 1355
- Van Dijck P W M. (1979) *Negatively charged phospholipids and their position in the cholesterol affinity sequence* Biochim. Biophys Acta 555, 89 – 101
- Yeagle P L. (1985) *Cholesterol and the cell membrane.* Biochim. Biophys. Acta. Rev. Biomem. 822, 267 – 287.

5. Phase Behaviour of Asymmetric Bilayers

The aim of this study was to attempt to model the asymmetric nature of membranes using the double bilayer samples. The results of three different asymmetric samples are given here, with respect to the fabrication, stability and phase behaviour.

5.1 Introduction

The distribution of lipids across many types of membranes is usually highly asymmetric. In Human erythrocyte and similar membranes phosphatidylcholines are mainly distributed in the outer exoplasmic-facing leaflet whilst phosphatidylethanolamines are mainly distributed in the inner cytoplasmic facing leaflet (Bretscher 1973). The asymmetric distribution of phospholipids is a fundamental feature of normal cell operation. For example, phosphatidylserine lipids, which are normally localised in the inner leaflet of an animal plasma membrane, are vital not only for exocytosis (fusion of membranes and secretory vesicles) and intracellular fusion processes, but also for lipid–protein interactions and signal transduction pathways (Kato 2002). The asymmetric nature of membranes is generated by the activity of an adenosine triphosphate (ATP)-dependent aminophospholipid translocase that specifically transports specific types of lipids between bilayer leaflets (Seigneuret 1984). This discovery underscored the prevailing concept that membrane lipid asymmetry was of major physiologic importance, because it showed that cells invest energy to catalyze lipid movement in order to maintain a specific transmembrane phospholipid distribution. Another membrane-bound enzyme involved in lipid asymmetry is the group known as flippases, which catalyse the exchange of lipids between the leaflets. Their working mechanism is still not fully understood (Boon 1999).

The Langmuir-Blodgett technique used to fabricate the double bilayers is highly suited to the fabrication of asymmetric bilayers. The technique has been used before to create supported asymmetric single bilayers (Merkel 1989, Bassereau 1997, Rinia 1999) but these single bilayers are likely to have the issues associated with their close proximity to the substrate.

In this chapter the results of three different asymmetric samples are given. The first sample recreates the asymmetric distribution of phosphatidylcholines and phosphatidylethanolamines across the membrane. The second sample consists of a lower bilayer of hydrogenated DPPC, and an upper bilayer with a hydrogenated DPPC lower leaflet and deuterated chain DPPC upper bilayer. The purpose of this sample was to study the asymmetric stability and effect on the phase behaviour. The third sample contains different concentrations of cholesterol in the upper and lower bilayers. This allows interesting biophysical studies of the effect of cholesterol upon various phase phenomena and is a predecessor of models the asymmetrically distribution of cholesterol across the leaflets of membranes, which in the case of brain synaptic plasma membranes of mice was observed to change with age (Igbavboa 1996).

5.2 Asymmetric bilayers of DPPC, DPPE and cholesterol

5.2.1 Introduction

In many membranes phosphatidylcholines and phosphatidylethanolamines are asymmetrically distributed across the leaflets of the bilayer. Figure 5.1 shows the asymmetric distribution of phospholipids and sphingomyelin for three common membranes. It can be seen that phosphatidylcholines are predominantly located in the exoplasmic facing leaflet and phosphatidylethanolamines in the cytoplasm-facing leaflet.

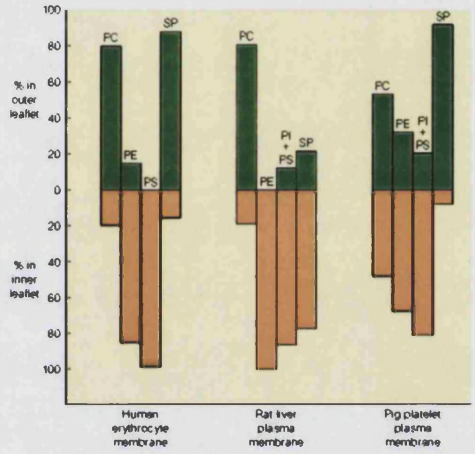

Figure 5.1 Schematic of the asymmetric distribution of phosphatidylcholines (PC), phosphatidylethanolamines (PE), phosphatidylserines (PS) and sphingomyelin (SP) in three different membranes.

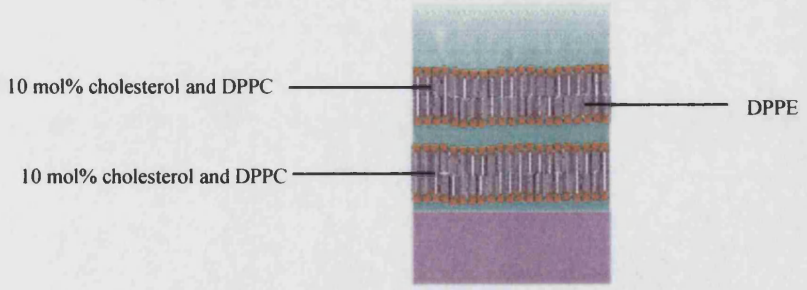

Figure 5.2 Schematic of asymmetric sample of DPPC, cholesterol, DPPE. The lower bilayer and upper bilayer outer leaflet consisted of 10 mol% cholesterol and DPPC. The inner leaflet was DPPE.

To model the asymmetric distribution of phosphatidylcholines and phosphatidylethanolamines, a sample consisting of a lower bilayer of DPPC and 10

mol% cholesterol and an upper bilayer with a inner leaflet of DPPE and outer leaflet of DPPC and 10 mol% cholesterol was fabricated (Figure 5.2). Cholesterol was not included in the DPPE leaflet as it was found to increase the instability of planar DPPE bilayers (Chapter 4). The stability, phase behaviour and asymmetric stability were studied by neutron reflectivity.

5.2.2 Fabrication Results

The fabrication of asymmetric samples was found to be rather difficult and very precise laboratory skills are necessary due to the exchange of the monolayers between the second and third deposition. The first two depositions of 10 mol% cholesterol and DPPC proceed in the way described in the fabrication chapter. After which the monolayer was removed and a monolayer of DPPE spread. The DPPE leaflet was then deposited. The final DPPC cholesterol leaflet was deposited by a Schaefer deposition. The transfer ratios and Schaefer results are listed in Table 5.1. The first and third depositions were excellent, however the second deposition transfer ratios was low. The Schaefer deposition was reasonable. The fabrication results show that it is possible to deposit subsequently different monolayers to form asymmetric bilayers with good transfer ratios.

	Tr1	Tr2	Tr3	Schaefer Deposition	
				Pressure	Area
Asym. PC PE Chol db	1.09	0.16	1.00	11mN/m	7cm²

Table 5.1 Transfer ratios (T_r) and Schaefer parameters results

5.2.3 Data fitting considerations

The data was fitted using the layered model approach in the AFit programme. A ten layer model was used. This allowed the upper bilayer chain region to be separated into two leaflets, rather than the usual one chain region. The incorporation of 10 mol% cholesterol reduced the DPPC chain SLD from -0.41×10^{-6} Å^{-2} to -0.36×10^{-6} Å^{-2}. The silicon oxide was found to have a thickness of 8Å and roughness of 3Å throughout.

5.2.4 Stability and Phase Behaviour

The sample was measured in D_2O at temperatures between 25.1 – 57.2°C. This temperature range covered the full phase behaviour of DPPC. Unfortunately due to beam-time constrains it was not possible to measure to temperatures above the gel – fluid of the DPPE (T_m is 64.5°C). Fitted profiles at 25.1°C, 43.4°C and 57.2°C are shown in Figure 5.3 and the parameters are listed in Table 5.2.

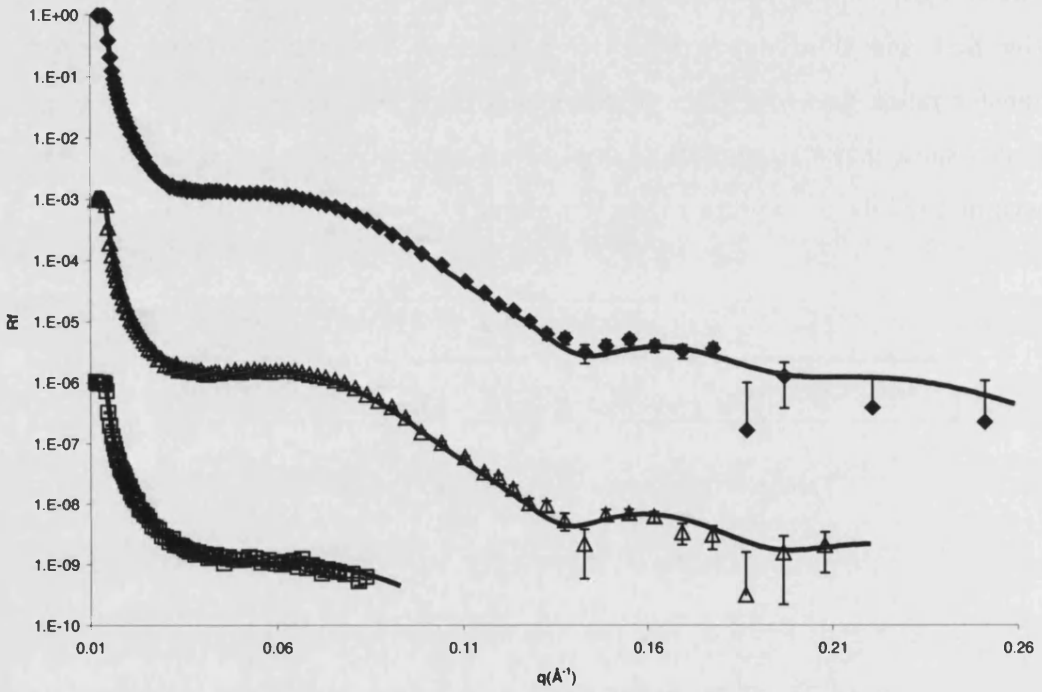

Figure 5.3 Fitted profiles of asymmetric DPPC – DPPE – 10 mol% cholesterol sample at 25.1°C (♦), 43.4°C (Δ) and 57.2°C (□).

The structural parameters show that it is indeed possible to fabricate stable asymmetric bilayers which are stable at temperatures above the DPPC T_m. The coverages of both leaflets of the upper bilayer are high, even though the lipids deposited onto different components from themselves.

	dw	lDb	lDc	lAPM	lRou	lCov	Dw	uDb	D_{DPPE}	$D_{DPPC-chol}$	uDc	uAPM	uRou	PE uCov	PC uCov
25.1°C	5±1	50±2	36±1	44±2	9±1	83±2	32±1	54±2	20±1	18±1	38±1	42±2	16±2	88±2	85±2
29.4°C	5±1	50±2	36±1	44±2	9±1	83±2	32±1	54±2	20±1	18±1	38±1	42±2	15±2	90±2	87±2
32.5°C	6±1	51±2	37±1	43±2	8±1	85±2	34±1	54±2	20±1	18±1	38±1	42±2	16±2	92±2	90±2
33.2°C	6±1	51±2	37±1	43±2	8±1	85±2	34±1	54±2	20±1	18±1	38±1	42±2	16±2	92±2	90±2
34.0°C	6±1	51±2	37±1	43±2	8±1	85±2	33±1	54±2	20±1	18±1	38±1	42±2	16±2	92±2	90±2
34.9°C	6±1	51±2	37±1	43±2	8±1	85±2	33±1	54±2	20±1	18±1	38±1	42±2	16±2	92±2	90±2
35.8°C	6±1	51±2	37±1	43±2	8±1	85±2	33±1	54±2	20±1	18±1	38±1	42±2	16±2	92±2	90±2
37.1°C	6±1	51±2	37±1	43±2	8±1	85±2	33±1	54±2	20±1	18±1	38±1	42±2	16±2	92±2	90±2
40.5°C	6±1	52±2	37±1	43±2	8±1	85±2	33±1	54±2	20±1	18±1	38±1	42±2	16±2	92±2	90±2
42.1°C	5±1	52±2	37±1	43±2	8±1	85±2	33±1	54±2	20±1	18±1	38±1	42±2	16±2	92±2	90±2
43.4°C	6±1	51±2	37±1	43±2	8±1	85±2	33±1	54±2	20±1	18±1	38±1	42±2	16±2	93±2	91±2
47.1°C	6±1	46±2	32±1	50±2	5±1	88±2	33±1	54±2	20±1	18±1	38±1	42±2	16±2	93±2	91±2
52.9°C	6±1	44±2	30±1	53±2	5±1	90±2	31±1	54±2	20±1	18±1	38±1	42±2	16±2	93±2	91±2
57.2°C	6±1	40±2	28±1	57±2	5±1	92±2	29±1	54±2	20±1	18±1	38±1	42±2	15±2	93±2	91±2

Table 5.2 Fitted parameters of asymmetric DPPC – DPPE – 10 mol% cholesterol sample.

The lower bilayer entered the fluid phase between 43.4°C – 47.1°C, after which its chain region thickness continued to progressively decrease (Figure 5.4). Its structure was similar to that of the 10 mol% cholesterol – DPPC double bilayer (Chapter 3), although the T_m was slightly higher. This may well be due to the closer proximity of the lower bilayer to the substrate than for the 10 mol% double bilayer.

The DPPC – cholesterol outer leaflet of the upper bilayer remained gel like throughout the temperature range studied. The surprising fact is that the DPPC leaflet remained gel like even when its T_m had been surpassed by 15°C. (The upper bilayer of the 10 mol% cholesterol DPPC double bilayer of chapter 3 had a T_m of between 39.1°C – 39.9°C). The presence of the DPPE leaflet therefore affects its phase behaviour.

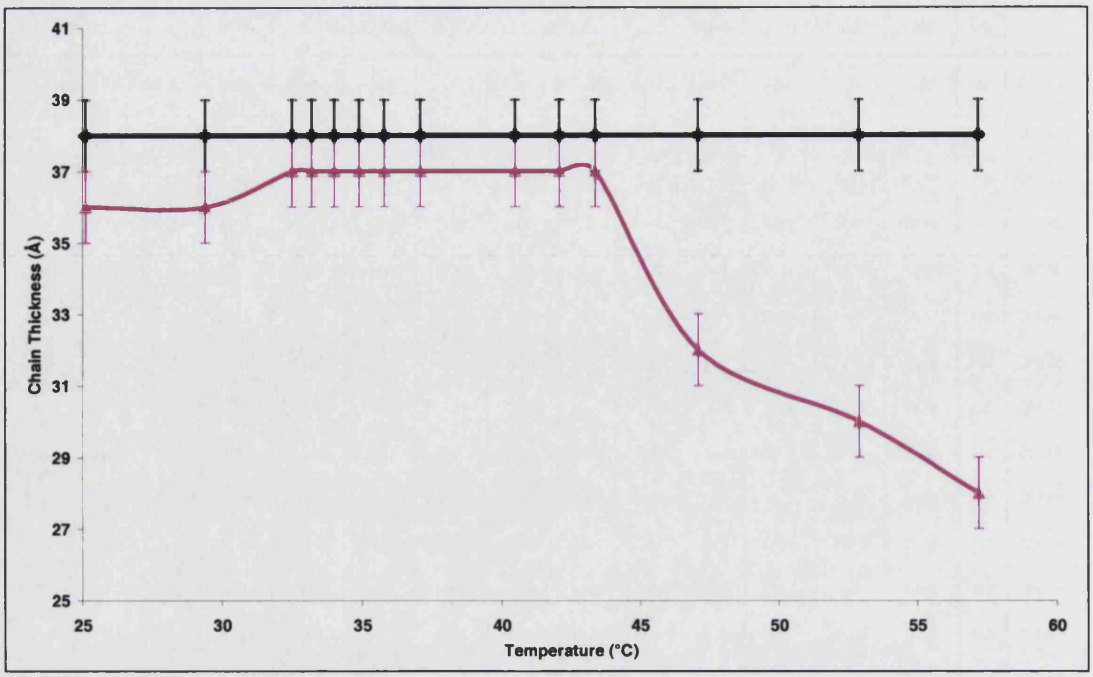

Figure 5.4 Thickness of chain region versus temperature. The upper bilayer is black, the lower bilayer pink.

The chain region thickness of the upper bilayer was very similar to the 10 mol% cholesterol DPPC double bilayer and the DPPE double bilayer, which both had a thickness of 37±1Å (Table 3.29 and Table 4.4). It was thicker than the DPPC sample (34Å±1 chapter 3.4), which was expected, as the cholesterol has been observed to reduce the tilt of DPPC chains (Leonard 2001) and the chains of DPPE are not tilted (Nagle 2000). The roughness of the upper bilayer was identical to the 10 mol% double bilayer, but much higher than the DPPE double bilayer of 5±2Å. The higher roughness could be due to formation of cholesterol rich and poor domains, which has been observed in vesicles of DPPC and 10 mol% (Knoll 1985). It is unlikely that depositing different monolayers compositions caused the higher roughness.

The gel phase chain region thickness of the lower bilayer was comparable to that of the 10 mol% cholesterol DPPC double bilayer of 35±1Å. The fluid phase thickness of 28 – 30Å was very similar as well, as was its roughness. The lower bilayer coverage was less than the other double bilayers, which is likely due to the lower quality of the second deposition. The similarities show that the lower bilayer acts independently of the upper bilayer, and that changing the components of the upper bilayer has no effect on the lower bilayer behaviour.

The main water layer thickness was comparable to the other double bilayers containing DPPC and cholesterol, which varied between 22 – 36Å. However, it was double the thickness of the DPPE double bilayer thickness of 16Å. It is thought that the water layer thickness is governed by the same balance of forces present in multilayers (Helfrich 1977), but also with the addition of substrate forces. More studies need to be conducted to fully understand the effect of different composition of leaflets upon the Helfrich forces. The lower water layer was only slightly thinner than that of the DPPC – cholesterol double bilayers, which had a thickness ranging between 8 – 12Å.

5.2.5 Asymmetric stability of upper bilayer

There was no indication in the scattering length density values that exchange of lipids between the two leaflets occurred (flip – flop). Although it is not possible to observe this unless very significant exchange occurred, as the two lipids have the same scattering length density for the chains and similar ones for the head-groups (PC 1.74 x 10^{-6} $Å^{-2}$, PE 2.66 x 10^{-6} $Å^{-2}$). For very significant exchange to occur it would be expected to take a very long time as flip-flop in model membranes and in real membranes is very slow (Smith, BD. 2003). A more sensitive way to assess the asymmetric stability would be to use deuterated versions of the lipids. An example of this is the next sample.

5.3 Asymmetric hydrogenated and deuterated bilayers

5.3.1 Introduction

The ability to deposit deuterated layers upon hydrogenated layers allows one to selectively label components and layers in the bilayers. A new variation on the double bilayer was therefore evaluated. The sample consisted of an upper bilayer with deuterated lipids in the outer leaflet and hydrogenated lipids in the inner leaflet. The lower bilayer had hydrogenated lipids (Figure 5.5). The deuterated lipid used was deuterated chain DPPC (d_{62}-DPPC) and the hydrogenated lipid was the normal DPPC used in the other studies. This sample is ideal for uses in experiments were adsorptions of peripheral proteins onto the surface of the bilayer are studied. The use of the deuterated outer leaflets provides a high scattering length contrast between the lipid and the proteins, allowing the vertical position of the proteins to be located more clearly.

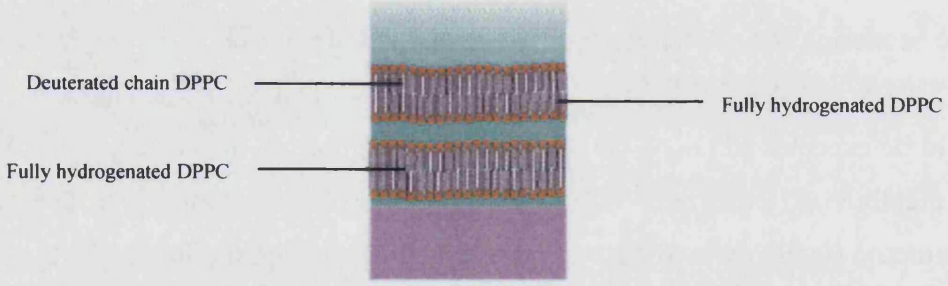

Figure 5.5 Schematic of the asymmetric hydrogenated and deuterated sample.

5.3.2 Fabrication

The d_{62}-DPPC needed mild heating to dissolve in chloroform. The results of the depositions are given in Table 5.3. The transfer ratios for the three hydrogenated chain DPPC depositions were good and almost identical to those of the DPPC double bilayer (Table 3.1). The Schaefer deposition parameters however were higher than that observed for h-DPPC, especially the area rise. This maybe intrinsic to d-DPPC or may signify a poorer quality deposition.

	Tr1	Tr2	Tr3	Schaefer Deposition	
				Pressure	Area
Asym. h-d-DPPC	1.03	0.47	0.96	10mN/m	10cm²

Table 5.3 Transfer ratios and Schaefer parameters of depositions of three hydrogenated DPPC layers followed by one d_{62}-DPPC layer.

5.3.3 Stability and Phase Behaviour

The reflectivity profiles were fitted using a ten-layer model, to enable the separation of the upper bilayer chain region into hydrogenated and deuterated layers. The scattering length densities are given in the Chapter 3. The sample was measured in D_2O from 25.2°C up to 49.1°C. The D_2O solvent used was found to have a scattering length density of 6.12 x 10^{-6} $Å^{-2}$ rather than 6.35 x 10^{-6} $Å^{-2}$, which indicates incomplete exchange of the H_2O for D_2O. The silicon oxide layer was found to have a thickness of 16Å and roughness of 3Å. Four fitted profiles are shown in Figure 5.6 and the parameters are listed in Table 5.4.

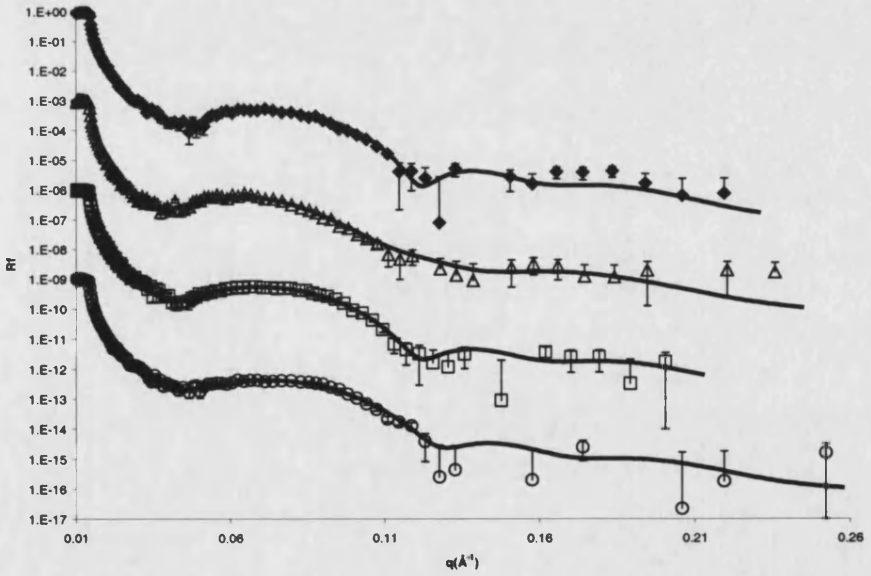

Figure 5.6 Fitted profiles of asymmetric hydrogenated and deuterated DPPC bilayer sample at 25.2°C (♦), 37.1°C (Δ), 42.1°C (□) and 49.1°C (○).

The sample exhibited phase behaviour consistent with gel, transition and fluid phases. The structure was stable over the temperature range measured.

5.3.3.1 Gel phase

The chain region thickness of the lower bilayer was comparable to that of the DPPC double bilayer of which had a thickness of 35Å (Table 3.3). The upper bilayer was slightly thicker in comparison. This difference is minimal, but may indicate that the hydrogenated and deuterated chains are not interdigitated. The roughness of both bilayers was much higher than that observed in the DPPC double bilayer which had a lower bilayer roughness of 3Å and upper bilayer of 5Å. The higher roughness of the upper bilayer could be due to the asymmetric nature of the layers or because, for reasons unknown, deuterated DPPC tends to give rougher layers. It is not understood why the lower bilayer has high roughness though. It is not expected to be affected by the asymmetric nature. It could be connected to its low coverage though as the coverage of both bilayers was lower than that expected.

	dw	lDb	lDc	lAPM	lRou	lCov	Dw	uDb	Dh	Dd	uDc	uAPM	uRou	h uCov	d uCov
25.2°C	5±1	55±2	36±1	44±2	10±2	63±2	36±1	53±2	17±1	19±1	36±1	44±1	15±2	74±2	69±2
29.5°C	5±1	56±2	37±1	43±2	11±2	82±2	37±1	52±2	17±1	18±1	35±1	46±1	15±2	74±2	70±2
31.3°C	5±1	56±2	37±1	43±2	11±2	84±2	36±1	52±2	17±1	18±1	35±1	46±1	15±2	74±2	70±2
33°C	6±1	56±2	37±1	43±2	11±2	83±2	37±2	53±2	17±1	18±1	35±1	46±1	15±2	70±2	70±2
33.8°C	6±1	56±2	37±1	43±2	11±2	83±2	37±2	53±2	17±1	18±1	35±1	46±1	15±2	70±2	70±2
34.3°C	6±1	56±2	37±1	43±2	11±2	83±2	37±2	52±2	16±2	18±1	34±1	47±1	15±2	70±2	70±2
34.8°C	7±1	56±2	37±1	43±2	11±2	82±2	38±2	53±2	17±1	18±1	35±1	46±1	15±2	69±2	71±2
35.9°C	5±1	57±2	37±1	43±2	12±2	81±2	39±2	53±2	18±1	16±1	34±1	47±1	20±2	63±2	65±2
37.1°C	5±1	55±2	37±1	43±2	11±2	82±2	44±2	54±2	18±1	17±1	35±1	46±1	24±2	65±2	60±2
38.6°C	5±1	57±2	37±1	43±2	11±2	81±2	44±2	54±2	18±1	17±1	35±1	46±1	24±2	65±2	60±2
40.4°C	5±1	56±2	37±1	43±2	11±2	81±2	43±2	54±2	18±1	17±1	35±1	46±1	22±2	64±2	60±2
42.1°C	6±1	55±2	37±1	43±2	10±2	81±2	35±2	47±2	14±1	14±1	28±1	57±1	14±2	71±2	69±2
43.8°C	6±1	55±2	37±1	43±2	10±2	81±2	35±2	47±2	14±1	14±1	28±1	57±1	14±2	71±2	69±2
45.5°C	5±1	55±2	36±2	44±2	10±2	80±2	35±2	45±2	13±1	14±1	27±1	59±1	14±2	74±2	67±2
47.3°C	5±1	52±2	32±2	50±2	10±2	86±2	35±2	44±2	12±1	13±1	25±1	64±1	13±2	75±2	72±2
49.1°C	5±1	52±2	32±2	50±2	9±2	85±2	35±2	44±2	12±1	13±1	25±1	64±1	13±2	77±2	72±2

Table 5.4 Fitted parameters asymmetric hydrogenated and deuterated DPPC bilayer.

5.3.3.2 Transition Phase

The sample started exhibiting transition phase behaviour at 35.9°C with an increase in the thickness of the main water layer and increase in the upper bilayer roughness.

This was the same as the gel – ripple transition temperature for h-DPPC of 35.7°C (Racansky 1987). The presence of a deuterated chain DPPC leaflet in the upper bilayer does not affect the bilayer phase behaviour. The variation with temperature of the water layer thickness and the bilayer chain thickness are shown in Figure 5.7. The increase in the water layer reached a maximum at 37°C that continued until close to the transition to the gel – fluid transition. The behaviour of the upper bilayer roughness parallels that of the water layer.

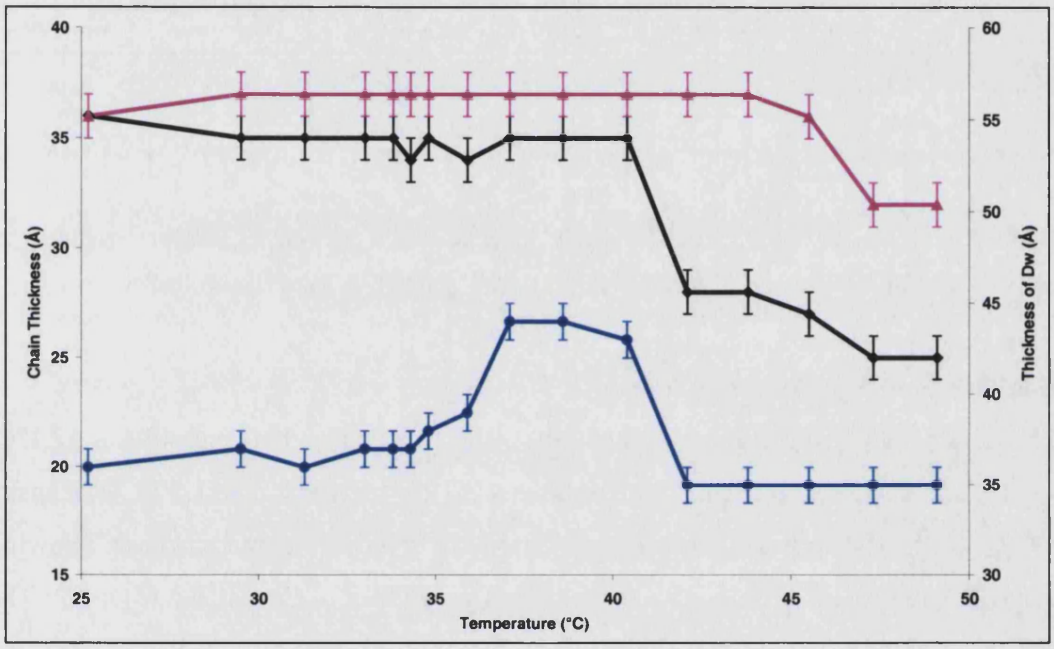

Figure 5.7 Variation versus temperature of: upper bilayer chain region (black), lower bilayer chain region (pink) and the main water layer (blue).

Table 5.5 shows a comparison of the maximum increase in the water layer thickness and upper bilayer roughness of this sample and the hydrogenated DPPC double bilayer of chapter 3. The maximum increase of the thickness of the water layer is considerably less than that of the hydrogenated double bilayer. However, the maximum increase in the roughness of the bilayers is similar. The difference in the maximum water layer thickness could be connected to the difference in the thicknesses in the gel phase at 25°C or due to the deuterated leaflet restricting the behaviour. The fact that the samples have the same maximum value could indicate that the former is the likely reason. The roughness has the opposite behaviour, where the maximum increases in the values are the same, but the maximum values are

different. The increase in the water layer during the transition phase has been compared for fully hydrogenated and fully deuterated DSPC bilayers. The maximum increase in the water layer in the deuterated DSPC was found to be in the order of a half less that that of the hydrogenated DSPC (Fragneto 2003). It is likely that the presence of the deuterated leaflet in the upper bilayer is actually causing the reduced transition phase behaviour of the water layer.

	Gel value (25°C)		Maximum transition phase value		Maximum increase	
	h-DPPC db	Asym DPPC	h-DPPC db	Asym DPPC	h-DPPC db	Asym DPPC
Dw	27±1Å	36±1Å	43±1Å	44±1Å	16±1Å	8±1Å
Urou	5±2Å	15±2Å	15±2Å	24±2Å	10±2Å	9±2Å

Table 5.5 Maximum increase in the water layer thickness and upper bilayer roughness of hydrogenated DPPC double bilayer and double bilayer containing deuterated outer leaflet.

5.3.3.3 Fluid phase

The upper bilayer undergoes a transition to the fluid phase between 40.4 – 42.1°C, which encompasses the transition temperature of h-DPPC of 41.8°C (Racansky 1987). Both of the upper bilayer leaflets exhibit a reduction in thickness, showing that the d-DPPC has a transition temperature very close to that of the h-DPPC. The fact that there are hydrogenated chains in contact with deuterated does not affect the gel – fluid transition temperature. This is particularly interesting, as the predominant change occurring in this transition is the melting of the chains, so the difference in the isotopic nature does not affect the temperature.

The difference in the upper bilayer roughness between the gel and fluid phase is minimal. The hydrogenated double bilayer roughness increased by 3Å (Chapter 3), but its value of 8Å was lower than here. The higher roughness of the deuterated leaflet sample could be an inherent factor of deuterated lipids. The upper bilayer coverage increased slightly upon becoming fluid. This is expected due to the increase in the lipid area per molecule (APM). The average APM of the lipids lies within the fluid phase range of values of 56 – 72Å^2 for h-DPPC (Nagle 2000). The average fluid phase chain thickness range of 28 – 25Å is less than that observed for the h-DPPC

double bilayer, which ranged between 30 – 28Å. It appears that the h-DPPC and d-DPPC chains were more interdigitated than the fully h-DPPC bilayer.

As in the h-DPPC double bilayer, the lower bilayer became fluid between 45.5°C – 49.1°C. Like the upper bilayer, the roughness of the lower bilayer did not significantly change upon becoming fluid, it remained high. The coverage however increased slightly. The reduction in chain thickness was slightly less than that observed in the upper bilayer and the fluid phase APM was lower than the literature range of 56 – 72Å^2 (Nagle 2000).

5.3.4 Stability of asymmetric nature

There was no indication in the scattering length densities that flip – flop of the deuterated and hydrogenated lipids occurred. All profiles needed the calculated values to obtain good fits. Unlike lateral diffusion, which is very rapid, the flip-flop of phospholipids across a model bilayer membrane is known to be a very slow process with a half-life of hours to days (Smith 2003). Flip-flop rates in vesicles have been found to be strongly dependent on the composition of the polar head-group and less dependent on the length of the acyl chains (Homan 1988). At neutral pH, flip-flop rates increase in the order PC < PG < PA < PE, where the rates for PE were at least 10-times greater than those of the homologous PC derivative. The double bilayer therefore would not be expected to have a fast exchange of lipids across the bilayer. The presence of holes in the bilayer could be expected to increase the rate though. To properly assess the asymmetric stability the sample would need to be repeatedly measured over a number of days. This is not usually viable with neutron reflectivity measurements due to beam-time restrictions. What can be said though is that this type of sample is asymmetrically stable over at least a day, which is the time it took to measure it. This stability timescale allows this type of sample to be used in hydrogenated/deuterated protein studies.

5.4 Asymmetric distribution of cholesterol

5.4.1 Introduction

Cholesterol is often asymmetrically distributed across the leaflets of membranes. To aid in the understanding of the effect of low amounts of cholesterol upon the ripple phase behaviour (chapter 3), a DPPC sample containing 6 mol% of cholesterol in the lower bilayer and 1 mol% of cholesterol in the upper bilayer was investigated (Figure 5.8). The stability and phase behaviour were measured by neutron reflectivity.

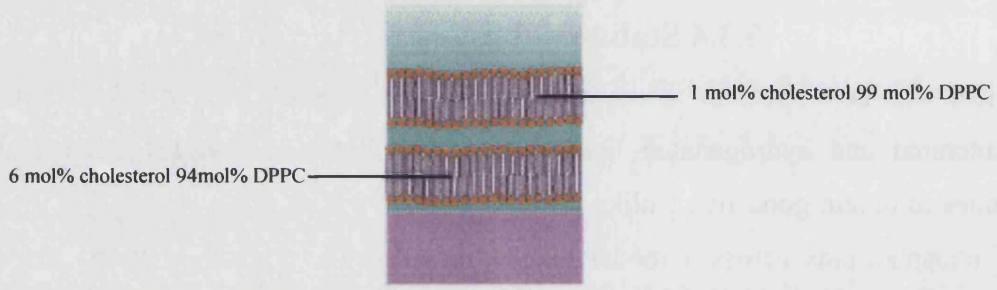

Figure 5.8 Lower bilayer consists of 6 mol% cholesterol and DPPC and the upper bilayer of 1 mol% cholesterol and DPPC.

5.4.2 Fabrication

The sample was fabricated using the technique detailed in chapter 2, except that after the second deposition, the monolayer was replaced by a lower cholesterol concentration monolayer. The transfer ratios and Schaefer parameters are given in Table 5.6.

	Tr1	Tr2	Tr3	Schaefer Deposition	
				Pressure	Area
Asym. 6% Lbl 1% Ubl	1.07	0.56	0.92	7mN/m	4cm²

Table 5.6 Transfer ratios of 6 mol% lower bilayer, 1 mol% upper bilayer, DPPC sample

The transfer ratios of the first and second depositions were excellent and comparable to those of the 6 mol% double bilayer (Table 3.1). The transfer ratio of the third deposition was lower than the normal unity observed.

5.4.3 Measurements

The reflectivity profiles were fitted using the AFit programme. The scattering length densities are given in the Chapter 3. The presence of 6 mol% cholesterol reduces the lipid chain scattering length density from -0.41 x 10^{-6} $Å^{-2}$ to -0.38 x 10^{-6} $Å^{-2}$. The presence of 1 mol% cholesterol does not significantly alter it to two decimal places. The reflectivity was measured in D_2O from 26.4°C to 48.3°C and then down to 26.1°C. The silicon oxide was found to have a thickness of 8Å and roughness of 3Å throughout. The sample exhibited stable gel, transition and fluid phase behaviour. The transition behaviour was different upon heating and cooling.

5.4.4 Gel phase structure

The structure of the gel phase differed before and after the temperature scan. This was a result of the large transition behaviour observed when cooling from the fluid phase. The gel phase after cooling is given after the transition region section as it may still be exhibiting properties of that phase. Fitted profiles at 26.4°C and 31.5°C are shown in Figure 5.9 and the parameters are listed in Table 5.7.

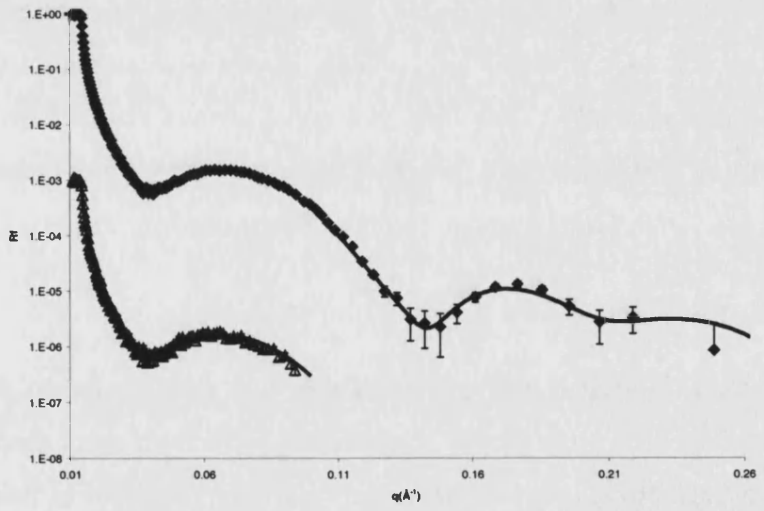

Figure 5.9 Fitted profiles of asymmetric 6 mol% and 1 mol% sample at 26.4°C (♦) and 31.5°C (Δ).

	dw	lDb	lDc	lAPM	lRou	lCov	Dw	uDb	uDc	uAPM	uRou	uCov
26.4°C	7±1	50±2	36±1	44±2	5±1	94±2	28±1	49±2	35±1	46±2	12±2	89±2
31.5°C	7±1	50±2	36±1	44±2	5±1	94±2	29±1	49±2	35±1	46±2	12±2	89±2

Table 5.7 Fitted parameters of asymmetric 6 mol% and 1 mol% sample in the gel phase

The deposition of the two bilayers with different concentrations gave a stable double bilayer structure and was not effected by the exchange of the monolayer after the second deposition.

The structure of the lower bilayer and that of the lower water layer were identical to those of the 6 mol% double bilayer (Table 3.20), confirming that the structure of the first two depositions is entirely reproducible. The upper bilayer had similar thickness and coverage parameters to that of the 1 mol% double bilayer (Table 3.8) but was rougher by 5Å. The cause of the higher roughness is unknown but maybe connected to the lower transfer ratio of the third deposition. The thickness of the main water layer was comparable that of the 1 mol% sample after the temperature scan and was similar to those of the other low ratio of cholesterol once equilibrated.

5.4.5 Fluid phase structure

The upper bilayer became fluid between 40.1°C to 41.0°C, whilst the lower bilayer became fluid between 41.0°C to 42.0°C. These transition temperatures were similar to those observed in the respective double bilayers counterparts. The bilayers therefore act independently in the fluid phase and are not affected by the different concentrations of cholesterol in the other bilayer. Fitted fluid phase profiles at 42.0°C, 48.3°C and 42.1°C upon cooling are shown in Figure 5.10 and the parameters are listed in Table 5.8.

The structures of the upper and lower bilayers were very similar to those of their double bilayers counterparts (Table 3.9 and Table 3.25). Both water layer thicknesses remained constant throughout the fluid phase and were identical to those of the gel phase.

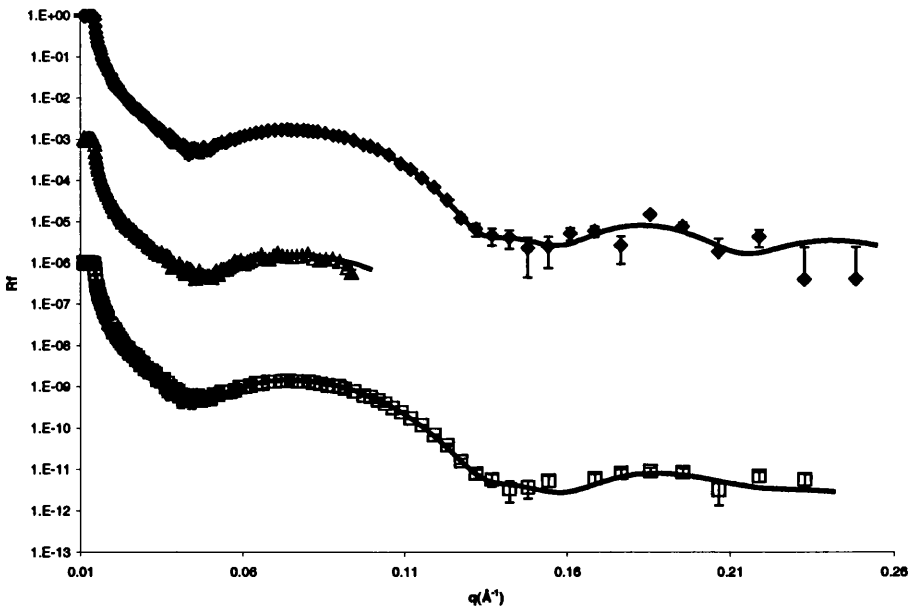

Figure 5.10 Fitted profiles of asymmetric the 6 mol% and 1 mol% sample at 42.0°C (♦), 48.3°C (Δ) and 42.1°C (□)

	dw	lDb	lDc	lAPM	lRou	lCov	Dw	uDb	uDc	uAPM	uRou	uCov
26.4°C	7±1	50±2	36±1	44±2	5±1	94±2	28±1	49±2	35±1	46±2	12±2	89±2
41.0°C	8±1	48±2	35±1	46±2	4±1	98±2	29±1	49±2	32±1	50±2	10±2	98±4
42.0°C	8±1	47±2	31±1	52±2	3±1	100±2	29±1	45±2	29±1	55±2	8±2	100±2
43.0°C	8±1	46±2	30±1	53±2	3±1	100±2	28±1	45±2	29±1	55±2	8±2	100±2
48.3°C	8±1	46±2	30±1	53±2	3±1	100±2	28±1	44±2	28±1	57±2	8±2	100±2
44.1°C	8±1	45±2	30±1	53±2	3±1	100±2	28±1	43±2	28±1	57±2	10±2	100±2
42.1°C	8±1	47±2	32±1	50±2	3±1	98±2	28±1	43±2	29±1	55±2	10±2	100±2

Table 5.8 Fitted parameters of asymmetric 6 mol% and 1 mol% sample in the fluid phase

5.4.6 Transition phase behaviour

The sample exhibited different transition phase behaviour upon heating and cooling. The difference in behaviour with the direction of temperature change matches the behaviour of the 1 mol% double bilayer. The behaviour upon heating will be given first, followed by the behaviour upon cooling.

5.4.6.1 Transition phase behaviour upon heating

Upon heating the sample exhibited transition phase behaviour between 34.1°C – 40.1°C. Fitted profiles at 35.0°C, 36.6°C and 39.1°C are shown in Figure 5.11 and the parameters are listed in Table 5.9.

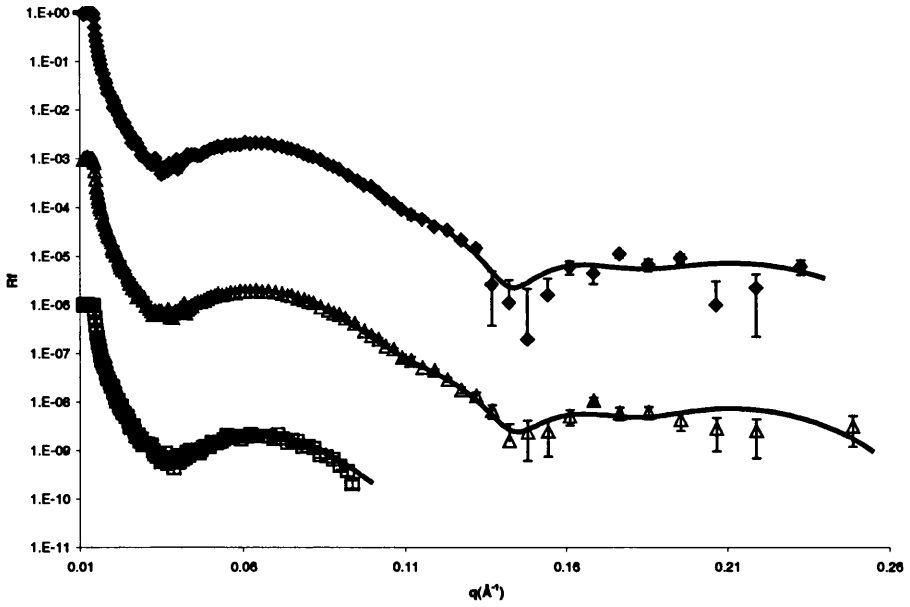

Figure 5.11 Fitted profiles of asymmetric 6 mol% and 1 mol% sample at 35.0°C (♦), 36.6°C (Δ) and 39.1°C (□).

As in the case of the double bilayers of cholesterol concentrations between 0 – 4 mol% (Chapter 3) increases were observed in the thickness of the main water layer, the upper bilayer roughness and the solvation of the upper bilayer, whilst the structure of the lower bilayer and lower water remained constant throughout. These increases versus temperature are shown in Figure 5.12. It can be seen that these parameters increase in value between 31.5°C to 34.1°C then remain relatively constant until 38.3°C where they start to decrease, finally giving the fluid phase structure at 41.0°C.

	dw	lDb	lDc	lAPM	lRou	lCov	Dw	uDb	uDc	uAPM	uRou	uCov
26.4°C	7±1	50±2	36±1	44±2	5±1	94±2	28±1	49±2	35±1	46±2	12±2	89±2
34.1°C	7±1	50±2	36±1	44±2	4±1	93±2	35±1	54±2	37±1	46±2	15±2	82±4
35.0°C	8±1	50±2	36±1	44±2	3±1	95±2	34±1	54±2	38±1	46±2	15±2	82±4
35.7°C	8±1	50±2	36±1	44±2	3±1	95±2	35±1	54±2	38±1	46±2	15±2	82±4
36.6°C	8±1	50±2	36±1	44±2	4±1	95±2	35±1	52±2	38±1	46±2	15±2	83±4
37.4°C	8±1	50±2	36±1	44±2	4±1	95±2	35±1	52±2	38±1	46±2	15±2	83±4
38.3°C	8±1	50±2	36±1	44±2	4±1	95±2	35±1	52±2	38±1	46±2	15±2	81±4
39.1°C	8±1	50±2	36±1	44±2	4±1	95±2	34±1	52±2	38±1	46±2	13±2	83±4
40.1°C	8±1	50±2	36±1	44±2	4±1	95±2	32±1	52±2	38±1	46±2	12±2	85±4
48.3°C	8±1	46±2	30±1	53±2	3±1	100±2	28±1	44±2	28±1	57±2	8±2	100±2

Table 5.9 Fitted parameters of asymmetric 6 mol% and 1 mol% sample upon heating in transition region

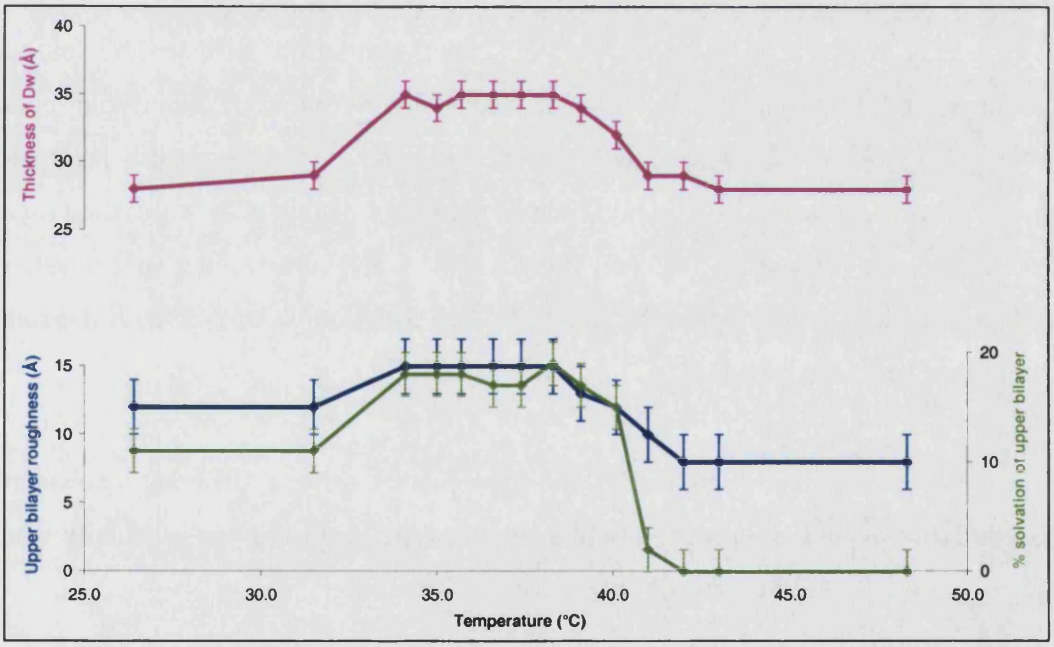

Figure 5.12 Variation in thickness of main water layer (pink) and upper bilayer roughness (blue) and solvation (green) versus temperature upon heating the sample.

The maximum increase in the water layer thickness, and upper bilayer roughness and solvation is given in Table 5.10 along with the values of the respective double bilayers from chapter 3. The increase in water layer thickness and upper bilayer

roughness of the asymmetric bilayer are considerably smaller than those of the 1 mol% double bilayer, but higher than the 6 mol% double bilayer. The sample is not reproducing the behaviour of the 1 mol% double bilayer even though the upper bilayer has a very similar structure. The presence of a lower bilayer with a different amount of cholesterol is affecting the transition phase behaviour.

	Gel value (25°C)			Maximum Transition value			Maximum Increase		
	Asym	1 mol%	6 mol%	Asym	1 mol%	6 mol%	Asym	1 mol%	6 mol%
Dw	28±1Å	22±1Å	33±1Å	35±1Å	37±1Å	37±1Å	7±1Å	15±1Å	4±1Å
Urou	12±2Å	7±2Å	10±2Å	15±2Å	16±2Å	11±2Å	3±2Å	9±2Å	1±2Å
uSolv	11±4%	14±4%	25±4%	19±4%	22±4%	29±4%	8±4%	8±4%	4±4%

Table 5.10 Comparison of gel phase, maximum transition values and the maximum increase of water layer thickness, and upper bilayer roughness and solvation of asymmetric sample, 1 mol% double bilayer and 6 mol% double bilayer.

In chapter 3, it was proposed, that due to the close similarities between the value of the upper bilayer roughness parameter and the amplitude of the ripple phase measured by AFM (Kaasgaard 2003), that the value of the roughness parameter could be proportional to be the amplitude of the ripple. If this is the case, then it can be said that the presence of a lower bilayer with a different amount of cholesterol reduces the size of the ripple structure compared to a double bilayer with the same cholesterol concentration.

It is unclear why the presence of a lower bilayer with a different cholesterol concentration would affect the phase behaviour of the upper bilayer, especially when the structure of the lower bilayer remains static throughout.

Whilst the structure of the ripple phase has been extensively studied in other systems the reasons for its appearance is still not clear and many theoretical models have been put forward to explain the formation, but no general model is able to account for all the features (Cunningham 1998). In the double bilayer system there is the additional interaction with the substrate and the fact the upper rippling bilayer is bound only on one side. Further experiments are needed with different ratios of

cholesterol and with different lipids in the upper and lower bilayer to understand more clearly the effect of the lower bilayer composition on the upper bilayer ripple.

5.4.6.2 Transition phase behaviour upon cooling

As in the case of the 1 mol% double bilayer, the asymmetric double bilayer exhibited different structural behaviour upon cooling compared to upon heating. Transitional behaviour was observed between 39.3°C to 34.9°C. The gel phase structures observed below this were heavily affected by the transition region. The sample was measured at three temperatures in the transition region (39.3°C, 36.7°C and 34.9°C). A complete profile was measured at 36.7°C, whilst for the other two only the first angle was measured which gave a maximum q of $0.09Å^{-1}$.

In the case of the pure 1 mol% double bilayer (chapter 3) due to the possible presence of two fringes in the first fringe, it was not possible to fit the overall profile using only one model. As in that sample, it was proposed also here that two models are needed to achieve a good fit, as it is possible that the upper bilayer was exhibiting two coexisting ripple structures. This behaviour has previously been observed by the Mouritsen group in DPPC double bilayers on mica by AFM measurements (Kaasgaard 2003). The group observed two coexisting ripple structures, consisting of a small amplitude ripple structure of $\geq$ 12Å, similar to that observed upon heating and a large ripple structure of $\geq$ 50Å. The two models to fit the asymmetric sample were the same as those used for the 1 mol% double bilayer profiles. They consisted of one model with a smaller upper bilayer roughness (~ 15Å) and another model with a high upper bilayer roughness (~ 50Å).

Unlike the profiles for the 1 mol% double bilayer, the reflectivity profiles of the asymmetric sample do not show clearly a first fringe consisting of two features. It is unclear whether the upper bilayer is behaves the same way as the 1 mol% double bilayer. The use of two ripple models is shown in Figure 5.13 and 5.14 for the sample at 39.3°C and 36.9°C, the ambiguity of the use of two models is clearly visible. The parameters are listed in Table 5.11

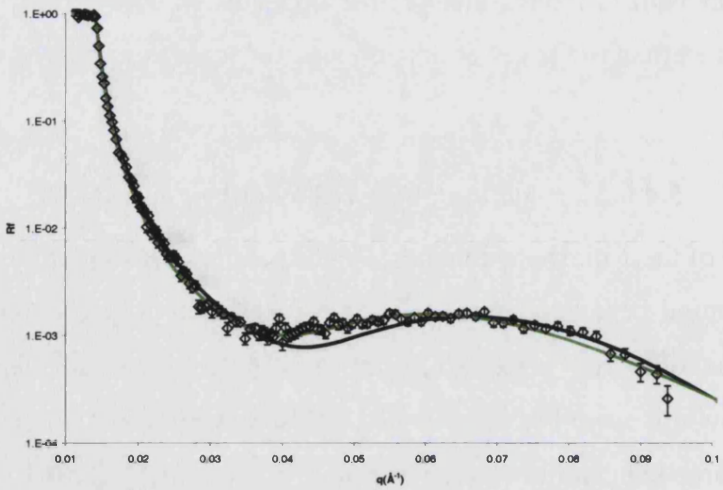

Figure 5.13 Profile of 6 mol% 1 mol% asymmetric sample at 39.3°C fitted using two different roughness ripple models. The black line is the smaller roughness model and the green line the larger roughness model.

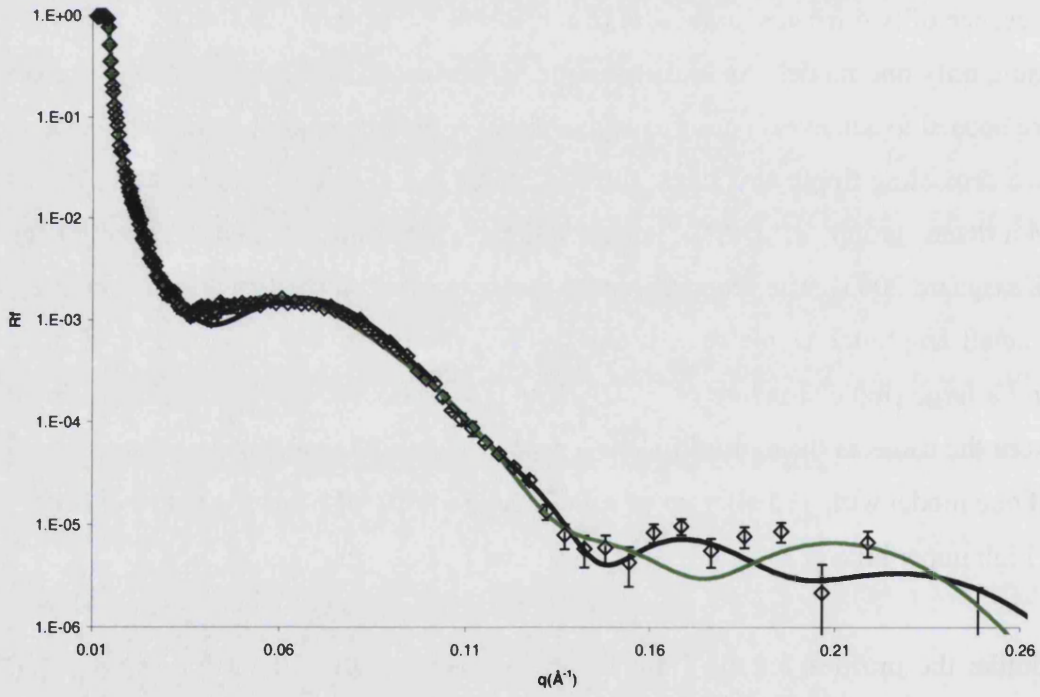

Figure 5.14 Profile of 6 mol% 1 mol% asymmetric sample at 36.9°C fitted using two different roughness ripple models. The black line is the smaller roughness model and the green line the larger roughness model.

		dw	lDb	lDc	lAPM	lRou	lCov	Dw	uDb	uDc	uAPM	uRou	uCov
39.3°C	small	8±1	47±2	35±1	46±2	6±1	95±2	35±1	51±2	35±1	46±2	15±2	93±2
	large	8±1	48±2	35±1	46±2	4±1	94±2	37±1	53±2	37±1	43±2	23±2	96±2
36.7°C	small	8±1	47±2	35±1	46±2	6±1	95±2	32±1	51±2	35±1	46±2	15±2	96±2
	large	8±1	48±2	35±1	46±2	4±1	94±2	39±1	53±2	36±1	44±2	25±2	100±2
34.9°C	small	7±1	47±2	34±1	47±2	7±1	96±2	32±1	52±2	37±1	43±2	16±2	96±2
	large	7±1	47±2	35±1	46±2	5±1	97±2	34±1	52±2	37±1	43±2	21±2	100±2

Table 5.11 Fitted parameter of 6 mol% 1 mol% asymmetric sample upon cooling down in transition region. The 'small' refers to the smaller amplitude ripple model and the 'large' label the larger amplitude ripple model.

It is possible that the profile measured at 36.9°C could be considered to be fitted sufficiently using only the large ripple structure shown in green. However, this fit does not account fully for the 0.07 – 0.10 $Å^{-1}$ and 0.12 – 0.14 $Å^{-1}$ parts of the profile. The profiles demonstrate that more measurements are needed on this type of sample, especially measuring the sample in many solvent contrasts. This was not conducted at the time with this sample due to beam-time constraints.

Whether the use of two models is valid or not, it can be confidently said that from the differences in the profile shape that the asymmetric bilayer is behaving differently to that of the 1 mol% double bilayer of chapter 3. It is likely then that the presence of a lower bilayer with a higher cholesterol concentration is affecting the phase behaviour of the upper bilayer.

If the use of two models was shown to be valid then the following discussion using two separate models is valid.

The two models used to fit the profiles had upper bilayer roughnesses ranging from 15Å to 16Å and 23Å to 25Å, which could be evidence of coexisting small amplitude ripples and large amplitude ripples. This would suggest that the size of the larger ripple is lowered by the presence of the bilayers with two different cholesterol concentrations, as it is much lower than that proposed for the 1 mol% double bilayer of 44±2Å (Chapter 3).

Both model fits indicated that the structure of the lower bilayers remained constant throughout the transition region. For the upper bilayer, the two models had the same thickness and similar coverage; however the larger roughness model had a thicker water layer. This is logical, as a larger rippling structure would be expected to have a thicker water layer due to the larger undulating bilayer structure.

The roughness of the smaller model is similar to that observed when heating in the transition region, but the water layer thickness differs slightly. It could be that the smaller ripples thought to be present upon cooling are different then to those upon heating. This would differ from the AFM study of pure DPPC double bilayers, where the small ripples observed upon cooling were the same as those observed upon heating (Kaasgaard 2003).

Phase behaviour at 34.9°C

The shape of the profile changed between 36.7°C – 34.9°C. It is equally possible to obtain good fits with either of the two ripple models proposed for the higher temperatures (Figure 5.15). The parameters were listed in Table 5.11 above. The first model consisted of a model of the small amplitude ripple with parameters similar to those used in fitting the 39.3°C and 36.7°C profiles. The second model consisted of a larger ripple model, but with lower parameters than that used for the 39.3°C and 36.7°C profiles.

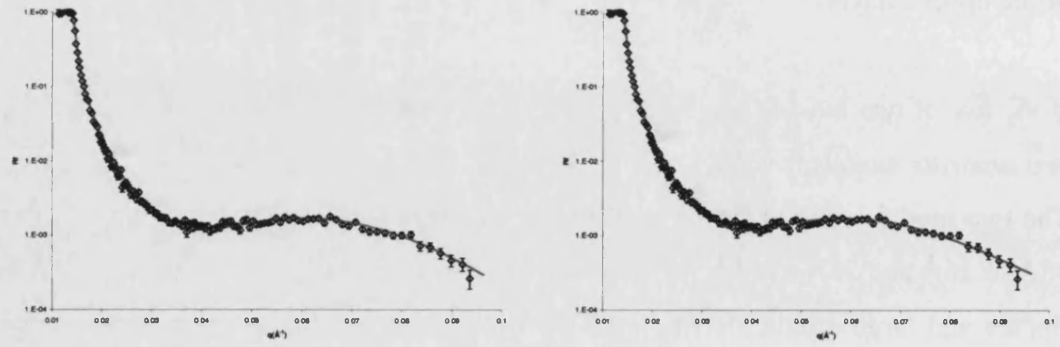

Figure 5.15 Possible fits of Profile of 6 mol% 1 mol% asymmetric sample at 34.9°C. (a) Fitted with a small roughness model and (b) fitted with a larger roughness model.

It is not possible to determine which of the two fits is likely to be closer to the real structure. Both fits have similar least square difference values and both match the contours of the profile.

The parameters of the small ripple model resemble closely those used in the 39.3°C and 36.7°C small ripple model, whilst the parameters of the large ripple model are significantly lower than those used in the large model parameters. The water layer was 3Å – 5Å less and the upper bilayer roughness by 2Å – 4Å less. If this was the actual structure, it could be said that a reduced ripple structure is observed at lower temperatures. This would parallel the behaviour observed in heating, where a maximum is observed in the middle of the transition temperature range.

Gel phase after cooling

The sample exhibited a gel phase between 32.3°C to 26.2°C. The fitted profiles at these two temperatures are given in Figure 5.16 and the parameters are listed in Table 5.12 along with the initial structure before heating.

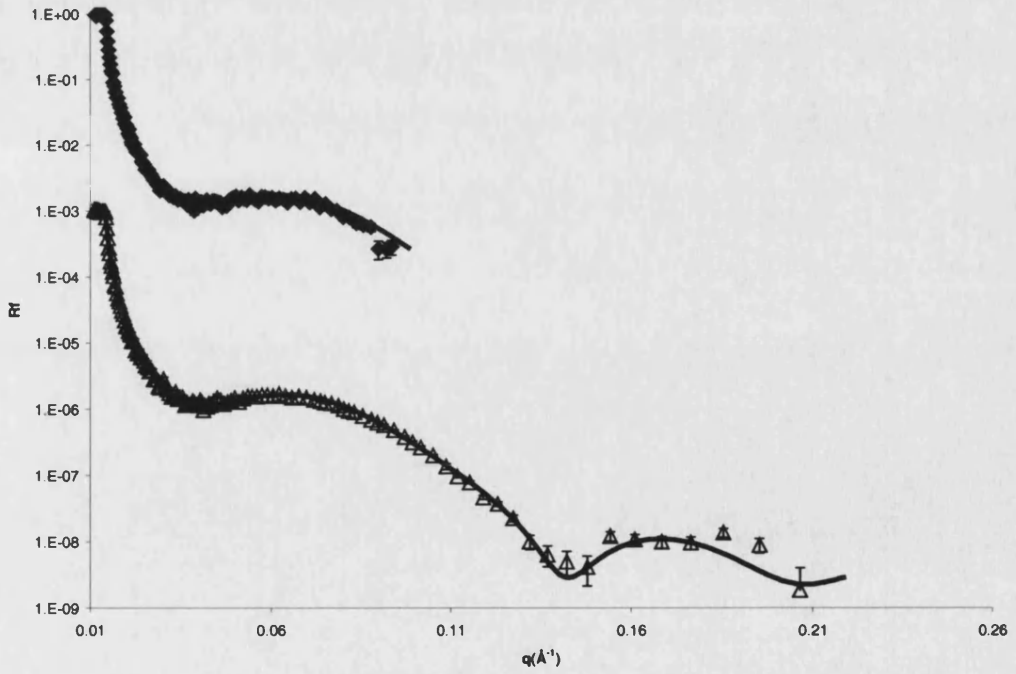

Figure 5.16 Fitted profiles of asymmetric 6 mol% and 1 mol% sample at 32.3°C (♦) and 26.2°C (Δ)

	dw	lDb	lDc	lAPM	lRou	lCov	Dw	uDb	uDc	uAPM	uRou	uCov
32.3°C	7±1	47±2	35±1	46±2	5±1	97±2	32±1	52±2	37±1	43±2	16±2	97±2
26.2°C	8±1	47±2	35±1	46±2	5±1	97±2	31±1	51±2	37±1	43±2	16±2	97±2
Initial 26.4°C	7±1	50±2	36±1	44±2	5±1	94±2	28±1	49±2	35±1	46±2	12±2	89±2

Table 5.12 Fitted parameters of asymmetric 6 mol% and 1 mol% sample in gel phase after cooling. The initial gel structure before heating is given for comparison.

The main differences between the initial gel phase and after the temperature scan are that it has a thicker upper bilayer chain region, thicker main water layer and higher coverage in both bilayers. These differences are all likely caused by an equilibrating of the structure by the temperature scan. There is one other significant difference though; the upper bilayer has a much higher roughness by 4Å. This behaviour mirrors that of the double bilayer of 1 mol% cholesterol, where the roughness was 3Å higher after the temperature scan (Table 3.8).

The presence of low amounts of cholesterol has previously been observed to stabilise the secondary long wavelength ripple structure, which is observed in the transition region, down to lower temperatures and into the gel phase. The cholesterol also increases the periodicity of the ripples (Mortensen 1988). It could be that the higher roughness of the gel phase is caused by the presence of these ripples.

5.5 Asymmetric Samples Conclusion

The results of this chapter have shown that it is possible to fabricate stable asymmetric double bilayer samples using a range of different components. This is an advantage of the use of the Langmuir-Blodgett-Schaefer technique, which allows a much greater control over each layer composition compared to vesicle adsorption methods.

The structural behaviour of the different phases was found to be affected by the presence of asymmetric bilayers and samples, especially the transition phase.

The asymmetric double bilayer of DPPE and DPPC-cholesterol was completely stable over the temperature range measured. Whilst the lower bilayer of DPPC-cholesterol exhibited full gel – fluid phase behaviour, the presence of the DPPE leaflet in the upper bilayer restricted the phase behaviour of the DPPC-cholesterol leaflet. The presence of a leaflet with a higher gel – fluid transition temperature in a bilayer is therefore able to restrict the gel – fluid transition of the other leaflet.

The double bilayer with an asymmetric upper bilayer of h_{62}-DPPC and d_{62}-DPPC was found to have a stable asymmetric nature over the temperature range measured. During the transition phase the asymmetric sample exhibited a lower increase in the water layer thickness and upper bilayer roughness compared to the fully hydrogenated sample of chapter 3. The presence of a deuterated lipid leaflet is restricting the phase behaviour of the upper bilayer. The temperature of the gel – fluid transition was not affected however.

The sample containing different amounts of cholesterol in the lower and upper bilayer was found to exhibit similar gel and fluid structures to the non-asymmetric 1 mol% and 6 mol% double bilayers of chapter 3. Upon heating in the transition phase the increase in the water layer thickness and upper bilayer roughness was less than that observed in the 1 mol% double bilayer. The profiles measured upon cooling in the transition phase were different to those of the 1 mol% double bilayer. The presence of a lower bilayer with a higher amount of cholesterol is therefore having

an effect on the behaviour of the upper bilayer. This is logical as the upper bilayer is held to the lower bilayer by a range of different Helfrich forces (Helfrich 1977).

5.6 References

- Bittman R, Blau L, Clejan S. et al. (1981) *Determination of cholesterol asymmetry by rapid kinetics of filipin-cholesterol association: effect of modification in lipids and proteins* Biochemistry 20, 2425 – 2432
- Boon J M, Smith B D. (1999) *Facilitated phospholipid translocation across vesicle membranes using low molecular weight synthetic Flippases* J. Am. Chem. Soc. 121, 11924 – 11925
- Bretscher M S. (1973) *Membrane structure: some general principles* Science 181, 662 – 629
- Clejan S, Bittman R, Rottem S. (1978) *Uptake, transbilayer distribution, and movement of cholesterol in growing Mycoplasma capricolum cells* Biochemistry 17, 4579 – 4583
- Clejan S, Bittmann R, Rottem S. (1981) *Effects of sterol structure and exogenous lipids on the transbilayer distribution of sterols in the membrane of Mycoplasma capricolum* Biochemistry 20, 2200 – 2204
- Cunningham B, Brown A D, Wolfe D H, Williams WP, Brain A. (1998) *Ripple phase PC Effect chain length, position, and unsaturation* Phys. Rev. E. 58, 3662 –3672
- Fragneto G, Charitat T, Bellet-Amalric E. et al. (2003) *Swelling of phospholipid floating bilayers: the effect of chain length* Langmuir 19, 7695 – 7702
- Helfrich W. (1977) *Steric interaction of fluid membranes in multilayer systems* Z. Naturforsch 33a, 305 – 315
- Homan R, Pownall H J. (1988) *Transbilayer diffusion of phospholipids: dependence on headgroup structure and acyl chain length* Biochim. Biophys. Acta 938, 155 – 166
- Igbavboa U, Avdulov N A, Schroeder F. et al. (1996) *Increasing age alters transbilayer fluidity and cholesterol asymmetry in synaptic plasma membranes of mice* J. Neurochem. 66, 1717 – 1725
- Kaasgaard T, Leidy C, Crowe J H. et al. (2003) *Temperature-controlled structure and kinetics of ripple phases in one- and two-component supported lipid bilayers* Biophys. J. 85, 350 – 360
- Kato N, Nakanishi M, Hirashima N. (2002) *Transbilayer asymmetry of phospholipids in the plasma membrane regulates exocytotic release in mast cells* Biochemistry 41, 8068 – 8074
- Knoll W, Schmidt G, Ibel K. et al. (1985). *Small-Angle Neutron Scattering Study of Lateral Phase Separation in Dimyristoylphosphatidylcholine-Cholesterol Mixed Membranes.* Biochemistry. 24, 5240 – 5246.
- Leonard A, Escrive C, Laguerre M. et al. (2001) *Location of Cholesterol in DMPC Membranes. A Comparative Study by Neutron Diffraction and Molecular Mechanics Simulation†* Langmuir 17, 2019 - 2030
- Merkel R, Sackmann E, Evans E. (1989) *Molecular friction and epitactic coupling between monolayers in supported bilayers* Journal de Physique 50, 1535 – 1555
- Nagle J F, Tristram-Nagle S. (2000) *Structure of lipid bilayers* Biochim. Biophys. Acta 1469 159 – 195
- Racansky (1987) *A study of the phase-transitions in phosphatidylcholine and phosphatidylethanolamine model membranes using polarizing microscopy* Acta Physica Slovaca 37, 166 – 176
- Rinia H A, Demel R A, Van der Eerden J P J M. et al. (1999) *Blistering of langmuir-blodgett bilayers containing anionic phospholipids as observed by atomic force microscopy* Biophys J. 77, 1683 – 93
- Seigneuret M, Devaux (1984) *ATP-dependent asymmetric distribution of spin-labeled phospholipids in the erythrocyte membrane: Relation to shape changes* Proc Natl Acad Sci 81, 3751 – 3755

- Smith B D, Lambert T N. (2003) *Molecular ferries: membrane carriers that promote phospholipid flip-flop and chloride transport* Chem. Comm. 2261–2268

6. Thesis Conclusions

The aim of this thesis was to incorporation of new components into supported lipid double bilayer systems and to study their effect on the phase behaviour and stability of the double bilayer. This would increase the understanding of the behaviour of the components in the field of biophysics and increase the applicability of the system as a biomembrane mimic.

In this thesis it has been shown that with the Langmuir-Blodgett-Schaefer technique it is possible to fabricate double bilayers with a range of different components, at different concentrations and with asymmetric distributions of lipids across the bilayer. This particular ability to fabricate asymmetric double bilayers opens an interesting new area in field of membrane mimics. It was not possible to fabricate high quality bilayers with deuterated chain DPPC (d_{62}-DPPC). However it was possible to fabricate single bilayers of this compound using 10 mol% cholesterol.

The main advance in the fabrication method was refinement of the procedures so that double bilayers could be fabricated with very reproducible results. This was in part due to the development of a micrometer controlled manual dipper for the Schaefer deposition. The manual dipper consistently gave better results than with the use of the computer controlled dipper. With this dipper the substrate can be brought within microns of the monolayer and the horizontality still be adjusted. The speed of deposition can also be a slow as microns per minute or less. This is not possible with the computer controlled dipper, which is not rigid enough whilst holding the weight of the large silicon substrates (8 x 5 x 2cm^2) and has a minimum speed of 1mm/min.

The thesis aim regarding the study of the phase behaviour of a range of different components was also met. Three studies of particular interest were undertaken. The phase behaviour of DPPC with low concentrations of cholesterol was studied; the stability and phase behaviour of DPPE with and without cholesterol was investigated and the effect of asymmetric distributions on the phase behaviour was investigated.

6.1 DPPC cholesterol phase behaviour

The phase behaviour of DPPC double bilayers containing 0, 1, 2, 4, 6 and 10 mol% cholesterol was investigated. They were all found to exhibit stable and reversible gel, transition and fluid phases.

The thickness of the gel phase bilayers was found to increase with increasing cholesterol concentration, whilst the fluid phase bilayer thickness did not vary with cholesterol content.

In the fluid phase the thickness of the water layer that separates the two bilayers was thinner for very low concentrations (1 – 2 mol%). Increasing the cholesterol concentration increased the sample thickness back to that of the pure DPPC.

Upon heating in the transition region, the samples containing 0 – 4 mol% cholesterol exhibited large increases in the upper bilayer roughness and the water layer thickness. This was interpreted as observation of a ripple structure. The addition of 1 – 4 mol% cholesterol progressively broadened the temperature range over which the increase in parameters was observed, and reduced the level of increase of the parameters compared to the pure DPPC sample. By a ratio of between 6 – 10 mol% it was not possible to determine whether a ripple structure is present, as only a swelling of the water layer was observed. The sample containing 10 mol% also exhibited different swelling behaviour of the water layer as a function of temperature compared to the 0 – 6 mol% samples. It is likely that this was caused by domain formation, which interferes with the transition behaviour.

Upon cooling in the transition region, the samples containing 0 – 4 mol% behaved differently from the behaviour observed for them upon heating. The reflectivity profiles seem to suggest that the upper bilayer exhibits two coexisting ripple structures. This has previously been observed in a very similar DPPC double bilayer using AFM. It was not possible to fit the reflectivity profiles successfully using only one model. The presence of two coexisting ripple structures requires different analytical methods for the data analysis, which are not currently available. In this thesis a simple approximation was used, that consisted of using two separate models

to fit different parts of the profiles. This gave results similar to other studies. Different measurement techniques such as AFM and off-specular reflectivity are necessary to confirm this interpretation.

Upon cooling in the transition region the samples containing 6 – 10 mol% behaved differently to those of lower cholesterol concentrations. The samples exhibited similar transitional structures both upon heating and cooling. The higher ratios of cholesterol are likely to be reducing the large amplitude ripple structure thought to be occurring in the 0 – 4 mol% samples upon cooling. It is suspected that only a small amplitude ripple occurs in the 6 – 10 mol% samples.

It was not possible to study the phase behaviour of d_{62}-DPPC double bilayers due to the poor quality of the samples. However the phase behaviour of single bilayers of d_{62}-DPPC and h_{62}-DPPC with 10 mol% was studied and compared. They both exhibited similar gel and fluid phase structures, except that the d_{62}-DPPC sample had a higher bilayer roughness in both phases.

6.2 DPPE with and without cholesterol phase behaviour

Double bilayers of DPPE were found to be partially unstable above the gel – fluid transition temperature. A Bragg peak was observed in the reflectivity profile, indicating that part of the bilayer had formed a structure with a repeating unit. The formation was found to be irreversible. The profiles indicated that the majority of the sample remained as a double bilayer. The reflectivity profiles were interpreted by the use of two models. First the profiles were fitted without consideration of the Bragg peak. This gave results showing that the double bilayers still retained high coverage and that they became a fluid phase structure. When the gel temperature profiles were fitted with this method the bilayers showed a gel phase structure. The Bragg peak was then fitted with a model having a repeat lamellar structure above a high coverage double bilayer. Unfortunately it was not possible to obtain realistic fits of the Bragg with this model. The interpretation of the presence of the Bragg peak is on-going work.

The study of the phase behaviour of a single DPPE bilayer exhibited stable gel and fluid phases. This showed that it is likely that it is the upper bilayer that forms the repeat structure as no Bragg peak was observed, even up to 15°C above the gel – fluid transition.

The phase behaviour of a sample containing 10 mol% cholesterol and DPPE was investigated to understand whether cholesterol is able to stabilise the DPPE double bilayer structure. The cholesterol however had the opposite effect, with the upper bilayer actually detaching completely at a temperature of between 8 – 12°C below the gel – fluid transition temperature of DPPE. It is thought that the cholesterol destabilises the upper bilayer by increasing the conical shape of the DPPE molecule. Future perspectives are to incorporate DPPE into mixed component double bilayers, in the hope that it would be stabilised as planar structure by influence of other lipids.

6.3 Phase behaviour of asymmetric samples

The phase behaviour of three different asymmetric samples was investigated. The phase behaviour was found to be affected by the asymmetric nature of the bilayers.

The first sample consisted of a double bilayer with an upper bilayer containing an outer leaflet of DPPC and 10 mol% cholesterol, and inner leaflet of DPPE. The presence of the DPPE leaflet with its higher gel – fluid transition temperature was found to restrict the gel – fluid transition of the DPPC and 10 mol% cholesterol leaflet. This is a very interesting result and needs more investigation using other lipid types.

The second sample investigated had an upper bilayer with an outer leaflet of d_{62}-DPPC and inner leaflet of h-DPPC. Whilst the presence of the deuterated leaflet did not affect the gel and fluid structure or the temperature of the gel – fluid transition, in the transition phase it reduced the level of increase in the thickness of the water layer that separates the bilayers and the bilayer roughness observed compared to the DPPC double bilayer.

The third sample had a lower DPPC bilayer containing 6 mol% cholesterol and upper DPPC bilayer containing 1 mol% cholesterol. The presence the lower bilayer with a higher concentration of cholesterol was found to reduce the level of increase in the upper bilayer roughness and water layer thickness observed in the transition region, in comparison to the 1 mol% double bilayer. The effect of the lower bilayer concentration is logical as the upper bilayer is held to the lower bilayer by a range of different Helfrich forces that would be expected to be altered for different compositions.

7. Future Perspectives

7.1 Future Samples

There are many areas of future work concerning the double bilayer. Firstly, the fabrication and phase behaviour of double bilayers containing charged lipids such as phosphatidylserines and phosphatidylglycerols should be investigated. Problems could be encountered with these charged lipids though, as previously it has only been possible to fabricate single bilayers containing the phosphatidylserine DPPS, whilst monolayers of the phosphatidylglycerol lipid DPPG were found to be unstable (one possible solution would be to use the longer chained DSPG). One area of investigation would be to evaluate the use of salts to stabilise the deposition of the charged lipid monolayers. It would also be useful to evaluate the incorporation of the sphingomyelin into the bilayer, which is commonly found in plasma membranes.

An interesting study would be to investigate whether it is possible to incorporate glycolipids into the outer leaflet of the double bilayer. Glycolipids are especially abundant in plasma membranes and have a lipid structure containing a head-group composed of saccharides. Their role is to provide energy and also serve as markers for cellular recognition. The incorporation of glycolipids would aid the study of cellular recognition by providing a model for the interaction of glycolipid containing bilayers and vesicles.

Variations of the bilayers within this thesis should be investigated. For example, it would be useful to investigate the effect on the phase behaviour of different structural types of phosphatidylcholines, such as DOPC (18:1-cis) with its asymmetric chain length and unsaturated chains. It would also be interesting to study the effect of mixed bilayers of phosphatidylcholines with different chain lengths (e.g. DPPC, DSPC) on the planar structure (Ipsen 1988) and the phase behaviour. This is also relevant as the chain length of phospholipids is usually C_{16} (palmitoyl), C_{18} (stearoyl) or C_{20} (arachidoyl) (Darnel, 3rd edition 1995).

Another relevant study would be to investigate whether it is possible to fabricate high cholesterol concentration (above 20 mol%) double bilayers by the small

unilamellar vesicle adsorption technique of the Mouritsen group (Kaasgaard 2003). This would allow the double bilayer to mimic biological ratios of cholesterol (Yeagle 1986).

The effect of low amounts of cholesterol upon the stability of DPPE double bilayers should also be investigated, as low concentrations of cholesterol behave differently to high amounts. It would also be interesting to study the stability and phase behaviour of different structural types of phosphatidylethanolamines, such as DOPE with its unsaturated chains. These could be more stable as a double bilayer compared to DPPE.

The behaviour of all these samples should also be studied in the presence of biological buffer solutions and salts, to mimic the nature extra-cellular environment of the cell. All the above studies should also be studied as single component double bilayers, mixed component bilayers and asymmetric bilayers. These studies would contribute to the use of the double bilayer as a biomembrane mimic. The double bilayer is currently being used in this form for protein studies

7.2 Application of different analytical methods

Other future work involves the application of different analytical techniques in studies using the double bilayer. Techniques such as AFM, surface plasmon resonance and Brewster angle microscopy at the liquid – solid interface can be applied. The use of these techniques has already been initiated and the preliminary results look promising.

7.3 References

- Ipsen J H, Mouritsen O G. (1988) *Modelling the phase equilibria in two-component membranes of phospholipids with different acyl-chain lengths* Biochim. Biophys. Acta 944, 121 –134
- Kaasgaard T, Leidy C, Crowe J H. et al. (2003) *Temperature-controlled structure and kinetics of ripple phases in one- and two-component supported lipid bilayers* Biophys. J. 85, 350 – 360
- Darnel (3ed 1995) *Molecular cell biology* Scientific American books, New York
- Yeagle P L. (1985) *Cholesterol and the cell membrane.* Biochim. Biophys. Acta. Rev. Biomem. 822, 267 – 287